Metabolomics as a tool to explore the staphylococcal biofilm

Laurence Harry Stipetic
BSc(Hons) MRes

Submitted in fulfilment of the requirements for the Degree of Doctor of Philosophy

School of Life Sciences
College of Medical, Veterinary and Life Sciences
Institute of Infection, Immunity & Inflammation
University of Glasgow

January 2016

Abstract

Orthopaedic infections can be polymicrobial existing as a microbiome. Infections often incorporate staphylococcal species, including *Staphylococcus aureus*. Such infections can lead to life threatening illness and implant failure. Furthermore, biofilm formation on the implant surface can occur, increasing pathogenicity, exacerbating antibiotic resistance and altering antimicrobial mechanism of action. Bacteria change dramatically during the transition to a biofilm growth state: phenotypically; transcriptionally; and metabolically, highlighting the need for research into molecular mechanisms involved in biofilm formation. Metabolomics can provide a tool to analyse metabolic changes which are directly related to the expressed phenotype. Here, we aimed to provide greater understanding of orthopaedic infection caused by *S. aureus* and biofilm formation on the implant surface.

Through metagenome analysis by employing: implant material extraction; DNA extraction; microbial enrichment; and whole genome sequencing, we present a microbiome study of the infected prosthesis to resolve the causative species of orthopaedic hip infection. Results highlight the presence of *S. aureus* as a primary cause of orthopaedic infection along with *Enterococcus faecium* and the presence of secondary pathogen *Clostridium difficile*. Although results were hindered by the presence of host contaminating DNA even after microbial enrichment, conclusions could be made over the potential increased pathogenicity caused by the presence of a secondary pathogen and highlight method and sample preparation considerations when undertaking such a study.

Following this finding, studies were focused on an orthopaedic clinical isolate of *S. aureus* and a metabolome extraction method for staphylococcal biofilms was developed using cell lysis through bead beating and solvent metabolome extraction. The method was found to be reproducible when coupled with liquid chromatography-mass spectrometry (LC-MS) and bioinformatics, allowing for the detection of significant changes in metabolism between planktonic and biofilm cultures to be identified and drug mechanism of actions (MOA) to be studied.

Metabolomics results highlight significant changes in a number of metabolic pathways including arginine biosynthesis and purine metabolism between the two cell populations, evidence of S. *aureus* responding to their changing environment, including oxygen availability and a decrease in pH. Focused investigations on purine metabolism looking for biofilm modulation effects were carried out. Modulation of the S. *aureus* biofilm phenotype was observed through the addition of exogenous metabolites. Inosine increased biofilm biomass while formycin B, an inosine analogue, showed a dispersal effect and a potential synergistic effect in biofilm dispersal when coupled with gentamycin.

Changes in metabolism between planktonic cells and biofilms highlight the requirement for antimicrobial testing to be carried out against planktonic cells and biofilms. Untargeted metabolomics was used to study the MOA of triclosan in S. *aureus*. The triclosan target and MOA in bacteria has already been characterised, however, questions remain over its effects in bacteria. Although the use of triclosan has come under increasing speculation, its full effects are still largely unknown. Results show that triclosan can induce a cascade of detrimental events in the cell metabolism including significant changes in amino acid metabolism, affecting planktonic cells and biofilms.

Results and conclusions provide greater understanding of orthopaedic infections and specifically focus on the S. *aureus* biofilm, confirming S. *aureus* as a primary cause of orthopaedic infection and using metabolomic analysis to look at the changing state of metabolism between the different growth states. Metabolomics is a valuable tool for biofilm and drug MOA studies, helping understand orthopaedic infection and implant failure, providing crucial insight into the biochemistry of bacteria for the potential for inferences to be gained, such as the MOA of antimicrobials and the identification of novel metabolic drug targets.

Table of Contents

List of Tables

List of Figures

List of Accompanying Material

Appendices

I. Publication: Stipetic *et al.*, 2015, *(PDF has been removed due to Copyright restrictions)*.

II. Publication: Stipetic *et al.*, 2016, *(PDF has been removed due to Copyright restrictions)*.

III. Supplementary data: Metabolomic data set comparing 3 alternative lysis methods - IDEOM macro-enabled spread sheet *(Spread sheet has been removed due to Copyright restrictions, accessible online via appendix II)*.

IV. Supplementary data: *S. aureus* biofilm versus planktonic metabolomic data set – Polyomics In-house Metabolomic Pipeline spread sheet *(Spread sheet has been removed due to Copyright restrictions, accessible online via appendix II)*.

V. Supplementary data: Inosine- and adenine-treated *S. aureus* biofilm metabolomic data set - Polyomics In-house Metabolomic Pipeline spread sheet.

VI. Supplementary data: Triclosan-treated *S. aureus* planktonic cell metabolomic data set - Polyomics In-house Metabolomic Pipeline spread sheet.

VII. Supplementary data: Triclosan-treated *S. aureus* biofilm metabolomic data set - Polyomics In-house Metabolomic Pipeline spread sheet.

VIII. Electronic copy (PDF) of Thesis.

Published papers

- Stipetic, L. H., Hamilton, G., Dalby, M. J., Davies, R. L., Meek, R. M. D., Ramage, G., Smith, D. G. E., & Burgess, K. E. V. (2015). Draft Genome Sequence of Isolate *Staphylococcus aureus* LHSKBClinical, Isolated from an Infected Hip. *Genome Announcements*, *3*, 2.

- Stipetic, L. H., Dalby, M. J., Davies, R. L., Morton, F. R., Ramage, G., & Burgess, K. E. V. (2016). A novel metabolomic approach used for the comparison of *Staphylococcus aureus* planktonic cells and biofilm samples. *Metabolomics*, *12*, 75.

Conference proceedings

Parts of the following thesis have been presented at the following conferences and various other local and national meetings.

- Gordon Research Conference in Staphylococcal diseases, Lucca (Barga), Italy, 2015
- Gordon Research Seminar in Staphylococcal diseases, Lucca (Barga), Italy, 2015
- Glasgow Orthopaedic Research Initiative (GLORI), Glasgow, UK, 2015
- Microbiology Society Meeting, Birmingham, UK, 2015
- Microbiology Society Annual Meeting, Liverpool, UK, 2014
- Joint Centres for Doctoral Training Conference, Warwick, UK, 2014

Acknowledgements

I would first like to thank my supervisory team, Karl E.V. Burgess, Matthew J. Dalby and Robert L. Davies. To my primary supervisor Karl Burgess, who has led me through the trials and tribulations of a PhD, thank you for all your support and being there to answer my favourite question; *'it's OK isn't it?'*

I would also like to thank for their support, help, wisdom and encouragement, in no particular order: Richard J. Burchmore; Gordon Ramage; Harry Birkbeck; Dominic Meek; Michael Barrett; David G.E. Smith; Stefan Weidt; Suzanne McGill; Ana Monteiro; Graham Hamilton; Gavin Blackburn; Jing Wang; Julie Galbraith; Jennifer Haggarty; Emma Boulton; Bogumila Pesko; James Newton; Donald Hansom; Fahd Mahmood; Hannah Rankin; Margaret Mullin; Fraser Morton; Tanita Casci; Allison Jackson; Amy Cattanach; & Pawel Herzyk.

Thank you to Glasgow Polyomics where I have been based and carried out my research and to the Doctoral Training Centre in Technologies at the Interface between Engineering & the Physical Sciences and the Life Sciences (previously Cell and Proteomic Technologies), of which I have been a member of, and to the funders; Biotechnology and Biological Sciences Research Council (BBSRC), and the Engineering and Physical sciences Research Councils (EPSRC).

I would like to thank my parents, Anthony and Alison Stipetic. I wouldn't be here without you and I couldn't have asked for more supportive parents, I can only hope I make you proud. A special thanks to my girlfriend Hazel Hamilton. Your help, support, proof reading skills, tea making, and overall 'Laurence rock', has been invaluable and I wouldn't be here without your help. I'm just happy that I will be able to return the favour when you come to write your PhD thesis.

To the Stipetic family, the Hamilton family, and all my friends that I have not named, thank you.

Dedication

I dedicate this thesis to my late Grandfathers; Harry Burns, and Edmund Laurence Stipetic. Not only do I share a combination of your names but also your enquiring minds.

Author's declaration

I declare that, except where explicit reference is made to the contribution of others, that this dissertation is the result of my own work and has not been submitted for any other degree at the University of Glasgow or any other institution.

Signature: 

Printed name: Laurence H. Stipetic

Definitions/Abbreviations

°C	Degrees Celsius
µM	Micro molar
2D	Two-dimensional
A	Adenine
Aap	Accumulation-associated protein
ABC	ATP-binding cassette
ackA	Acetyl phosphate
ACP	Enoyl-acyl carrier protein
ADH	Arginine dihydrolase
Agr	Accessory gene regulator
AHLs	N-Acyl homoserine lactones
AIP	Autoinducing peptides
AMP	Adenosine monophosphate
AMPA	α-amino-3-hydroxy-5-methyl-4-isoxazolepropionic acid
amu	Atomic mass unit
antiSMASH	Antibiotics and Secondary Metabolite Analysis SHell
API	Analytical profile index
arcD	Arginine/ornithine antiporter gene
B	Biofilm
Bap	Biofilm-associated protein
BC	Before Christ
BHI	Brain heart infusion
BLAST	Basic local alignment search tool
C	Chloramphenicol
C	Cytosine
C. difficile	Clostridium difficile
C18	Octadecyl carbon chain
CFU	Colony forming unit
CI	Confidence interval(s)
CidA	Holin-like protein
CO_2	Carbon dioxide
CV	Crystal violet
ddH_2O	Double-distilled water

dGMP	Deoxyguanosine monophosphate
dH_2O	Distilled water
DNA	Deoxyribonucleic acid
DNase	Deoxyribonuclease
E	Erythromycin
E. coli	*Escherichia coli*
E. faecium	*Enterococcus faecium*
EC	Enzyme commission
ECM	Extracellular matrix
eDNA	Extracellular deoxyribonucleic acid
EDTA	Ethylenediaminetetraacetic acid
EPM	Extracellular polymeric material
ESI	Electrospray ionisation
et al.	*et alii*
FC	Fusidic acid
FDA	Food and Drug Administration
FDR	False detection rate
FnBPs	Fibronectin binding protein
FRU	Fructose
FT-ICR	Fourier transform ion cyclotron resonance
fwhm	Full width at half maximum
g	Gram
G	Guanine
GDP	Guanosine diphosphate
GLU	Glucose
GMP	Guanosine monophosphate
h	Hour(s)
HILIC	Hydrophilic interaction chromatography
HMDB	Human metabolite database
HMDS	Hexamethyldisilazane
HPLC	High pressure liquid chromatography
$HRMS_a^1$	High-resolution full scan mass spectrum and match to an authentic compound
$HRMS_{PL}^1$	High-resolution full scan mass spectrum and match to a public library/database

ica	Intercellular adhesion
isaA	Immunodominant antigen A
isD	Iron regulated surface determinant
Kb	Kilo-bases
KEGG	Kyoto Encyclopedia of Genes and Genomes
LAC	Lactose
LC	Liquid chromatography
LC-MS	Liquid chromatography- mass spectrometry
lrg	LytSR (sensor and response regulator proteins)-regulated genes
LSTR	Lysostaphin
M	Molar
M+H	Protonated mass
MAL	Maltose
MAN	Mannitol
MDG	Methyl-αD-glucopyranoside
MEL	Melibiose
MetaPhlAn	Metagenomic Phylogenetic Analysis
M-H	Deprotonated mass
MIC	Minimum inhibitory concentration
min(s)	Minute(s)
ml	Millilitre
MLST	Multilocus sequence typing
Mm	Millimetre
mM	Millimolar
MNE	Mannose
MOA	Mechanism/mode of action
Mr	Molecular mass
MRSA	Methicillin resistant *Staphylococcus aureus*
MS	Mass spectrometry
MSCRAMM	Microbial surface components recognizing adhesive matrix molecules
MSI	Metabolomics Standards Initiative
MSSA	Methicillin susceptible *Staphylococcus aureus*
NAD	Nicotinamide adenine dinucleotide
NAG	N-acetyl-glucosamine

NC	Negative control
NCBI	National Center for Biotechnology Information
ng	Nano-gram
NHS	National Health Service
NIT	Potassium nitrate
NMR	Nuclear magnetic resonance
NO	Novobiocin
NRPS	Nonribosomal peptide synthetase
O	Oxygen
OD	Optical density
OD_{595}	Optical density at 595 nm
OX	Oxacillin
P	Planktonic
PAGE	Polyacrylamide gel electrophoresis
PAL	B-naphthyl phosphate
PC	Principal component
PCA	Principal component analysis
PCR	Polymerase chain reaction
PG	Penicillin G
PIA	Polysaccharide intercellular adhesion
PNAG	Poly-N-acetylglucosamine
ppm	Parts per million
PPP	Pentose-phosphate pathway
PSMs	Phenol-soluble modulins
PTS	Phosphotransferase system
PurR	Purine metabolism regulator
PVL	Panton-Valentine Leukocidin
Q	Quarter
qPCR	Quantitative PCR
RAF	Raffinose
RAST	Rapid Annotation using Subsystem Technology
Rbf	Regulator of biofilm formation
RNA	Ribonucleic acid
RPM	Revolutions per minute
Rsd	Relative standard deviation

R_t	Retention time
R_{ta}	Retention time matched to an authentic standard
S	Streptomycin
S. aureus	*Staphylococcus aureus*
S.D.	Standard deviation
SAC	Saccharose (sucrose)
SAID	*S. aureus* identification agar
SaPI	*S. aureus* pathogenicity islands
SarA	Staphylococcal accessory regulator
SCV	Small colony variants
Sdr	Serine-aspartate repeat
SEM	Scanning electron microscopy/microscope/micrograph
sigB	Sigma factor B
SpA	Protein A
Spf	Sophoraflavanone
spp	species
ssaA	Staphylococcal secretory antigen
T	Tetracycline
T	Thymine
TA	Teichoic acid
TAE	Tris-acetate-EDTA
TCA	Tricarboxylic acid
tcaR	Teicoplanin-associated locus regulator
TE	Tris EDTA
TIFF	Tagged Image File Format
TOF	Time of flight
TRE	Trehalose
Tris	Tris(hydroxymethyl)aminomethane
UK	United Kingdom
URE	Urea
USA	United States of America
V	Volts
VP	Voges-Proskauer
VRE	Vancomycin-resistant Enterococcus
VRSA	Vancomycin resistant *Staphylococcus aureus*

WGS	Whole genome sequencing
XLT	Xylitol
XYL	Xylose

Chapter 1 Introduction

1.1 Bacteria and Biofilms

1.1.1 *Staphylococcus aureus*

Staphylococcus aureus is a Gram-positive, coccal, facultative anaerobe found as part of the normal skin flora of humans (Cogen et al., 2008). The name *Staphylococcus* comes from the Greek meaning bunch of grapes (*staphyle*) and berry (*kokkos*), due to its ability to divide in multiple plains giving it an appearance of bunches of grapes or berries when growing (Tzagoloff and Novick, 1977). First described by the Scottish surgeon Sir Alexander Ogston in 1880, Aberdeen, it was 4 years later that the German physician, Friedrich Julius Rosenbach differentiated the bacteria based on colony colour (Anon, 1984; Licitra, 2013). *S. aureus* from the Latin for gold *aurum* and *S. albus* from the Latin for white, later to be renamed *S. epidermidis* due to its association with the skin.

S. aureus are encased in a phospholipid bi-layer cell membrane, peptidoglycan cell wall that provides cell rigidity maintaining cell shape, and a capsule (Figure 1-1).

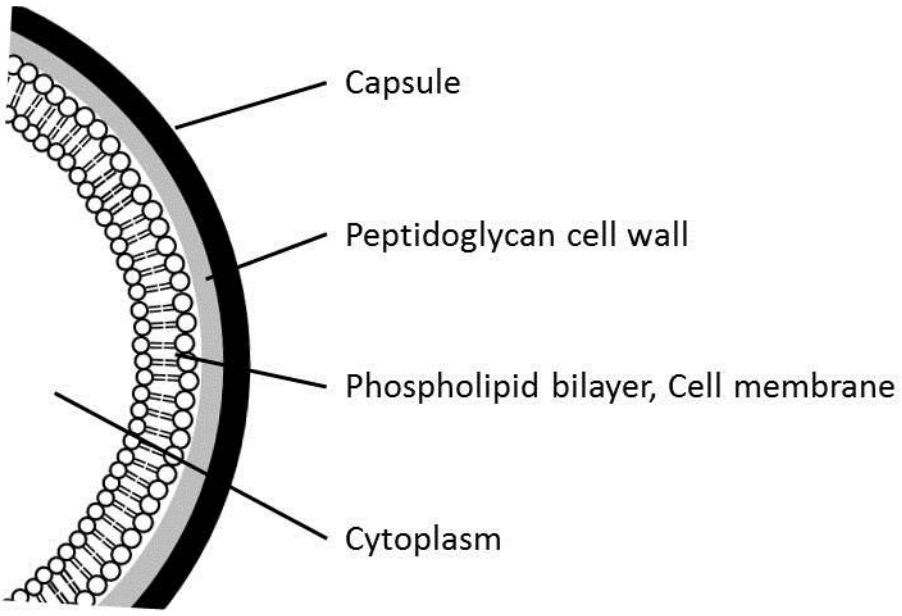

Figure 1-1: Diagram of the structure of a *S. aureus* cell

Commonly found as a commensal pathogen, *S. aureus* can be asymptomatic to their carrier (Brown et al., 2013). However, infection can cause a wide spectrum of disease including: localised infections of the skin such as a wound infection; toxinoses such as toxic shock syndrome; or potentially life-threatening, systemic illnesses such as septicaemia, septic arthritis, endocarditis, osteomyelitis, pneumonia, brain abscesses, meningitis, and bacteraemia (Aires de Sousa and De Lencastre, 2004; Bien et al., 2011).

The bacterium can be spread through host-host contact and can be carried in and colonise the anterior nares (Brown et al., 2013; Kluytmans et al., 1997). *S. aureus* infection can be community acquired (Salmenlinna et al., 2002), health care associated or hospital acquired (nosocomial), the latter two being closely related in terms of strains, mortality, and treatment management (Bishara et al., 2012). *S. aureus* can infect a number of different mammalian hosts and has several natural reservoirs including livestock animals such as cows (Devriese et al., 1972) and pigs (Lewis et al., 2008), as well as companion animals such as dogs, cats and horses (Loeffler and Lloyd, 2010). Often infecting livestock and with animal contact being a cause of human infection, it is believed host adaption and cross species jumping has led to the emergence of virulent and antibiotic resistant strains (Price et al., 2012).

S. aureus strains can be broadly divided into two groups depending on their susceptibility to beta-lactam antibiotics, namely; Methicillin-resistant *S. aureus* (MRSA) and Methicillin-sensitive *S. aureus* (MSSA). MRSA strains are a great medical concern as they are resistant to widely used conventional antibiotics. However, MSSA strains, although antibiotic susceptible, still present a significant health threat. Previous *in vitro* studies have shown virulence to be unaltered between MRSA and MSSA (Duckworth and Jordens, 1990). A clinical cohort study by Melzer *et al.* 2003, looking at 815 patients with nosocomial *S. aureus* bacteraemia shows that both MRSA and MSSA patients presented a similar incidence of dissemination and that some virulence factors such as adherence did not differ between MRSA and MSSA, thus, highlighting MSSA as an important pathogen (Melzer et al., 2003). Furthermore, David *et al.* 2011, report a study which suggests MSSA had become a health-care-associated pathogen among patients in the study and not always a community acquired infection. While

MRSA had become a community acquired pathogen and not always a health-care-associated infection, as in the past (David et al., 2011). They further concluded from their study that MSSA patients were more likely to have bacteraemia, endocarditis, or sepsis than MRSA patients. However, MSSA and MRSA patients had a similar likelihood of having an invasive infection (David et al., 2011). In Scotland and England the number of MSSA reported cases is far larger in comparison to the number of reported MRSA cases. In Scotland, July to September 2014 (Q3 of Year 2014), 410 new cases of *S. aureus* bacteraemia were reported with only 7.6% of them being MRSA cases (National Health Service (NHS) Scotland, 2015). In England, 2014-15, the total number of reported cases of MSSA increased by 5.8% from the preceding year, compared to cases of MRSA which decreased by 7.1% from the preceding year (Public Health England, 2015).

In addition to MRSA, other antibiotic resistant strains of *S. aureus* have emerged including Vancomycin-resistant *S. aureus* (VRSA), which have quickly become a serious medical concern due to the onset of persistent infections failing to respond to antibiotic treatment (Appelbaum, 2006).

There are a number of antibiotic resistance mechanisms in *S. aureus* including enzymatic inactivation of the antibiotic, target modulation, antibiotic trapping and efflux pumps (Kaatz et al., 1993; Pantosti et al., 2007; Wright, 2005).

Antibiotic resistance mechanisms are mediated through horizontal gene transfer or through spontaneous mutations and positive selection (Pantosti et al., 2007).

1.1.2 *S. aureus* pathogenesis and orthopaedic surgery

Due to the presence of *S. aureus* on the skin, infections have been associated with eczema and other skin damaging conditions, in which the upper skin layers (epidermis and dermis) are compromised, allowing the bacteria to cause a wound infection (Gong et al., 2006; Kumar et al., 2015). Further to this, members of the *Staphylococcus* genus, including *S. aureus*, are primarily responsible for orthopaedic implant infections (Dempsey et al., 2007; Esteban et al., 2010; Montanaro et al., 2011; Zimmerli et al., 2004). Such implants can include joint and other skeletal component replacements. *Staphylococcus*

infections have an historic connection with orthopaedics, being first seen and described in the pus from a surgical abscess located in a knee joint.

The most common type of arthroplasty surgery is knee and hip replacements (National Health Service (NHS), 2014), carried out due to diseases such as arthritis affecting the joint or because of a trauma (break) causing damage to the joint.

Infections post-arthroplasty surgeries are a main cause of disease and implant failure (Dempsey et al., 2007; Esteban et al., 2010; National Health Service (NHS), 2014; Zimmerli et al., 2004).

Orthopaedic infections can lead to debilitating illness and lower life expectancy post-surgery. Septic loosening is the second highest cause of orthopaedic implant failure after aseptic loosening caused by mechanical failure and other factors (National Health Service (NHS), 2014). However, some studies have shown that aseptic loosening may be a misdiagnosis, where bacteria causing an unidentified infection inducing loosening may be present (Bereza et al., 2013). Such misdiagnosis is attributed to bacteria which are not identified through conventional techniques and culture preparations, for example anaerobic organisms.

Although the orthopaedic infection rate is relatively low at 0.75-2% of all knee and hip replacements in Scotland (a percentage infection rate seen nationally, UK), around 15 000 Knee and hip arthroplasty procedures, whether elective or because of trauma, are carried out annually in Scotland, and thus the number of cases per year are significant, at around 100-300 (NHS, 2014). Furthermore, this percentage represents clinically diagnosed septic cases and does not include aseptic cases were by infection may be present but not diagnosed. Infection rates in Scotland have shown to stay stable even though the number of hip and knee replacement surgeries is increasing.

A significant factor in implant failure and the failure of antimicrobial therapy is biofilm formation on the prosthesis surface (Esteban et al., 2010; Smith et al., 2008; Zimmerli et al., 2004). This persistent infection can lead to the requirement for a revision procedure usually involving complete removal of the

implant and potentially meaning replacement of the stem and acetabular component of the prosthesis (Figure 1-2). If infection cannot be cleared from the site or too ensure the infection has been depleted, the surgeon can use an antibiotic impregnated cement spacer which is left *in situ* temporally at the removal site for a period of time after which it is then removed and replaced with a more permanent implant (Zimmerli et al., 2004). Although an effective way to administer antibiotics directly to the infection site and ensuring microbial eradication so the infection will not return, this procedure requires an additional operation, causing further trauma and risk to the patient. Additionally, persistent orthopaedic infections can cause bone erosion, which have to be rectified through larger implants, the addition of secondary implants, or cement (Figure 1-2). For example, Figure 1-2 shows an infected hip replacement where infected material surrounds the stem component of the prosthesis. The infection appears to have induced some bone erosion, thus resulting in damage to the femur. In order to get a clear margin of uninfected material the whole distal femur condyles had to be removed. There would have been no support for a stem this far down the femur other than a knee replacement, therefore requiring a knee, femur and hip replacement (Figure 1-2). Such procedures are a huge cost burden to the NHS (Kallala et al., 2015; Vanhegan et al., 2012), as well as causing significant trauma to the patients, which are commonly elderly. In a study by Vanhegan *et al*. (2012), they analyse the financial cost of revision hip arthroplasty between 1999 and 2008 at a UK tertiary referral centre. They document that the mean total cost of revision surgery in aseptic cases (n = 194) was £11,897 (S.D. £4,629), whereas the cost was almost doubled for septic revision cases (n = 76) at £21,937 (S.D. £10,965) (Vanhegan et al., 2012). They further highlighted that surgery for infection cases was associated with increased: operating times, blood loss, complications and inpatient stay, compared to revisions for aseptic loosening (Vanhegan et al., 2012). Patients may have to undergo numerous separate operations and treatments, including pre- and post- operative antibiotic treatments and physiotherapy. Thus, research into modes of infection, biofilm formation and drug target and drug discovery are crucial strategies in preventing these infections.

Figure has been removed due to Copyright restrictions.

Figure 1-2: Infected orthopaedic hip revision surgery.

(A) Surgeons first have to expose the implant, figure illustrating the complexity and evasiveness of the procedure. (B) The acetabular component of the hip replacement is also removed and replaced. (C) Figure depicts the removed femur with the distal femur condyles. The old stem still in place and infection has led to bone erosion and damage of the femur (C (i)). (D) The entire femur has had to be removed and replaced as well as the knee and hip joints, thus, ensuring a clear uninfected tissue margin around and removal of all infected material. Images used with permission from the Trauma and Orthopaedic surgery department at the Queen Elizabeth University Hospital, Glasgow, Scotland, UK. Photos taken by medical illustration, NHS Greater Glasgow & Clyde, 2015.

1.1.3 *S. aureus* virulence factors

The virulence of *S. aureus* is due to a number of factors including adhesins and exoproteins (Bien et al., 2011). These virulence factors are responsible for the onset of infection, disease, immunosuppression, immune evasion and increased pathogenicity. *S. aureus* virulence factors can be expressed in both planktonic cells and biofilms (Flemming and Wingender, 2010). Expression can be triggered by environmental changes including bacterial cell density and nutrient availability (Bien et al., 2011).

1.1.3.1 Exoproteins: toxins and enzymes

S. aureus has the capability to produce several cytolytic toxins namely; α-haemolysin, β–haemolysin, γ-haemolysin, δ-haemolysin, leukocidin, and Panton-Valentine leukocidin (PVL), promoting virulence (Bien et al., 2011; Kaneko and Kamio, 2004; Nilsson et al., 1999; Tomita and Kamio, 1997; Williams and Harper, 1947).

These toxins work through the formation of β-barrel pores in cell membranes inducing cell leakage and lysis (Foster, 2005; Kaneko and Kamio, 2004). Each toxin has specificity to different mammalian cell types. For example, α-haemolysin causes membrane damage to many mammalian cell types but is particularly effective against platelets and monocytes (Menestrina et al., 2001). Further, PVL and leukocidin have toxicity specificity to leukocytes, while γ-haemolysin has toxicity specificity erythrocytes (Kaneko and Kamio, 2004). In addition to these toxins, *S. aureus* can produce additional groups of exotoxins including: the exfoliative toxins and the pyrogenic toxin superantigens, the

latter comprising of the two further sub-groups; toxic shock syndrome toxin-1 and the enterotoxins (Holtfreter and Broker, 2005; Lina et al., 2004).

Through the production of excreted enzymes *S. aureus* can use host tissues as a nutrient source leading to increased growth and subsequent pathogenicity (Bhakdi and Tranum-Jensen, 1991; Dinges et al., 2000; Harshman et al., 1989). Enzymes including nucleases, proteases, lipases, hyaluronidases, and collagenases are produced.

1.1.3.2 Adhesins

Antigens in the form of the capsule and adhesins allow *S. aureus* to further evade the host immune response protecting the bacterium and allowing adhesion to surfaces leading to biofilm formation. Attachment and further colonisation is controlled by a number of adhesins including microbial surface component recognising adhesive matrix molecules (MSCRAMM). MSCRAMMs are a group of covalently anchored peptidoglycan proteins responsible for cell adhesion to host plasma or host extra cellular matrix (ECM) components (Foster and Hook, 1998; Maresso and Schneewind, 2008; Marraffini et al., 2006; Speziale et al., 2009). MSCRAMMs include staphylococcal protein A, fibronectin-binding proteins A and B, collagen-binding protein, and clumping factor A and B proteins (Archer et al., 2011; Foster and Hook, 1998; Lowy, Franklin, 1998).

1.1.4 Biofilm formation

The growth of bacteria in a liquid medium is generally known as a planktonic state and remains the most commonly employed method for bacterial cell culture studies. However, it is a general consensus that most bacteria species possess the ability to grow as a biofilm (McDougald et al., 2012).

The defining characteristics of a biofilm are: firstly, a colony of cells encased in and stuck together with an ECM consisting of excretions from the cells themselves (Flemming and Wingender, 2010); and secondly, attachment to a living or inert surface (O'Toole et al., 2000; Stewart and Costerton, 2001).

Biofilms can be found in a number of locations including medical, industrial and natural environments. Biofilm formation is known to be the root cause of spoiling and bio-fouling in industries which utilise fluid processing operations, where biofilm build up on machines and within systems can lead to manufacturing inefficiencies, machine breakdowns and product spoilage (Mittelman, 1998). Biofilms are also noted to form in the natural environment for example on stream and river beds where they display a slimy appearance (Lubarsky et al., 2012).

Medical associated biofilms are a serious concern as formation can lead to persistent and serious infections. It has been estimated that 80% of all microbial infections are caused by or involve biofilms (Archer et al., 2011; Stowe et al., 2011). By utilising biofilm formation, indwelling bacteria are provided with increased protection from the environment, for example protection from antibiotics, subsequently aiding the onset of persistent infection and exacerbating antibiotic resistance (Drenkard and Ausubel, 2002; Ramage et al., 2003). Biofilm formation by a range of bacteria has also been attributed to causing and exacerbating diseases such as cystic-fibrosis, gingivitis and otitis media (Costerton et al., 1999). As well as being attributed to medical implant infections and subsequent failure as previously described.

Although S. *aureus* can be infectious without; they can employ biofilm formation as a mechanism of infection *in vivo*, and along with the presence of persister cells and small-colony variant (SCV) bacteria, antibiotic resistance can be severely worsened (Singh et al., 2010). Persister cells are described as subpopulations of cells that have high antibiotic tolerances, whereas SCVs form small colonies compared to that of the parental strain, expressing a lowered growth rate, altered virulence factor production and increased antibiotic resistance (Singh et al., 2009).

However, it has been shown that strain type and external environmental factors can alter the ability of some strains to start forming a biofilm (Smith et al., 2008). Biofilm formation is regulated through signalling and can be altered depending on the surface to which they are exposed, as discussed later in sections 1.1.5 and 0.

1.1.4.1 Stages of Biofilm formation

The stages of biofilm formation have been documented in the literature (McDougald et al., 2012; Moormeier et al., 2014; O'Toole et al., 2000). Biofilm formation starts with an attachment stage, followed by aggregation, micro-colony formation, mature biofilm development and then dispersal (Figure 1-3). Cell dispersal can lead to further colonisation in subsequent areas. Further to these documented stages of biofilm formation, research into *S. aureus* biofilm formation has shown the presence of two further intermediate stages namely; multiplication and exodus (Figure 1-3). These stages occur after initial attachment and before maturation, resulting in changes in the ECM and cellular organisation in the mature biofilm (Moormeier et al., 2014). Moormeier *et al.*, 2014 observe that in the development of biofilm formation by the *S. aureus* strain UAMS-1 using a BioFlux microfluidics system, multiplication into a confluent "lawn" occurs at 6 h after primary attachment of the cells and then is followed by an exodus stage at 11 h in a subpopulation of the biofilm, followed by mature biofilm formation at 17 h. They further highlight that the exodus stage is mediated by staphylococcal nuclease (Moormeier et al., 2014).

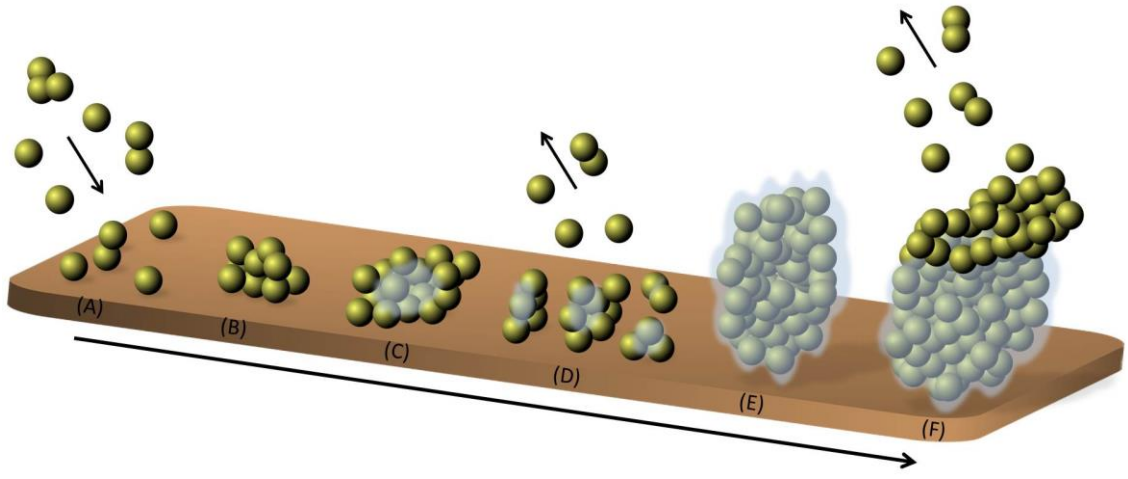

Figure 1-3: Diagram illustrating the stages of *S. aureus* biofilm formation.

(A) Initial colonisation and surface attachment. (B) Micro-colony formation, accumulation/maturation. (C) Multiplication into a confluent 'lawn'. (D) Exodus. (E) Mature biofilm development, including the ECM. (F) Cell dispersal from the biofilm (dissemination).

The start of the biofilm lifecycle is considered as the attachment stage, at which the bacteria have been able to breech the hosts defence mechanisms and adhere to a surface (McDougald et al., 2012; Roilides et al., 2015). As described earlier

a number of virulence factors and adhesions are responsible for this including molecules expressed on the cell surface. It is believed that cells come into contact with a surface through either gravitational forces, Brownian motion or hydrodynamic forces (Anselme et al., 2010). Once a surface is available for attachment and initial contact is made a change in gene expression allows the bacteria to initiate attachment mechanisms and mature into a micro-colony, further developing into a three-dimensional complex encased in the ECM (Monds and O'Toole, 2009). *S. aureus* MSCRAMMs, covalently bound to the cell surface, bind to human matrix proteins (Foster and Hook, 1998; Patti et al., 1994). Further cell surface proteins include: Serine-aspartate-repeat family (Sdr) proteins with cell-wall spanning domains (McCrea et al., 2000), and several non-covalently bound surface proteins, such as the autolysin, Atl. Autolysins have been shown to represent the most abundant proteins on the cell surface (Peschel et al., 2000). Furthermore the lipase GehD has been described to have a functional role in adherence (Bowden et al., 2002).

Following attachment, biofilm maturation occurs through a combination of adhesive forces causing intercellular aggregation and disruptive forces leading to biofilm structuring. Polysaccharide intercellular adhesin (PIA) (alternative name: poly-N-acetylglucosamine (PNAG)) is the molecule primarily responsible for intercellular adhesion (Mack et al., 1996; Otto, 2008). PIA is a polymer component of the extracellular matrix along with teichoic acids and proteins (Otto, 2008). PIA is a partially de-acetylated polymer of beta-1-6-linked N-acetylglucosamine. PIA synthesis results in the molecule being positively charged attracted to the negatively charged cell surface and subsequently attracting and sticking cells together through electrostatic interaction. Teichoic acids (TA) on the cell surface are thought to provide the negative charge to which PIA is attracted to (Otto, 2008), and thus have been attributed to *S. aureus* biofilm formation (Gross et al., 2001).

PIA is synthesised from UDP-N-acetylglucosamine via products of the intercellular adhesion (*ica*) locus (Cramton et al., 1999). The *ica* locus is comprised of the *icaR* gene, involved in regulation and the *icaADBC* operon, involved in biosynthetic processes (Archer et al., 2011; Otto, 2008). Genes belonging to the *ica* locus have been shown to be up regulated under anaerobic growth and are required for biofilm formation (Cramton et al., 2001). The

synthesis of PIA has been shown to be regulated by a number of genes including: staphylococcal respiratory response regulator, SrrAB (Ulrich et al., 2007); TcaR, a transcriptional regulator of the teicoplanin-associated locus (Jefferson et al., 2004); *IcaR*; Rbf, the protein regulator of biofilm formation (Cue et al., 2009); and Spx, a stress response gene regulator (Pamp et al., 2006). In addition, a number of environmental stimuli and changes can have a regulatory effect on *ica*, subsequently altering PIA production, for example, glucose availability, ethanol, osmotic pressure, temperature and antibiotic challenge (Fitzpatrick et al., 2005). However, PIA independent biofilm formation and strains lacking the *ica* genes isolated from biofilms have been shown to occur (Arciola et al., 2006; Rohde et al., 2005).

Alternative proteins to PIA, for example protein A (SpA), the fibronectin-binding proteins (FnBPs) and biofilm-associated protein (Bap), have been implemented in PIA independent biofilms (Cucarella et al., 2001; Houston et al., 2011; Merino et al., 2009). Cucarella *et al*. 2001, show that Bap is involved in a number of biofilm formation processes including cell to cell aggregation and abiotic surface adherence (Cucarella et al., 2001). In *S. epidermidis*, a protein called accumulation-associated protein (Aap) has been described to be involved and implemented in PIA-independent biofilm formation (Hennig et al., 2007; Hussain et al., 1997; Rohde et al., 2007).

1.1.4.2 The Biofilm Extracellular Matrix (ECM)

The mature biofilm is encased in an ECM composed of proteins, exopolysaccharides and extracellular DNA (eDNA), each produced by the encased bacterial cells (Barken et al., 2008; Flemming and Wingender, 2010; McDougald et al., 2012). The ECM acts as a scaffold, immobilising cells, thus providing support and protection (Flemming and Wingender, 2010). DNA can link other molecules together in the biofilm matrix. As a negatively charged molecule it can interact with positively charged molecules through electrostatic interactions, for example the positively charged PIA. Autolysis (cell lysis) is understood to be the main mechanism for the production of eDNA, present in the ECM. A number of regulators controlling autolysis have been identified including *cidA* and *Irg* (Figure 1-4) (Rice et al., 2007). Studies by Rice *et al*. 2007, describe the *cidA* gene which encodes a murein (bacterial peptidoglycan)

hydrolase regulator. They show reduced DNase I activity in a *cidA* gene mutant compared to the parental strain, providing evidence that the gene is involved in cell lysis (Rice et al., 2007). In addition to *cidA* other regulators of murein hydrolase and cell death have been described, for example the *lrg* gene, known to reverse the function of *cidA*, and genes encoding autolysin, a hydrolytic enzyme (Archer et al., 2011).

Figure has been removed due to Copyright restrictions.

Figure 1-4: Flowchart of *S. aureus* eDNA regulation and biofilm formation

eDNA enhances biofilm formation. Cell lysis is regulated by the *lrg* and *cidA* genes. DNase activity can degrade biofilm eDNA. Adapted from Archer *et al.* 2011.

The ECM acts as external protection mechanism, protecting against harmful substances, for instance antimicrobials or toxins, which may kill the bacteria contained within (Hall-Stoodley et al., 2004; Monds and O'Toole, 2009). The ECM has the ability to trap nutrients and other biological molecules required for a number of processes including metabolism and signalling (Flemming and Wingender, 2010; McDougald et al., 2012). It has been shown that biofilms have a digestive property containing expelled enzymes available for degrading substrates brought into the matrix, for example nutrients too large to cross individual cell membranes, which are broken down and are available for the uptake by individual cells (Flemming and Wingender, 2010).

A mature biofilm 3-dimensional structure is formed through disruptive forces. Fluid nutrient channels weave between towering structures supplying nutrients to cells deeply embedded in the biofilm (Costerton et al., 1995; Otto, 2008). Such channels are not only utilised for the distribution and transportation of nutrients and other growth factors but have an additional role in the expulsion of waste consisting of bacteria metabolism by-products (Costerton et al., 1995; Davey and O'toole, 2000; Flemming and Wingender, 2010). By-products excreted into the biofilm ECM can lead to a change in the ECM environment, for example a decrease in pH or pH gradient across the biofilm (Foulston et al., 2014).

The formation of the mature biofilm structure is thought to occur through quorum-sensing controlled expression of surfactants. Studies looking at biofilm formation by Otto 2008, have suggested the implementation of quorum-sensing controlled surfactant peptides involved in biofilm structuring (Otto, 2008). These results correspond to similar findings of quorum-sensing controlled expression of the surfactant rhamnolipid involvement in *P. aeruginosa* biofilm structuring (Davies et al., 1998; Otto, 2008). Peptides, specifically phenol-soluble modulins (PSMs) display surfactant-like properties in *S. aureus* (Periasamy et al., 2012).

The final stage of the biofilm life cycle is cell dispersal. Dispersed cells are planktonic and can migrate to new surfaces to further colonise subsequent areas (McDougald et al., 2012). Cues for cell dispersal are thought to come from a number of different signals including: when cell density within the mature biofilm reaches a critical level, variations in the surrounding environment, nutrient availability such as carbon sources, oxygen availability, nitric oxide levels, or iron levels (McDougald et al., 2012). A combination of mechanical forces acting on the biofilm, changes in metabolism resulting in a change in the production of biofilm components and the production of molecules including enzymes or surfactants as employed in biofilm structuring, are responsible for the onset of biofilm cell dispersal. Cell dispersal is controlled by the quorum-sensing accessory gene regulator (*agr*) system discussed in 1.1.5.1.

Finally, it is worth noting that the account of biofilm formation presented here is focused on staphylococcal biofilm formation and more specifically *S. aureus* biofilm formation. Biofilm formation mechanisms can vary between species and although they have similarities they can be very species specific.

1.1.5 Biofilm regulation

Bacteria generally regulate biofilm synthesis through quorum sensing, two-component systems or sigma factors (Rachid et al., 2000; Yarwood et al., 2004; Zhang and Powers, 2012; Zhu et al., 2007).

Regulatory systems include *rbf* (regulator of biofilm formation) (Cue et al., 2009; Lim et al., 2004). Bacteria can produce signalling molecules for cell-cell communication which can lead to the regulation of biofilm formation (Davies et

al., 1998). These molecules represent a potential drug target. Signalling and quorum sensing molecules, for example autoinducing peptides (AIP) in *S. aureus*, have been shown to allow the bacteria to sense and respond to changes within the environment, and to modulate virulence traits (Daines et al., 2005). These molecules are excreted during stages of biofilm development, therefore up and down regulated at different time points of growth (Yarwood et al., 2004).

Interestingly, quorum sensing molecules from other species for example N-Acyl homoserine lactones (AHLs) produced by Gram-negative bacteria have been shown to down-regulate virulence gene expression including the staphylococcal accessory regulator (*SarA*) and the *agr* in *S. aureus*, but are themselves not produced by *S. aureus* (Qazi et al., 2006).

Biofilm cells display an altered gene expression profile (Resch et al., 2005) and metabolism in contrast to their planktonic counterparts (Ammons et al., 2014; Gjersing et al., 2007; Zhang and Powers, 2012). Differences occur in biofilm capability between *S. aureus* strains, with certain strains forming biofilms more readily than others (Smith et al., 2008).

Biofilm regulation occurs at all stages of biofilm formation. In *S. aureus* biofilm formation can be controlled through regulation of the synthesis of PIA, by regulating N-acetylglucosamine and glucosamine that make up PIA (Figure 1-5) (Gerke et al., 1998; Otto, 2008). A number of genes result in changes in the expression of *icaADBC* leading to altered expression of PIA (Figure 1-5). In addition, PIA production can be ceased through the insertion of insertion element IS256 into the *ica* genes (Conlon et al., 2004; Otto, 2008; Ziebuhr et al., 1999). Cramton *et al*. 2001, highlight a further regulation mechanism of PIA, whereby anaerobic conditions induced expression of PIA.

Figure has been removed due to Copyright restrictions.

Figure 1-5: Flowchart of S. *aureus* PIA dependent biofilm formation regulation

In PIA-dependent biofilm formation (blue) the *icaADBC* gene cluster leads to PIA expression which can be suppressed by *tcaR and icaR.* The *icaR* gene can be regulated by the Spx (up-regulator) and Rbf (down-regulator) proteins. Under anaerobic conditions SrrAB induces *icaADBC* expression. PIA independent biofilm formation (red) is mediated through cell wall-associated protein cell-to-cell adhesion. Adapted from Archer *et al*. 2011.

A number of global regulators have been implicated in the regulation of biofilms, including the DNA-binding protein sarA, and the alternative sigma factor sigB (Figure 1-6).

1.1.5.1 *Agr* and *sarA* regulation

The *sarA* and *agr* genes are involved in regulating biofilm formation (Figure 1-6). *SarA* expression induces attachment and early biofilm formation followed by *agr* expression leading to immune responses through the production of virulence factors and then up regulating mechanisms involved in cell dispersal. In *S. aureus* the quorum-sensing system is encoded by *agr* (Boles and Horswill, 2008; Ji et al., 1997). The molecules that are produced and used for signalling by *agr* are AIPs. AIPs have an eight-residue peptide, the last 5 of which are in a cyclic thiolactone ring, structure (Boles and Horswill, 2008; Ji et al., 1997).

Studies looking at *Pseudomonas aeruginosa* quorum sensing have shown it to have a pivotal role in biofilm formation (Boles and Horswill, 2008; Davies et al., 1998); however this is not true for *S. aureus*. Studies looking at *S. aureus* have shown that quorum sensing actively restricts cell colonisation and biofilm formation through the production of detergent-like peptides and nucleases (Beenken et al., 2003, 2010; Kong et al., 2006; Vuong et al., 2000).

Quorum-sensing regulation involves the up-regulation of adhesion factors inducing colonisation. Following this the *agr* quorum-sensing system stops colonisation factors through negative regulation of MSCRAMMs (Novick, 2003; Otto, 2008; Patti et al., 1994).

The *agr* quorum-sensing system regulates PSM expression. Furthermore, *agr* mutants and *agr*-negative phenotypes are common (Somerville et al., 2002; Vuong et al., 2004). *In vitro agr* mutants display an altered phenotype with thicker and more compact biofilm formation (Vuong et al., 2000, 2003).

Yarwood et al. (2004), hypothesise and later shown by Boles & Horswill 2008, that the *agr* quorum-sensing system may be involved in biofilm detachment, based on the observations that *agr* activity is increased in dispersed cells and through adding exogenous AIP to increase *agr* activity (Boles and Horswill, 2008; Yarwood et al., 2004).

The regulatory role of *sarA* has been shown using transcriptomic studies showing the up regulation of the gene in biofilms and through studying the inability of *sarA* mutants to form biofilms (Beenken et al., 2003; Valle et al., 2003). A reason for the inability of the *sarA* mutant to form a biofilm have been shown to be through the production of a nuclease, *nuc* or through the production of proteases (Tsang et al., 2008).

Further biofilm regulation studies have shown that the agr quorum sensing system can down regulate genes of cell wall-associated adherence factors (Chan et al., 2004).

The *arg* and *sarA* genes further regulate *arlRS* which encodes a two-component regulatory gene locus. The products of which can alter peptidoglycan hydrolase activity regulating surface attachment and preventing biofilm formation (Fournier et al., 2001).

1.1.5.2 *sigB* regulation

Further biofilm regulation is achieved through sigmaB the product of *sigB* (Pane-Farre et al., 2006) which represses *icaR* subsequently repressing *icaADBC* (Figure 1-6) (Conlon et al., 2002; Knobloch et al., 2004). SigmaB up regulates factors involved in cell adherence and biofilm formation including clumping factor, fibronectin binding protein A (FnbpA) and coagulase, while negatively controlling factors involved in cell dispersal including ß-haemolysin, enterotoxin B, serine protease (SplA), cysteine protease (SplB), metalloprotease (Aur), staphopain and

leukotoxin D (Kullik and Giachino, 1997; Nair et al., 2003; Nicholas et al., 1999). It has been reported that *sigB* activity may be strain specific (Archer et al., 2011).

Figure has been removed due to Copyright restrictions.

Figure 1-6: *agr/sarA/sigB* regulation in *S. aureus*

sarA gene expression down regulates proteases and nuclease. The *sigB* gene down-regulates protease production and induces adherence factor expression. Following an increase in cell density and mature biofilm formation AIPs involved in quorum sensing leads to *agr* gene expression. This subsequently up regulates detergent-like peptide, protease and thermostable nuclease expression leading to biofilm dispersal (seeding dispersal). From Archer *et al.* 2011.

1.1.6 Current staphylococcal biofilm treatment and prevention strategies

1.1.6.1 Biofilm removal and antimicrobial treatment

Biofilm infections are usually treated through surgical removal of the origin (nidus) of infection. Surgical practices include debridement to remove dead and damaged tissue, incision and drainage of the infection site and finally indwelling medical device removal as described earlier (Otto, 2008). These treatments are typically followed by antimicrobial treatment administered intravenously, orally or applied directly to the site of infection through the use of an antibiotic impregnated spacer.

Antimicrobial therapies are important in eliminating and reducing damage caused by infection. The death rate caused by infection will be considerably higher without the intervention of antimicrobial therapies for example antibiotics.

Antimicrobial therapy as a sole means of eliminating infection caused by a biofilm is ineffective due to the antimicrobial resistance properties induced by the biofilm structure and ECM, stopping antimicrobials and host immune components from penetrating encased cells. However, antimicrobial treatment, depending on the resistance status of the causative pathogen, is usually coupled

with the primary route of biofilm treatment, surgical removal of the nidus of infection (Archer et al., 2011; Osmon and Berbari, 2002; Osmon et al., 2012).

Antimicrobials previously employed in the treatment of biofilm infections include: ß-lactam agents, for example Penicillin G and oxacillin; fluoroquinolones and aminoglycosides; glycopeptides, for example vancomycin; and rifampin (Davies, 2003; Fraimow, 2009; Lynch and Abbanat, 2010; Lynch and Robertson, 2008; Nguyen and Graber, 2010). However, as mentioned above, these would be ineffective against biofilms without additional surgical intervention, which is invasive, time-consuming and costly, and could even introduce the risk of further infection. This is therefore not an ideal therapy for the treatment of biofilm infections.

With a view to improving the traditional approach of using an effective antimicrobial to treat an infection, agents that interfere with factors required for biofilm growth have been suggested. For instance, a PIA degrading enzyme called dispersin B has been reported, which may act as an anti-biofilm drug (Kaplan et al., 2003). Research has also highlighted the synergistic effect of compounds when coupled with certain antimicrobials.

One study by Rogers *et al.* (2010), examined the synergistic activity of 2-aminoimidazole-derived compounds, which have been shown to be anti-biofilm agents with biofilm dispersal capabilities. They show that combining these compounds with commonly used antibiotics resulted in a reduction in MICs against biofilms of *P. aeruginosa*, *Acinetobacter baumannii*, *Bordetella bronchiseptica* and *S. aureus*. Furthermore, the addition of such compounds resensitised multidrug-resistant strains of bacteria including MRSA and multidrug-resistant *Acinetobacter baumannii* (Rogers et al., 2010). A second study observed synergistic effects of plant metabolites salvipisone and aethiopinone when coupled with ß-lactam antibiotics against MRSA through changing cell hydrophobicity and permeability (Walencka et al., 2007).

It is clear that the currently used methods of treatment for infections caused by biofilms are not satisfactory. There is a significant lack of available therapies which will penetrate or disperse the biofilm without resorting to mechanical surgical disruption.

1.1.6.2 Biofilm prevention strategies

As in many situations, prevention methods are often the best strategy to lower the risk of infection. Antimicrobials can also be used in a preventative manner as well as other chemical and physical methods of biofilm prevention.

Antimicrobials in biofilm prevention

In many cases of disease, prevention is often the best strategy to lower the risk of infection. A number of products contain antimicrobials for the prevention of bacterial growth including soaps and dentifrices. In high risk situations of infection, for example operating theatres, surgical scrubs and washes containing antimicrobial agents are employed. Compounds including iodine and silver have been employed in bacterial growth prevention strategies (Jansen and Kohnen, 1995; Jansen et al., 1992). In operating theatres it is also worth mentioning that these strategies are also often coupled with additional bacterial contamination prevention strategies including air-flow systems, autoclavable equipment and sterile scrubs. Many antimicrobial agents used in bacterial growth prevention can be used in the prevention of biofilm formation.

An antimicrobial agent that has been more commonly used in the prevention of biofilm infection is triclosan (Irgasan; 5-chloro-2-(2,4-dichlorophenoxy)phenol)). Triclosan is an antibacterial compound that has been applied to topical preparations, including personal and surgical soaps (Bhargava and Leonard, 1996); dental hygiene applications, for example a component of dentifrices (Riley and Lamont, 2013); and is regularly used in the cosmetic industry (Bhargava and Leonard, 1996). Triclosan is a broad spectrum drug effective against a wide range, but not all Gram-positive and Gram-negative bacteria (Russell, 2004; Schweizer, 2001). High triclosan activity has been reported against staphylococci, some streptococci, some mycobacteria, *Escherichia coli* and *Proteus* species (Bhargava and Leonard, 1996; Lilly and Lowbury, 1974; Russell, 2004; Schweizer, 2001). The antimicrobial agent has also been shown to be anti-fungal against some fungi (Bhargava and Leonard, 1996).

The target and mechanism of action (MOA) of triclosan in bacteria has previously been characterised (McMurry et al., 1998a). Previous work using sequencing and

gene knockout approaches, has shown triclosan to block lipid synthesis in *S. aureus* and *E. coli* (Heath and Rock, 2000; Levy et al., 1999; McMurry et al., 1998a). Triclosan activity occurs through inhibiting an NADH-dependent enoyl-acyl carrier protein (ACP) reductase, or FABI (Heath and Rock, 2000; Levy et al., 1999; McMurry et al., 1998a). Further to inhibiting lipid biosynthesis, the antimicrobial agent can employ other toxic and bactericidal effects including potassium ion leakage, and detrimental membrane effects, including damage and destabilizing behaviour, thus highlighting multiple bacteriostatic and bactericidal mechanisms of action (Suller and Russell, 1999, 2000; Villalain et al., 2001).

Furthermore, a number of studies utilising high throughput screening of thousands of small molecules have highlighted multiple compounds which inhibit *S. aureus* biofilm formation (Ma et al., 2012; Opperman et al., 2009; Panmanee et al., 2013; Sambanthamoorthy et al., 2011).

However, mechanisms of action of a majority of these small molecules are still unclear meaning more work is needed to evaluate them (Chen et al., 2013). Some known mechanisms involve the inhibition of gene expression in *S. aureus* altering biofilm formation. These compounds could represent novel-antimicrobials.

Further molecules including Cis-2-decenoic acid produced by *P. aeruginosa* has shown biofilm dispersal effects and inhibitory effects on biofilm development in *S. aureus* (Davies and Marques, 2009). In addition to this d-amino acids have been shown to have inhibitory effects on *S. aureus* biofilm formation (Kolodkin-Gal et al., 2010). Chelators that remove cations including Ca^{2+} and Mg^{2+} that are involved in adherence and biofilm formation may be potential anti biofilm formation compounds (Abraham et al., 2012).

And finally, although undeveloped, untested and controversial due to the diverse nature of biofilms, antisera containing human monoclonal antibodies tested in animal models, has led to the suggestion of possible vaccinations targeting specific biofilm factors for example PIA (Archer et al., 2011).

Anti-biofilm surfaces

It is well known that surface interactions and alterations in surface topography can cause both molecular and phenotypic changes in cells through mechanotransduction (Alenghat and Ingber, 2002; Belas, 2014; Chatterjee and Fisher, 2014).

Biofilm formation has also been found to change depending on the surface bacteria are exposed to (Díaz et al., 2007). Alterations in surface topography of commonly colonised surfaces, for example medical implants, could therefore be proposed as a potential preventative strategy. A study by Díaz *et al.* 2007, shows that biofilm forming bacteria; *Pseudomonas fluorescens* and various streptococcal species, produce different biofilm phenotypes depending on what surface they are grown on (Díaz et al., 2007). The authors conclude from the study that surface composition; including roughness and the nano-topography have a profound effect on initial biofilm growth. They also observe that bacteria change the quantity of extracellular polymeric material (EPM), the biofilm matrix, produced in response to the roughness of the surface (Díaz et al., 2007).

A further study by Komaromy *et al.* (2012), looks at the consequence of cell survival of *S. aureus* and *E. coli* when cultured on a nano-patterned surface (Komaromy et al., 2012). Results confirmed that the surface nano-pattern, bacterial cell size and physiology had an adverse effect on cell survival and adhesion with some pattern topographies causing high cell death to certain bacteria (Komaromy et al., 2012). Nano-patterned surfaces have been successfully applied to a number of cell growth and attachment applications, for example using nano-patterned materials to study the colonisation of oral pathogens on different surfaces and subsequently in demoting dental biofilms (Pelaez-Vargas et al., 2012).

In addition to altering the physical topography of a surface to alter biofilm formation, alternative approaches have been to coat or impregnate medical implants with antimicrobials (Otto, 2008), although these approaches have had little success (Archer et al., 2011). However, it is common clinical practice for surgical cements to be impregnated with antimicrobials, to prevent infection, or for the surgeon to use antimicrobial impregnated spacers, to treat infection (Klemm, 1979).

To conclude, as attachment is a defining characteristic of a biofilm formation and the bacteria require a surface to attach onto, altering surface chemistry and topography to discourage cell adherence is a clear research interest.

1.1.7 Studying biofilms

There are a number of techniques to study biofilm formation *in vitro*. Approaches commonly involve cell culture approaches to allow for biofilm development (Merritt et al., 2005) followed by an exploratory field of science, either at a phenotypic (McLean et al., 2007) or molecular level (Zhang and Powers, 2012).

1.1.7.1 Growing biofilms *in vitro*

Studies in the literature that investigate *S. aureus* show that it can be grown *in vitro* as a biofilm (Smith et al., 2008). Different media can be used for biofilm culture, for example brain heart infusion (BHI) broth, a commonly used nutrient rich medium for bacteria growth (Smith et al., 2008). Through allowing the bacteria to become confluent and colonise a living or inert surface, for example a polymer well base, they naturally form collective colonies subsequently creating a mature biofilm as described above. *S. aureus* are known to stick well to plastic surfaces, a quality that has been fundamental in the study of *in vitro* biofilm formation (Otto, 2008).

Biofilm cultivation approaches can be broadly separated into two types; static and dynamic. Static cultivation involves seeding bacteria culture on a surface that is then maintained in static conditions, for example in a static cell culture incubator. Previously used dynamic cultivation methods can be found in the literature including the use of angulated glass slides in a shaking incubator and the use of flow media systems (Merritt et al., 2005). Flow cell culture media set-ups allow for a culture to be grown in similar conditions as *in vivo* (Merritt et al., 2005). In these systems media flow removes planktonic cells and circulates media in the system, subsequently circulating nutrients. However, problems can persist in, for example; experimental set-up complexity, and difficulties in the multiplexing of samples.

1.1.7.2 Imaging and quantification of biofilm growth

Once a biofilm is suspected to have grown on a surface there are a number of techniques to visualise phenotypic detail and quantify the levels of biofilm formation. Conventional techniques incorporating staining and microscopy approaches have been applied. Stains such as alcian blue, which stains acidic polysaccharides, have been used in the past to identify areas of biofilm formation when coupled with light microscopy (Kolari, 2003; Solano et al., 2002).

Other traditional stains such as crystal violet (CV) can be used to visualise biofilm forming cells when coupled with light microscopy (Christensen et al., 1985; O'Toole, 2011). CV is a non-specific biomass stain that will stain biological material adhered to a surface, such as a biofilm. CV is a cationic dye that binds to the bacterial cell surface and has been suggested to bind to other substances for example expelled DNA located in the biofilm matrix (Moxon et al., 2008). Previous publications have described biofilm quantification methods employing fast staining procedures coupled with stain solubilisation and absorbance measurements (Mowat et al., 2007; Murphy and Kirkham, 2002; O'Toole, 2011; O'Toole and Kolter, 1998; Smith et al., 2008). CV assays have been previously used for antimicrobial screening in biofilms (Frank et al., 2007; Ramage et al., 2001). It has been suggested that biofilm analysis using CV alone is only semi-quantitative (Moxon et al., 2008).This is based on the unspecific staining of CV. For example, CV can stain dead cells, extracellular material and lysed bacteria, which some argue may not constitute a biofilm (Moxon et al., 2008). However, others suggest these components do represent biofilm components and therefore should be included in biofilm quantification (Flemming and Wingender, 2010; Ma et al., 2009).

Fluorescence staining can be used to target specific components of the biofilm, for example allowing the distinction between live and dead cells (Chai et al., 2012; Passerini de Rossi et al., 2007; Tunney et al., 1999). However, fluorescence staining methods can come with associated imaging problems, for example auto-fluorescence and photo-beaching (Lichtman and Conchello, 2005).

To achieve greater magnification, allowing for further in-depth visualisation of a biofilm, electron microscopy (Erlandsen et al., 2004) and atomic force microscopy (Hennig et al., 2007) can be applied.

1.1.7.3 Molecular study of biofilms

Techniques to investigate the molecular make-up of a biofilm at a molecular level have been explored. These include studies at multiple levels of metabolic regulation fitting the central dogma of molecular biology: genomics; transcriptomics; proteomics; and metabolomics. Proteomics and metabolomics are both still relatively in their infancy in terms of potential applications, but greater in-depth detail and understanding of biofilm formation at a molecular level can be obtained with the application of these approaches. Furthermore, little is known about the metabolic requirements of *S. aureus* during biofilm growth (Zhu et al., 2007).

Zhu *et al*. (2007), presented a study showcasing the influence of arginine on PIA synthesis, biofilm formation and pathogenesis. Through using arginine/ornithine antiporter gene (arcD) mutants they inhibit arginine transport and reduce PIA accumulation however mutants continued to produce biofilms. Studies suggested that glucose is catabolized to pyruvate via the lactate dehydrogenase, pyruvate formate-lyase, and butanediol pathways. Additionally, they show that *S. aureus* strains acquired the amino acids: serine; proline; arginine; glutamine; glycine; and threonine from the culture medium (Zhu et al., 2007).

Proteome analysis and transcriptome profiling of the molecular mechanisms of biofilm formation can be explored. Studies by Resch *et al*. (2005 and 2006), carried out such studies in *S. aureus* biofilm and planktonic cells (Resch et al., 2005, 2006). Utilising 2D PAGE gel electrophoresis to identify secreted cell wall-associated and cytoplasmic proteins expressed in *S. aureus* planktonic cells & biofilm and RNA expression profiling, differences in the proteome and the transcriptome were observed. They note that 9 enzymes involved in glycolysis were up regulated in biofilm samples, along with proteins involved in cell attachment, peptidoglycan synthesis, fibrinogen-binding proteins, enzymes involved in pyruvate and formate metabolism and SarA. Down-regulated proteins

included: proteases, immunodominant antigen A (isaA) and staphylococcal secretory antigen A (ssaA) (Resch et al., 2005, 2006).

In addition to proteins, metabolites also play key roles both in biofilm formation and regulation (Gjersing et al., 2007; Zhang and Powers, 2012; Zhu et al., 2007). Changes in metabolism between bacterial growth states may highlight targets for novel treatment and prevention strategies; therefore metabolomics is an increasingly exciting area of biofilm research.

1.2 The application of metabolomics to the study of bacteria and biofilms

1.2.1 Metabolomics

As an -omic technology, metabolomics is still in its infancy compared to proteomics and genomics, however it is fast becoming a fundamental part of molecular biology studies and expanding rapidly with more technologies supporting its analysis (Griffin and Nicholls, 2006; Oldiges et al., 2007). This said, early concepts of metabolomics can be dated back to Ancient Chinese doctors (1500–2000 BC) who used ants that moved towards the direction of sweet tasting urine as a measure of sugar presence in urine, an early diagnostic method for diabetes (van der Greef and Smilde, 2005). Further, the ancient Greeks were reported to have looked at the concept of changes in human tissues and fluids corresponding to various medical conditions. Phenotypes of urine that have metabolic origins for example colours, smells and tastes, often taste-tested by the physician, were used to diagnose certain conditions and were displayed in ‘urine charts’ (Nicholson and Lindon, 2008). Even though these examples are primitive studies, these types of analyses where essentially a form of metabolomics, looking at changes in abundance of molecules, in this instance sugar, within a sample from a system, in this case urine.

It was not until the 1940s and 1950s that Roger Williams made a profile of human metabolites using in excess of 200,000 paper chromatograms (Williams et al. 1951). Throughout history and to the present day, chemical changes within

samples such as urine and blood have been used as diagnostic tools for many diseases.

The term metabolomics was first coined in 1998 (Oliver et al., 1998) although the concept of 'metabolic profiling' can be dated back to the 1970s (Horning and Horning, 1971).

Metabolomics is defined as the measurement of small molecules (Mr<1200) within a given system, providing a 'snap-shot' of metabolism. Metabolites play fundamental roles in the cell, notably energy metabolism and signalling in bacteria and biofilms, as mentioned earlier (van der Werf et al., 2007). Through employing metabolomic approaches, metabolism of a biological system, for example a cell can be studied providing a unique way of detecting and quantifying a large set of molecules simultaneously, thus allowing metabolomics to establish itself as a fundamental science for understanding metabolism and the small molecule component of biological systems.

Metabolomic analysis allows for changes in metabolite abundance to be studied and related to corresponding metabolic pathways (Fiehn, 2002). At the tip of the central dogma of molecular biology (Figure 1-7), proceeding genomics, transcriptomics and proteomics, metabolomics is the closest to the expressed phenotype, as metabolites can be effector molecules, products and cofactors of enzymatic reactions. However, it is a greater aim to integrate genomic, transcriptomic, proteomic and metabolomic data together (Villar et al., 2015).

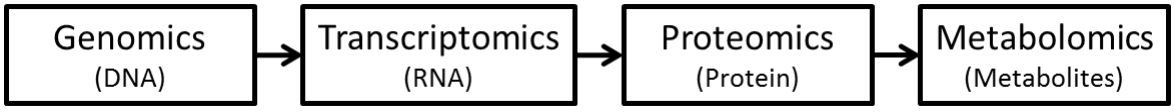

Figure 1-7: The central dogma of molecular biology and related molecules.

Metabolites are directly associated with cell metabolic activity and can be final end products that are responsible for pathogenicity and disease (Fiehn, 2002). Takahashi (2005), highlights a number of specific metabolites related to oral disease which can involve bacteria colonisation and biofilm formation, including: organic acids involved in dental caries; short fatty acids and sulphides involved in periodontal diseases; and sulphides and ammonia involved in halitosis (Takahashi, 2005).

Metabolism can be divided into metabolic pathways, including: glycan biosynthesis and metabolism; nucleotide metabolism; biodegradation of xenobiotics; carbohydrate metabolism; lipid metabolism; energy metabolism; amino acid metabolism; metabolism of cofactors and vitamins; biosynthesis of secondary metabolites.

The study of metabolism is important in the study of *S. aureus* pathogenicity. Changes in metabolism can be responsible for the virulence and pathogenicity of an organism (Liebeke et al., 2011). Metabolism can change in response to growth conditions leading to altered pathogenicity. Metabolites can be cofactors in virulence and induce disease phenotypes (Archer et al., 2011; Bien et al., 2011; Wyatt et al., 2010). For example, the TCA cycle is involved in and is central to the synthesis of capsular polysaccharide, through the supply of phosphoenolpyruvate for gluconeogenesis and the regulation of PIA synthesis, through transcriptional repression of *icaADBC* (Sadykov et al., 2008; Vuong et al., 2005).

It has previously been shown in *S. epidermidis* that environmental stress, such as iron limitation, can lead to TCA cycle stress resulting in an increase in ribose concentration, indicating increased activity in the pentose-phosphate pathway (PPP) (Sadykov et al., 2010).

1.2.2 Untargeted metabolomics

Untargeted metabolomics looks at chemical effects across the network of metabolic processes allowing for in-depth knowledge and greater understanding of the biological responses at a single cell to a complex system/organism level (Nicholson and Lindon, 2008).

Untargeted metabolomics provides qualitative data that can be used to profile the metabolite complement of a system and essentially tells you what small molecules are present. It aims to measure every metabolite present but is biased by the chosen sample preparation methods and equipment capabilities. Untargeted approaches are generally intended to be hypothesis generating and allow for the potential of novel mechanisms in metabolism to be detected in a

sampled system (Alonso et al., 2015; Patti et al., 2012; Tang, 2011; Vincent et al., 2012, 2014).

1.2.3 Targeted metabolomics

Targeted metabolomics is employed to target a specific pathway within a system. Targeted metabolomics can also allow for quantification of metabolites to be carried out whereby labelled metabolites spiked into a sample can be added at varying concentrations and detected, thus allowing the creation of a calibration curve which the detected metabolite can be fitted to and concentration measured (Kiefer et al., 2008; Psychogios et al., 2011; Wu et al., 2005). As of yet there is no global method for metabolite quantification. Targeted metabolomics is usually regarded as hypothesis testing and is often guided by previous investigation, for example an untargeted metabolomics study, highlighting areas of interest in the metabolome. Targeted approaches can be an alternative methodology in biomedical testing were enzyme assays or untargeted metabolomic approaches were traditionally used (Chan et al., 2016; Fiehn, 2002).

1.2.4 Microbial metabolomics

Previous studies have shown the application of metabolomic techniques to bacterial cell metabolism (Liebeke et al., 2012; Tang, 2011). Microbial metabolomic studies have included the examination of: human ecosystems; the gut microbiota; and environmental ecosystems (Tang, 2011). Furthermore, methods published by Liebeke *et al.* (2012); Meyer *et al.* (2010); and Lei *et al.* (2014), have highlighted protocols to study the metabolomes of Gram-positive cells such as *S. aureus* (Lei et al., 2014; Liebeke et al., 2012; Meyer et al., 2010).

In a study by Liebeke *et al.* (2011), the adaption of *S. aureus* metabolism was studied during glucose starvation (Liebeke et al., 2011). Through proteomic and metabolomic approaches a time-resolved examination of *S. aureus* was performed, describing the activity of 500 proteins and 94 metabolites during the transition from exponential growth to glucose starvation. The extracellular and intracellular metabolome was measured. Distinct changes in amino acid

metabolism were noted. Under glucose excess during planktonic cell growth, cells displayed high levels of proteins involved in glycolysis and protein-synthesis. Following this, when stationary phase had started an increase in the TCA cycle and gluconeogenesis activity was noted (Liebeke et al., 2011). These results support other studies showing that up-regulation in TCA cycle activity in response to glucose concentration is a regulating factor of biofilm formation (Mack et al., 1992). These studies highlight the use of metaboliocs to study metabolic shifts in bacterial meatbolism during different growth states and under different conditions.

In a recent study by Aros-Calt *et al.* (2015), metabolomic approaches were utilised to examine the *S. aureus* cell metabolome and provide insight into methicillin resistance mechanisms (Aros-Calt et al., 2015). The intracellular metabolome was extracted and analysed with the study characterising 210 metabolites in *S. aureus*. The study also compares the metabolic profiles of different methicillin resistant and susceptible strains; however, as yet, has not revealed resistance mechanisms but does highlight changes caused by growth rate characteristics of the strains (Aros-Calt et al., 2015). This study highlights method development to study the intracellular metabolome of *S. aureus* and the application of metabolomics to potentially understand and provide further insight into resistance mechanisms. This is important as it has been shown that *S. aureus* can adapt its metabolism to permit growth under antibiotic challenge, subsequently inducing resistance (Nelson et al., 2007).

1.2.5 Biofilm Metabolomics

In addition to planktonic growth, bacteria can grow as biofilms as discussed in section 1.1.4. Biofilm formation can influence and alter the metabolome of bacteria (Gjersing et al., 2007). Studying biofilms is challenging in comparison to other cell cultures due to their unique characteristics as discussed in section 1.1.7. As biofilm growth is initiated through a number of cellular processes in response to environmental stimuli, notable changes in the metabolome of the bacteria can be identified and studied. Previously, metabolomics has been applied to the study of biofilms from multiple species of biofilm forming bacteria (Gjersing et al., 2007; Tang, 2011; Zhang and Powers, 2012). Gjersing *et al.* 2007; Zhang & Powers 2012; and Ammons *et al.* 2014, describe studies in which

nuclear magnetic resonance (NMR) spectroscopy is used to study the changes in metabolism between planktonic cells and biofilms (Ammons et al., 2014; Gjersing et al., 2007; Zhang and Powers, 2012).

In the study by Gjersing *et al*. (2007), metabolite profiles of *Pseudomonas aeruginosa* cells living in either a planktonic state or growing as a biofilm were created (Gjersing et al., 2007). Through analysis of spent media samples (media in which the cells had been cultured in) and bacterial cells, they were able to decipher differences in the metabolomes between the two growth states. They initially found no difference in the metabolome between the spent media samples from the different growth states, but identified distinct differences in the intracellular metabolite composition between the growth states. They further highlight that biofilm metabolites typically displayed a depleted peak intensity compared to planktonic cells, hypothesised to be because cells closer to the substrate will operate at a lower metabolic rate (Gjersing et al., 2007).

A study by Workentine *et al*. (2010), looking at changes between planktonic cells and biofilm samples of *Pseudomonas fluorescens*, shows distinct changes in amino acid metabolism, specifically involving the amino acids: Aspartate; Glutamate; Glycine; Methionine; Phenylalanine; Proline; Trptophan; and Valine. They also highlight changes in acetate, glutathione and pyruvate, thus indicating alterations in exopolysaccharide production, a response to oxidative stress and restricted amino acid metabolism (Workentine et al., 2010).

In a further study, Booth et al. (2011), looked at differences in metabolism between the biofilm forming and planktonic cells of *Pseudomonas fluorescens* in response to metal stress (Booth et al., 2011). They noted distinct variation in metabolite profiles between biofilm and planktonic cells. A number of metabolites that they found to have altered expression rates were involved in exopolysaccharide related metabolism and energy metabolism pathways, for example the tricarboxylic acid (TCA) cycle, glycolysis and amino acid metabolism (Booth et al., 2011).

In addition to examining the differences in metabolome profile of planktonic cells and biofilms, metabolomics has also been utilised to examine the structure and functional characteristics of the biofilm. One such study carried out by Vogt

et al. (2000); employed metabolomic led investigations to study small-molecule diffusion within *Pseudomonas aeruginosa* biofilms (Vogt et al., 2000).

Takahashi *et al*. (2012), describe a metabolomic approach to study and characterise oral associated biofilms (Takahashi et al., 2012). Using MS approaches they analysed the metabolomic profiles of oral biofilms after rinses with different dentifrices containing glucose, fluoride and xylitol *in vivo*. They demonstrate the usefulness of MS approaches to describe metabolic properties of oral biofilms previously unseen, including the function of key carbon metabolism pathways including glycolysis, the pentose-phosphate pathway (PPP), and the TCA cycle. Furthermore, they highlight the effects of different oral rinses on the metabolome of oral biofilms, with changes identified in carbon metabolism between the different rinses (Takahashi et al., 2012).

A further use of metabolomic approaches with respect to biofilms is in understanding biofouling (Beale et al., 2013). Biofouling can occur when microorganisms accumulate on wetted surfaces. An example of this is biofilm formation in water pipes which are understood lead to disease, accelerate corrosion and can taint the water with foul tastes and odours (Beale et al., 2013). A pilot study carried out by Beale *et al*. (2013), evaluates the usefulness of metabolomics to assess microbial activity in biofilms in an urban water pipe network. They were able to detect metabolites associated with microbial activity in the water supply using metabolomics approaches, highlighting a distinction between biofilms and planktonic bacteria. They conclude that metabolomics could provide in-depth analysis of biofilms and microbial activity thus proving analysis of water quality (Beale et al., 2013).

A related application of MS to biofilm metabolomics was highlighted in a review by Zhang & Powers (2012). They describe metabolomic profiling as a way of analysing medical biopsies for diagnosis of infections caused by biofilm formation. An example given by the authors was in diagnosing infection of tympanostomy tubes that may be a result of biofilm formation on the surface of the tube (Zhang and Powers, 2012). Previous methods that would have been used to analyse such samples included: polymerase chain reactions or direct microscopy of biopsy samples. Using MS in this way implicates metabolomic profiling as a possible diagnostic tool (Zhang and Powers, 2012).

Staphylococcal biofilm formation is widely studied but relatively little insight into the changing cell metabolism is provided in the literature. This is partially due to two main reasons; lack of method development to study molecular changes in metabolism and complications that arise from the study of biofilm cultures. Metabolites including: nutrient molecules; signalling molecules; structural components; and amino acids, as discussed in the review above on biofilm formation, have all been shown to change in response to *S. aureus* biofilm formation (Zhang and Powers, 2012).

Studies by Ammons *et al.* (2014), show that through profiling metabolite differences of MRSA and MSSA isolates they are able to discriminate between biofilm and planktonic phenotypes using quantitative NMR (Ammons et al., 2014). They highlight that the cells, independent of strain type, switch to anaerobic metabolism in the biofilm and initiate mixed acid fermentation. Furthermore, they also highlight distinct changes in amino acid metabolism incorporating intracellular pools of arginine, aspartate, glutamine, leucine, and serine and extracellular pools of alanine, asparagine, histidine, isoleucine, methionine, threonine, and tyrosine. They suggest amino acid metabolism in the biofilm is important but the intracellular profile of amino acids is not a determining factor between planktonic growth and biofilms (Ammons et al., 2014). Intracellular amino acids alanine, leucine, isoleucine and histidine function as electron donors while; leucine and sarcosine function as electron acceptors for amino acid fermentation by the Stickland reaction (Nisman, 1954), oxidation and reduction of amino acids (Ammons et al., 2014).

Metabolomic studies have also been used to investigate how *S. epidermidis* and *S. aureus* initiate biofilm formation in response to environmental signals such as those previously mentioned above including nutrient availability, osmolality, and temperature. Studies by Sadykov *et al.* (2008); Sadykov *et al.* (2010); and Zhang *et al.* (2011), highlight the presence of a single changeable signalling pathway centred around the tricarboxylic acid (TCA) cycle in *S. epidermidis* (Sadykov et al., 2008, 2010; Zhang et al., 2011).

In a recent paper by Johnson *et al.* (2015), metabolomics was used to show a link between bacterial biofilms and colon carcinogenesis. Biofilm formation can occur in the colon by the present microbiota (Johnson et al., 2015). They have

previously highlighted that the presence of biofilms is associated with cancer (Dejea et al., 2014). In the metabolomics study, targeted and untargeted metabolomic approaches were performed to examine metabolic changes in colon tissues caused by biofilms. They assessed metabolite origin and metabolite biological role in both the host and in the bacteria. The paper describes the discovery of changes in polyamine metabolism in colon cancers using untargeted metabolomic approaches followed by stratified analysis of tissues with biofilms to those without (Johnson et al., 2015). Acetylated polyamines, including the N^{1}, N^{12}-diacetylspermine molecule, were shown to be up regulated in biofilm cancer tissues and decreased following antibiotic treatment to clear biofilms. This was confirmed with targeted analysis and metabolite spatial specificity studies using *in situ* imaging (Johnson et al., 2015). Finally, they show that N1, N12-Diacetylspermine is potentially acetylated by bacterial enzymes and is a metabolic end product, with both host and bacterial cells contributing to polyamine metabolite up regulation (Johnson et al., 2015). The authors propose that polyamine metabolism in the host and bacteria act synergistically, promoting biofilm formation and creating carcinogenic conditions (Johnson et al., 2015). Changes in host cell metabolism may provide polyamines to stimulate biofilm development with up regulation of polyamine metabolism shown to enhance cancer growth (Soda, 2011).

Such studies highlight the importance of biofilms in not only bacterial infections but in other diseases such as cancer. In addition metabolomics has proved to be a powerful tool in providing molecular insight into biofilms and subsequent disease.

1.2.6 Mechanism-of-action (MOA) studies

Finally, an area of research that has benefited greatly from metabolomics is in drug mechanism-of-action (MOA) and toxicity research (Vincent et al., 2010, 2012, 2014). MOA studies aim to study the effects of chemical compounds/drugs on the metabolism of a system, looking at the metabolic state after a compound has been administered. Through applying metabolomics the effects of drugs, including antimicrobial chemotherapy, on a system can be studied, potentially identifying specific metabolic targets and pathways inhibited by the drug. This type of study can be important for the licencing of drugs as it can allude to a

specific mechanism of the drug, but also allow for side effect predictions to be made by comparing affected pathways in the pathogen system to pathways that may be affected in the host (Terstappen et al., 2007). Furthermore, resistance mechanisms can also be predicted and studied (Almeida Da Silva and Palomino, 2011). Either time kinetics, the effect a drug has on a system over time or concentration kinetics, the effect of changing drug concentration on a system, can be studied, thus providing different insights into the drug MOA.

Metabolomics can be employed in different ways to undertake a MOA study, namely:

- Metabolic fingerprinting of the drug's response on metabolism compared to drugs with known mechanisms of action (Yi et al., 2007).

- Analysis of metabolite abundance changes after drug challenge (Le Roch et al., 2008).

- Metabolic profiling (untargeted metabolomics) of the drug's response on metabolism (Taylor et al., 2010).

In a study by Yi *et al.* (2007), looking at the MOA of berberine on *S. aureus*, metabolic profiling of *S. aureus* treated with berberine and nine other antibacterial substances with known MOA was carried out (Yi et al., 2007). Using principle component analysis the drugs were classified according to their MOA and the possible MOA of berberine was determined (Yi et al., 2007). In a further study metabolic fingerprinting was used to study the effect of antifungals on *Saccharomyces cerevisiae* (Allen et al., 2004). Predicted MOA could be made through comparing the effects of known drugs to the effects seen by the tested ones (Allen et al., 2004). These studies relied on pattern recognition analysis to determine the MOA of the drug meaning novel MOAs could not be established and subtle effects may be missed.

Untargeted metabolomics has been applied to determine the MOA of toxins on daphnid metabolism (Taylor et al., 2010). Through focusing investigations on the toxicants: cadmium; fenvalerate; dinitrophenol; and propranolol, and through

using multivariate models, the Taylor study looks at the effects of these toxins to discover changes to specific pathways (Taylor et al., 2010). They highlighted toxicant-induced metabolic effects which could be seen through analysis of the metabolome, with specific changes identified in fatty acid metabolism, eicosanoid biosynthesis and amino sugar metabolism (Taylor et al., 2010).

In more recent studies by Vincent *et al*. (2010, 2012 and 2014), metabolomic approaches were utilised to look at the MOA of eflornithine and nifurtimox in African trypanosomes, and miltefosine in *Leishmania* species (Vincent et al., 2010, 2012, 2014). In the most recent Vincent study, an untargeted metabolomics approach was utilised to determine metabolic changes involved in miltefosine action. Looking at MOA over time, they note significant changes in the metabolome at different time points. At 3.75 h they identified changes relating to reactive oxygen species production, DNA damage, thiols and polyamines. While at 5 h they identified metabolite depletion indicating the cells membrane has been compromised (Vincent et al., 2014). This type of study highlights the potential for untargeted metabolomics to be employed in MOA studies. Since this type of study is not reliant on previous knowledge of the compound it can provide an unbiased view of the metabolic effect a compound induces.

In biofilm research, a MOA study was carried out by Takahashi & Washio (2011), looking at the effects of Xylitol and Fluoride on plaque biofilm *in vivo* (Takahashi and Washio, 2011). Fluoride and xylitol have been widely used as a tooth-decay preventative based on inhibitory effects relating to bacterial acid production. Using a MS approach Takahashi & Washio (2011) showed that fluoride inhibited lactate production along with an increase in 3-phosphoglycerate and a decrease in phosphoenolpyruvate in the Embden–Meyerhof–Parnas (glycolysis) pathway in oral biofilms confirming that fluoride inhibited bacterial enolase and repressed acid production *in vivo* (Takahashi and Washio, 2011). On the other hand, xylitol had no effect on acid production or on the biofilm metabolome suggesting an alternative MOA possibly acting as a non-fermentative sugar alcohol (Takahashi and Washio, 2011).

These studies highlight the potential use of metabolomics to derive the MOA of drugs. However, due to the number of compounds available and the number of

organisms and systems to be tested there isn't metabolic knowledge of all drugs on every system. In addition, time kinetics, looking at how a compound alters metabolism over a given time, or concentration kinetics, looking at how varying concentrations of a compound can alter metabolism, can be studied.

Studying the MOA is crucial to the understanding of the effectiveness, resistance mechanisms and potential side effects associated with the drugs (Iorio et al., 2010; Terstappen et al., 2007). There is a void in the number of studies looking at the MOA of commonly used antimicrobial compounds.

The increasing numbers of studies incorporating an aspect of metabolomics research have coined a large subset of terminology (Dunn, 2008), some of these terms are listed in (Table 1-1).

Table 1-1: A glossary of terminology related to metabolomic investigations.

Term	Description	References
Metabolomics	Study of the metabolome	(Dunn, 2008)
Metabonomics	Quantitative analysis of metabolism in response to pathophysiological stimuli or genetic modification	(Dunn, 2008)
Fingerprinting	A metabolome snap-shot of the intracellular metabolome.	(Dunn, 2008)
Secretome analysis (footprinting)	Environment sampling of the extracellular metabolome surrounding of an organism, for example spent media.	(Dunn, 2008)
Profiling	Untargeted analysis. An attempt at global analysis of the metabolome. Aiming to detect as many metabolites as possible. Often used to compare two test conditions for example treated vs. non-treated. Can by hypothesis generating.	(Dunn, 2008; Kell and Oliver, 2004)
Flux analysis (fluxomics)	The rate at which a molecule is metabolised in a metabolic pathway. Typically using stable isotope or radio-isotope labelling of metabolites. An example of this is using carbon-13 labelled glucose, in which the standard carbon-12s of glucose have been substituted for carbon-13. Other stable isotope incorporated metabolites can also be used, for example labelled with	(Fan et al., 2009; Olszewski et al., 2010)

	nitrogen-15, a stable isotope of nitrogen.	
Targeted analysis	Targeted analysis (identification and quantitation) of a specific pathway or subset of metabolites.	(Kiefer et al., 2008; Psychogios et al., 2011; Wu et al., 2005)
Choke points	Critical enzymatic points in metabolic pathways with no alternative route.	(Rahman and Schomburg, 2006)
Biomarker discovery	Detection of metabolite markers (biomarkers) of disease or toxicity. May lead to novel diagnostic tests. May involve the comparison of disease vs. healthy. Metabolite biomarkers that distinguish between biofilm and planktonic phenotypes, providing noninvasive diagnostics for detecting biofilm growth have been a research interest.	(Ammons, 2010; Mamas et al., 2011; Secor et al., 2012)

To summarise, metabolomic approaches can be used to carry out in-depth analysis of microbial metabolism. Studies of the changing metabolic phenotypes of different growth states of bacteria, including biofilms, can lead to the understanding of pathogenicity, virulence and possible anti-microbial resistance mechanisms. Metabolic pathways and metabolites represent possible anti-microbial targets and changes identified between growth states could highlight novel drug targets against bacterial cells and biofilms. For example, bacterial cells are known to produce D-amino acids in stationary phase and in biofilms. It has been reported that D-amino acids inhibit biofilm formation and can trigger biofilm disassembly in *S. aureus* and *Pseudomonas aeruginosa* (Hochbaum et al., 2011; Kolodkin-Gal et al., 2010). This finding, however, was not found to be conclusive (Sarkar and Pires, 2015), but illustrates that metabolites may have modulatory effects and more research into small molecule interactions is required.

Furthermore, metabolomic studies can be employed in MOA studies looking at the effects of compounds on biological systems. These studies can lead drug validation and insight into potential host side-effects.

1.2.7 Metabolomic methods

Metabolomics can be carried out using a number of techniques and technologies. A commonly used technique for the detection of metabolites is MS. MS measures the mass to charge ratio of metabolites allowing for the identification of a metabolite through analysis of the mass-spectra produced. Further techniques developed by M.G. Horning established ways to quantify metabolites, looking at fluctuations of peaks of metabolites over time (Horning and Horning, 1971). Raman spectroscopy detects vibrations or rotations in metabolites as they are excited by a laser, but does not provide a large coverage of the metabolome like MS approaches. In the 1980s Jeremy Nicholson created the commonly used technique of NMR. NMR is used frequently for targeted analyses as it is much more facile to quantify metabolites using a single internal standard, requires minimal separation, is non-destructive and is very reproducible (Beckonert et al., 2007). However, it is far less sensitive than MS (Zhang and Powers, 2012).

Since the 1980's approaches employing highly accurate and reproducible MS technologies, for example the Orbitrap MS, have been applied to metabolomics, providing greater sensitivity in creating metabolomic profiles of present metabolites in a given system (Hu et al., 2005; Makarov et al., 2006).

A number of separation techniques typically utilising gas chromatography, high pressure liquid chromatography or capillary electrophoresis have been coupled with accurate MS allowing for the characterisation of a wide range of metabolites present in the metabolome (Blow, 2008; Fiehn, 2002; Horning and Horning, 1971; Kell, 2004; Kiefer et al., 2008; Wilson et al., 2005).

Current and developing metabolomic approaches can be used for resolving the complex metabolome of bacterial cells (Dunn, 2008; Tang, 2011). Initially metabolite extraction has to be performed to extract the metabolome to be analysed and deplete it from other macromolecules such as proteins (t'Kindt et al., 2010). One metabolomics study approach is outlined in Figure 1-8, depicting the stages carried out in such a study.

Figure 1-8: Metabolomics study pipeline from sample collection to data interpretation.

1.2.7.1 Sample collection and metabolome extraction for metabolomics

Initial experimental design starts with a hypothesis to be tested. This will lead to the type of metabolomics experiment to be designed, for example whether an un-targeted or targeted approach is required. After hypothesis creation and experimental design, samples can be collected and extracted. An example pipeline of this process is depicted in Figure 1-9.

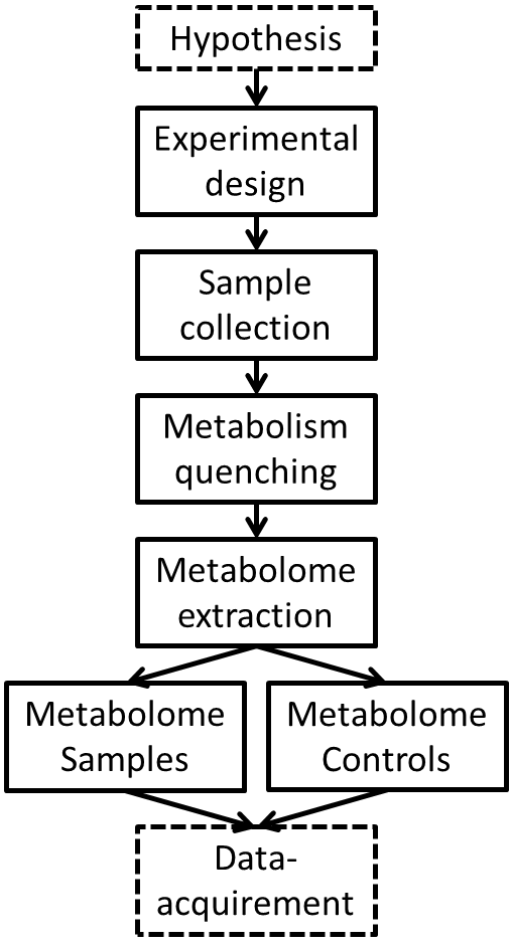

Figure 1-9: An example pipeline of sample collection and metabolome extraction for a metabolomics experiment.

Typically, samples have to be quenched to slow or stop metabolism (enzymatic reactions) and then washed to remove contaminants, from for example media. A number of quenching methods can be applied for example: hot or cold solvent quenching, such as ice cold methanol; or frozen steel beads (Theobald et al., 1997), used to increase the speed of heat transfer to quench the sample more rapidly (Bolten et al., 2007; Faijes et al., 2007; Mashego et al., 2003).

Quenching is important because the sample to be analysed needs to be a true reflection of the metabolic phenotype to be studied (Faijes et al., 2007). Intracellular metabolite turnover can occur rapidly, potentially skewing results (Faijes et al., 2007). Also, inadequate quenching may induce a biological stress response, altering results and not truly reflecting tested conditions.

Metabolome extraction can then be carried out to remove the metabolome in a suitable solvent for down-stream analysis. Different protocols have been used to

extract the metabolome involving different solvent mixtures and altering temperature depending on the sample type and metabolites of interest to be detected (Danielsson et al., 2010; Darghouth et al., 2010; Kim and Verpoorte, 2010; Masson et al., 2010; Saunders et al., 2010; Shin et al., 2010; t'Kindt et al., 2010).

Shin *et al.* (2010), report the testing of multiple extraction solvents and mixes metabolite extraction from *Saccharophagus degradans* (Gram-negative bacteria), including methanol, acetonitrile, isopropanol, water and a combination of said solvents (Shin et al., 2010). They concluded that combinations of solvents performed well but different mixes favoured different sets of metabolites (Shin et al., 2010). Further to this, t'Kindt *et al.* (2010), show a reproducible metabolome extraction method using cold chloroform/methanol/water in a ratio of 1:3:1 which provides comprehensive metabolite extraction (t'Kindt et al., 2010). Care needs to be taken when deciding on extraction method to use. Extraction method and solvent used can introduce sample bias favouring some metabolites better than others.

In samples such as bacterial cells, where the internal cellular metabolome is to be tested, a lysis method may have to be employed. In some cells, for example Gram-negative bacteria, this can happen through osmotic pressure and solvent degradation but in others for example Gram-positive cells that have a dense peptidoglycan cell wall and possibly a capsule (Figure 1-1), a more vigorous and possibly mechanical method of disrupting the cell has to be employed (Maharjan and Ferenci, 2003). Metabolome extraction methods for Gram-positive cells can be found in the literature employing different cell disruption approaches, including: filtration (Liebeke et al., 2012; Meyer et al., 2010; Soga et al., 2002, 2003), sonication (Takahashi et al., 2010), and bead-beating (Liebeke et al., 2012). However, many of these are unsuitable and incompatible with metabolome extraction from biofilms.

If quenching and extraction methods are inadequate the metabolic phenotype can change and a stress response can be expressed skewing results. A number of methods currently presented in the literature can lead to problems with: metabolite degradation or inadequate quenching of metabolism during

extraction; media contamination; or failure to lyse the bacterial cell (Bolten et al., 2007; de Koning and van Dam, 1992).

1.2.7.2 Data acquisition

Data acquisition is achieved through employing analytical chemistry approaches for the detection of metabolites for example MS. One approach is outlined in Figure 1-10.

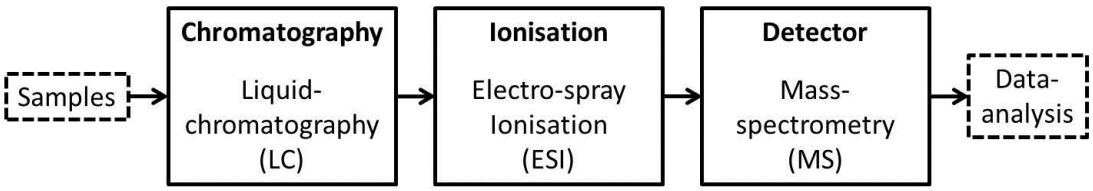

Figure 1-10: An example of a data acquirement approach for the detection of metabolites

Liquid-Chromatography (LC)

Liquid-chromatography (LC) is a method for separating analytes in solution and is arguably the most important part of a liquid chromatography-mass spectrometry (LC-MS) system. It is a useful tool for reducing complexity in complex samples for example cell or biofilm extracts (Cubbon et al., 2010; Kiefer et al., 2008). Through utilising LC, molecules of the same mass can be separated allowing for more accurate annotation. In addition, initial separation can reduce ion suppression and matrix effects, reducing chemical interactions within samples (Cubbon et al., 2010). An LC system typically consists of a pump which drives solvent and injected sample into a separation column. The column then separates the analytes which are then directed to a detector, in this case a MS (Figure 1-11).

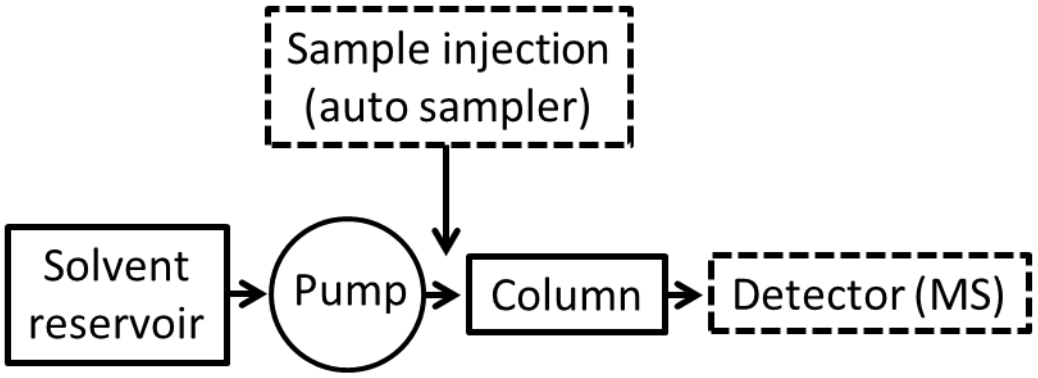

Figure 1-11: Schematic of a liquid-chromatography (LC) system.

Column selection is made depending on the physicochemical properties of the compounds to be separated (Figure 1-12). Figure 1-12 illustrates a flowchart of compound physicochemical properties and the LC column choices most suited to their respective separation.

Figure has been removed due to Copyright restrictions.

Figure 1-12: Liquid chromatography column selection guide.
(Adapted from http://chromtracker.com/hplc-columns_column-selection-guide/, site accessed 05/04/16)

A liquid ‘mobile phase’ is passed through a column packed with a functional material, the ‘stationary phase’. Chromatography employing small stationary phase particles and a high pressure is termed high performance liquid chromatography (HPLC). Metabolites are eluted from the column using gradient elution of the mobile phase. HPLC resolution in terms of separation can be severely limited, for example isomers with similar structures may be poorly separated.

Normal and reverse phase are two different commonly used separation approaches. Normal phase has a more polar stationary phase than the mobile phase while reverse phase has a less polar stationary phase than the mobile phase. Retention time (R_t) of a compound decreases with increasing polarity in reverse phase separation.

Through altering the polar gradient of the mobile phase elution of metabolites from the column can be staggered. Isocratic separation, were the mobile phase remains constant, can be applied for some separation approaches, however more often a gradient chromatography has to be applied for the elution of all molecules in a time period while retaining peak resolution. A gradient changes the ratio of polar to non-polar mobile phase. Eluent starting out with polar solvents changing gradually to non-polar is termed a reverse phase gradient. Gradient elution is applied when samples potentially contain compounds of multiple polarities allowing best available separation of peaks. Reversed-phase LC is commonly used for lipophilic compounds, however, polar compounds are not retained on these columns so are not separated. Hydrophilic interaction liquid chromatography (HILIC) incorporates hydrophilic stationary phases with reversed-phase eluents. A type of column that can be used is a ZIC-pHILIC column, these use a polymer bead as the packing material with a zwitterionic functional group bonded to the polymer (Figure 1-13). The stationary phase active site can be altered depending on the separation required for example the most commonly used reverse-phase columns have an octadecyl carbon chain (C18) functional group. HILIC is frequently used for separating complex mixes of compounds as they can separate both polar and non-polar metabolites (Cubbon et al., 2010). Other columns preferred for the separation of different compounds include reverse phase, and chiral columns.

A limiting factor of liquid chromatography is the high level of contaminant molecules in the metabolome extract, including high salt and protein concentrations (Theobald et al., 1997).

Figure has been removed due to Copyright restrictions.

Figure 1-13: Functional group of a zwitterionic, polymer, hydrophilic interaction liquid chromatography (zic-pHILIC) column.
Sulfoalkylbetaine zwitterionic bonded stationary phase (Image from Cubbon et al. (2010))

Ionisation and mass spectrometry (MS)

After separation of a complex mixture of analytes by LC, mass spectrometry (MS) can then be used to determine the mass of the molecules in the LC-separated fractions. First, the analytes must be ionised. There are many different methods of ionisation used in MS with electrospray ionisation (ESI) being the most commonly used method in LC-MS. ESI can operate in either positive or negative polarity. Being able to operate in two polarities means more molecules with different physicochemical properties can be detected. For example acidic compounds such as phosphates are more stable when deprotonated so will be detected in negative mode while molecules such as amines are more stable in a protonated state so will be detected in positive mode (Watson, 2010). ESI uses high voltage applied to solvent pumped through a narrow-bore needle (the source), which results in the production of mostly protonated or deprotonated charged species (Figure 1-14) (Careri and Mangia, 2011). Charged solvent droplets can then leave the needle through evaporation of the solvent which subsequently increases the charge density (Figure 1-14). Eventually surface tension is overcome and electrostatic repulsion between ions takes effect transferring ions to a gas phase through which they enter the mass spectrometer (Figure 1-14). ESI is a relatively low energy form of ionisation, so that the molecular ion is commonly observable. However, the creation of multi-charged ions can occur and some labile molecules can still undergo fragmentation in source (Careri and Mangia, 2011).

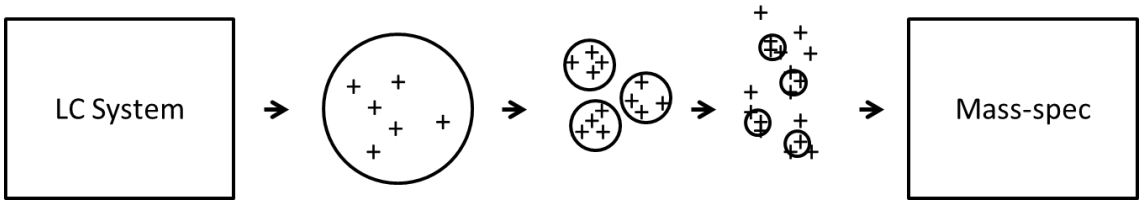

Figure 1-14: A schematic of electrospray ionisation (ESI).

After ionisation, mass-analysers coupled with a detection system detect charged species and distinguish ions according to their mass to charge ratio. Mass-spectrometry tells you the masses of the components of a mixture of chemicals. With accurate mass spectrometers you can obtain an estimate of the empirical chemical formula by looking at the mass defect of each element. This allows you to, in many cases, narrow down the number of possible molecules detected to a handful, or even one in some cases. MS alone cannot distinguish between molecules of the same molecular weight, for example fructose and glucose by one full scan mass spectrum (MS^1). However, when coupled with the ability to separate molecules based on their physicochemical properties using chromatography, it is possible to exploit the mass and chromatography data to further annotate detected molecules. Identification (according to the Metabolomics Standards Initiative (MSI) (MSI Board Members, 2007)) can be achieved by measuring accurate mass and R_t data compared to standards (Sumner et al., 2014). Furthermore, a way to increase the confidence achieved is to carry out fragmentation, were a molecule is broken up, providing information on the molecule's structure.

Different mass-analysers can be used but vary in resolution and mass-accuracy. Different mass-analysers include: Fourier transform ion cyclotron resonance (FT-ICR) spectroscopy, which measures ion oscillations in a magnetic field; Quadrupole, which filters ions based on mass and charge; Orbitrap mass analysers, which measures how ions travel laterally across a central electropole in orbit creating oscillations in current; and Time of flight (TOF) spectroscopy, which measures the time taken for an ion to travel a defined distance (Dunn, 2008).

In this project an Orbitrap mass spectrometer was utilised (Figure 1-15). Developed by Alexander Makarov, the Orbitrap instrument is a hybrid mass spectrometer comprising of a linear ion trap and an Orbitrap mass analyser (Figure 1-15) (Makarov et al., 2006). Through the use of a C-trap (trapping quadrupole) ions are injected into a changing electric field in the Orbitrap (Figure 1-15). Ions with high kinetic energies are trapped in the Orbitrap and orbit a central electrode. Ions are then detected when they pass the outer Orbitrap electrodes once a stable electrostatic field is established. Fourier transformation is performed allowing for mass detection (Makarov et al., 2006). The Orbitrap mass spectrometer achieves ultra-high mass accuracy reported to be within 0.21, 2 or 5 parts per million (ppm), depending on the mass calibration approach used; internal with internal background ions (Scheltema et al., 2008), internal, or external respectively (Makarov et al., 2006). Makarov *et al*. (2006) report the resolving power to be over 100, 000 fwhm (full width at half maximum) permitting up to three spectra per second to be produced (Makarov et al., 2006).

The instrument used for mass detection has a detectable mass range meaning some molecules will not be detected, for example small molecules that are under the standard cut-off of 70 amu. Further limitations of ionisation and MS analysis can include: compounds that do not ionise easily or ion suppression. Ion suppression can occur when molecules that are ionised easily inhibit the ionisation of other molecules. Furthermore, compounds may be undetected because they are below a detectable concentration range or are unstable in the sample.

Figure has been removed due to Copyright restrictions.

Figure 1-15: A diagram of an Orbitrap mass spectrometer.
Separated samples from a chromatography system are ionised and are filtered and guided by the transfer multipole to the C-trap where they are then passed into the Orbitrap mass analyser. Mass to charge ratios are calculated and recorded with the retention time (R_t) from the chromatography system, allowing for metabolite identification. (Image adapted from www.planetorbitrap.com, Thermo Scientific, 2015, site accessed Nov 2015)

1.2.7.3 Data analysis (bioinformatics) and data interpretation

Once raw data (MS data output) has been generated it has to be processed, filtered, annotated and interpreted, usually with the incorporation of multi-variate analysis and statistics (Figure 1-16) (Roessner and Bowne, 2009; Scheltema et al., 2011).

Figure has been removed due to Copyright restrictions.

Figure 1-16: An example metabolomics mass spectrometry data analysis pipeline used at Glasgow Polyomics
Includes utilised software for each stage (From personal communication with Yoann Gloaguen (2015) and (Scheltema et al., 2011))

Peak assignment and metabolite annotation

Initial analysis will normally involve the conversion of raw data from an instrument manufacturer-specific file format into a standard input file format; this can aid the processing and subsequent analysis of data. Analysis then involves the detection and selection of features based on abundance, peak shape and R_t across replicates, thus permitting mass identification and comparison between samples (Smith et al., 2006). Computer software can detect, combine, and filter features according to a number of factors such as their relative standard deviation (rsd) and related peaks. The features are then combined into one data set, taking into account compound chemistry, for example isomer production (Scheltema et al., 2011). Further analysis can then be performed to incorporate mass chromatogram extraction, noise filtering, and normalisation, thus lowering the false detection rate (FDR) (Scheltema et al., 2011).

Statistical analysis enables confidence intervals and fold-changes to be calculated. Batch correction and sample normalisation can also be employed to increase data analysis robustness. R_t prediction algorithms can also aid the annotation of metabolites that are not matched to an internal standard.

Any machine drift across the sample batch can be taken into account by the inclusion of ‘burn-in’ samples, to stabilise and condition the instrument, and the inclusion of pooled samples containing an aliquot of each individual sample.

These pooled samples are run multiple times throughout the batch which then allows for batch correction algorithms to be incorporated into the data analysis pipeline to account for machine drift across the run (Dunn, 2008).

After data processing metabolite identifications and annotations can be made. Compound databases such as: the Human Metabolome Database (HMDB) (Wishart et al., 2007, 2009, 2013); Lipid Maps (Byrnes et al., 2009; Cotter et al., 2006; Fahy et al., 2007, 2009; Sud et al., 2007); Kyoto Encyclopedia of Genes and Genomes (KEGG) (Kanehisa and Goto, 2000); PubChem (Kim et al., 2016); ChemSpider (Pence and Williams, 2010); MassBank (Horai et al., 2010); and Metlin (Smith et al., 2005) assist in the annotation and identification of metabolites.

Pathway analysis

Metabolites don't exist as singular entities in a biological system but form pathways which can subsequently make up complex metabolic networks. Metabolic pathways typically follow a generalised branched format existing as linear or cyclic systems. Pathways can also incorporate feedback loops. Simply put, enzymes can act on metabolites changing them into another structure possibly with the release of by-products. Analysis of metabolites in pathways also allows for multiple –omic data sets to be incorporated into one, for example proteomic data used to determine enzymes present in metabolic pathways. Databases such as KEGG are useful for the incorporation of identified metabolites into their corresponding pathways.

Data analysis caveats

False positives (false metabolite associations) and false negatives (discarding true associations) are a problem in metabolomic data analysis (Alonso et al., 2015). These can lead to misidentification and incorrect biological interpretation. This can be reduced by having stringent parameters in data analysis. However, too stringent parameters can lead to the loss of features and subsequent data.

Further issues with data analysis can arise from the data acquirement stage as mentioned above. These can include in-source fragmentation and multi-charged

species creating multiple peaks from one metabolite (Careri and Mangia, 2011). Isomers, isotopes and adducts can also lead to problems with analysis and subsequent identification and annotation. In addition, poor data reduction, the conversion of raw data to interpretable biological information, in metabolomic data analysis can lead to an increase in false positives and poor biological interpretation.

Finally, it is noteworthy to comment on the availability of metabolite data repositories. There are a lack of such repositories compared to the numbers available for genomic and proteomic studies. A move to create curated central databases have been made with the release of such repositories as MetaboLights (Haug et al., 2012), but there is a greater need to increase their use and increase the amount and quality of data sharing in the field.

1.3 Aims

Biofilm formation can lead to persistent infections that are hard to treat and can exacerbate antibiotic resistance (Ramage et al., 2003; Soto, 2013; Stewart and Costerton, 2001). Staphylococcal infections are a particular medical concern as they are known to commonly involve biofilm formation. Metabolomics presents a novel way to study the biofilm phenotype allowing for an in-depth analysis of metabolism. It is clear from early metabolomic studies that the metabolism of bacteria changes during biofilm formation compared to their planktonic counterparts (Ammons et al., 2014; Gjersing et al., 2007; Sadykov et al., 2010; Zhang and Powers, 2012). Techniques to study *S. aureus* biofilm metabolism at a molecular level are needed to understand the formation and growth of the cells and biofilm. Techniques such as LC-MS can be applied to resolve the complex metabolome of the clinically important organism *S. aureus*. Metabolomic studies may be used to identify drug targets in biofilm metabolism that could be targeted to induce dispersal. Such studies will also allow for the effects, toxicities and MOAs of antimicrobial agents on the biofilm and biofilm forming cells to be analysed.

The overall aim of this research project is to provide greater understanding of orthopaedic infection caused by *S. aureus* and biofilm formation on the implant surface.

1. We aim to carry out microbiome analysis of orthopaedic infections and further study *S. aureus* biofilm cultivation of a clinical isolate.

2. Develop metabolome extraction techniques for staphylococcal planktonic cells and biofilms to study differences in metabolism between bacterial growth states, and look for novel therapeutic targets.

3. Use metabolomic approaches to look at the MOA of triclosan in *S. aureus* planktonic cells and biofilms.

The number of orthopaedic infections and the lack of knowledge regarding biofilm involvement leads us to hypothesise that studies presented here will provide further insight and knowledge into orthopaedic infections caused by

biofilm formation on the implant surface. We further hypothesise that S. *aureus* is primarily responsible for these infections and metabolomic approaches can be used to study S. *aureus* biofilms and find significant metabolic differences between different bacterial growth states and in response to antimicrobial challenge.

Chapter 2 Microbiome analysis, isolate characterisation and biofilm cultivation

Sections of this chapter have been submitted for publication (Appendix I)

2.1 Introduction

Orthopaedic infection is an area of medical research in which the analysis of biofilms and subsequent infections has become a focus (Dempsey et al., 2007; Esteban et al., 2010; National Health Service (NHS), 2014; Zimmerli et al., 2004). Biofilm formation has been associated with antimicrobial resistance and an altered pathogenicity (Drenkard and Ausubel, 2002; Ramage et al., 2003). There are a number of microbial species that have been described as the causative pathogens of orthopaedic infection (Bereza et al., 2013; Dempsey et al., 2007; Osmon et al., 2012; Ramage et al., 2003; Tunney et al., 1998, 1999); however, species belonging to the *Staphylococcus* genus have been detected the most and are predicted to be the greatest causative species of orthopaedic infection (Dempsey et al., 2007; Esteban et al., 2010; Montanaro et al., 2011; Zimmerli et al., 2004).

Orthopaedic infections are generally diagnosed through imaging and subsequent biopsies and/or swabs of associated tissue (Bauer et al., 2006; Del Pozo and Patel, 2009). The causative species are typically identified based on the culture of the micro-organisms obtained from the site. It is often the case that hospitals empirically prescribe broad spectrum antibiotics, such as cephalosporins, vancomycin, aminoglycosides, and carbapenems to treat infection or for surgical prophylaxis (Fraimow, 2009; McMillan et al., 2011; Tunney et al., 1998). Antibiotic-impregnated cement or spacers are also used to reduce infection (Zimmerli et al., 2004). There are a number of risks associated with using broad-spectrum antibiotics compared to narrow spectrum antibiotics that are designed to target a specific type of bacteria. Broad-spectrum antibiotics are nonspecific leading to the depletion of organisms that are part of the normal micro flora, allowing for an increase in drug resistant organisms to flourish and secondary infections to develop (Giuliano et al., 1987; Wynne et al., 2004). However, a number of studies have highlighted that orthopaedic infections can be polymicrobial, existing as a multi-species community (Bereza et al., 2013; Gomez et al., 2012; Makaritsis et al., 2009; Moran et al., 2007); supporting the use of broad-spectrum antibiotics. These conflicting views demonstrate the need for better diagnosis and understanding of polymicrobial infections, which will allow for improved use of antibiotics targeting specific groups of species present.

A bacterial population with two or more bacterial species present, occupying a defined habitat, has been termed a microbiome, defined as a microbial community (Whipps et al., 1988). A polymicrobial infection of the prosthetic joint has been referred to as a microbiome (Hartley and Harris, 2014). Microbiome studies, looking at the presence of multiple bacterial species living in one location have been carried out (Feehery et al., 2013; Hartley and Harris, 2014; Liu et al., 2012; Tang, 2011; Ventura et al., 2009). Microbiome communities have been associated with disease and inflammation, including oral infections (Liu et al., 2012) and conditions such as atherosclerosis (Koren et al., 2011).

Early work on the infected prosthesis microbiome focused on culturable organisms, using samples taken through swabbing the implant (Atkins et al., 1998; Moran et al., 2007; Tunney et al., 1998). These techniques do not represent the whole microbiome as results are biased towards laboratory conditions, for example the use of specific culture media which may be selective, deficient in some nutrients, and anaerobic culture requirements. Many micro-organisms have different growth conditions, including differing culture temperatures and oxygen requirements. Some organisms require exogenous growth factors for example *Haemophilus* species which require nicotinamide adenine dinucleotide (NAD) and haemin (Rao et al., 1999). Furthermore, some microorganisms are strongly adherent and embedded in a biofilm *in vivo* on the implant surface (Arciola et al., 2006; Costerton et al., 1999; Esteban et al., 2010; Ramage et al., 2003), making detachment and isolation more challenging.

Therefore, complete evaluation of present microorganisms is challenging via conventional culture practices. In recent studies a move towards genomic methods has been favoured for microbiome analyses, which do not rely on being able to culture the organisms. Genomic DNA studies have allowed analysis of microbiome species identification, abundance, and functional characteristics to be carried out (Kinross et al., 2011; The NIH HMP Working Group et al., 2009).

Previous studies looking at the microbiome of infected hip prostheses have employed 16S rRNA amplicon sequencing methods, which aim to identify the specific 16S rRNA gene (Bereza et al., 2013; Dempsey et al., 2007; Gomez et al., 2012; Tunney et al., 1999). The 16S rRNA region is a component of the 30S small

subunit of prokaryote ribosomes which has highly conserved regions flanking variable regions. Through utilising polymerase chain reaction (PCR) employing universal 16S rRNA primers annealing to the conserved regions, elongation and subsequent amplification of the flanked variable regions can be achieved. Amplified variable regions can then be matched to a database library containing known bacterial 16S rRNA genes. This approach allows for microbiome species to be detected independent of culturable ability and abundance level (Dempsey et al., 2007; Shah et al., 2011; Tunney et al., 1999).

However, this approach lacks the ability to look at virulence factors, and if using PCR, introduce amplification bias due to the use of specific primers, meaning only certain variable regions of the genome are targeted. Additionally, it has been reported that PCR based assays cannot be used to determine antimicrobial susceptibly status of a detected microorganism nor identify individual pathogens of a mixed infection (Zimmerli et al., 2004). Panousis *et al.* (2005) and (2006), report that broad-range PCR exhibits a poor predictive value for the detection of orthopaedic infections (Panousis et al., 2005, 2006). They conclude that PCR based methods are sensitive in the detection for diagnosis of infection but have poor specificity due the occurrence of false positives, potentially due to contamination, and positive results in non-infected cases, potentially due to over sensitivity of the method (Panousis et al., 2005, 2006).

There are also caveats to removal of material from the implant and DNA extraction. These can include external bacterial contamination during the prosthesis removal and DNA extraction protocol, host tissue contamination masking bacterial DNA, and inappropriate cell lysis for DNA extraction, often involving an enzymatic reaction (Feehery et al., 2013).

Commercial kits have been developed for efficient cell lysis and extraction of DNA from bacterial cells, also kits are available to separate microbial DNA from the contaminating host DNA thus enriching microbial DNA and improving sequencing efficiency (Feehery et al., 2013).

Further to microbiome analysis, clinical isolates taken from clinically relevant infections, as in orthopaedic infection cases, through biopsies or swabbing, can also be sequenced to allow for strain identification and in-depth gene analysis.

Whole genome sequencing can provide answers and insights into pathogenicity, for example the presence of genes encoding pathogenicity islands and genes known to be involved in biofilm formation and production. As well as sequencing, individual clinical isolated species can be cultured in the laboratory and used for *in vitro* testing.

2.2 Aims

The Aims of this project were to:

1. Carry out a preliminary microbiome study of infected hip prostheses to investigate what species of bacteria cause infection.

2. Characterise a clinical isolate of *S. aureus*.

3. Optimise bacterial cell and biofilm cultivation methods and test a clinical isolate of *S. aureus* for biofilm formation capabilities.

We aim to improve microbiome analysis of the infected hip prosthesis and to provide further evidence of what species cause infection using metagenome sequencing. Whole genome shotgun sequencing (WGS) has previously been utilised to study microbial populations (Diaz et al., 2012). This coupled with new sample preparation methods to eliminate host DNA contamination can improve microbiome analysis through providing greater coverage of indwelling bacteria and polymicrobial infections. Using a microbial DNA sample enrichment method and WGS DNA sequencing, we carried out a genomic study of the infected hip prosthesis microbiome. Such experiments will allow for species, strain, and pathogenicity genomic analysis to be undertaken. This microbiome study may also support the finding that staphylococcal species are a primary cause of infection. We hypothesise that metagenome sequencing will provide identification of the bacteria present in an orthopaedic prosthesis polymicrobial infection. We further hypothesise that the methods presented here will provide a metagenome study approach to study other cases of infected hip prostheses.

Secondly, we aim to characterise a clinical isolate of *S. aureus* taken from an orthopaedic infection case, and test its *in vitro* biofilm forming capabilities. *S. aureus* was selected as an organism to study so that specific capabilities of a single bacterium known to be involved in orthopaedic infections could be analysed. We hypothesise that the characterised clinical isolate of *S. aureus* studied here produces biofilms *in vitro* allowing for future orthopaedic infection studies.

2.3 Materials and Methods

2.3.1 Microbiome analysis

2.3.1.1 Clinical sample collection

Over a year, four samples of clinically infected hip prostheses removed during revision surgery were collected from the Southern General Hospital, Glasgow and the Royal Alexandra Hospital, Paisley, both NHS, Greater Glasgow and Clyde (Table 2-1). The patients were informed about the study and each of them gave consent to participate. The infected prostheses were covered under the residual human tissue ethics scheme for Glasgow hospitals and the Caldicott Guardian scheme for protecting the confidentiality of the patient and service user, and enabling appropriate information sharing. Hospital bacteriology results obtained from aspirate and tissue samples taken during prosthesis removal surgery by the operating surgeon and analysed in the hospital bacteriology department by laboratory technicians and analysts are indicated in Table 2-1.

Table 2-1: List of infected prosthetic implant samples collected from operating theatres

Sample number	Removal date	Clinical Diagnosis	Implant type	Implant Components	Bacteriology results	Culture method
1	09/01/14	Infected	Hip	Acetabular, stem & head	*Staphylococcus warneri* & *Corynebacterium striatum*	Broth
2	30/05/14	Infected	Hip	Acetabular, stem & head	*Staphylococcus caprae*	Broth
3	11/03/14	Infected	Hip	Acetabular, stem & head	n.d.	n.d.
4	11/12/14	Infected	Hip	Acetabular, stem & head	*Staphylococcus aureus*	aspirate, From Broth

n.d., not determined, *Results from aspirate and tissue samples taken during surgery

Following routine sample collection, surgeons removed the prostheses in a controlled environment operating theatre. The removed prostheses were then placed into a sterile bag and were handled using aseptic techniques in a category 2 containment flow-hood. Samples were collected directly from the hospital theatres and transported to the laboratory within 40 minutes from being removed from the patient. Direct sample collection from the operating theatre ensured sample storage and transportation methods were kept the same between samples and the disturbance to the procedure and theatre staff was kept to a minimum.

2.3.1.2 Processing of clinical samples

All reagents and chemicals were purchased from Sigma-Aldrich, Dorset, UK, unless stated otherwise.

The stem and acetabular components of each sample prosthesis were placed in separate sterile plastic bags. Plastic bags were sterilised through ultra-violet irradiation for 60 mins. To each component 40 ml of ultrapure ddH_2O from a Milli-Q® system (Millipore, Watford, UK) was added. The components were then sonicated separately for 5 mins in a Grant XUB5 sonication bath (Grant, Shepreth, UK) operating at a frequency of 38 kHz at 21°C to remove material adhered to the surface of the implant, a method adapted from Dempsey *et al.*, 2007. Sonicate from each sample was placed in separate 50 ml falcon tubes (Corning, St. David's Park, UK) and pelleted at 1000 xg for 20 mins at 4°C in a Heraeus™ Megafuge™ bench top centrifuge (Thermo Scientific, Waltham, MA, USA). The supernatant was then discarded and the pellet was resuspended in 0.5 ml of ultrapure ddH_2O per sample. Corresponding samples from each prosthesis were then pooled in reaction tubes (Greiner Bio-One, Stonehouse, UK) and stored at -80°C until DNA extraction. A negative control was made using an unused prosthetic hip that was sterilised through 70% ethanol washing and UV light treatment for 60 min in a category 2 containment flow-hood. The negative control was then treated in the same way as the samples.

2.3.1.3 Microbiome DNA extraction

DNA extraction was performed on sonicated material. The Qiagen DNeasy® blood & Tissue Gram-positive cell lysis and DNA extraction kit (Qiagen, Manchester,

UK) and corresponding protocol (Qiagen, 2006) was used according to the manufacturer's instructions. All stages were carried out in DNase free reaction tubes (Greiner Bio-One, Stonehouse, UK). Samples were initially pelleted by centrifugation in a bench top centrifuge at 5000 xg for 10 mins. Cell pellets were then resuspended in 180 µl of enzymatic cell lysis buffer containing 20mM Tris-Hydrochloride (pH 8), 2mM sodium ethylenediaminetetraacetic acid (EDTA), 1.2% Triton™ X-100 and 20 mg/ml of lysozyme, and then incubated overnight at 37°C on a Grant QBT2 block heater. After incubation, proteinase K at a concentration of 20 mg/ml was added along with buffer AL both from the Qiagen DNeasy® kit, followed by vortexing and incubation at 56°C for 2 h on the block heater. After 2 h a further 25 µl proteinase K from the Qiagen DNeasy® kit was added and the samples were incubated for a further 1 h at 56°C, increasing and ensuring protein degradation/depletion. RNase A at a concentration of 100 mg/ml was added to the samples, followed by sample vortexing and incubation at room temperature for 2 mins. Following this 100% ethanol was added to the samples and the samples were mixed thoroughly by vortexing, producing a homogenous solution. The solution was then pipetted into a DNeasy Mini spin column and centrifuged at 6000 xg for 1 min retaining the DNA on the column filter. The column containing the filter was then washed with buffers AW1 and AW2 from the Qiagen DNeasy® kit by centrifugation at 6000 xg for 1 min and 20 000 xg for 4 mins respectively to clean up the DNA. The column was then placed in a fresh collection tube and the DNA was eluted from the column with buffer AE from the Qiagen DNeasy® kit, by centrifugation at 6000 xg for 1 min. The extracted DNA was then stored at 4°C until further analysis.

2.3.1.4 NanoDrop™ spectrophotometer

A Thermo Scientific NanoDrop™ spectrophotometer was used to calculate the concentration of DNA present in samples through measuring the DNA extract absorbance at 260 nm and the purity of DNA through calculating absorbance ratios, 260/280 and 260/230. A 260/280 ratio of ~1.8 is generally accepted as "pure" for DNA, a lower ratio may indicate the presence of contaminants including: protein, phenol, or other contaminants that absorb at or near 280 nm. A 260/230 ratio of 2.0-2.2 is generally accepted as "pure" for nucleic acid, a lower ratio may indicate the presence of contaminants including: EDTA, carbohydrates, phenol or other contaminants that absorb at or near 230 nm.

2.3.1.5 DNA gel electrophoresis

DNA samples were then analysed by gel electrophoresis. DNA was separated in a 0.7% agarose gel in 1x TAE buffer (40 mM Tris-base, 20 mM acetic acid and 1mM EDTA). 6x blue gel loading dye (New England Biolabs, Hemel Hempstead, UK) was added to all samples to a final concentration of 1x, with a final DNA concentration of at least 1.7 ng/µl per sample (based on the NanoDrop reading), and ddH_2O was added to a total of 30 µl. A lambda DNA-HindIII digest ladder (New England Biolabs) in TE buffer (10 mM Tris-HCl pH 8, 1 mM EDTA) and 6x loading buffer, was run in parallel to DNA samples. The gel was run at 100 V until the dye line had gone 80% down the gel. The gel was stained with SYBR® safe (Life-technologies, Paisley, UK) solution (SYBR® safe and TAE buffer), for 30 mins at room temperature, with shaking at 50 rpm. The gel was then imaged using a G:Box imaging system (Syngene, Cambridge, UK) under ultraviolet light excitation.

2.3.1.6 Qubit™ fluorometric DNA quantitation

The Qubit® Fluorometer model 2.0 (Invitrogen™, Thermo Scientific, Paisley, UK) was used for DNA quantitation. Qubit analysis was carried out using the supplied Qubit DNA quantitation assay kit used according to the manufacturer's instructions. Briefly, samples were mixed with the Qubit kit dilution buffer and Qubit fluorescence DNA dye, in Qubit assay thin-walled reaction tubes. DNA concentration is calculated by comparing sample fluorescence readings to Qubit standards containing known DNA concentrations. Standards are made by adding Qubit kit standard solutions 1 and 2 to Qubit kit buffer and Qubit fluorescence dye.

2.3.1.7 Microbial DNA enrichment

The NEBNext® Microbiome DNA Enrichment kit (New England Biolabs) was utilised to remove host DNA contamination enriching microbial DNA. Enrichment is performed by separating DNA containing methyl-CpG (cytosine-phosphate-guanine) from a complex mixture of human and bacterial DNA. Through specific binding of methyl-CpG elements in host DNA to methylated CpG-specific binding protein, MBD2, which is fused to the Fc fragment of human IgG (MBD2-Fc), separation can be carried out based on differences in abundance of CpG

methylation (Hendrich and Bird, 1998; Lewis et al., 1992; Lister et al., 2009; Tucker, 2001). The Fc fragment of MBD2-Fc readily binds to Protein A which is attached to magnetic beads allowing for easy separation using a magnet.

The following steps of the kit were followed in accordance with the manufacturer's instructions and described by Feehery *et al*. 2013: pre-binding MBD2-Fc protein to magnetic beads; capturing methylated host DNA; collection of enriched microbial DNA; and ethanol precipitation.

The amount of MBDS-Fc bound magnetic beads required (Y) is calculated by the following equation.

$$Y = \frac{Input\ DNA\ (ng)}{6.25\ ng/\mu l}$$

To bind the beads and protein, MBD2-Fc protein and Protein A magnetic beads, both from the NEBNext® kit, were mixed with 1x Bind/wash buffer from the NEBNext® kit in Ambion® nuclease-free water (Thermo Scientific) in DNase free reaction tubes (Greiner Bio-One). Through placing tubes on a Dynal magnetic rack (DynaMag™, Invitrogen™, Thermo Fisher Scientific) the supernatant can be separated from the beads. Bound beads were washed twice in 1x Bind/wash buffer through centrifugation (2000 xg) and finally resuspended in 1x Bind/wash buffer. Beads were at 4°C for a maximum of 7 days prior to use.

Capturing methylated host DNA was carried out by adding a maximum of 1 µg of DNA extract to prepared bound beads and 1x Bind/wash buffer, followed by incubation for 15 mins at room temperature.

Collection of enriched microbial DNA was carried out by using the magnetic rack to collect the beads and removing the microbial DNA containing supernatant.

To purify the DNA samples ethanol precipitation was performed by adding 2.5 volumes of ethanol (Fisher Scientific, Loughborough, UK), incubating on ice for 10 mins and centrifuging at 16 000 xg. Residual ethanol was removed and the DNA pellet was resuspended in 50 µl of TE buffer (as previously described in section 2.3.1.5). The enriched DNA was stored at 4°C until sequencing.

2.3.1.8 Microbiome metagenome sequencing and data analysis

Library construction and setting up the sequencing run was performed by Julie Galbraith at the Glasgow Polyomics Next Generation Sequencing facility.

Microbiome sequencing and data analysis was performed using the pipeline depicted in Figure 2-1.

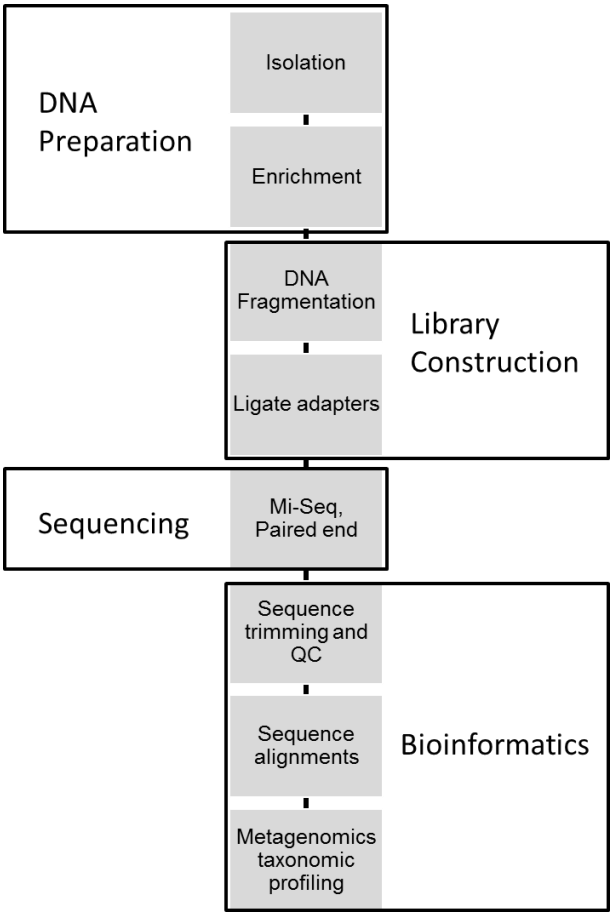

Figure 2-1: Microbiome pipeline used for the acquirement and analysis of microbiome studies of the infected hip prosthesis.

The NEBNext® Ultra DNA library prep kit for Illumina platforms (New England Biolabs) was used due to the small amount of DNA input required (5ng-1µg). The kit was used according to the manufacturer's instructions. Metagenomic sequencing was carried out using the Illumina MiSeq platform incorporating 300 bp paired end sequencing.

Sequence trimming and QC was performed using Cutadapt (Martin, 2011) and FastQC (Babrahan Bioinformatics), respectively. Metagenome bioinformatics was performed using MetaPhlAn (Metagenomic Phylogenetic Analysis) 2 (version 2.2.0) (Segata et al., 2012; Truong et al., 2015), which aligns reads and data base matches or MetaVelvet (version 1.2.02) (Namiki et al., 2012), which aims to assemble mixed reads *de-novo*.

2.3.2 Characterisation of a *S. aureus* clinical isolate

An orthopaedic clinical isolate of *S. aureus*, cultured from the pus aspirated from the hip of a 75-year-old female, was obtained from isolate collections held at the Southern General Hospital Microbiology laboratories (Glasgow, United Kingdom). The hospital microbiology laboratory confirmed the isolate was *S. aureus* using a positive Staph Xtra latex test (Pro-Lab Diagnostics, Wirral, UK) and growth on chromID® agar, for the selective isolation of staphylococci and the direct identification of *S. aureus* (SAID) (BioMérieux, Durham, NC, USA). Once transported to the laboratory here, identification and further characterisation was carried out. This isolate was used for all future *S. aureus* studies here.

2.3.2.1 Bacterial culture

S. aureus isolates were cultured on Brain Heart Infusion (BHI) agar plates (Oxoid, Basingstoke, UK), at 37°C in a humidified static aerobic incubator. For planktonic *S. aureus* cell culture, single colonies were taken from an agar plate and inoculated into BHI broth media (Oxoid) in 50 ml falcon tubes (Corning). Liquid cultures were then incubated overnight up to 24 h, at 37°C, shaking at 180 RPM in an Orbital shaker to stationary phase growth, which was used for subsequent planktonic and biofilm studies. Glycerol stocks (30% glycerol (Sigma-Aldrich), 70% BHI) of *S. aureus* culture in BHI were stored at -80°C until required. Growth was recovered by streaking an aliquot of the stock on a BHI agar plate followed by culturing as above.

2.3.2.2 Growth curve

The increase in absorbance/optical density (OD) caused by the increase of cell culture density can allow for the creation of a growth curve and growth phase to

be estimated. A growth curve was made through measuring OD of culture against time. To do this, single colonies from an overnight cultured BHI agar plate of the clinical *S. aureus* isolate were inoculated and resuspended in BHI broth as in section 2.3.2.1 in a falcon tube (Corning). This was carried out in triplicate. The tubes were incubated as in section 2.3.2.1. At each time point 100 µl was removed and placed in a 96-well microtitre plate (Corning). Using fresh BHI as a blank, the OD at 595 nm (OD_{595}) was measured using a GENios plate reader (Tecan, Männedorf, Switzerland), or a GeneQuant™ Pro cuvette absorbance reader (GE Healthcare, Pollards Wood, UK). 'n' numbers represent technical replicates.

2.3.2.3 Miles-Misra colony forming unit (CFU) counts

The Miles-Misra method was used here to measure cell density. First published in 1938 (Miles and Misra, 1938), the Miles-Misra colony forming unit (CFU) counting method provides a fast, reproducible and low cost way to assess culture concentration. Serial dilutions of the culture to be counted were made to 10^{-8} in sterile PBS (Fisher Scientific). A 20µl aliquot of each serial dilution was then pipetted onto a segmented BHI agar plate and incubated as described in section 2.3.2.1 this was always repeated in triplicate for each dilution. After incubation and growth each sector containing one dilution was examined for growth. Sectors containing high concentrations of bacteria experienced luxurious growth producing plaques of merges colonies. Colonies were counted in sectors were the highest number of separated colonies could be observed. The following equation was then used to calculate the colony forming unit count per ml.

$$CFU\ per\ ml = average\ number\ of\ colonies * 50 * dilution\ factor$$

2.3.2.4 Species identification with the API® Staph test

Once collected and transported to the laboratory, the isolate was sub-cultured and the API® (analytical profile index) Staph test (BioMérieux, Durham, NC, USA) was used to confirm the clinical isolate was *S. aureus*. The test incorporates a single strip that 20 biochemical tests which are run simultaneously, including: acid production from sugar metabolism; reduction of nitrates to nitrites; alkaline phosphatase activity; acetyl-methyl-carbinol production; arginine dihydrolase activity; and urease activity (Table 2-2). The addition of scores assigned to the

reactions in a pre-determined pattern produce a 7-digit numerical code that can be matched to the API allowing bacterial species identification. The test cannot be used for polymicrobial cultures and can only identify species listed in the API database. In 2014, assay performance was tested by carrying out multiple tests on collection strains and strains belonging to the species included in the API database. 92.49% of strains were correctly identified while 4.42% and 3.09% were not identified or misidentified, respectively.

Here, the API assay was performed according to the manufacturer's instructions. To prepare the inoculum colonies of the isolate to be tested were taken from a BHI agar plate, cultured as described in section 2.3.2.1, and resuspended in an ampule of API Staph medium from the API Staph test kit, until a homogeneous bacterial suspension was created to a turbidity equivalent to a 0.5 McFarland standard, a turbidity standard used to standardise bacterial suspensions. Each of the 20 microtubes on the test strip were then filled with the inoculum followed by adding oil to tests ADH and URE to create a convex meniscus. The strip was then placed in the strip incubation box with ddH_2O added to wells within the box to create a humidified atmosphere and incubated overnight at 37°C in a static aerobic incubator.

Following incubation API Staph test kit reagents VP 1 and VP 2 are added to the sodium pyruvate (VP) test and incubated at room temperature for 10 mins. A violet-pink colour indicates a positive result while a light pink colour indicates a negative result. Reagents NIT 1 and NIT 2 are added to the Potassium nitrate (NIT) test and incubated at room temperature for 10 mins. A red colour indicated a positive reaction. Reagents ZYM A and ZYM B are added to the B-naphthyl phosphate (PAL) test and incubated at room temperature for 10 mins. A violet colour indicated a positive reaction. The strip was then interpreted, scores assigned and summed to create the 7 digit numerical code. API tables were then interrogated to match the numerical code to identify the bacterial species.

A 21st test is performed to test lysostaphin resistance. This was carried out by flooding a BHI plate with inoculum and leaving to dry for 20 mins at 37°C. After the plate has dried a drop of 200 µg/ml lysostaphin solution (Sigma-Aldrich) is pipetted onto the agar surface. The plate was then incubated as described in

section 2.3.2.1. Resistance to the enzyme is a recorded as a positive result while partial to total lysis of the culture indicates susceptibility to the enzyme and a negative result.

Table 2-2: API Staph test result scoring system

Test	Scoring system
0 (Negative control)	1
D-Glucose (GLU) (Positive control)	2
D-fructose (FRU)	4
D-mannose (MNE)	1
D-maltose (MAL)	2
D-lactose (LAC)	4
D-trehalose (TRE)	1
D-mannitol (MAN)	2
Xylitol (XLT)	4
D-melibiose (MEL)	1
Potassium nitrate (NIT)	2
B-naphthyl phosphate (PAL)	4
Sodium pyruvate (VP)	1
D-raffinose (RAF)	2
D-xylose (XYL)	4
D-saccharose (sucrose) (SAC)	1
Methyl-αD-glucopyranoside (MDG)	2
N-acetyl-glucosamine (NAG)	4
L-arginine (ADH)	1
Urea (URE)	2
Lysostaphin (LSTR)	4

2.3.2.5 Antibiotic susceptibility testing

A MASTRING-S™ Gram-positive M-13 antibiotic susceptibility ring (Bootle, UK) was used to test antibiotic susceptibility. The rings test bacteria susceptibility to chloramphenicol (C) (25 µg), erythromycin (E) (5 µg), fusidic acid (FC) (10 µg), oxacillin (OX) (5 µg), novobiocin (NO) (5 µg), penicillin G (PG) (1 unit), streptomycin (S) (10 µg) and tetracycline (T) (25 µg). A stationary phase culture was diluted to an OD_{595} of 0.1. The diluted culture (100 µl) was then spread on a BHI agar plate. Following this a MASTRING-S™ M-13 ring was placed on the surface of the agar plate. The plate was then incubated described in section 2.3.2.1. Following overnight incubation plates were inspected for growth. Zones of growth inhibition around antibiotic impregnated tips were observed around susceptible antibiotics. Antibiotic impregnated tips which had continuous and

luxurious growth with no growth inhibition were classed as antibiotics that the S. *aureus* isolate was resistant too.

2.3.2.6 DNA extraction from a single isolate

The Qiagen DNeasy® blood & Tissue Gram-positive cell lysis and DNA extraction protocol (Qiagen) as used in section 2.3.1.3 was used here for the DNA extraction and isolation from a stationary phase overnight culture of the S. *aureus* clinical isolate. The kit was used according to the manufacturer's instructions and as above in section 2.3.1.3.

2.3.2.7 Genome Sequencing and Data Analysis

Library construction and setting up the sequencing run was performed by Julie Galbraith at the Glasgow Polyomics Next Generation Sequencing facility.

Sequencing and data analysis was performed using the pipeline depicted in (Figure 2-2). The Illumina MiSeq platform with 300 bp paired end sequencing as used in section 2.3.1.8, was utilised here for sequencing the genome of the clinical S. *aureus* isolate.

De-novo assembly was performed using CLC workbench version 7.5.1 (Qiagen). Proteins potentially encoded were predicted using the Rapid Annotation using Subsystem Technology (RAST) resource (Aziz et al., 2008; Overbeek et al., 2014). Further genome analysis was carried out using Multilocus sequence typing (MLST) (Enright et al., 2000; Maiden et al., 1998; Spratt, 1999), National Center for Biotechnology Information (NCBI) Basic Local Alignment Search Tool (BLAST) searches (Altschul et al., 1990) and Mauve analysis software (Darling et al., 2004). The genome sequence was also analysed using the Antibiotics and Secondary Metabolite Analysis SHell (antiSMASH) web server to look for secondary metabolite biosynthesis gene clusters in the genome (Medema et al., 2011).

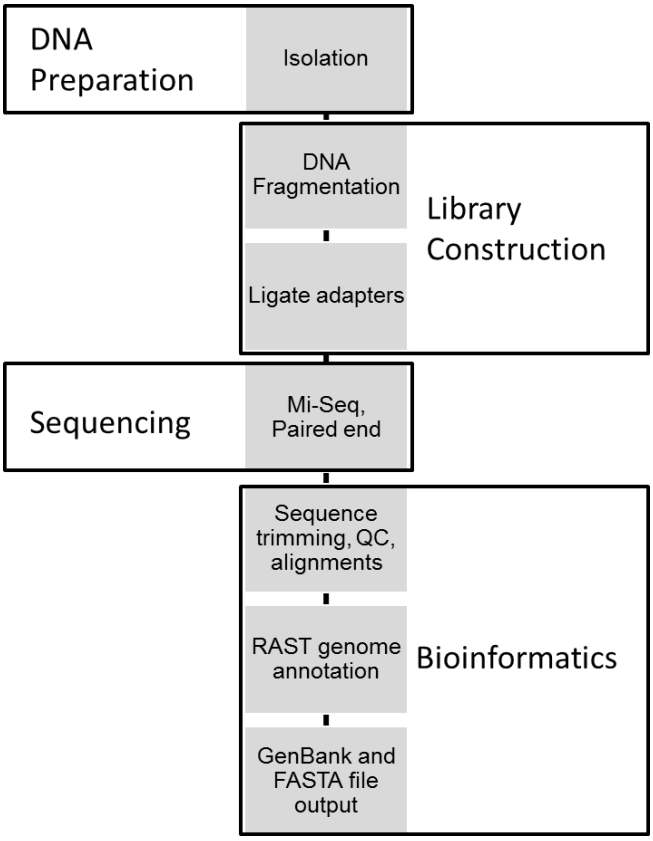

Figure 2-2: Sequencing pipeline used for the acquirement and analysis of *S. aureus* genome sequencing data.

2.3.3 *In vitro* biofilm studies

In all *in vitro* biofilm experiments 'n' numbers represent technical replicates.

2.3.3.1 Biofilm cultivation

Biofilms were grown either on Nunc™ Thermanox™ coverslips (Thermo Fisher Scientific, Nunc, Roskilde, Denmark) or on the base of a well of a 96-well flat bottomed plate (Corning). Overnight stationary phase culture was diluted to an OD_{595} of 0.1 in fresh BHI. 200 µl of cell dilution per well was incubated in a 96-well plate or 500 µl was added to coverslips placed in a 24-well plate (Corning), for up to 24 h in a static aerobic humidified incubator at 37°C. Following incubation spent media was removed through pipetting and biofilms were washed by dunking the plate or coverslip using forceps into 10 mM ammonium bicarbonate or ddH_2O and blotted to remove excess liquid.

2.3.3.2 Crystal violet (CV) assay

The biofilm crystal violet (CV) assay as first described by Christensen *et al*. in 1985 and later by O'Toole and Kolter in 1998 and 2011 (Christensen et al., 1985; O'Toole, 2011; O'Toole and Kolter, 1998), was utilised here. The method carried out according to the published methods. Here, 0.1% CV stain (Acros organics, Geel Belgium) in ddH_2O was added to biofilms and incubated for 15 mins at room temperature. As a negative control and to act as a blank reading deducted from optical density readings, blank wells were stained in the same way biofilm samples were, included due to the ability of CV to stain plastics inducing a false positive result.

Following staining excess stain was removed and the biofilms were washed as described in section 2.3.3.1 in ddH_2O. The CV of stained biofilms was then solubilised using 95% ethanol. The solvent was added to the biofilm samples and the plate was incubated at room temperature on a shaker (70 RPM) for 15 mins. To quantify biofilm formation, solubilised stain was then transferred to a fresh flat bottomed 96-well plate and the OD_{595} was measured using the GENios plate reader previously described.

To assess *S. aureus* biofilm formation over time multiple wells in several plates (one for each time point) were cultured with a biofilm as described in section 2.3.3.1. At each time point the CV staining assay mentioned above was used to quantify biofilm formation of simultaneous samples.

2.3.3.3 Scanning electron microscopy (SEM) imaging

SEM sample processing was performed by Margaret Mullin at the Integrated Microscopy Facility, The University of Glasgow.

For SEM analysis biofilms were cultured on Thermanox™ coverslips for 24 h described in section 2.3.3.1. Samples were processed and imaged as previously described by Erlandsen *et al.* (2004).

Briefly, biofilm samples were washed as described in section 2.3.3.1 and fixed overnight in a mixture of 2% paraformaldehyde and 2% glutaraldehyde (Sigma-Aldrich) in 0.15 M sodium cacodylate buffer (pH 7.4) (Agar Scientific, Stansted, UK) with 0.15% w/v of the cationic dye Alcian blue (Agar Scientific). After fixing the samples were washed twice in 0.15 M cacodylate buffer and post-fixed for 1 h in 1% Osmium tetroxide (Agar Scientific) in 0.15 M cacodylate buffer. Samples were then rinsed in 0.15 M cacodylate buffer and dehydrated with an ascending ethanol concentration series consisting of; 50%, 70%, 80%, 95%, and twice with 100%, before drying with hexamethyldisilazane (HMDS), 3 x 5min changes, and then leaving to air dry. The fixed and dried samples were then gold-palladium coated and mounted on SEM pin mounts. Samples were imaged under a JEOL JSM-6400 scanning electron microscope running at 10 kV, with images collected in TIFF format captured using Olympus scandium software.

2.4 Results

2.4.1 Microbiome analysis of orthopaedic infections

Mr Fahd Mahmood, NHS Greater Glasgow and Clyde, assisted with sample preparation and sonication treatments of samples. Hannah Rankin assisted with DNA extraction, enrichment and the running of gels under my supervision. Dr Graham Hamilton assisted with bioinformatics workflows and sequencing data analysis.

2.4.1.1 Microbial DNA extraction from infected orthopaedic prostheses

To ascertain what species of bacteria are responsible for orthopaedic implant failure, a metagenome study of orthopaedic infection was carried out. Cases of infected orthopaedic prostheses removed during revision surgery were collected for microbiome analysis and transported to the laboratory.

Once in the laboratory, sonication was used to remove biological material from the implant surface, which included not only bacteria but human tissue and fluids. Through using a Gram-positive cell extraction kit, both Gram-positive and Gram-negative species were lysed and DNA extracted from the bacteria and any host tissue present. After the DNA extraction and before microbial DNA enrichment, NanoDrop measurements were used to calculate DNA concentrations and to check the DNA quality (Table 2-3). Gel electrophoresis was also carried out to check the DNA fragment sizes were suitable for enrichment (Figure 2-3). Sample 1 had a low DNA concentration and a low 260/280 ratio representing poor quality, meaning the DNA concentration measurement may be a consequence of contamination (Table 2-3). Gel electrophoresis confirmed this observation as sample 1 appeared to have a very low DNA concentration compared to the other 3 samples. Samples 2, 3 and 4 each demonstrated a high DNA concentration and the presence of large DNA fragments (Table 2-3 & Figure 2-3). The negative control had no visible DNA contamination (Figure 2-3). Given the presence of non-bacterial DNA in the samples as alluded to above, a microbial DNA enrichment kit was used to remove host DNA contamination.

Table 2-3: DNA concentration from microbiome samples of infected orthopaedic prostheses measured using the NanoDrop spectrophotometer.

Sample number	DNA concentration (ng/µl)	260/280 ratio	260/230 ratio
1	4.7	1.17	2.6
2	23.5	1.87	1.99
3	190.8	1.85	2.43
4	107.6	1.88	2.33
NC	1.5	1.03	0.56

NC (Negative control)

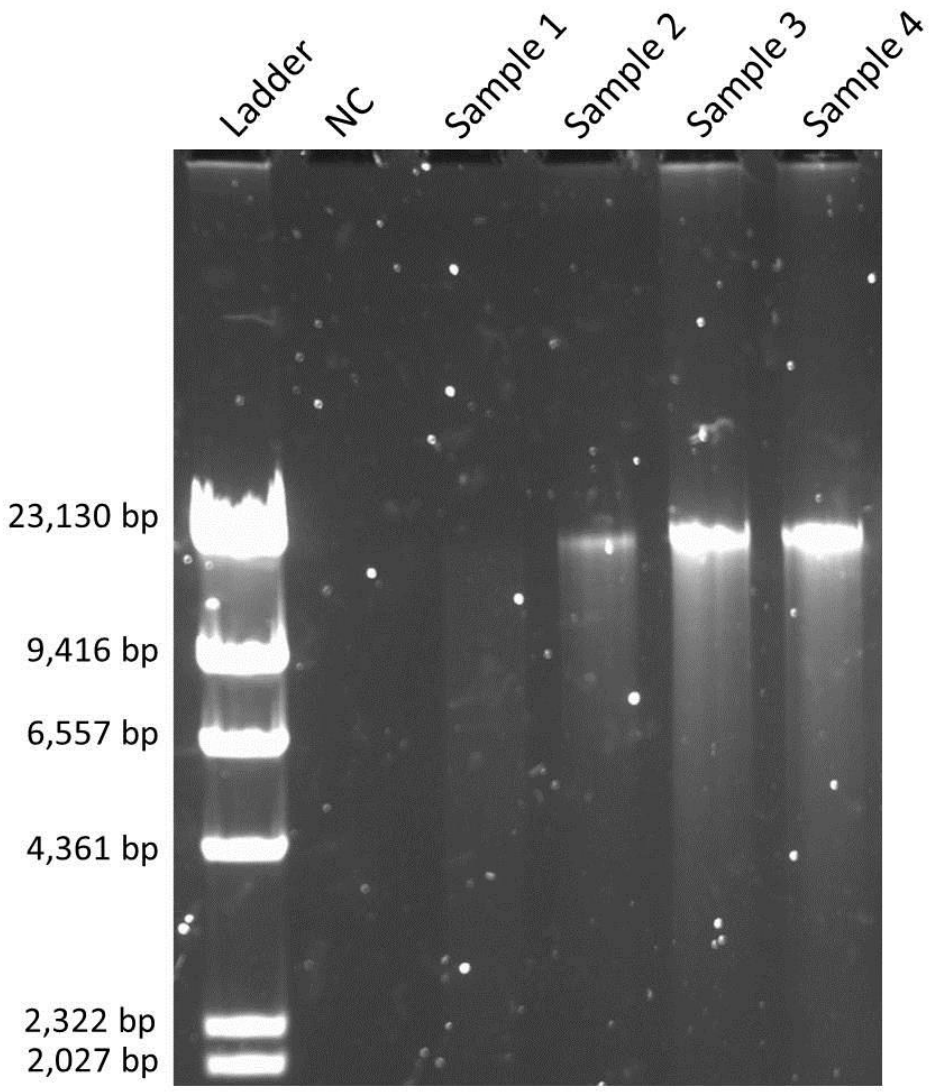

Figure 2-3: Gel electrophoresis of DNA extracts from infected hip prostheses
An infected prosthesis samples 1-4 and a negative control (NC). Infected prostheses were collected from operating theatres and prepared by sonication to remove material followed by DNA extraction. NC (Negative control) was an uninfected sterilised prosthesis. The gel is a 0.7% agarose gel run at 100 V and the ladder is a lambda DNA-HindIII digest.

2.4.1.2 Microbial DNA enrichment and removal of contaminant host DNA

A microbial DNA enrichment kit was used to remove human DNA based on methylation. It is reported that 4-6% of cytosines are methylated in human DNA and 60-90% of these are at CpG sites, compared to microbial DNA were CpG site methylation is very rare (Lister et al., 2009; Tucker, 2001). Therefore, separation could be carried out based on differences in abundance of CpG methylation (Feehery et al., 2013). The kit works optimally with large (>15 Kb) fragments of DNA, confirmed here by gel electrophoresis (Figure 2-3).

Here, the NEB kit proved to be very efficient in removing methylated DNA as a drop in DNA concentration is seen after enrichment (Table 2-4). This highlights the presence of high levels of contaminant DNA in the samples, emphasising the importance of carrying out an enrichment protocol. However, it was found that following enrichment, microbial DNA concentration was extremely low in each sample due to the limitation of the amount of input DNA in each reaction (Table 2-4). This meant pooling of multiple enrichments was required. The overall low DNA concentration post-enrichment compared with pre-enrichment measurements highlights a decrease in the DNA concentration (Table 2-4). Sample 1 and the negative control (NC) did not give a Qubit measurement post-enrichment. DNA concentration was too low in these samples; therefore metagenome sequencing could not be performed on these samples. In sample 2, 4.6% of the extracted DNA sample was un-methylated DNA, while 95.4% was methylated DNA. In sample 3, >0.16% of the extracted DNA sample was un-methylated DNA, while 99.84% was methylated DNA. In sample 4, >0.15% of the extracted DNA sample was un-methylated DNA, while 99.85% was methylated DNA.

Table 2-4: DNA concentration in non-enriched and enriched microbiome samples from infected orthopaedic prostheses measured using the Qubit fluorometric DNA quantitation assay.

Sample Number	Qubit reading of DNA extractions (ng/µl)	
	Non-enriched	Enriched[(a)]
1	<0.5	<0.5
2	31.6	1.45
3	>600	0.946
4	>600	0.9
NC[(b)]	<0.5	<0.5

[(a)]Enrichment by selective removal of methylated DNA

[(b)]NC = Negative Control

2.4.1.3 Microbiome sequencing and analysis of orthopaedic infections reveals polymicrobial infections

Different sequencing platforms can be used for sequencing acquisition. Here, the Illumina platform was chosen as it provided highly accurate short reads compared to the alternative Ion Torrent platform. Next generation sequencing was used because it is much faster, meaning lower running costs, and allows for greater accuracy as it is not reliant on gels or polymers for separation as in Sanger sequencing.

Metagenome analysis software was used including, MetaVelvet which assembles mixed short reads *de-novo* (Namiki et al., 2012), and MetaPhlAn 2 which aligns reads and matches them to a data-base (Segata et al., 2012; Truong et al., 2015). Processing errors due to high levels of host DNA resulted in no result when MetaVelvet was used here so following metagenome sequencing and sequence processing, MetaPhlAn 2 was used to profile the microbial composition of the samples. Sample reads were further aligned against the human genome to ascertain the level of human DNA contamination. Results show a low level of microbial DNA detected compared to human DNA (Table 2-5). Furthermore, a high number of reads from the sequence data did not align to microbial nor human DNA.

One sample had a very low number of reads (66 in total) matched to microbial DNA and was too low to assign taxonomy. Through alignment to the human

genome it was found that a majority of sequenced DNA was human (Table 2-5). This coupled with high human DNA reads in all other samples indicated the microbial DNA enrichment protocol may not have been as efficient as first thought. Further analysis using MetaPhlAn2 identified taxonomic identifications of bacterial reads (Table 2-6).

Table 2-5: Metagenome data analysis using MetaPhlAn2 of infected orthopaedic hip prosthesis samples and alignment against the human genome.
Number of reads belonging to bacterial species and human. Also shown are the numbers of unaligned reads.

Sample Number	Bacterial reads	Human reads	Unaligned reads	Total reads	% bacteria
2	206,098	2,428,351	206,309	2,840,758	7.26
3	66	4,365,455	53,097	4,418,618	0
4	6,404	6,237,339	87,865	6,331,608	0.1

Table 2-6: Metagenome data analysis using MataPhlAn2 of infected orthopaedic hip samples: identified bacterial species

Sample Number	Clade Name (Species ID)	Relative abundance	Coverage (%)	Estimated number of reads from the clade
2	*Enterococcus faecium*	99.96256	0.0673	191891
	Clostridium difficile	0.03744	2.5209×10^{-5}	108
4	*Staphylococcus aureus*	99.21101	0.0021	5950
	Clostridium difficile	0.78899	1.6508×10^{-5}	71

Here, we aimed to improve microbiome analysis of the infected hip prosthesis and to provide further evidence of what species cause infection using metagenome sequencing. Our results represent a microbiome study using new sample preparation methods to eliminate host DNA contamination to improve microbiome analysis. Results of the sequencing analysis highlight multiple species responsible for infection, including *S. aureus*, a commonly isolated organism from orthopaedic infections. Further, we show the presence of secondary organisms in these infections.

2.4.2 Characterisation of LHSKBClinical, an orthopaedic clinical isolate of *S. aureus*

An orthopaedic clinical isolate of *S. aureus*, termed LHSKBClinical herein, was obtained from isolate collections held at the Southern General Hospital Microbiology laboratories, for orthopaedic staphylococcal infection studies. This clinical isolate was isolated from a different orthopaedic infection case to the ones used in the microbiome study, but was received and used in parallel to the above study.

2.4.2.1 Growth Curve

A classical growth curve of LHSKBClinical was established, showing a lag phase for 2 hours, followed by exponential growth (Figure 2-4). Stationary phase was not reached at 24 h but growth had declined from exponential growth. Longer monitoring would have to be applied to see a plateau in growth. Furthermore, cell death would not be observed using this method due to dead cells absorbing light. Two deviations in the growth curve, between 5 h and 10 h and between 15 h and 20 h, may represent a diauxic shift in the culture due to the depletion of nutrient sources in the media. However, this would have to be confirmed with further replicates.

An overnight culture (16 h) of LHSKBClinical was grown and the Miles-Misra CFU method was used to calculate cell concentration. An overnight culture of LHSKBClinical grew to >2 x 10^9 cells/ml. An overnight culture of LHSKBClinical diluted to an OD_{595} of 0.1 gave a cell concentration of 2.5 x 10^6 cells/ml. This optical density was then used throughout this PhD project to standardise future studies. The Miles-Misra CFU method proved to be reproducible and gave an indication of cell number. However, there was variation between replicate counts of the same culture due to some colonies not growing on the agar plate or pipetting errors.

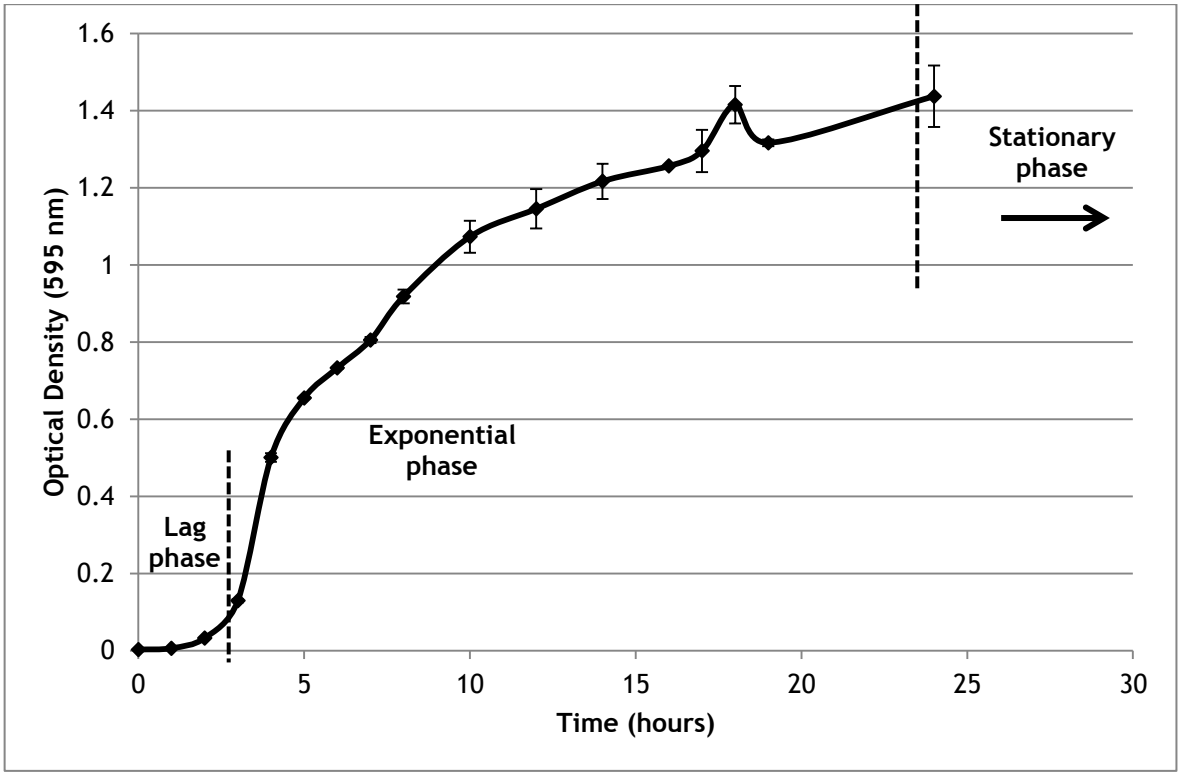

Figure 2-4: LHSKBClinical growth curve
Planktonic cell growth of *S. aureus* in BHI broth media. Optical density at 595 nm of the culture was measured at set time points. Lag, exponential and stationary growth phases are marked on the curve. Error bars ± S.D., n=3.

2.4.2.2 API Staph of LHSKBClinical

To confirm the species identification, bacterial species identification was carried out using the BioMérieux API Staph system. The results for LHSKBClinical gave the numerical code 6736153, indicating *S. aureus* (Andollina et al., 2004).

2.4.2.3 MAST antibiotic resistance testing of LHSKBClinical

To establish the antibiotic resistance status of the LHSKBClinical isolate, MAST ring antibiotic susceptibility testing was carried out (Table 2-7). The isolate displayed a zone of inhibition around all antibiotics tested on the M13 Gram-positive ring, apart from around the Streptomycin disc where growth occurred up to the disc perimeter indicating resistance (Table 2-7). However, this requires confirmation through minimum inhibitory concentration (MIC) experiments.

Table 2-7. MAST Stock ring M13 antibiotic susceptibility testing of LHSKBClinical

M13	
Chloramphenicol (C)	Sensitive
Erythromycin (E)	Sensitive
Fusidic acid (FC)	Sensitive
Oxacillin (OX)	Sensitive
Novobiocin (NO)	Sensitive
Penicillin G (PG)	Sensitive
Streptomycin (S)	Resistant
Tetracycline (T)	Sensitive

2.4.2.4 Genome sequencing of the *S. aureus* LHSKBClinical isolate

Sequencing data analysis and bioinformatics workflows were carried out by Dr Graham Hamilton, University of Glasgow. This work has been submitted for publication (Appendix I).

Following initial identification and characterisation experiments of LHSKBClinical, a full draft genome sequence was obtained. Sequencing was carried out by the Glasgow Polyomics Next Generation Sequencing facility and the draft genome sequence was submitted to the National Center for Biotechnology Information (NCBI), U.S. National Library of Medicine (accession number: JZAL00000000.1), along with a NCBI Bioproject (accession number: PRJNA276072) and a NCBI Biosample report (accession number: SAMN03365925) (Stipetic et al., 2015).

Following sequencing, reads were assembled into contigs allowing for species taxonomy to be identified and confirmed as *S. aureus*. Sequencing analysis assembled 24 scaffolds; consisting of a total of 2,762,774 bp. Contigs had a N_{50} of 587,246 bp and an A-T content of 67%. Using the RAST resource, the genome sequence was predicted to encode 2,566 proteins. After initial *de novo* assembly, genome analysis was performed using MLST, NCBI BLAST searches and Mauve analysis software. MLST analysis gave the sequence type as 3311441 which was not found to be a known type when searched against the MLST *S. aureus* database. NCBI BLAST analysis of the sequenced genome compared to genomes of *S. aureus* revealed 99% sequence coverage but with regions of heterogeneity. Finally, Mauve analysis, a multiple genome alignment tool, highlighted regions of

heterogeneity compared to other genomes of *S. aureus*, indicating that LHSKBClinical is a novel previously un-typed *S. aureus* isolate.

In addition, antiSMASH was used to search the genome sequence for secondary metabolite biosynthesis gene clusters. Returned results indicated gene similarity of 36%, 75%, and 87% to gallidermin (siderophore), staphyloferrin (siderophore) and staphylobactin (lantipeptide) biosynthetic gene clusters, respectively. Furthermore, gene clusters classed as a terpene cluster, a nonribosomal peptide synthetase (NRPS) cluster, and bacteriocin cluster were annotated from the genome sequence.

Here, we aimed to biotype and sequence a clinical isolate of *S. aureus* taken from an orthopaedic infection case. Our results show the biotyping, including antimicrobial resistance status testing, and genome sequencing, with some primitive analysis, of a clinical isolate of *S. aureus*, named LHSKBClinical.

2.4.3 *In vitro* biofilm studies of LHSKBClinical

2.4.3.1 LHSKBClinical biofilm formation

LHSKBClinical was tested for biofilm formation using a CV assay. The assay is a non-specific biomass test employed to stain biological material adhered to the surface, normalised to blank stained wells. Biofilm formation was measured over 24 h in wells of a 96-well plate. Cell adherence and biofilm formation of LHSKBClinical increased over time (Figure 2-5). Large variation between replicates was seen at 24 h (Figure 2-5).

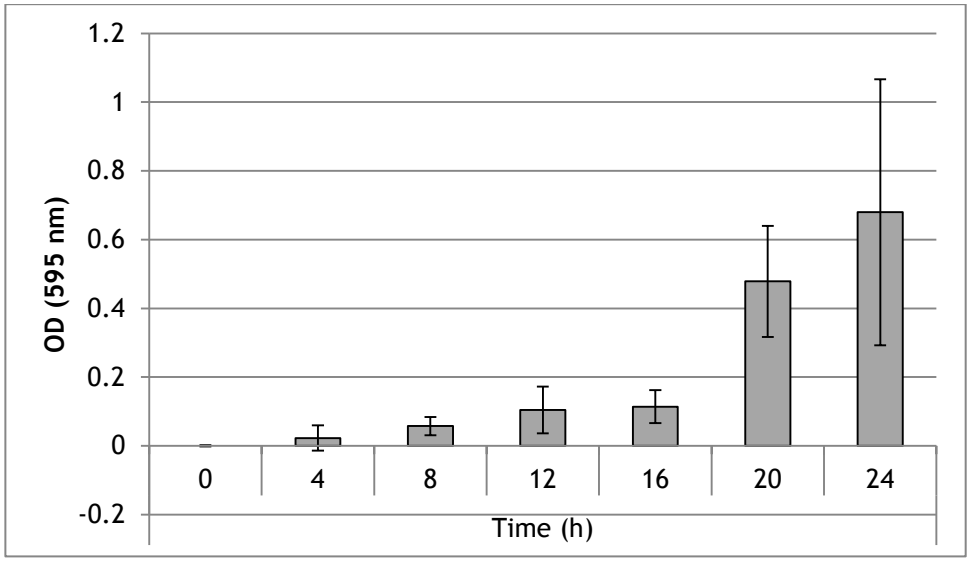

Figure 2-5: Crystal Violet (CV) assay of biofilm formation
Biofilm formation on the base of a 96-well microtitre plate. Standardised cell culture was inoculated in the wells and incubated for up to 24 hours. CV staining, stain solubilisation and an OD_{595} measurement of solubilised stain was carried out at each time point. Error bars ± S.D., n=8.

2.4.3.2 Scanning Electron Microscopy (SEM) of LHSKBClinical biofilms

Scanning electron microscopy was carried out on 24 h biofilms (Figure 2-6). Three-dimensional structures of *S. aureus* cells adhered to the cover slip surface are seen with areas of extracellular matrix (ECM) visible between the cells (Figure 2-6B).

Figure has been removed due to Copyright restrictions.

Figure 2-6: Scanning electron microscopy (SEM) imaging of LHSKBClinical biofilm formation on ThermanoxTM coverslips.
Standardised cell culture was incubated on cover-slips for 18h. After which cover-slips were washed, prepared for SEM imaging and imaged under a SEM running at 10 kV at 500X (A) and 5000X (B) magnification. Arrows a, b, c, d highlight areas of ECM.

Here, we aimed to test a clinical isolate of *S. aureus* for *in vitro* biofilm formation. Our results highlight the optimisation and use of bacterial cell and biofilm cultivation methods to test the biofilm forming capabilities of LHSKBClinical. The isolate forms a biofilm and is used for future *S. aureus* biofilm studies.

2.5 Discussion

2.5.1 Microbiome analysis of Orthopaedic infections

Orthopaedic infections can be polymicrobial (Bereza et al., 2013; Gomez et al., 2012; Makaritsis et al., 2009; Moran et al., 2007). Due to their sensitivity, techniques employing the use of genomic approaches have been considered a valuable tool to study the hidden microbiome of such infections (Gomez et al., 2012). Furthermore, genomic approaches eliminate the need for culture-based identification methods, which can miss many species that are difficult to culture *in vitro*, for example obligate anaerobes.

Here, metagenome analysis of infected prosthetic hips was carried out providing identification of the causative bacterial species. Therefore we can accept our hypothesis that metagenome sequencing will provide identification of the bacteria present in an orthopaedic prosthesis polymicrobial infection and that the methods presented here will provide a metagenome study approach to further study the infected hip prosthesis.

Results reveal the presence of different bacteria species causing infection and polymicrobial infections, correlating with other published papers looking at the microbiome of the infected prosthetic hip (Bereza et al., 2013; Dempsey et al., 2007; Osmon et al., 2012; Ramage et al., 2003; Tunney et al., 1998, 1999).

Dempsey *et al*. (2007) used 16S rRNA sequencing to identify bacteria present on the surface of 10 revised hip prostheses identifying species from the genera *Leifsonia*, *Staphylococcus*, *Proteus*, *Brevundimonas*, *Salibacillus*, *Methylobacterium*, and *Zimmermannella* (Dempsey et al., 2007). Other studies found the presence of: *Ralstonia pickettii*; *Propionibacterium acnes*; *Pseudomonas* spp.; *Brevibacterium* spp.; *Lactobacillus* spp.; *Propionibacterium* spp.; and *Staphylococcus* spp. (Bereza et al., 2013; Osmon et al., 2012; Ramage et al., 2003; Tunney et al., 1998, 1999). These studies all found *Staphylococcus* spp. and other commensal and environmental bacteria corresponding with our findings.

Through aseptic handling of samples and the use of a negative control, confidence in identifications was achieved. Similar negative controls have been used in other studies (Dempsey et al., 2007), but appear to have been missed out in others (Bereza et al., 2013).

Sonication has been described previously as a method for removing viable bacteria cells from orthopaedic implant surfaces (Takahashi et al., 2010; Trampuz et al., 2007; Tunney et al., 1998, 1999).

Trampuz *et al*. (2007), describe the use of sonication to remove material from the prosthesis to then carry out culture approaches for the diagnosis of hip and knee orthopaedic infections, thus highlighting the viability of bacterial cells after sonication treatment.

A problem with microbiome analysis when dealing with primary samples is host tissue contamination (Lim et al., 2014), leading to inefficient sequencing as reads may be derived from host DNA, inducing false positives and complicating molecular findings (Zimmerli et al., 2004). To counter this problem microbial enrichment can be performed, as previously described (Feehery et al., 2013). This enrichment method has previously been successfully applied to partition human DNA from other DNA sources including plant and microbial DNA (Feehery et al., 2013; Yigit et al., 2014; Zheng et al., 2014).

The number of identified species from the infected prostheses studied here was less than those identified in published studies employing PCR approaches (Bereza et al., 2013; Dempsey et al., 2007). Dempsey *et al*. (2007), identified a total of 16 bacterial genera/groups from 10 infected prosthetic hips using 16S rRNA gene sequencing (Dempsey et al., 2007). However, direct comparison of numbers is not possible as all infections are different and with the small sample size used here.

The identification of *S. aureus* (Table 2-6) corresponds with previous observations highlighting staphylococcal species as a primary cause of orthopaedic infections (Dempsey et al., 2007; Esteban et al., 2010; Montanaro et al., 2011; Zimmerli et al., 2004).

Enterococcus faecium was also identified in a sample; it has previously been isolated from prosthetic joint infections (Tornero et al., 2014). Interestingly, the hospital microbiology lab result for this sample, identifying *Staphylococcus caprae*, did not match our result, possibly a miss-identification or both organisms were present in polymicrobial infection. Sequencing results presented here represent a small fraction of genome coverage and therefore the identification based on the sequence data here may be inaccurate.

The intestinal pathogen, *C. difficile* was detected as a secondary organism present at low levels in two samples (Table 2-6). *C. difficile* has been previously associated with orthopaedic surgery causing infection in patients undergoing antibiotic prophylaxis (Jenkins et al., 2010; Kakwani et al., 2010) and is a common nosocomial pathogen (Khanna and Pardi, 2012).

Simultaneous infections of *S. aureus* and *C. difficile* have previously been reported to be the cause of Pseudomembranous Intestinal diseases, resulting in antibiotic treatment failure (Froberg et al., 2004). Furthermore, a number of *C. difficile* infection cases have been reported as secondary infections following a wound infection, often caused by faecal contamination (Mattila et al., 2012, 2013). A secondary pathogen may cause increased pathogenicity and virulence of other pathogens and as little as 7 spores/cm^2 of *C. difficile* have been shown to induce infection in murine models (Lawley et al., 2009).

The presence of a polymicrobial infection could be resulting in increased pathogenicity. A study by Moran *et al.* (2007), reviewing patients admitted with prosthetic joint infections to one unit over a 64 month period, looked at the microbial spectrum of infection through traditional microbiology approaches. They show 37% of 112 patients were found to have polymicrobial infections (Moran et al., 2007).

Furthermore, the identification of the presence *C. difficile* may influence the antibiotic therapy chosen, due to the risk of antibiotic-associated diarrhoea caused by *C. difficile* (Khanna and Pardi, 2012), generally when broad spectrum antibiotics are administered (Wistrom et al., 2001). If *C. difficile* is found to be present, an antimicrobial treatment less likely to promote *C. difficile* infection may be considered (Gerding et al., 2008). Low numbers of *C. difficile* reads

equate to a low level of relative abundance and a small coverage of the genome (Table 2-6). Environmental contamination from the operating theatre or laboratory could account for this result. However, environmental contamination can present an infection risk and be the cause of secondary infections (Dancer, 2004); therefore such results still have high clinical relevance. *C. difficile* is used as an indicator species from hospital hygiene standards if detected above a certain level, a quantitative aerobic colony count of <5 CFU/cm^2 (Dancer, 2004).

Low numbers of microbial reads in samples and reads matched to the human genome indicate the enrichment protocol was not efficient at removing all contaminating host DNA. A reason for this may be from sonication treatment lysing host cells and shearing host DNA, an application of sonication (Deininger, 1983), meaning only methylated parts of the DNA were removed leaving sheared non-methylated parts of host DNA. Furthermore, it has been suggested that bacteria may be more sensitive to sonication if they are stressed by both the removal during surgery, and the transportation to the laboratory, after living *in vivo* (Tunney et al., 1999).

Alternative methods could be applied to avoid shearing the host DNA, discussed further in section 2.5.1.1. Finally, unaligned reads in the analysis are most probably due to errors in the sequence, a common result of next generation sequencing studies (Schirmer et al., 2015).

Here, through using microbiome sequencing approaches compared to conventional culturing approaches, different species of bacteria were identified as the cause of the orthopaedic infection. This observation is significant when considering antimicrobial therapy. Risks are associated with the use of broad spectrum antibiotics, which are commonly prescribed in these cases, due to unspecific action. If more is known about the primary causes of infection antimicrobial therapy tailored to orthopaedic infection cases could be designed. Furthermore, as demonstrated here such infections can exist as polymicrobial communities containing multiple species of bacteria favouring the use of a broad spectrum antibiotic. In such cases broad spectrum antibiotics may be the preferred choice but selection can be guided by the understanding of what species are present, therefore not exacerbating resistance or altering the bacteria important to the natural flora.

We show that metagenome sequencing of the microbiome of the infected hip prosthesis can be used as a way to detect present pathogens in polymicrobial communities and confirms *S. aureus* as primary orthopaedic infection pathogen.

2.5.1.1 Microbiome study future steps

Method optimisation would certainly be a future step for the approach presented here, looking at alternative sample preparation approaches. Alternatives to sonication for material extraction, for example surface scraping of the implant surface, as previously described by Takahashi *et al.* (2010), should be explored. Removal of host material before extraction may circumvent the need for microbial DNA enrichment. Lim *et al.* (2014), describe complications with human DNA contamination in Cystic Fibrosis sputum samples (Lim et al., 2014). They describe a method through which they use DNase I prior to DNA extraction, thus breaking down host DNA before carrying out a DNA extraction on the microbes present (Lim et al., 2014). Direct DNA extraction from the implant surface might also be possible. Finally, a larger study employing a much larger cohort of samples will allow conclusions on causative species to be made.

2.5.2 Characterisation of LHSKBClinical

Due to the prevalence of staphylococcal species identified as a primary cause of orthopaedic infections, a clinical isolate of *S. aureus* was obtained from a different orthopaedic infection to the ones used in the microbiome study for this PhD project and biofilm studies. LHSKBClinical (Stipetic et al., 2015), a novel previously un-typed *S. aureus* isolate confirmed by genome analysis was characterised and sequenced confirming species identification as *S. aureus* after transportation and re-culturing in the laboratory. The genome was annotated, giving encoded protein information.

Biofilm formation on the implant surface is associated with the onset of orthopaedic infections and subsequent implant failure (Esteban et al., 2010; Smith et al., 2008; Zimmerli et al., 2004); therefore, genes associated with biofilm formation were looked for. Genes encoding proteins associated with biofilm formation were annotated from the genome. These included polysaccharide intracellular adhesion (PIA) proteins, icaA and icaD, previously

described (Resch et al., 2005). Biofilm formation requires cell to cell adhesion which has been shown to involve PIA (Cramton et al., 1999). Cramton *et al.* (1999) investigated numerous *S. aureus* strains and found them all to contain the *ica* locus. When the *ica* locus was deleted they found the strains lost the ability to form biofilms and produce PIA (Cramton et al., 1999). In addition to this, *sarA*, another gene implicated in biofilm formation by *S. aureus* (Beenken et al., 2003, 2004), was also found to be in the genome. It has been shown that mutation in the *sarA* gene limits the production of the biofilm phenotype by *S. aureus* (Beenken et al., 2003). Moreover, *fnbB* was found to be present in the genome, perceived as a possible genetic marker for biofilm formation (Lim et al., 2013).

Additionally, several genes encoding *S. aureus* virulence factors including exotoxins or superantigens were annotated. Super-antigen-encoding *S. aureus* pathogenicity islands (SaPI), a known virulence factor of *S. aureus* implemented in exacerbating pathogenicity (Lindsay and Holden, 2004; Novick, 2003) was also found.

Secondary metabolite biosynthesis gene clusters were also looked for that may play a crucial role in the metabolism and pathogenicity of this isolate. Results indicated the presence of siderophores, terpene, NRPS, lantipeptide and bacteriocin gene clusters. Terpene metabolites are plant or fungal metabolites, however a number have been detected with bacterial origin but not including *S. aureus* (Yamada et al., 2015). Siderophores (Dale et al., 2004), lantipeptides, bacteriocins and NRPSs play a role in the virulence of *S. aureus*. *S. aureus,* like most other microorganisms, require iron for growth. To establish successful growth and infection in the human body bacteria have to overcome iron restriction. Low concentrations of free iron in the human body are too low to support infection (Braun et al., 1998). A common mechanism employed by bacteria to overcome this deficit is through siderophores. Siderophores are high-affinity iron chelators. There iron chelators compete with the hosts iron-binding glycoproteins. Bacteriocins and lantipeptides are ribosomally synthesised peptides produced by Gram-positive bacteria with antimicrobial properties (Hofmann et al., 2012; Varella Coelho et al., 2007; Willey and van der Donk, 2007). NRPSs are bacterial secondary metabolites found in microorganisms,

examples of which are found in *S. aureus*, were they have been found to regulate virulence factor expression (Wyatt et al., 2010).

The LHSKBClinical isolate and corresponding genome provides a novel sequence type for this species and a reference genome for *S. aureus* isolated from an orthopaedic infection. This isolate could be further utilised in future pathogenicity, virulence factor and biofilm studies of *S. aureus*.

2.5.3 *In vitro* biofilm studies of LHSKBClinical

Biofilm studies show that LHSKBClinical can form biofilms *in vitro* therefore we can accept our hypothesis that LHSKBClinical produces biofilms *in vitro* allowing for future orthopaedic infection studies.

Due to the ability of *S. aureus* strains to grow in BHI media in both a planktonic and biofilm state, this media was selected as the media of choice throughout this project. Smith *et al*. (2008), screened and differentiated approximately 1000 clinical isolates for biofilm forming capabilities in different media types, concluding that BHI, a nutrient rich media, was the best for biofilm formation and growth (Smith et al., 2008). The biofilm formation capability of LHSKBClinical in BHI was tested (Figure 2-5). This assay was carried out under static conditions were biomass was determined through employing a CV assay and SEM imaging, correlating with the reported characteristics of a biofilm: adhered three-dimensional structures with ECM production (Flemming and Wingender, 2010; McDougald et al., 2012; O'Toole et al., 2000; Stewart and Costerton, 2001). However, the level of ECM production looks low, this may be due to the static culturing method utilised here or the effect of drying during SEM sample processing. Biofilm formation can occur under static conditions but it has been shown that biofilm biomass can increase when cultured under dynamic conditions (Weaver et al., 2012; Yarwood et al., 2004). In addition, the CV assay of static biofilm formation will show the increase in biofilm biomass over time in parallel samples as the assay is not a live assay. Therefore, it is challenging to resolve the separate stages of biofilm formation with this assay.

It is important to note that static conditions for biofilm cultivation will also alter oxygen availability. Differences between aerobic and anaerobic conditions can

alter bacterial metabolism and may subsequently alter biofilm formation. This represents a future developmental step for biofilm cultivation studies carried out here, using dynamic cultures to create an aerobic environment.

However, for the ease of culturing biofilms for future experiments in this PhD project, static conditions were always utilised allowing for easily scaled up experiments and multiplexing of simultaneous replicates through using a multi-well plates, as previously shown (Lopez-Ribot, 2014; Pierce et al., 2008; Srinivasan et al., 2013). Cultivating biofilms in the 96-well plate format as described here has previously been published for use in biofilm investigations (Christensen et al., 1985; Merritt et al., 2005; O'Toole, 2011; Otto, 2008).

The methods used here provide a quick, easy and inexpensive way to cultivate *S. aureus* cells and biofilms *in vitro*. These methods of biofilm cultivation and analysis will be utilised throughout this PhD project for studying the changing and altered phenotype of biofilm formation by LHSKBClinical.

2.5.4 Conclusions

Here we carried out microbiome analysis of the infected hip prosthesis, providing a preliminary metagenome sequencing study showing the species that cause orthopaedic infection. Metagenome sequencing has the capability to provide identification of bacterial species from orthopaedic infections. In addition, although not explored here because of a low number of microbial reads due to host DNA contamination, metagenome analysis can give strain, gene and encoded protein information. This extra information can allow for conclusions to be made about virulence and pathogenicity, for example the presence of genes responsible for biofilm formation. Important considerations in sample preparation for metagenome analysis have been explored here, with an emphasis on the care not to shear host DNA to ensure efficient enrichment.

The identification of *S. aureus* in one of the samples tested here provides evidence that staphylococcal species can be responsible for orthopaedic infections. In addition, the identification of secondary pathogens highlights the potential for these infections to be polymicrobial. Additionally, many of these secondary pathogens were not identified in the initial hospital laboratory

analysis of the aspirate. This further demonstrates the discrepancy between species identification methods which rely on *in vitro* culture, and more sensitive, genomic methods which do not rely on the ability to culture the organism for identification.

Secondly, we aimed to characterise a clinical isolate of *S. aureus* taken from an orthopaedic infection case. LHSKBClinical was successfully sequenced with a draft genome established (Stipetic et al., 2015). Using the draft genome sequence, genes involved in biofilm formation were identified. Through *in vitro* microbiological approaches, the biofilm formation capabilities of LHSKBClinical were evaluated. This isolate will give us a reference strain for orthopaedic infections and can be used for future staphylococcal biofilm studies.

Chapter 3 A novel metabolomics approach used for the comparison of *Staphylococcus aureus* planktonic cells and biofilm samples targeting biofilm purine metabolism

Sections of this chapter have been submitted for publication (Appendix II)

3.1 Introduction

S. aureus biofilm formation has been attributed to a number of diseases including orthopaedic infection and implant failure (Esteban et al., 2010; Smith et al., 2008; Zimmerli et al., 2004). Understanding the molecular mechanisms involved in biofilm formation can lead to greater understanding of biofilm growth and may lead to novel treatment strategies. Metabolomics is a tool which can allow the molecular mechanisms of biofilm formation to be explored. Metabolism and associated biochemical processes are a vital part of bacterial cell growth. Changes incurred during biofilm formation and molecules synthesised contribute to the virulence of *S. aureus* (Liebeke et al., 2011). Such virulence factors are potential drug targets. Metabolites directly involved in energy metabolism and signalling pathways can change in response to planktonic or biofilm growth so their study and identification may lead to further insight into the pathogenicity of *S. aureus* (Archer et al., 2011; Bien et al., 2011; Wyatt et al., 2010).

Metabolomic approaches can be applied to measure the metabolic profile of a system, such as a bacterial cell (Fiehn, 2002). Through utilising untargeted metabolomics the chemical effects across cellular metabolism can be studied (Nicholson and Lindon, 2008). Metabolomic investigations include drug mechanism of action studies, clinical diagnostic biomarker discovery and the identification of novel drug targets aimed at biofilm dispersal.

Previous studies have applied metabolomic approaches to investigate bacterial cell metabolism (Liebeke et al., 2012; Tang, 2011), however, significant constraints in sample preparation and processing have had to be addressed. Microbial metabolome extraction and metabolic quenching methods have a number of associated problems including metabolite degradation, inadequate quenching of metabolism during extraction, media contamination, and failure to lyse the bacterial cell (Bolten et al., 2007; de Koning and van Dam, 1992). Moreover, the lysis and extraction methods of a number of earlier studies that have focussed on Gram-negative bacteria are unsuited to Gram-positive bacteria due to the presence of a peptidoglycan cell wall (Maharjan and Ferenci, 2003).

In addition, many bacteria also have the capacity to form biofilms (O'Toole et al., 2000). Adherent cells are encased in an extracellular matrix (ECM), protecting bacteria by providing a physical barrier to the external environment. Mature *S. aureus* biofilm formation occurs from 17 h to 24 h, as shown in chapter 2 and by Moormeier *et al.*, (2014), so for experiments here 24 h was selected for biofilm cultivation. For planktonic cell culture, the transition from exponential cell growth to stationary phase growth for this strain of *S. aureus* generally occurs around 24 h, as shown in chapter 2, so this was selected as a time point for planktonic cell culture in experiments carried out here.

The protective nature of the biofilm complicates the ability to extract the intracellular metabolome from indwelling bacteria, as well as making them recalcitrant to antimicrobial chemotherapy (Drenkard and Ausubel, 2002; Ramage et al., 2003). These factors make the metabolic analysis of Gram positive cells and biofilms problematic, with published metabolite quenching and extraction methods unsuited to biofilm analysis due to a number of factors including metabolite leakage during quenching and the need for pre-removal of the biofilm from the surface.

Cells in a biofilm growth state display an altered phenotype and biochemistry in comparison to free floating planktonic cells, with changes observed at multiple levels of regulation, including: transcriptomic; proteomic; and metabolomic changes (Gjersing et al., 2007; Resch et al., 2005, 2006; Zhang and Powers, 2012; Zhu et al., 2007). Changes in metabolism subsequently alter the metabolic profile of the bacteria (Gjersing et al., 2007).

There have been published metabolomic analyses utilising NMR spectroscopy to study the molecular differences between planktonic cells and biofilms. These have revealed interesting changes in a number of fundamental metabolic pathways including amino-acid metabolism (Ammons et al., 2014; Gjersing et al., 2007; Zhang and Powers, 2012). However, NMR has low resolution compared to LC-MS approaches; therefore results present low metabolome coverage (Zhang and Powers, 2012).

3.2 Aims

The aims of this project were to:

1. Develop a metabolome extraction method for staphylococcal planktonic cells and biofilms for LC-MS metabolomics.

2. Characterise and compare the metabolome of a clinical isolate of *S. aureus* in planktonic or biofilm states using LC-MS.

3. Target pathways that have displayed an altered metabolic profile between planktonic and biofilm growth states, to look for novel biofilm modulation methods.

Through the development and optimisation of a direct metabolome extraction method for Gram-positive bacterial cells and biofilms, we aim to characterise and compare the metabolome of the clinically important bacterium, *S. aureus,* living in a planktonic or biofilm state, using LC-MS. Utilising untargeted metabolomics we aim to demonstrate the reproducibility of the method and highlight differences in metabolism between the two growth states. Due to the lack of studies and methodologies to study biofilm metabolism, we hypothesise that with the developed metabolome extraction method significant changes in metabolism will be observed between planktonic cells and biofilms.

Following this, we aim to target pathways that have displayed an altered metabolic profile between planktonic and biofilm growth states by spiking in metabolite intermediates, flooding metabolic pathways, or by using small molecule analogues, to look for novel biofilm modulation and biofilm dispersal targets. We hypothesise that biofilm formation will be altered by modulating these metabolic pathways.

3.3 Materials and Methods

3.3.1 Cell culture

The *S. aureus* clinical isolate LHSKBClinical, characterised in Chapter 2 of this thesis, was cultured as described in section 2.3.2.1.

3.3.2 Biofilm cultivation

In vitro biofilms of clinical isolate LHSKBClinical were cultivated as described in section 2.3.3.1.

3.3.3 Metabolome extraction from *S. aureus* planktonic cells

Reagents and chemicals were purchased at HPLC grade from Fisher Scientific, Loughborough, UK, unless stated otherwise.

Initially, an overnight stationary phase culture of LHSKBClinical was grown as described in section 2.3.2.1 in either a 50 ml falcon tube (Corning) or a 150 ml conical flask.

To compare different mechanical cell lysis methods, sonication and bead beating were tested against *S. aureus* planktonic cells. To do this, 1 ml of cell culture was added to 1.5 ml reaction tubes. To the bead beating samples, 0.1 mm acid washed glass beads (Sigma-Aldrich) (1 g of beads to 1 ml of cell culture) was added. Reaction tubes were then either placed on a cell disrupter, Disrupter Genie® bead beater (Scientific industries, Inc., New York, USA), operating at a speed of 3000 RPM, at 4°C, for 5-10 mins or placed in a sonication bath as described in section 2.3.1.2, with ice and water and sonicated for 30 mins. Samples were then vortexed briefly and CFU counts were performed as described in section 2.3.2.3.

To compare different metabolome extraction methods, three alternative methods of metabolome extraction from *S. aureus* planktonic cells were tested. A filter (Soga et al., 2002, 2003), a sonication (Takahashi et al., 2010) and a bead beating (Liebeke et al., 2011, 2012) method were compared. Modifications to the published methods were made. These included: extraction solvents were

altered to a chloroform/methanol/water 1:3:1 mix; and water/PBS washes were replaced with 10 mM ammonium bicarbonate to ensure differences between the methods were due to lysis rather than extraction solvent. Sonication was altered from 30 s probe sonication to 30 mins bath sonication to minimise heating and provide compatibility with microtitre plate extractions.

A filter method described by Soga *et al.* (2002) and (2003), was utilised (Soga et al., 2002, 2003). Briefly, 10 ml of stationary phase culture was passed through a 0.45 µm pore size Whatman™ filter (Sigma-Aldrich) using a Nalgene 250 ml filter unit (Thermo-scientific) attached to a vacuum pump. Cells on the filter were then washed with 10 ml of 10 mM ammonium bicarbonate (Sigma-Aldrich). Following washing, the filter was removed and placed in a 15 ml falcon tube (Corning) where 5 ml of 10 mM ammonium bicarbonate was used to wash and detach cells from the filter. Cells were then centrifuged at 1900 xg for 5 mins at 4°C, discarding the supernatant. The cell pellet was resuspended in 1 ml ice cold metabolite extraction solvent mix consisting of chloroform:methanol:ddH_2O at a ratio of 1:3:1, described by (t'Kindt et al., 2010), and incubated at room temperature, shaking, for 5 mins.

A sonication method adapted from Takahashi *et al.*, (2010), was utilised. Briefly, 10 ml of stationary phase culture was washed twice in 10 mM ammonium bicarbonate by centrifugation at 1900 xg for 5 mins at 4 °C. Cells were then resuspended in 1 ml of ice cold metabolite extraction solvent mix in 1.5 ml reaction tubes as described above. Samples were then sonicated for 30 mins in the sonication bath described in section 2.3.1.2 and then vortexed briefly.

Finally, a bead beating method adapted from Liebeke *et al.* (2011) and (2012), and developed here, was utilised. 10 ml of stationary phase culture was washed twice in 10 mM ammonium bicarbonate through centrifugation at 1900 xg for 5 mins at 4 °C. Cells were then resuspended in a 1 ml suspension of ice cold metabolite extraction solvent mix, as described above, with added glass beads, as described above (1 g of beads to 1 ml extraction solvent mix), in 1.5 ml reaction tubes. Reaction tubes were then placed on a cell disrupter for 10 mins as described above.

Following the alternative extraction methods CFU counts were performed as described in section 2.3.2.3, on the different sample extracts to measure extraction efficiency through viable cells remaining.

After CFU counting all samples were centrifuged at 1900 xg at 4°C for 10 mins, to pellet and remove cell debris, proteinaceous material and, in the case of the final extraction method, glass beads. The metabolome-containing supernatant was then transferred to a fresh reaction tube (Greiner Bio-One) and stored at -80°C until LC-MS metabolomic analysis. All extraction methods were carried out in triplicate.

For metabolomic comparison between planktonic culture (cells grown in a falcon tube at 37°C, 180 RPM) and biofilms (static cultivation at 37°C), the planktonic cell metabolome was extracted directly within the wells of a microtitre plate by pelleting 200 µl of stationary phase planktonic cells in the wells of a 96-well plate by centrifugation at 1900 xg at 4°C for 3 min. Spent media was removed and the cells were resuspended and washed in 10 mM ammonium bicarbonate by centrifugation at 1900 xg at 4°C for 3 min. The metabolome was then extracted by resuspending cells in 200 µl of glass beads and solvent solution, as described above and sealing the plate with a 96-well Cap Mat (Greiner Bio-One, Stonehouse, UK). 24 technical replicates were carried out for planktonic cell comparison to biofilms.

3.3.4 Metabolome extraction from *S. aureus* biofilms

For metabolome extractions from biofilms, biofilms were cultured for 24 h in 96-well plates as described in section 2.3.3.1. Biofilm samples were washed by submerging the plate in a beaker of sterile 10 mM ammonium bicarbonate and blotted to remove excess liquid. The biofilm metabolome was extracted directly *in situ* within the wells of a microtitre plate by adding 200 µl of glass beads and extraction solvent solution as described in section 3.3.3. A 96-well Cap Mat was then used to seal the plate and the plate was bead beaten on the cell disrupter described in section 3.3.3, for 10 min. Following bead beating the plate was centrifuged at 1900 xg at 4°C for 10 min, to remove beads and cell debris. The metabolome-containing supernatant was then transferred to a fresh reaction tube (Greiner Bio-One) and stored at -80°C until LC-MS metabolomic analysis.

Metabolome extractions from biofilms for the comparison of planktonic cells to biofilms represent one experiment with 24 technical replicates intended to demonstrate the utility of the method.

3.3.5 Liquid metabolite extraction

For a liquid metabolite extraction from BHI to analyse purine content, 5 µl of fresh BHI was added to solvent mix as described in section 3.3.3 and vortexed briefly. Samples were then stored at -80°C until LC-MS analysis.

3.3.6 Liquid Chromatography - Mass Spectrometry (LC-MS)

LC-MS analysis was performed as follows. Samples were analysed by hydrophilic interaction liquid chromatography (HILIC) coupled with mass spectrometry (LC-MS) (UltiMate 3000 RSLC, Thermo Fisher, San Jose, California, USA) using a 150 x 4.6 mm ZIC-pHILIC column (Merck SeQuant, Umea, Sweden) running at 300 µl/min and Orbitrap Exactive (Thermo Fisher) detection. Mass spectrometer parameters were: 50,000 resolving power in positive/negative switching mode. Electrospray ionisation (ESI) voltage was 4.5 kV in positive and 3 kV in negative modes. Buffers consisted of A: 20 mM ammonium carbonate in ddH_2O and B: Merck SeQuant: acetonitrile. The gradient ran from 20% A: 80% B to 80% A: 20% B in 15 min, followed by a wash at 95% A: 5% B for 3 min, and equilibration at 20% A: 80% B for 5 min.

3.3.7 Metabolomic data analysis and statistics

Raw mass spectrometry data was processed using our standard pipeline (Creek et al., 2012), consisting of XCMS (Smith et al., 2006) (for peak picking), MzMatch (Scheltema et al., 2011) (for filtering and grouping) and in-house R-scripts (for further filtering, post-processing and identification). Peaks were visualised using PeakML Viewer (Scheltema et al., 2011). Core metabolite identifications were validated against a panel of unambiguous authentic pure standards (Sigma-Aldrich) using accurate mass and R_t (error of 5 % was allowed), and could therefore be classified using the alphanumeric metabolite coding scheme as $HRMS_a^1$, R_{ta}, as described by Sumner *et al.* (2014). Additional putative identifications were assigned by accurate mass along with a R_t prediction

algorithm (error of 35 % allowed) (Creek et al., 2011) and as such were classified as $HRMS^{1}_{PL}$ (Sumner et al., 2014).

Quantile normalisation was carried out across the data, normalising both data sets (Bolstad et al., 2003). Once identified and filtered, detected peak intensities were logged (base 2) and quantitation was performed on sets of biological replicates by applying differential statistics to generate P values. Metabolites with apparently different levels were assessed using Bayes moderated t-tests (Smyth, 2004). Benjamini and Hochberg false discovery rate adjustment for multiple testing was applied (Hochberg and Benjamini, 1990) and the resulting data was used to query the KEGG (Kyoto Encyclopaedia of Genes and Genomes) database for pathway analysis (Kanehisa and Goto, 2000). This was then cross-referenced to enzyme annotations for *S. aureus* and the available genome sequence for this isolate, described in section 2.4.2.4, to ensure the enzymes and subsequent metabolic pathways assigned were present in this isolate.

Comparative metabolomic analysis of extraction methods was further processed using the IDEOM software (Creek et al., 2012), without normalisation applied.

3.3.8 Metabolomic data presentation

Statistics, including principal component analysis (PCA), were performed and presented using R, employing appropriate standard R libraries and Microsoft Excel. ChemDraw Std version 14.0 was used to draw metabolic pathways and GraphPad Prism 4 and Microsoft® Excel were used to create figures.

3.3.9 Testing purine metabolites for biofilm modulation effects

All reagents and chemicals were purchased from Sigma-Aldrich, Dorset, UK, unless stated otherwise.

Stock solutions of inosine and adenosine in ddH_2O, adenine in boiling ddH_2O and hypoxanthine in 1N NaOH, were made and diluted in fresh BHI to make final working concentrations. 24 h biofilms of *S. aureus* were cultivated in the wells of a 96-well microtitre plate, as described in section 2.3.3.1. Following biofilm

growth, spent media was removed and biofilms were washed in ddH_2O as described in section 2.3.3.1, and blotted to remove excess liquid. Following washing, concentration ranges of inosine, adenine, hypoxanthine and adenosine, including controls with solvent only, were individually added to biofilms and then the samples incubated for 4 h at 37°C, in a static humidified incubator. Following incubation, excess purine solutions were removed and the biofilms were washed as above.

Inosine and hypoxanthine standards for LC-MS analysis were made to 100 µM in 80% acetonitrile (Fisher Scientific) in ddH_2O.

3.3.9.1 Crystal violet assay

The CV biofilm assay, as described in section 2.3.3.2, was used to quantify biofilms following treatment. Appropriate negative controls were utilised including biofilm samples treated with BHI only and biofilm samples treated with BHI containing the working concentration of NaOH solvent. Experiments were carried out in technical replicates of 4.

3.3.9.2 Scanning Electron Microscopy imaging

SEM imaging was used to visualise biofilm modulation caused by inosine and adenine. Biofilms were cultivated on Thermanox™ coverslips as described in section 2.3.3.1 and treated for 4 h with 10 mM final concentrations of inosine and adenine made as above. Biofilm samples were then washed as described in section 2.3.3.1, processed for SEM and imaged as described in section 2.3.3.3. As a negative control, biofilms were treated with BHI only containing ddH_2O and processed in parallel to purine treated samples. SEM samples were made in replicates of 3.

3.3.9.3 Quantitative PCR

Quantitative PCR (qPCR) was performed as described by O'Donnell *et al.*, 2015. Briefly, primers targeting the SAR0234 gene (L-lactate dehydrogenase), Forward-ATTTGGTCCCAGTGGTGTGGGTAT and Reverse- GCTGTGACAATTGCCGTTTGTCGT, were obtained from Prof. Gordon Ramage, Glasgow Dental School University of Glasgow. Oligonucleotide primers were made by Eurogentec (Southampton, UK).

Primers were previously checked for specificity to *S. aureus* and amplification efficiencies were optimised to be >90%.

Biofilm samples were cultured on Thermanox™ coverslips, treated with either inosine or adenine at 10 mM in BHI as described in section 3.3.9, and washed in ddH_2O as previously described in section 2.3.3.1. Following this, samples were sonicated for 5 mins in ddH_2O and placed in 7ml bijou bottles in a sonication bath as previously described in section 2.3.1.2, to remove material from the coverslip surface. After sonication treatment sonicate was placed in DNase free reaction tubes (Greiner Bio-One) and the DNA was extracted as described in section 2.3.1.3. As a negative control, biofilm samples were treated with BHI only and were processed in the same way as the other samples.

qPCR sample preparation was carried out by taking 200 ng of sample DNA and adding to a qPCR master mix consisting of SYBRR® GreenERTM (Life Technologies, Paisley, UK), RNase-free ddH_2O, and forward/reverse primers (10 µM). qPCR was then performed using the step one plus real-time PCR unit (Applied Biosciences, Paisley, UK), using the following programme: 50°C for 2 mins, 95°C for 2 mins, followed by 40 cycles of 95°C for 3 sec and 59°C for 30 sec. The StepOne software V2.3 (Life Technologies) was used to analyse the data and calculate the Ct values by taking the baseline threshold value of the samples and adjusting to correspond with the equivalent standard curve. Standard curves of Ct versus known cell densities were created from qPCR analysis, as above. Known cell densities were created by serial two-fold dilutions of the *S. aureus* isolate LHSKBClinical, allowing cell density approximations to be calculated for each sample. Three biological replicates with 3 technical replicates each were performed with different biofilm cultures and DNA extractions performed. As a qPCR negative control, samples containing master mix only with no added DNA were run in parallel to other qPCR reactions and returned no detectable readings.

3.3.9.4 Minimum inhibitory concentration (MIC) testing of inosine and adenine

MIC testing of planktonic *S. aureus* cells treated with inosine and adenine was performed. MIC testing was performed by first making a metabolite dilution in a

round-bottom 96-well microtitre plate with sterile BHI starting at a metabolite concentration of 20 mM and decreasing 2-fold in concentration with each step. To prepare cells, an inoculum was made by taking *S. aureus* colonies from a BHI agar plate and resuspending in BHI until an OD_{595} of 0.1 was reached. A 1 in 100 dilution was made of the inoculum and 50 µl was added to each well containing 50 µl of the different metabolite concentrations, thus making final concentrations of 10, 5, 2.5, 1.25, 0.63, 0.31, 0.16, 0.08, 0.04, 0.02 and 0 mM. The 0 mM samples had BHI only added and acted as a negative control. The plate was then incubated overnight at 37°C with shaking at 50 RPM. After incubation the contents of each well was transferred to a sterile flat-bottom 96-well microtitre plate and the OD_{595} was measured using the plate reader, as previously described in section 2.3.2.2, with fresh BHI used as a blank to normalise readings. Results were recorded and an inhibitory concentration graph plotted. Eight technical replicates were performed.

3.3.9.5 Metabolomics of biofilms treated with exogenous metabolites

For metabolomics, biofilms were cultivated and treated with 10 mM inosine and adenine on Thermanox™ coverslips as above. Following inosine and adenine treatment, coverslips were washed in 10 mM ammonium bicarbonate as described in section 2.3.3.1 and placed in a sterile 7 ml Sterilin™ bijou (Thermo-Scientific). Metabolite extraction was carried out as previously described in section 3.3.4 by adding 1 ml of metabolome extraction solvent mix and glass-beads to each bijou. The bijous were then bead beaten as described in section 3.3.4, after which all contents of the bijou was transferred to a 1.5 ml reaction tube (Greiner Bio-One) and centrifuged at 1900 xg at 4°C for 10 min, to remove beads and cell debris. The metabolome-containing supernatant was then transferred to a fresh reaction tube (Greiner Bio-One) and stored at -80°C until LC-MS metabolomic analysis. Metabolomic extractions were performed in replicates of 3. As a negative control extractions were performed on biofilms treated with BHI only containing ddH_2O.

LC-MS, data analysis and data presentation was performed as described in sections 3.3.6, 3.3.7 and 3.3.8, respectively.

3.3.10 Biofilm DNase treatment

24 h biofilms cultivated on Thermanox™ coverslips, treated with and without 10 mM inosine, were challenged with DNase I from bovine pancreas (Sigma-Aldrich) using the same method as previously described by Rajendran *et al.*, 2013. Concentrations of DNase including, 0.125, 1 and 4 mg/ml were prepared in 0.15 M NaCl supplemented with 5 mM $MgCl_2$. Samples were incubated overnight at 37°C with a non-treated buffered sample used as a negative control. Following DNase treatment, coverslips were removed and washed in ddH_2O as described in section 2.3.3.1. The CV assay described in section 2.3.3.2 was then used to quantify the biofilms. Non DNase-treated biofilm samples treated with and without 10 mM inosine were used as negative controls. Percentage biofilm biomass was calculated by calculating the biomass of biofilm after varying treatment conditions as a percentage of non DNase-treated biofilms.

3.3.11 Formycin B

3.3.11.1 *S. aureus* biofilm formycin B treatment

A structural analogue of inosine, formycin B (Berry & Associates, Dexter, MI, USA) was tested for biofilm modulation effects. *S. aureus* biofilms were cultivated for 24 h in a 96-well microtitre plate and washed as described in sections 2.3.3.1 and 3.3.4, respectively. A stock solution of inosine in ddH_2O was added to BHI to a final concentration of 10 mM, as described in section 3.3.9, and a stock solution of formycin B in ddH_2O was also made to a final concentration of 10 mM in BHI. These were then added to biofilm samples separately and together. Biofilm samples were incubated for 4 h and analysed using a CV assay (2.3.3.2). As a negative control BHI only was added to parallel samples and percentage change in biofilm biomass by comparing treated and non-treated biofilms was calculated. Three technical replicates were performed.

3.3.11.2 Minimum inhibitory concentration (MIC) testing of formycin B and gentamycin

MIC experiments of formycin B and gentamycin in planktonic *S. aureus* cells were carried out as described in section 3.3.9.4. Final concentrations of formycin B in BHI tested included; 0, 0.0098, 0.0195, 0.0391, 0.0781, 0.1563 0.3125, 0.6250,

1.25, 2.5, 5, and 10 mM. The 0 mM samples had BHI only added and acted as a negative control. For the gentamycin MIC, gentamycin solution at 50 mg/mL in deionized water was purchased from Sigma-Aldrich. Final concentrations of gentamycin in BHI tested included; 0, $4x10^{-11}$, $4x10^{-10}$, $4x10^{-9}$, $4x10^{-8}$, $4x10^{-7}$, $4x10^{-6}$, $4x10^{-5}$, $4x10^{-4}$, $4x10^{-3}$, and $4x10^{-2}$ mg/ml. The 0 mg/ml samples had BHI only added and acted as a negative control.

For both MIC experiments the 96-well microtitre plate was incubated overnight at 37°C with shaking at 50 RPM. After incubation, the contents of each well for the gentamycin MIC and 50 µl for the formycin B MIC experiment was transferred to a sterile flat-bottom 96-well microtitre plate and the OD_{595} was measured using the plate reader, as previously described in section 2.3.2.2, with fresh BHI used as a blank to normalise readings. Results were recorded and an inhibitory concentration graph plotted. Three technical replicates for the formycin B MIC and eight technical replicates for the gentamycin MIC were performed.

3.3.11.3 Gentamycin treatment of biofilms

S. aureus biofilms were cultivated for 24 h in a 96-well microtitre plate and washed as described in sections 2.3.3.1 and 3.3.4, respectively. Gentamycin was added at varying concentrations in fresh BHI. Final gentamycin concentrations of; 0, $2x10^{-9}$, $2x10^{-8}$, $2x10^{-7}$, $2x10^{-6}$, $2x10^{-5}$, $2x10^{-4}$, $2x10^{-3}$, $2x10^{-2}$, 0.2, 2, and 20 mg/ml were tested. Biofilm samples were incubated overnight at 37°C, and analysed by CV assay (2.3.3.2). As a negative control BHI only (0 mg/ml gentamycin samples) was added to parallel biofilm samples. Eight technical replicates were performed.

3.3.11.4 Biofilm antibiotic synergistic experiments

S. aureus biofilms were cultivated for 24 h in a 96-well microtitre plate and washed as described above. Varying gentamycin solution concentrations in BHI were added as described in sections 3.3.11.2 and 3.3.11.3 to biofilms with and without 10 mM formycin B as described in section 3.3.11.1. Biofilm samples were incubated overnight at 37°C and washed as described in sections 2.3.3.1 and 3.3.4, respectively, and analysed by CV assay (2.3.3.2). As a negative control BHI only was added to parallel samples. Three technical replicates were performed.

3.3.12 Statistics and data presentation

Data was presented using Microsoft® office programmes; PowerPoint and Excel. GraphPad Software, Prism V4, was used for statistical analysis. ChemDraw Std version 14.0 was used to draw and create molecules.

3.4 Results

3.4.1 Method development for metabolome extraction from *S. aureus* planktonic cells and biofilms

This work has been submitted for publication (Appendix II).

For efficient metabolome extraction from Gram-positive bacteria the peptidoglycan coat of the cell must be lysed. Bead beating can be used to lyse Gram-positive cells: here, the method was optimised using 0.1mm beads, as recommended for bacterial species by the cell disrupter manufacturer's guidelines (Scientific industries, inc, New York, USA). Through applying bead beating to planktonic cell culture, initial studies show that 10 min induced significant cell death compared to 30 min sonication bath treatment ($P<0.009$), and further viable cell reduction compared to 5 min bead beating ($P<0.002$) (Figure 3-1). Increasing bead beating time can have detrimental effects on metabolome samples due to motor heating from the cell disrupter; here, the disrupter was maintained at 4°C. After 30 min sonication treatment an increased viable cell count was observed compared to the control thus giving >100 % viable cell count in some sample replicates, however replicates displayed large variation (Figure 3-1). It can be concluded that sonication treatment is unsuitable for Gram-positive cell lysis and 10 mins bead beating causes significant cell death (Figure 3-1).

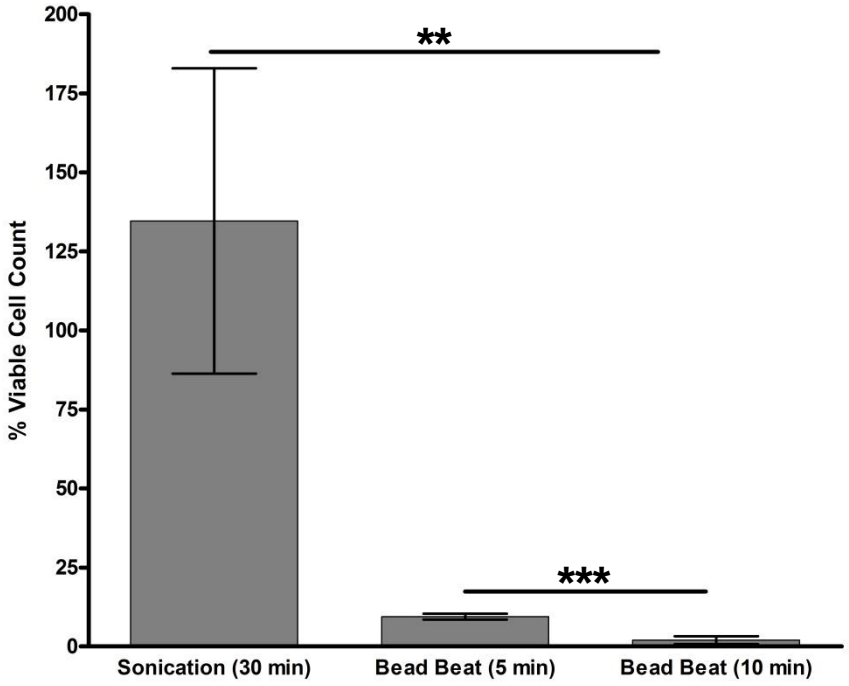

Figure 3-1: Bead Beating induces significant cell death.
Percentage viable colony forming unit (CFU) counts post sonication bath treatment for 30 min or bead beating for 5 or 10 min, with beads added to overnight *S. aureus* cell culture at a ratio of 50:50, compared to overnight starting cell culture colony forming unit counts. Bead beating for 10 min compared to 5 min significantly reduces the viable cell count (Unpaired t tests, bead beat for 5 min compared to 10 min percentage viable cell count, ***P=0.0012 and sonication bath treatment for 30 min compared to 10 min bead beating, **P=0.0089). Error bars ± S.D. (n = 3).

Once mechanical bead beating to lyse planktonic *S. aureus* cells was optimised, 10 mins bead beating was coupled with a metabolite extraction solvent mix containing chloroform: methanol: ddH_2O, at a ratio of 1:3:1, subsequently quenching metabolism. The solvent mix was added ice cold to further quench metabolism and prevent degradation of labile intermediates. As a relatively polar solvent, methanol is appropriate for extraction of small organic molecules. Chloroform is added for hydrophobic metabolite extractions, for example lipid compounds in the sample. In addition, the high organic solvent concentration is effective at precipitating out macromolecules, such as proteins and nucleic acids.

To compare different Gram-positive bacterial cell extraction methods, 3 approaches were compared. A filtering, sonication and bead beating method, coupled with the extraction solvent mix, were compared using CFU counts and LC-MS analysis. CFU counts showed no viable cells remaining after using any of the described methods (data not shown). By LC-MS analysis average signal intensities of the metabolites from each method showed no significant difference between the lysis methods (Figure 3-2). However, further analysis revealed that the filtration method resulted in an overall decrease in signal intensity of identified ($HRMS_a^1$, R_{ta}) metabolites, compared to bead beating results. In the data 84 metabolites were identified ($HRMS_a^1$, R_{ta}), where 31 were significantly lower in intensity while only 3 were significantly higher between bead beating and filtration. Similar overall results were achieved with the bead beating and sonication methods (Appendix III). Additionally, the bead beating method showed less variation between replicates compared to the other two methods.

Metabolite identifications can be classed as identified or annotated. Identified metabolite identifications ($HRMS_a^1$, R_{ta}) have been matched by R_t and molecular mass to an authenticated standard run in parallel to the samples. Annotated metabolite identifications ($HRMS_{PL}^1$) have not been matched to standard but to a molecular mass from a data base entry. Further peak fragmentation to elucidate exactly what compound has been detected would be required for further annotation. Although they are not conclusive identifications due to the occurrence of isomers with the same molecular mass, annotated metabolite

identifications can provide additional confidence in the detected pathway changes.

Figure has been removed due to Copyright restrictions.

Figure 3-2: Comparison of 3 Gram-positive bacterial metabolome extraction methods by LC-MS.
For planktonic cells, bead beating for 10 mins was compared to filtration and 30 mins sonication, coupled with metabolite extraction using chloroform, methanol, water (1:3:1). Average peak intensities were established by taking the average of the peak intensities between the sample replicates. No significant difference in the average metabolite peak intensities between the methods was seen. Error bars ± S.D., n=3.

For analysis using the LC-MS metabolomics platform used here, a minimum sample volume of 10 µl is required, with a minimum metabolite concentration in the micromolar range for small molecules (dependent on the molecule studied) (Gross, 2011). We are able to demonstrate here that in the 96-well microtitre plate format, the biomass of biofilm adhered to the base of a well provided sufficient material for LC-MS analysis.

Ammonium bicarbonate was selected as a LC-MS appropriate and compatible buffer, subsequently removing residual media but not leaving or depositing inorganic salts in the extraction leading to inefficient LC-MS analysis downstream, causing poor ionisation through creating blockages in the needle and skimmer (Mashego et al., 2007).

There was concern that the volume of solvent and beads added to lyse and extract the metabolome from the samples would dilute the metabolite concentrations below that of detectable limits for our LC-MS system, but with the results yielding the detection of hundreds of metabolites per well/biofilm, this highlights the effectiveness and utility of the method.

3.4.2 Metabolomics as a tool to explore *S. aureus* planktonic cell vs. biofilm metabolism

An initial study comparing the metabolic profile of planktonic cells and biofilms of LHSKBClinical was carried out. The study utilised the previously developed and optimised bead-beating metabolome extraction method.

3.4.2.1 Liquid chromatography-mass spectrometry (LC-MS) data analysis

This metabolomics study analysed a clinically relevant strain of *S. aureus* derived from an orthopaedic infection. Detailed metabolic analysis of this pathogenic organism living in a planktonic or biofilm growth state reveals significant metabolic differences; therefore we can reject the null hypothesis that there is no difference in metabolism between planktonic cell and biofilm growth.

Principal component analysis (PCA) of LC-MS metabolomic data sets, comparing planktonic cells and biofilm samples, revealed clustering of biological replicates (Figure 3-3), highlighting the reproducibility of the method. The plot also shows variation in detected metabolites between the planktonic and biofilm data. Principal components 1 and 2 (PC1 and PC2) are responsible for 78.4% and 10.91% of the variation, respectively. Furthermore, the plot shows an outlier in the biofilm data set, not clustered along PC2, highlighting the importance of having a number of replicates. From examining the data from this extraction replicate, it can be seen that relative abundance values display '0', with very low peak intensities of metabolites in the sample compared to other replicates in the set (see supplementary data, sample B20). This indicates an undetermined preparation problem with the sample or a problem with the injection of the sample into the liquid chromatography system. Data relating to this outlier were removed in further metabolomic comparisons and analyses.

Using the average peak intensities of aspartate as an example metabolite identification, and calculating the standard deviations between replicates of the sample groups, the reproducibility of the extraction method is shown by small standard deviation of the replicates within each group (Figure 3-4). This metabolite was also identified to be changing between the two groups and demonstrates that there is a clear discrimination between the two groups, shown by non-overlapping standard deviations (Figure 3-4).

Figure has been removed due to Copyright restrictions.

Figure 3-3: Principal component analysis (PCA) plots of planktonic (blue) and biofilm (red) metabolomic data sets.
Samples generated utilising a 10 mins bead beating extraction method; beads in a 50:50 suspension in extraction solvent of chloroform; methanol; water (ratio 1:3:1), followed by liquid-chromatography-mass spectrometry. Red and blue data plots represent planktonic cells and biofilm

biological sample replicates, respectively. The arrow indicates an outlier in the planktonic cell data set not clustered along Principal component 2 (PC2).

Figure has been removed due to Copyright restrictions.

Figure 3-4: Aspartate average peak intensity in *S. aureus.*
The average peak intensities for features identified as aspartate taken across replicates of the *S. aureus* planktonic and biofilm sample sets. Error bars ± S.D. (n=24). *** Unpaired t-test, P<0.01.

In both extraction sample sets, 530 metabolites were identified ($HRMS^1_a$, R_{ta}) or annotated ($HRMS^1_{PL}$) with significant log_2 fold changes of >0.1 (adjusted P value of <0.05) (null hypothesis: there is no difference between planktonic cell and biofilm extractions, is rejected). Of these, 151 metabolites demonstrated a significant up-regulation in expression in planktonic cells compared to biofilms with log_2 fold changes of 1 to 8.53 and 177 metabolites were found to be significantly up-regulated in biofilms compared to planktonic cells, with log_2 fold changes of 1 to 6.25. The remaining 202 metabolites had log_2 fold changes <1.

Metabolites were identified ($HRMS^1_a$, R_{ta}) by matching mass and R_t to internal standards or annotated ($HRMS^1_{PL}$) by mass-matching to a database entry. Data analyses, including raw peak data, metabolite identification, planktonic compared to biofilm samples analysis, and R_t errors are shown in Appendix IV.

Identified and annotated metabolites were then matched to pathways defined by the KEGG database. 128 biochemical pathways demonstrated changes in expression of two or more metabolites between planktonic cells and biofilm samples. Table 3-1 lists these 128 pathways, which contained a minimum of two identified or annotated metabolites that demonstrated significant (P<0.05) changes in expression.

Table 3-1: **Metabolic pathways that have intermediate and end-product metabolites detected to display significant changes in intensity rates between *S. aureus* planktonic cells and biofilm samples.**

Table has been removed due to Copyright restrictions.

3.4.2.2 Identified differences in arginine metabolism between *S. aureus* planktonic cells and biofilms

One of the pathways that demonstrated significant changes when comparing planktonic cells to biofilms was arginine biosynthesis (KEGG pathway: 00220). Enzymatic information specific to the LHSKBClinical *S. aureus* isolate, from the available genome sequence (Stipetic et al., 2015) was included in the construction of the metabolic pathways (Figure 3-5). It was found that 5 identified and 4 annotated (total of 9) metabolites found here, are involved in this pathway (Table 3-2) (Figure 3-5). Of these, 7 metabolites (4 identified and 3 annotated) were seen to have significant ($P<0.05$) $\log_2$ fold changes between planktonic and biofilm sample sets. Peak annotation results of the 9 arginine biosynthesis metabolites detected in negative mode are listed in Table 3-2. Metabolites that were identified or annotated in both data sets could have a fold-change difference in intensity calculated (Table 3-2). These results suggest that flux through the arginine biosynthesis pathway is amplified in biofilms.

L-arginosuccinate was seen to be present in the planktonic data set only. The absence in biofilms may be because the metabolite is simply not present or because its concentration is below the limits of detection of our instrumentation. In the urea cycle, *S. aureus* can produce the enzyme arginine deiminase which catalyses the reaction between citrulline and arginine. This metabolic shunt allows cellular metabolism to bypass a section of the urea cycle to metabolise arginine directly from citrulline (Figure 3-5).

Table 3-2: Arginine biosynthesis metabolites identified from *S. aureus* planktonic and biofilm data sets

Table has been removed due to Copyright restrictions.

Figure has been removed due to Copyright restrictions.

Figure 3-5: Arginine metabolism (Urea cycle) in the *S. aureus* clinical isolate LHSKBClinical. Metabolites identified (bold) and annotated by LC-MS. Colour coding indicates $\log_2$ fold changes of metabolites identified and annotated from planktonic cell samples (overnight planktonic cells cultured at 37°C, shaking at 180 RPM) compared to biofilms (24 h biofilm cultivation, at 37°C, static). A negative fold change indicates a decrease in metabolite intensity in planktonic samples compared to biofilm samples. A positive fold change indicates an increase in metabolite intensity planktonic samples compared to biofilm samples. *Fold change unable to be formulated as only detected in the planktonic data set and not in the biofilm data set. Enzyme commission (E.C.) numbers are based on the KEGG database and crossed matched with the available genome sequence for LHSKBClinical (Stipetic et al., 2015).

3.4.2.3 Identified differences in purine metabolism between *S. aureus* planktonic cells and biofilms

Further analysis of *S. aureus* planktonic cells compared to biofilm samples highlighted significant differences in purine metabolism (KEGG pathway: 00230) between the two different growth states (Table 3-3) (Figure 3-6). Fifteen peaks identified or annotated to be involved in purine metabolism were found, 5 of which exhibited a fold-change increase in planktonic cells compared to biofilms and 2 of which displayed a fold-change increase in biofilm samples compared to planktonic cells (Table 3-3) (Figure 3-6). These results suggest different levels of expression in purine metabolism between biofilms and planktonic cells and may suggest that purine metabolism is up regulated in biofilms (Table 3-3) (Figure 3-6). Furthermore, a number of peaks identified or annotated to be involved in purine metabolism were found to be at a static level between data sets (Table 3-3) (Figure 3-6). Several peaks, peak numbers; 997, 1768, 3033 and 3742 were matched to two metabolite identifications (Table 3-3).

Table 3-3: Purine Biosynthesis metabolites identified from *S. aureus* planktonic and biofilm data sets.

Peak number	Metabolite	Elemental formula	KEGG ID[(a)]	Metabolite code[(b)]	Adduct	Mass (Da)	R_t (sec)	Log_2 fold change[(c)]
134	Adenosine	$C_{10}H_{13}N_5O_4$	C00212	$HRMS_a^1$, R_{ta}	M+H	268.104	544.2	8.53
997*	AMP/dGMP	$C_{10}H_{14}N_5O_7P$	C00020/C00362	$HRMS_a^1$, R_{ta}	M+H	348.071	685.3	7.48
3742	3'-GMP[(d)]/GMP	$C_{10}H_{14}N_5O_8P$	C06193/C00144	$HRMS_{PL}^1$	M-H	362.051	791.3	4.94
194	Adenine	$C_5H_5N_5$	C00147	$HRMS_a^1$, R_{ta}	M+H	136.062	572.8	0.76
1787	Guanine	$C_5H_5N_5O$	C00242	$HRMS_a^1$, R_{ta}	M+H	152.057	705.1	0.53
78	L-Glutamine	$C_5H_{10}N_2O_3$	C00064	$HRMS_a^1$, R_{ta}	M+H	147.077	778.3	n/a[(e)]
162	dGDP/ADP	$C_{10}H_{15}N_5O_{10}P_2$	C00361/C00008	$HRMS_{PL}^1$	M+H	428.037	728.3	n/a[(e)]
3033	3',5'-Cyclic GMP/2',3'-Cyclic GMP	$C_{10}H_{12}N_5O_7P$	C00942/C06194	$HRMS_{PL}^1$	M-H	344.040	650.5	n/a[(e)]
2650	Deoxyinosine	$C_8H_9N_3O_4$	C05512	$HRMS_{PL}^1$	M+H	253.093	603.4	-1.51
1796	Hypoxanthine	$C_5H_4N_4O$	C00262	$HRMS_a^1$, R_{ta}	M+H	137.046	597.2	-6.25
495	Xanthine	$C_5H_4N_4O_2$	C00385	$HRMS_{PL}^1$	M+ACN+H	194.067	622.6	n/a[(f)]
1394	Deoxyadenosine	$C_{10}H_{13}N_5O_3$	C00559	$HRMS_a^1$, R_{ta}	M+H	252.109	491.3	n/a[(f)]
1788	Guanosine	$C_{10}H_{13}N_5O_5$	C00387	$HRMS_a^1$, R_{ta}	M+H	284.099	705.4	n/a[(f)]
1768	2',3'-Cyclic AMP/3',5'-Cyclic AMP	$C_{10}H_{12}N_5O_6P$	C02353/C00575	$HRMS_{PL}^1$	M+H	330.060	292.8	n/a[(g)]
3740	GDP	$C_{10}H_{15}N_5O_{11}P_2$	C00035	$HRMS_{PL}^1$	M-H	442.018	834.9	n/a[(g)]

[(a)]See reference Kanehisa and Goto (2000).
[(b)]See reference Sumner *et al*. (2014).
[(c)]Log_2 fold-change in expression of metabolite between planktonic cell and biofilm data sets (planktonic to biofilm).
[(d)]Alternative name; Guanosine 3'-phosphate.
[(e)]Not available, fold change unable to be formulated as peak intensities did not significantly change between sample sets (0 fold change).
[(f)]Not available, fold change unable to be formulated as only detected in the planktonic data set and not in the biofilm data set.
[(g)]Not available, fold change unable to be formulated as not detected in all sample replicates in the planktonic and/or biofilm data set.
* Peak 997 was matched to two standards, AMP and dGMP, by mass and R_t. Through further analysis looking at R_t errors for these two standards, the most likely metabolite to be responsible for the peak, having with smallest R_t error, is dGMP.

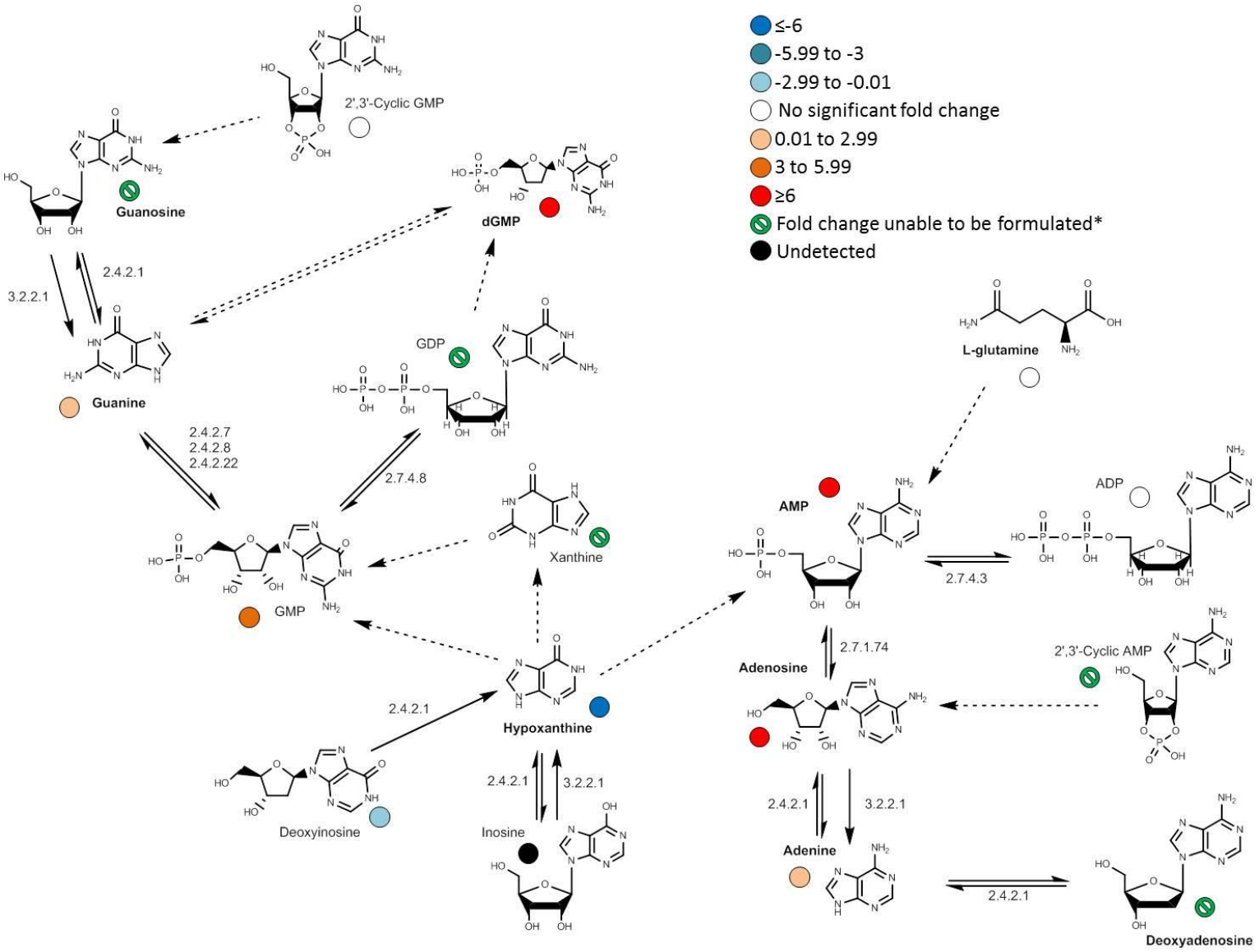
≤-6
-5.99 to -3
-2.99 to -0.01
No significant fold change
0.01 to 2.99
3 to 5.99
≥6
Fold change unable to be formulated*
Undetected
2',3'-Cyclic GMP
Guanosine
dGMP
3.2.2.1
2.4.2.1
Guanine
GDP
2.4.2.7
2.4.2.8
2.4.2.22
2.7.4.8
Xanthine
GMP
Hypoxanthine
2.4.2.1
Deoxyinosine
2.4.2.1
3.2.2.1
Inosine
L-glutamine
AMP
ADP
2.7.4.3
2.7.1.74
Adenosine
2',3'-Cyclic AMP
2.4.2.1
3.2.2.1
Adenine
2.4.2.1
Deoxyadenosine

Figure 3-6: Purine metabolism in the *S. aureus* clinical isolate LHSKBClinical.
Metabolites identified (bold) and annotated by LC-MS. Colour coding indicates $\log_2$ fold changes of metabolites identified and annotated from planktonic cell samples (overnight planktonic cells cultured at 37°C, shaking at 180 RPM) compared to biofilms (24 h biofilm cultivation, at 37°C, static). A negative fold change indicates a decrease in metabolite intensity in planktonic samples compared to biofilm samples. A positive fold change indicates an increase in metabolite intensity in planktonic samples compared to biofilm samples. *Fold change unable to be formulated. Xanthine, deoxyadenosine and guanosine only detected in the planktonic data set and not in the biofilm data set. GDP and 2',3'-Cyclic AMP was not detected in all sample replicates in the planktonic and/or biofilm data set. Enzyme commission (E.C.) numbers are based on the KEGG database and crossed matched with the available genome sequence for LHSKBClinical (Stipetic et al., 2015).

3.4.3 Targeting purine metabolism of *S. aureus* biofilms

3.4.3.1 Biofilms treated with exogenous purines

Due to significant changes identified in purine metabolism and in specific purines between *S. aureus* planktonic cells and biofilms samples, shown in section 3.4.2.3, purine metabolism was targeted in biofilms by flooding metabolism through spiking in exogenous purines into the biofilm culture media, to look for biofilm modulation effects.

Initially, fresh BHI as an undefined media was analysed for purine content using LC-MS. A number of exogenous purines were identified to be present in BHI media (Table 3-4).

Table 3-4: Purine content of brain heart infusion (BHI) media.

Purine name	Formula	Annotation[(a)]
GMP	$C_{10}H_{14}N_5O_8P$	$HRMS^1_a$, R_{ta}
Guanosine	$C_{10}H_{13}N_5O_5$	$HRMS^1_a$, R_{ta}
Guanine	$C_5H_5N_5O$	$HRMS^1_a$, R_{ta}
Xanthine	$C_5H_4N_4O_2$	$HRMS^1_a$, R_{ta}
Hypoxanthine	$C_5H_4N_4O$	$HRMS^1_a$, R_{ta}
Adenine	$C_5H_5N_5$	$HRMS^1_a$, R_{ta}
Adenosine	$C_{10}H_{13}N_5O_4$	$HRMS^1_a$, R_{ta}
AMP	$C_{10}H_{14}N_5O_7P$	$HRMS^1_a$, R_{ta}
Adenosine-3'-monophosphate	$C_{10}H_{14}N_5O_7P$	$HRMS^1_{PL}$
2',3'-cyclic AMP	$C_{10}H_{12}N_5O_6P$	$HRMS^1_{PL}$

[(a)]See reference Sumner *et al.* (2014)

The purines inosine, hypoxanthine, adenosine and adenine were then tested at varying concentrations for 4 h, against 24 h biofilms of LHSKBClinical. CV staining was used to ascertain the effect of these purines on the biofilm phenotype (Figure 3-7). Inosine at a concentration of >0.01 mM was shown to cause an increase in biofilm biomass compared to the BHI control (Figure 3-7). Further, adenine at a concentration of >0.01 mM appeared to cause a slight decrease in biofilm biomass compared to the BHI control (Figure 3-7). No

significant change was seen in biofilm biomass following hypoxanthine and adenosine treatment (Figure 3-7).

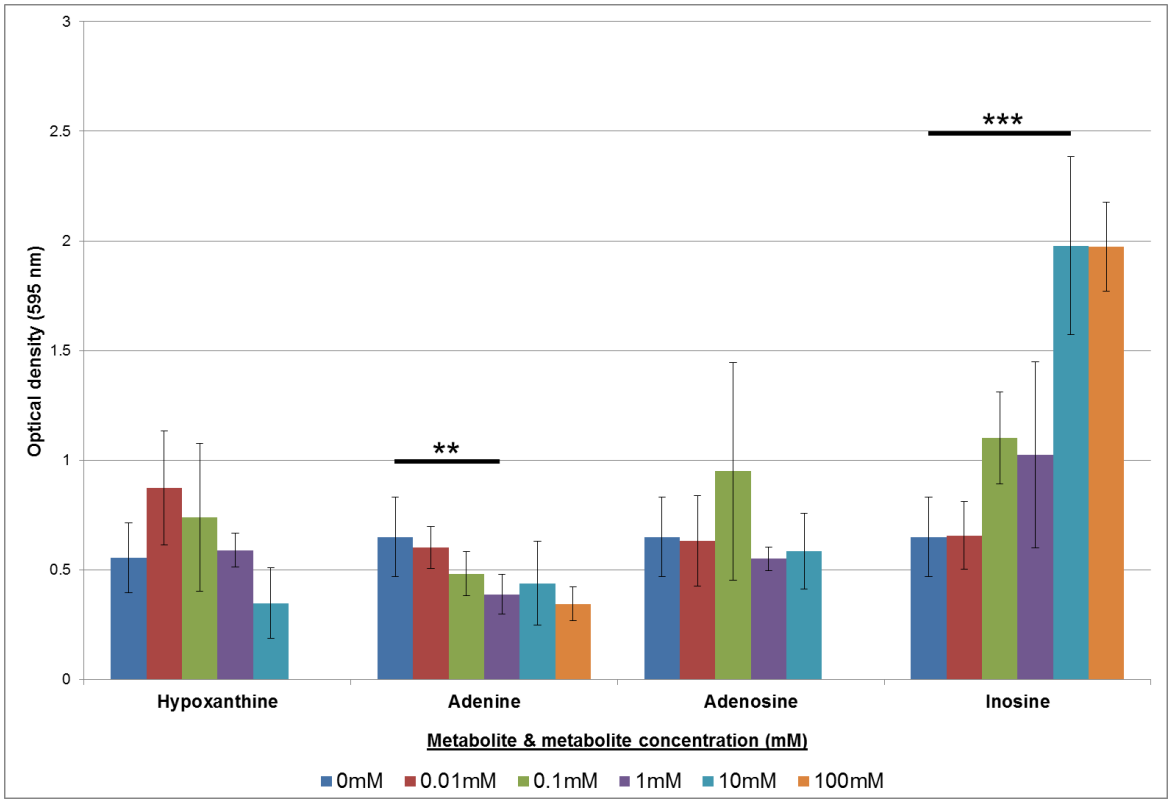

Figure 3-7: CV assay of 24 h LHSKBClinical biofilms treated with inosine, hypoxanthine, adenosine and adenine for 4 h.
Error bars ± S.D. deviation (n=4). ***Unpaired t-test between 10 mM inosine treated and non-treated biofilm samples, very significant, P = 0.001, (two-tailed). **Unpaired t-test between 1 mM adenine treated and non-treated biofilm samples, significant, P = 0.04, (two-tailed).

SEM imaging of non-treated 24 h S. *aureus* LHSKBClinical biofilms, with BHI only added for 4 h, illustrated cell adherence and biofilm formation (Figure 3-8). Samples appeared as a mono-layer of adhered cells, potentially displaying signs of detachment due to the absence of multiple layers (Figure 3-8).

SEM imaging illustrated little obvious difference between BHI controls (Figure 3-8) and adenine treated biofilms (Figure 3-9). However, it was observed that biofilm thickness appeared to vary in adenine treated samples from mono-layers of cells to complex multi-layers (Figure 3-9).

SEM imaging further illustrated that biofilm samples treated with exogenous inosine had an increased biofilm thickness (Figure 3-10) compared to non-treated BHI control samples (Figure 3-8).

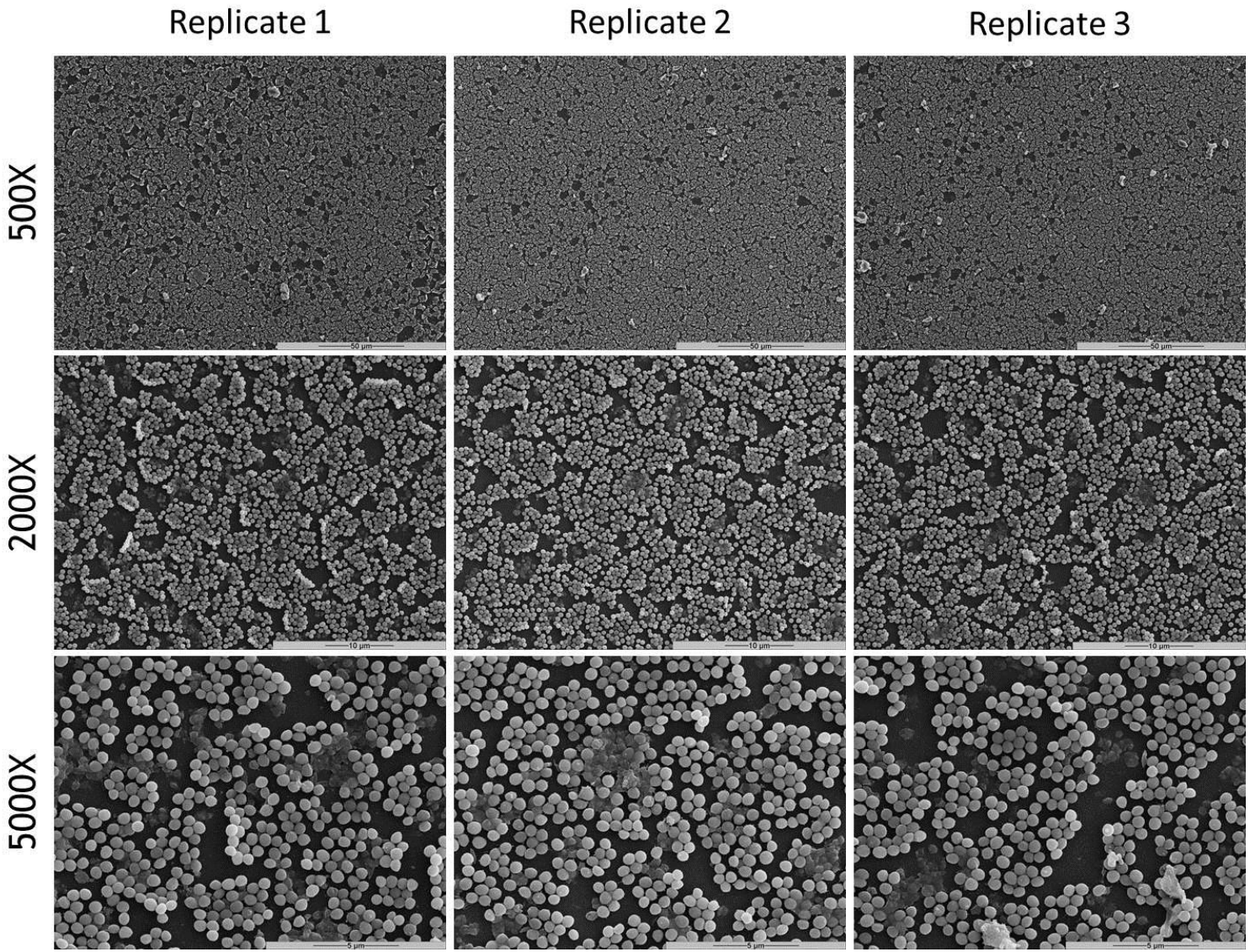
Replicate 1
Replicate 2
Replicate 3
500X
2000X
5000X

Figure 3-8: SEM images of 24 h *S. aureus* biofilms treated with ddH_2O.
Biofilms were grown on Thermanox coverslips for 24 h and then subsequently washed and treated with BHI (ddH_2O) for 4 h. Following treatment samples were washed, prepared for SEM imaging and imaged under a SEM running at 10 kV at 500X, 2000X and 5000X magnification, n = 3.

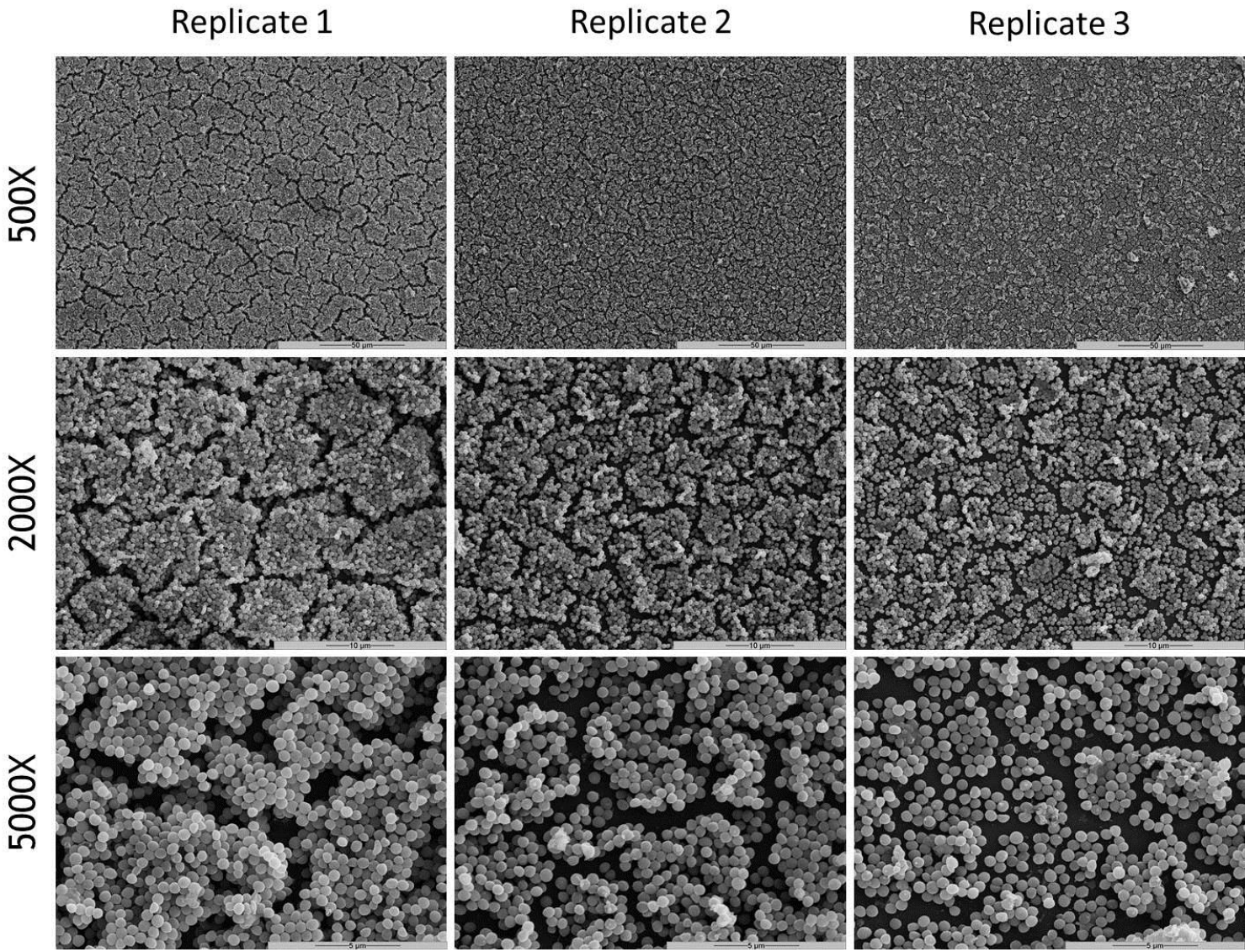
Replicate 1
Replicate 2
Replicate 3
500X
2000X
5000X

Figure 3-9: SEM images of 24 h *S. aureus* biofilms treated with 10mM adenine for 4 h.
Biofilms were grown on Thermanox coverslips for 24 h and then subsequently washed and treated with 10 mM adenine in BHI for 4 h. Following treatment samples were washed, prepared for SEM imaging and imaged under a SEM running at 10 kV at 500X, 2000X and 5000X magnification, n = 3.

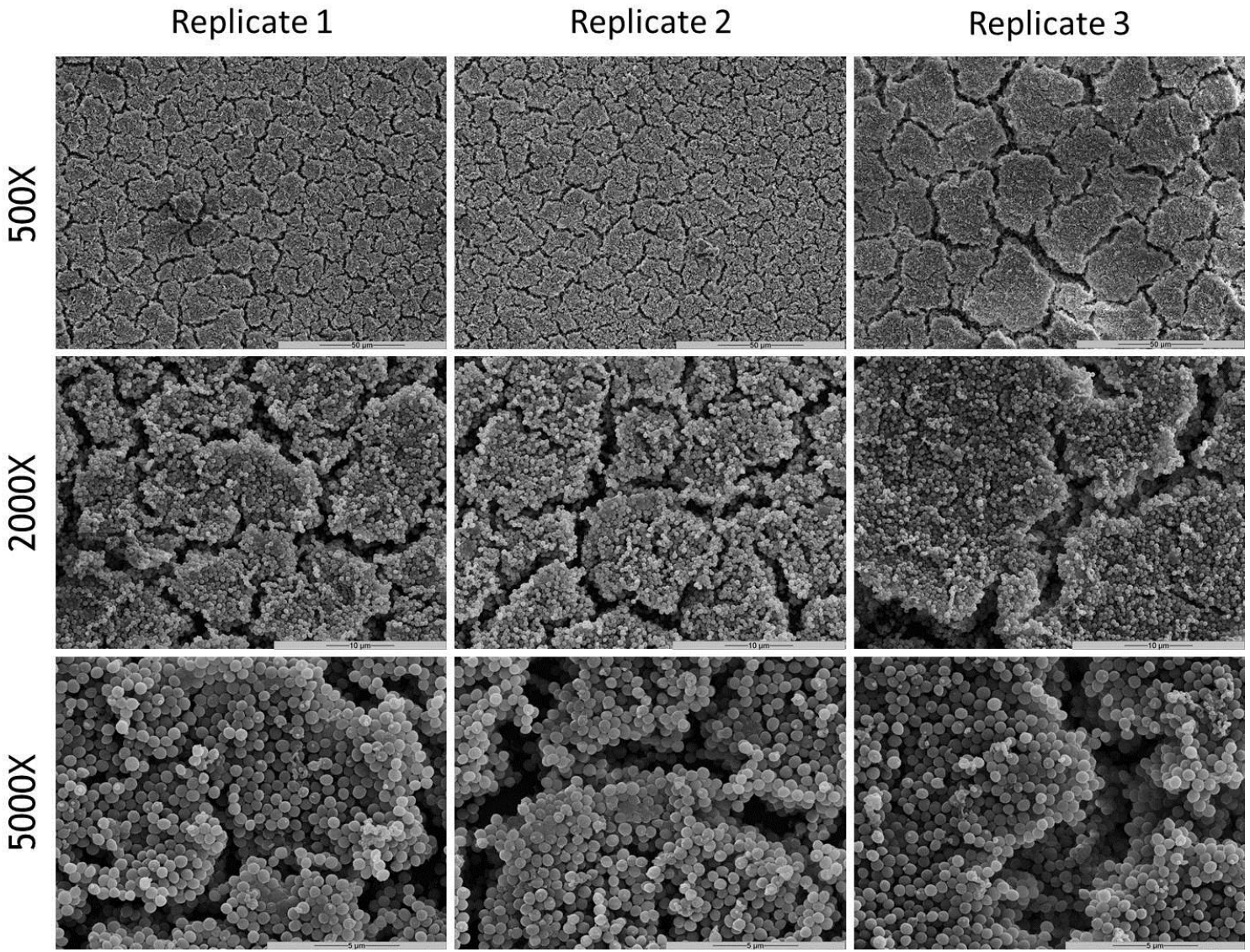
Replicate 1
Replicate 2
Replicate 3
500X
2000X
5000X

Figure 3-10: SEM images of 24 h *S. aureus* biofilms treated with 10mM inosine for 4 h.
Biofilms were grown on Thermanox coverslips for 24 h and then subsequently washed and treated with 10 mM inosine in BHI for 4 h. Following treatment samples were washed, prepared for SEM imaging and imaged under a SEM running at 10 kV at 500X, 2000X and 5000X magnification, n = 3.

Using a q-PCR approach with specific primers for *S. aureus*, analysis of LHSKBClinical biofilms treated with inosine for 4 h compared to dH_2O treated biofilm samples shows that the increase in biofilm biomass was not caused by an increase in viable cell number across the sample (Figure 3-11).

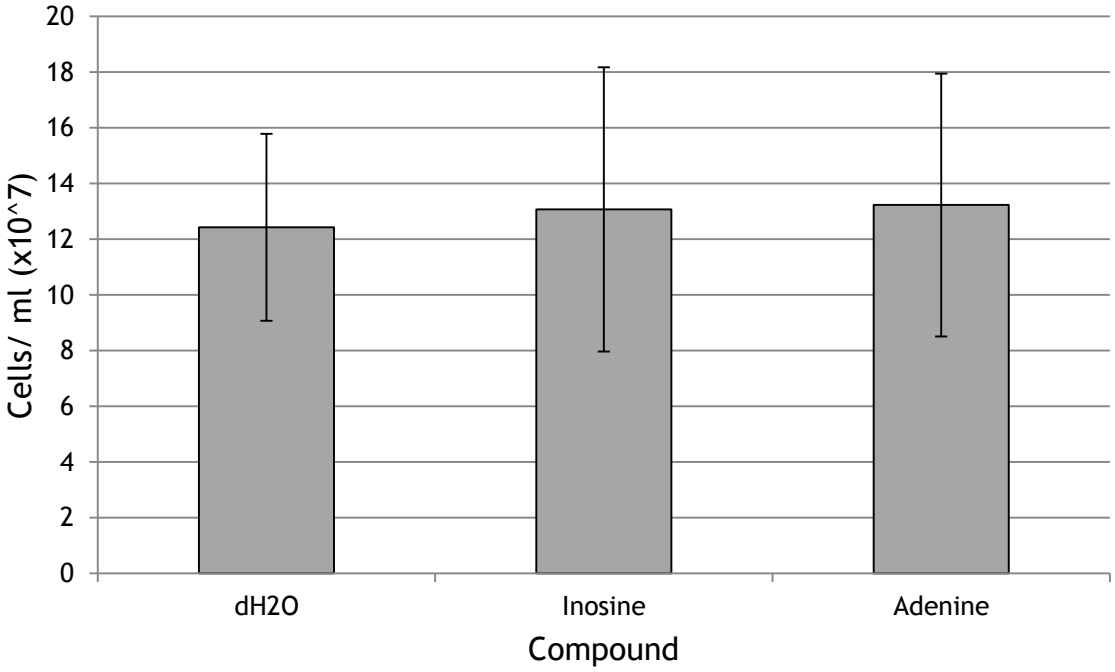

Figure 3-11: q-PCR analysis of *S. aureus* biofilms
24 h Biofilms treated with 10 mM inosine, 10 mM adenine and dH_2O, all in BHI, for 4h. Error bars ± S.D., n=3.

3.4.3.2 Minimum inhibitory concentration (MIC) testing of inosine and adenine on LHSKBClinical

The minimum inhibitory concentration (MIC) of inosine and adenine were tested on planktonic cells of LHSKBClinical (Figure 3-12 and Figure 3-13). This would tell us if inosine and adenine had an effect on planktonic cells of LHSKBClinical. Low overnight growth is most likely due to the slow shaking and therefore reduced aeration of the culture, and only a 100 µl culture volume was measured. Results show that varying concentrations of inosine and adenine had no effect on planktonic cultures. However, excluding observations for 10 mM adenine there appears to be a decreasing trend in the average OD_{595} of cell culture as the adenine concentration increased. Despite this, replicates for adenine appeared

highly variable, especially at high concentrations, and therefore conclusions about this cannot be drawn without further testing.

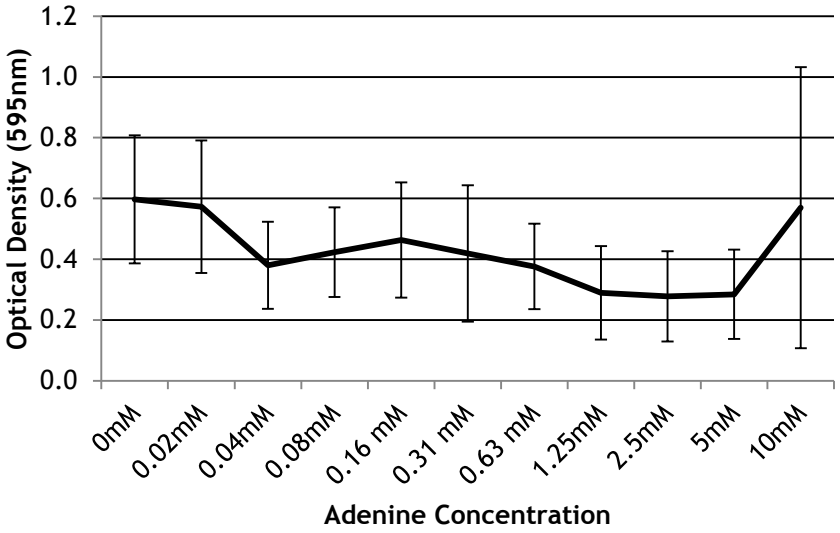

Figure 3-12: Adenine MIC testing against planktonic *S. aureus* (LHSKBClinical) culture.
A concentration gradient of adenine was tested against planktonic *S. aureus* culture overnight in a 96-well microtitre plate, at 37°C, shaking at 50 RPM. An OD_{595} measurement of each concentration was then taken, n = 8.

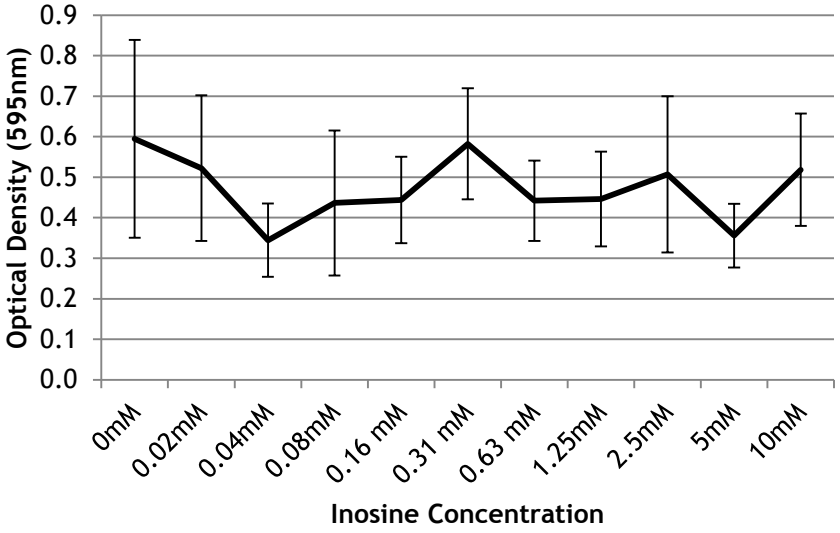

Figure 3-13: Inosine MIC testing against planktonic *S. aureus* (LHSKBClinical) culture.
A concentration gradient of inosine was tested against planktonic *S. aureus* culture overnight in a 96-well microtitre plate, at 37°C, shaking at 50 RPM. An OD_{595} measurement of each concentration was then taken, n = 8.

3.4.3.3 Metabolomic analysis of biofilms treated with inosine

Initial metabolomics results identified changes in purine metabolism between planktonic cells and biofilms. Additionally, CV assays and SEM imaging showed changes in biofilm phenotype induced by the addition of exogenous inosine.

Taken together, these results suggested purine metabolism is important in biofilm formation and as a result metabolomic analysis of inosine treated biofilms was performed to look at the molecular changes induced by the addition of exogenous inosine.

Before carrying out a metabolomics experiment of biofilms treated with inosine, an authentic standard of inosine was run through the LC-MS set-up utilised here. This test was carried out to ensure inosine could be detected on the metabolomics platform used here, as it was not detected in the original analysis comparing planktonic cells and biofilms. Through peak analysis, the mass of inosine was detected (Figure 3-14). However, a secondary peak in the spectra was detected, eluting at the same R_t as inosine and matching the mass of hypoxanthine. This peak was confirmed to match hypoxanthine by running an authentic standard of hypoxanthine in parallel. This provides evidence that inosine is not broken down in solution as two peaks are not visible in the in LC chromatogram, but through spontaneous fragmentation during ionisation, dissociating the ribose group from the hypoxanthine group. The capability to detect inosine with our system allowed us to run an authentic standard of inosine in parallel to samples to allow for identification.

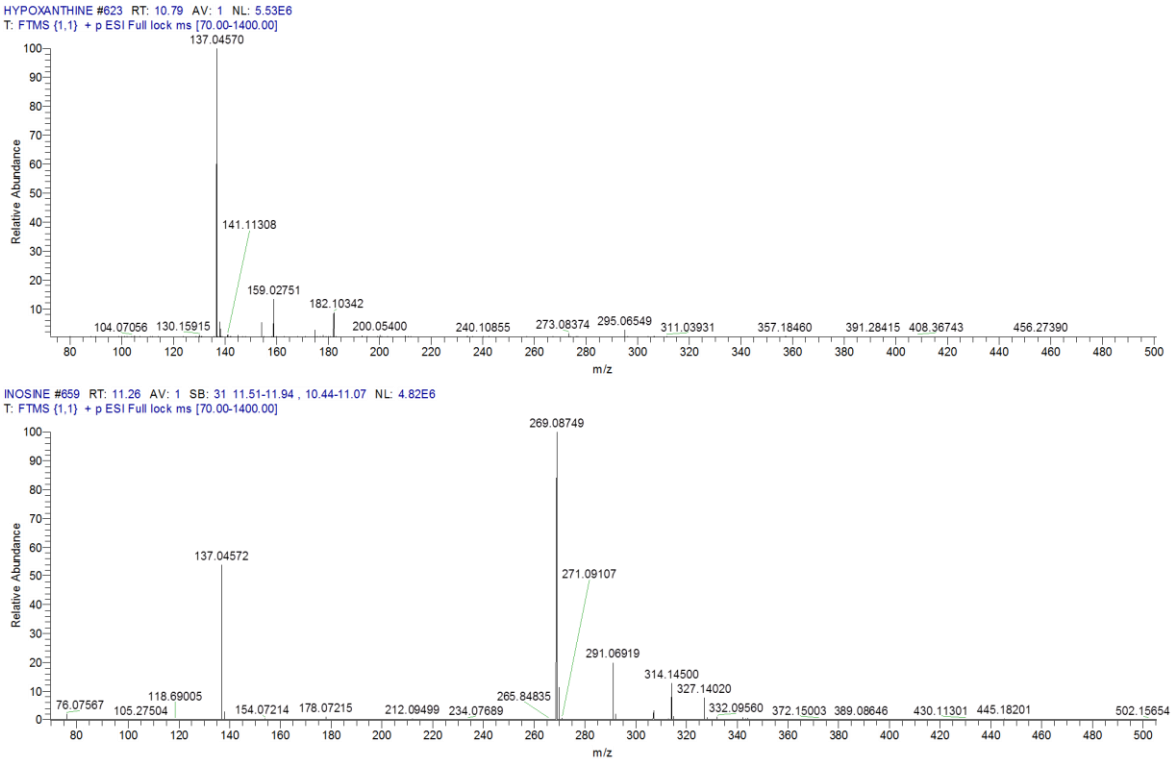

Figure 3-14: Spectra of hypoxanthine and inosine analysed using LC-MS.
Authentic standards of inosine and hypoxanthine at 100 µM in 80% acetonitrile were analysed by LC-MS analysis. Top: Hypoxanthine mass spectra at retention (R_t) time 10.79 mins showing a peak at m/z 137.04 matching to hypoxanthine (adduct M+H). Bottom: Inosine mass spectra at retention time (R_t) 11.26 mins showing a peak at m/z 269.087 matching to inosine (adduct M+H).

To analyse the metabolic effect of inosine on biofilm metabolism, mature 24 h biofilms of LHSKBClinical were treated with 10 mM exogenous inosine, spiked into media for 4 h. As a control, mature biofilms were treated with BHI and ddH_2O only, under the same conditions. Post treatment, the extraction method described earlier was utilised to extract the metabolome for LC-MS analysis.

Analysis of metabolite extractions of inosine-treated compared to ddH_2O-treated biofilms revealed 14 peaks to be highly up-regulated by 2 Log_2 fold change or greater (Table 3-5). In addition to this, the same data set revealed 7 peaks to be highly down-regulated by 2 Log_2 fold change or greater (Table 3-6). Results had an adjusted P value of <0.05 (null hypothesis: there is no difference between biofilms treated with inosine to BHI, reject null hypothesis).

Since inosine is a purine it was suspected that purine biosynthesis would be significantly changed by spiking this metabolite into the biofilm growth media. Therefore, the metabolites involved in purine biosynthesis could be looked for in the data set comparing inosine treated to non-treated biofilms. This analysis

revealed 13 peaks matched to metabolites involved in purine biosynthesis (Table 3-7). Of these, 6 were up-regulated in biofilms treated with inosine with the remaining 7 either not changing in abundance, expression or not identified in one data set (Table 3-7). For full metabolomic data analysis see supplementary data Appendix V.

Table 3-5: Metabolites up regulated by >2 Log_2 fold change in *S. aureus* biofilms in response to treatment with inosine compared to BHI (ddH_2O) controls.

Peak Number	Mass (Da)	R_t (Sec)	Elemental formula	KEGG[(a)]/HMDB[(b)] ID	Metabolite Name	Adduct	Metabolite code[(c)]	Log_2 Fold change[(d)]
1593	135.031	593.6	$C_5H_4N_4O$	C00262	Hypoxanthine	M-H	$HRMS^1_a$, R_{ta}	6.23
142	137.046	595.1	$C_5H_4N_4O$	C00262	Hypoxanthine	M+H	$HRMS^1_a$, R_{ta}	5.84
308	268.104	541.3	$C_{10}H_{13}N_5O_4$	C00212	Adenosine	M+H	$HRMS^1_a$, R_{ta}	4.72
2034	203.068	608.2	$C_7H_{12}N_2O_5$	HMDB11667	5-L-Glutamylglycine	M-H	$HRMS^1_{PL}$	2.89
			$C_7H_{12}N_2O_5$	HMDB11162	L-beta-aspartyl-L-alanine	M-H	$HRMS^1_{PL}$	
			$C_7H_{12}N_2O_5$	HMDB28746	Aspartyl-Alanine	M-H	$HRMS^1_{PL}$	
			$C_7H_{12}N_2O_5$	HMDB28683	Alanyl-Aspartate	M-H	$HRMS^1_{PL}$	
1088	247.129	305.9	$C_{10}H_{18}N_2O_5$	HMDB11172	L-gamma-glutamyl-L-valine	M+H	$HRMS^1_{PL}$	2.69
			$C_{10}H_{18}N_2O_5$	HMDB28756	Aspartyl-Isoleucine	M+H	$HRMS^1_{PL}$	
			$C_{10}H_{18}N_2O_5$	HMDB28925	Leucyl-Aspartate	M+H	$HRMS^1_{PL}$	
			$C_{10}H_{18}N_2O_5$	HMDB11166	L-beta-aspartyl-L-leucine	M+H	$HRMS^1_{PL}$	
			$C_{10}H_{18}N_2O_5$	C19972	2,4-Bis(acetamido)-2,4,6-trideoxy-beta-L-altropyranose	M+H	$HRMS^1_{PL}$	
			$C_{10}H_{18}N_2O_5$	C20424	2,4-Diacetamido-2,4,6-trideoxy-D-mannopyranose	M+H	$HRMS^1_{PL}$	
			$C_{10}H_{18}N_2O_5$	HMDB59717	Glu-Val	M+H	$HRMS^1_{PL}$	
			$C_{10}H_{18}N_2O_5$	HMDB28903	Isoleucyl-Aspartate	M+H	$HRMS^1_{PL}$	
			$C_8H_{15}NO_5$	C15480	N-Acetyl-D-fucosamine	M+ACN+H	$HRMS^1_{PL}$	
			$C_8H_{15}NO_5$	C15481	N-Acetyl-D-quinovosamine	M+ACN+H	$HRMS^1_{PL}$	
			$C_8H_{15}NO_5$	HMDB36394	N-Methylcalystegine C1	M+ACN+H	$HRMS^1_{PL}$	
			$C_{10}H_{18}N_2O_5$	HMDB28757	Aspartyl-Leucine	M+H	$HRMS^1_{PL}$	
2133	217.083	569.4	$C_8H_{14}N_2O_5$	HMDB29040	Serinyl-Hydroxyproline	M-H	$HRMS^1_{PL}$	2.69
			$C_8H_{14}N_2O_5$	HMDB03764	Glutamylalanine	M-H	$HRMS^1_{PL}$	

			$C_8H_{14}N_2O_5$	HMDB28872	Hydroxyprolyl-Serine	M-H	$HRMS^1_{PL}$	
			$C_8H_{14}N_2O_5$	HMDB36301	N-gamma-L-Glutamyl-D-alanine	M-H	$HRMS^1_{PL}$	
			$C_8H_{14}N_2O_5$	C03738	gamma-L-Glutamyl-D-alanine	M-H	$HRMS^1_{PL}$	
			$C_8H_{14}N_2O_5$	HMDB06248	5-L-Glutamyl-L-alanine	M-H	$HRMS^1_{PL}$	
1882	181.072	744.0	$C_6H_{14}O_6$	C01722	L-Glucitol	M-H	$HRMS^1_{PL}$	2.62
			$C_6H_{14}O_6$	C01697	Galactitol	M-H	$HRMS^1_{PL}$	
			$C_6H_{14}O_6$	C00794	D-Sorbitol	M-H	$HRMS^1_{PL}$	
			$C_6H_{14}O_6$	C00392	Mannitol	M-H	$HRMS^1_{PL}$	
			$C_6H_{14}O_6$	C01507	L-Iditol	M-H	$HRMS^1_{PL}$	
			$C_6H_{14}O_6$	C01489	D-Iditol	M-H	$HRMS^1_{PL}$	
2163	176.057	586.9	$C_6H_{11}NO_5$	C06034	4-Hydroxy-4-methylglutamate	M-H	$HRMS^1_{PL}$	2.48
			$C_6H_{11}NO_5$	C17576	3-Keto-scyllo-inosamine	M-H	$HRMS^1_{PL}$	
552	147.076	775.0	$C_5H_{10}N_2O_3$	C00064	L-Glutamine	M+H	$HRMS^1_a$, R_{ta}	2.40
1739	124.007	775.7	$C_2H_7NO_3S$	C00245	Taurine	M-H	$HRMS^1_a$, R_{ta}	2.28
1200	366.148	480.7	$C_{15}H_{20}N_2O_4S$	C13778	HMR1556	M+ACN+H	$HRMS^1_{PL}$	2.20
			$C_{15}H_{20}N_2O_4S$	C13820	Chromanol 293B	M+ACN+H	$HRMS^1_{PL}$	
			$C_{15}H_{20}N_2O_4S$	C06806	Acetohexamide	M+ACN+H	$HRMS^1_{PL}$	
2089	181.051	767.7	$C_9H_{10}O_4$	C12622	cis-3-(3-Carboxyethenyl)-3,5-cyclohexadiene-1,2-diol	M-H	$HRMS^1_{PL}$	2.14
			$C_9H_{10}O_4$	HMDB29232	3-Hydroxyphenyllactate	M-H	$HRMS^1_{PL}$	
			$C_9H_{10}O_4$	HMDB00333	Isohomovanillic acid	M-H	$HRMS^1_{PL}$	
			$C_9H_{10}O_4$	HMDB59763	3,4-Dimethoxybenzoic acid	M-H	$HRMS^1_{PL}$	
			$C_9H_{10}O_4$	HMDB00423	3,4-Dihydroxyhydrocinnamic acid	M-H	$HRMS^1_{PL}$	
			$C_9H_{10}O_4$	C10447	3,4-Dihydroxyphenylpropanoate	M-H	$HRMS^1_{PL}$	
			$C_9H_{10}O_4$	C10680	2',6'-Dihydroxy-4'-methoxyacetophenone	M-H	$HRMS^1_{PL}$	
			$C_9H_{10}O_4$	HMDB33624	(±)-2-Hydroxy-3-(2-hydroxyphenyl)propanoic acid	M-H	$HRMS^1_{PL}$	

			$C_9H_{10}O_4$	HMDB41270	2',4'-Dihydroxy-6'-methoxyacetophenone	M-H	$HRMS^1_{PL}$	
			$C_9H_{10}O_4$	C03964	(R)-3-(4-Hydroxyphenyl)lactate	M-H	$HRMS^1_{PL}$	
			$C_9H_{10}O_4$	HMDB00755	Hydroxyphenyllactic acid	M-H	$HRMS^1_{PL}$	
			$C_9H_{10}O_4$	C03672	3-(4-Hydroxyphenyl)lactate	M-H	$HRMS^1_{PL}$	
			$C_9H_{10}O_4$	HMDB02643	3-(3-Hydroxyphenyl)-3-hydroxypropanoic acid	M-H	$HRMS^1_{PL}$	
			$C_9H_{10}O_4$	HMDB29273	2,6-Dimethoxybenzoic acid	M-H	$HRMS^1_{PL}$	
			$C_9H_{10}O_4$	HMDB37274	Maltol propionate	M-H	$HRMS^1_{PL}$	
			$C_9H_{10}O_4$	C05582	Homovanillate	M-H	$HRMS^1_{PL}$	
			$C_9H_{10}O_4$	C04044	3-(2,3-Dihydroxyphenyl)propanoate	M-H	$HRMS^1_{PL}$	
			$C_9H_{10}O_4$	C05583	3-Methoxy-4-hydroxyphenylglycolaldehyde	M-H	$HRMS^1_{PL}$	
728	252.109	492.1	$C_{10}H_{13}N_5O_3$	C00559	Deoxyadenosine	M+H	$HRMS^1_a$, R_{ta}	2.12
1388	263.074	808.0	$C_8H_{16}O_8$	HMDB29954	D-glycero-L-galacto-Octulose	M+Na	$HRMS^1_{PL}$	2.01

[(a)]See reference Kanehisa and Goto (2000).
[(b)]See references Wishart *et al.*, (2007, 2009, 2013).
[(c)]See reference Sumner *et al.* (2014).
[(d)]Log_2 fold-change in metabolite expression between *S. aureus* biofilms treated with inosine, and non-treated BHI only (ddH_2O) control data sets (treated to non-treated).

Table 3-6: Metabolites down regulated by >2 Log_2 fold change in biofilms in response to treatment with inosine compared to BHI (ddH_2O) controls.

Peak Number	Mass (Da)	RT (sec)	Elemental formula	KEGG[a]/HMDB[b]/Lipids[c] ID	Metabolite Name	Adduct	Metabolite code[d]	Log_2 Fold change[e]
1057	170.118	427.9	$C_7H_{12}O_2$	HMDB29165	1,3-Diacetylpropane	M+ACN+H	$HRMS^1_{PL}$	-5.07
			$C_7H_{12}O_2$	HMDB30330	1-Methoxy-3-methylene-2-pentanone	M+ACN+H	$HRMS^1_{PL}$	
			$C_7H_{12}O_2$	C10976	1-Oxa-2-oxo-3-methylcycloheptane	M+ACN+H	$HRMS^1_{PL}$	
			$C_7H_{12}O_2$	LMFA01020121	2,2-dimethyl-4-pentenoic acid	M+ACN+H	$HRMS^1_{PL}$	
			$C_7H_{12}O_2$	LMFA12000013	2,3-Heptanedione	M+ACN+H	$HRMS^1_{PL}$	
			$C_7H_{12}O_2$	HMDB39819	2,4-Dimethyl-2-pentenoic acid	M+ACN+H	$HRMS^1_{PL}$	
			$C_7H_{12}O_2$	LMFA01020118	2-butyl acrylic acid	M+ACN+H	$HRMS^1_{PL}$	
			$C_7H_{12}O_2$	HMDB31484	2-Heptenoic acid	M+ACN+H	$HRMS^1_{PL}$	
			$C_7H_{12}O_2$	HMDB38271	2-Hexenyl formate	M+ACN+H	$HRMS^1_{PL}$	
			$C_7H_{12}O_2$	LMFA01020122	2-isopropyl trans-crotonic acid	M+ACN+H	$HRMS^1_{PL}$	
			$C_7H_{12}O_2$	LMFA01020101	2-methyl-2E-hexenoic acid	M+ACN+H	$HRMS^1_{PL}$	
			$C_7H_{12}O_2$	LMFA01020100	2-methyl-2Z-hexenoic acid	M+ACN+H	$HRMS^1_{PL}$	
			$C_7H_{12}O_2$	HMDB31477	3,4-Heptanedione	M+ACN+H	$HRMS^1_{PL}$	
			$C_7H_{12}O_2$	C11950	3-Isopropyl-3-butenoic acid	M+ACN+H	$HRMS^1_{PL}$	
			$C_7H_{12}O_2$	LMFA01030793	3-Methyl-2E-hexenoic acid	M+ACN+H	$HRMS^1_{PL}$	
			$C_7H_{12}O_2$	LMFA01030794	3-Methyl-2Z-hexenoic acid	M+ACN+H	$HRMS^1_{PL}$	
			$C_7H_{12}O_2$	HMDB32391	3-Methyl-3-butenyl acetate	M+ACN+H	$HRMS^1_{PL}$	
			$C_7H_{12}O_2$	LMFA01020119	4,4-dimethyl-2E-pentenoic acid	M+ACN+H	$HRMS^1_{PL}$	
			$C_7H_{12}O_2$	LMFA01020120	4,4-dimethyl-2Z-pentenoic acid	M+ACN+H	$HRMS^1_{PL}$	
			$C_7H_{12}O_2$	LMFA07040012	4-heptanolide	M+ACN+H	$HRMS^1_{PL}$	

$C_7H_{12}O_2$	HMDB33793	4-Heptenoic acid	M+ACN+H	$HRMS^1_{PL}$
$C_7H_{12}O_2$	HMDB31174	4-Methyl-5-hexanolide	M+ACN+H	$HRMS^1_{PL}$
$C_7H_{12}O_2$	HMDB32460	4-Pentenyl acetate	M+ACN+H	$HRMS^1_{PL}$
$C_7H_{12}O_2$	LMFA01030452	4Z-heptenoic acid	M+ACN+H	$HRMS^1_{PL}$
$C_7H_{12}O_2$	HMDB31593	5-Methyl-2,3-hexanedione	M+ACN+H	$HRMS^1_{PL}$
$C_7H_{12}O_2$	LMFA01020117	5-methyl-5-hexenoic acid	M+ACN+H	$HRMS^1_{PL}$
$C_7H_{12}O_2$	HMDB40591	Allyl butyrate	M+ACN+H	$HRMS^1_{PL}$
$C_7H_{12}O_2$	C13714	alpha-EMGBL	M+ACN+H	$HRMS^1_{PL}$
$C_7H_{12}O_2$	LMFA01030012	alpha-heptenoic acid	M+ACN+H	$HRMS^1_{PL}$
$C_7H_{12}O_2$	C13717	beta-EMGBL	M+ACN+H	$HRMS^1_{PL}$
$C_7H_{12}O_2$	LMFA01030013	beta-heptenoic acid	M+ACN+H	$HRMS^1_{PL}$
$C_7H_{12}O_2$	C10921	Butyl acrylate	M+ACN+H	$HRMS^1_{PL}$
$C_7H_{12}O_2$	LMFA07040011	cis-2-Methyl-5-hexanolide	M+ACN+H	$HRMS^1_{PL}$
$C_7H_{12}O_2$	HMDB40214	cis-3-Hexenyl formate	M+ACN+H	$HRMS^1_{PL}$
$C_7H_{12}O_2$	C09822	Cyclohexane-1-carboxylate	M+ACN+H	$HRMS^1_{PL}$
$C_7H_{12}O_2$	HMDB31351	Cyclohexyl formate	M+ACN+H	$HRMS^1_{PL}$
$C_7H_{12}O_2$	LMFA01030015	delta-heptenoic acid	M+ACN+H	$HRMS^1_{PL}$
$C_7H_{12}O_2$	HMDB31681	Dihydro-5-propyl-2(3H)-furanone	M+ACN+H	$HRMS^1_{PL}$
$C_7H_{12}O_2$	LMFA01030016	epsilon-heptenoic acid	M+ACN+H	$HRMS^1_{PL}$
$C_7H_{12}O_2$	HMDB31603	Ethyl 4-pentenoate	M+ACN+H	$HRMS^1_{PL}$
$C_7H_{12}O_2$	C08487	Ethyl tiglate	M+ACN+H	$HRMS^1_{PL}$
$C_7H_{12}O_2$	LMFA01030014	gamma-heptenoic acid	M+ACN+H	$HRMS^1_{PL}$
$C_7H_{12}O_2$	LMFA12000245	Heptan-2,5-dione	M+ACN+H	$HRMS^1_{PL}$
$C_9H_{15}NO_2$	HMDB38321	Homoarecoline	M+H	$HRMS^1_{PL}$
$C_7H_{12}O_2$	HMDB29314	Isopentenyl acetate	M+ACN+H	$HRMS^1_{PL}$
$C_7H_{12}O_2$	HMDB31504	Methyl (Z)-3-hexenoate	M+ACN+H	$HRMS^1_{PL}$

			$C_7H_{12}O_2$	HMDB31500	Methyl 2E-hexenoate	M+ACN+H	$HRMS^1_{PL}$	
			$C_7H_{12}O_2$	LMFA06000026	Pimelic dialdehyde	M+ACN+H	$HRMS^1_{PL}$	
			$C_9H_{15}NO_2$	C17730	Piperidione	M+H	$HRMS^1_{PL}$	
321	161.092	613.6	$C_4H_9NO_3$	C11108	(-)-erythro-(2R,3R)-Dihydroxybutylamide	M+ACN+H	$HRMS^1_{PL}$	-2.52
			$C_4H_9NO_3$	C02115	2-Methylserine	M+ACN+H	$HRMS^1_{PL}$	
			$C_6H_{12}N_2O_3$	HMDB31411	4-Acetamido-2-aminobutanoic acid	M+H	$HRMS^1_{PL}$	
			$C_4H_9NO_3$	C03678	4-Amino-3-hydroxybutanoate	M+ACN+H	$HRMS^1_{PL}$	
			$C_6H_{12}N_2O_3$	C00993	D-Alanyl-D-alanine	M+H	$HRMS^1_{PL}$	
			$C_4H_9NO_3$	C12317	D-Allothreonine	M+ACN+H	$HRMS^1_{PL}$	
			$C_6H_{12}N_2O_3$	C10996	Daminozide	M+H	$HRMS^1_{PL}$	
			$C_4H_9NO_3$	C00820	D-Threonine	M+ACN+H	$HRMS^1_{PL}$	
			$C_4H_9NO_3$	HMDB61148	Hydroxyethyl glycine	M+ACN+H	$HRMS^1_{PL}$	
			$C_4H_9NO_3$	C05519	L-Allothreonine	M+ACN+H	$HRMS^1_{PL}$	
			$C_4H_9NO_3$	C00263	L-Homoserine	M+ACN+H	$HRMS^1_{PL}$	
			$C_4H_9NO_3$	C00188	L-Threonine	M+ACN+H	$HRMS^1_{PL}$	
			$C_6H_{12}N_2O_3$	C06442	N(gamma)-Acetyldiaminobutyrate	M+H	$HRMS^1_{PL}$	
			$C_6H_{12}N_2O_3$	C03153	N5-Methyl-L-glutamine	M+H	$HRMS^1_{PL}$	
			$C_6H_{12}N_2O_3$	C19929	N-alpha-Acetyl-L-2,4-diaminobutyrate	M+H	$HRMS^1_{PL}$	
1398	182.140	571.3	$C_6H_{12}N_4$	HMDB29598	Metenamine	M+ACN+H	$HRMS^1_{PL}$	-2.40
2174	111.020	509.1	$C_4H_4N_2O_2$	HMDB60760	4-Carboxypyrazole	M-H	$HRMS^1_{PL}$	-2.37
			$C_4H_4N_2O_2$	C18474	Maleic hydrazide	M-H	$HRMS^1_{PL}$	
			$C_4H_4N_2O_2$	C00106	Uracil	M-H	$HRMS^1_{PL}$	
1650	159.078	611.8	$C_6H_{12}N_2O_3$	HMDB31411	4-Acetamido-2-aminobutanoic acid	M-H	$HRMS^1_{PL}$	-2.28
			$C_6H_{12}N_2O_3$	C00993	D-Alanyl-D-alanine	M-H	$HRMS^1_{PL}$	

			$C_6H_{12}N_2O_3$	C10996	Daminozide	M-H	$HRMS^1_{PL}$	
			$C_6H_{12}N_2O_3$	C06442	N(gamma)-Acetyldiaminobutyrate	M-H	$HRMS^1_{PL}$	
			$C_6H_{12}N_2O_3$	C03153	N5-Methyl-L-glutamine	M-H	$HRMS^1_{PL}$	
			$C_6H_{12}N_2O_3$	C19929	N-alpha-Acetyl-L-2,4-diaminobutyrate	M-H	$HRMS^1_{PL}$	
2102	137.036	607.3	$C_6H_6N_2O_2$	HMDB34174	(E)-Urocanic acid	M-H	$HRMS^1_{PL}$	-2.27
			$C_6H_6N_2O_2$	C02126	4-Nitroaniline	M-H	$HRMS^1_{PL}$	
			$C_6H_6N_2O_2$	HMDB31338	5-Oxo-2(5H)-isoxazolepropanenitrile	M-H	$HRMS^1_{PL}$	
			$C_6H_6N_2O_2$	HMDB02730	Nicotinamide N-oxide	M-H	$HRMS^1_{PL}$	
			$C_6H_6N_2O_2$	C19345	para-Benzoquinone dioxime	M-H	$HRMS^1_{PL}$	
			$C_6H_6N_2O_2$	C00785	Urocanate	M-H	$HRMS^1_{PL}$	
178	198.087	581.8	$C_6H_8N_2O_3$	C03817	(S)-3-(Imidazol-5-yl)lactate	M+ACN+H	$HRMS^1_{PL}$	-2.16
			$C_6H_8N_2O_3$	C03680	4-Imidazolone-5-propanoate	M+ACN+H	$HRMS^1_{PL}$	
			$C_6H_8N_2O_3$	HMDB00544	5-Hydroxymethyl-4-methyluracil	M+ACN+H	$HRMS^1_{PL}$	
			$C_8H_{11}N_3O_3$	C19430	HC Red No. 3	M+H	$HRMS^1_{PL}$	
			$C_6H_8N_2O_3$	C05568	Imidazole lactate	M+ACN+H	$HRMS^1_{PL}$	
			$C_8H_{11}N_3O_3$	C12245	Methyl5-(but-3-en-1-yl)amino-1,3,4-oxadiazole-2-carboxylate	M+H	$HRMS^1_{PL}$	
			$C_8H_{11}N_3O_3$	C02997	N-Acetyl-L-histidine	M+H	$HRMS^1_{PL}$	
			$C_6H_8N_2O_3$	C19481	N-Nitrosoguvacine	M+ACN+H	$HRMS^1_{PL}$	

[(a)]See reference Kanehisa and Goto (2000).
[(b)]See references Wishart *et al.*, (2007, 2009, 2013).
[(c)]See references: Byrnes *et al.*, (2009); Cotter *et al.*, (2006); Fahy *et al.*, (2007, 2009); and Sud *et al.*, (2007).
[(d)]See reference Sumner *et al.* (2014).
[(e)]Log_2 fold-change in metabolite expression between *S. aureus* biofilms treated with inosine, and non-treated BHI only (ddH_2O) control data sets (treated to non-treated).

Table 3-7: Purine metabolites identified in biofilms treated with inosine compared to ddH_2O control data sets

Peak Number	Metabolite	Elemental formula	KEGG ID[(a)]	Metabolite code[(b)]	Adduct	Mass (Da)	R_t (sec)	Log_2 fold change[(c)]
142	Hypoxanthine	$C_5H_4N_4O$	C00262	$HRMS^1_a$, R_{ta}	M+H	137.046	595.1	5.84
308	Adenosine	$C_{10}H_{13}N_5O_4$	C00212	$HRMS^1_a$, R_{ta}	M+H	268.104	541.3	4.72
308	Deoxyguanosine	$C_{10}H_{13}N_5O_4$	C00330	$HRMS^1_{PL}$	M+H	268.104	541.3	4.72
552	L-Glutamine	$C_5H_{10}N_2O_3$	C00064	$HRMS^1_a$, R_{ta}	M+H	147.076	775.0	2.4
728	Deoxyadenosine	$C_{10}H_{13}N_5O_3$	C00559	$HRMS^1_a$, R_{ta}	M+H	252.109	492.1	2.12
2155	Guanine	$C_5H_5N_5O$	C00242	$HRMS^1_a$, R_{ta}	M-H	150.042	692.1	1.41
918	3',5'-cyclic AMP/2',3'-cyclic AMP	$C_{10}H_{12}N_5O_6P$	C02353/C00575	$HRMS^1_{PL}$	M+H	330.06	511.0	n/a[(d)]
1503	Adenine	$C_5H_5N_6$	C00147	$HRMS^1_a$, R_{ta}	M-H	134.047	566.4	n/a[(d)]
1591	Xanthine	$C_5H_4N_4O_2$	C00385	$HRMS^1_a$, R_{ta}	M-H	151.026	634.2	n/a[(d)]
1846	Carbamoyl phosphate	CH_4NO_5P	C00169	$HRMS^1_{PL}$	M-H	139.976	866.9	n/a[(d)]
493	Inosine	$C_{10}H_{12}N_4O_5$	C00294	$HRMS^1_a$, R_{ta}	M+H	269.088	623.7	n/a[(e)]
726	Guanosine	$C_{10}H_{13}N_5O_5$	C00387	$HRMS^1_{PL}$	M+Na	306.081	698.1	n/a[(e)]
1387	Glycine	$C_2H_5NO_2$	C00037	$HRMS^1_a$, R_{ta}	M+H	76.039	802.6	n/a[(f)]

[(a)]See reference Kanehisa and Goto, (2000).
[(b)]See reference Sumner *et al.* (2014).
[(c)]Log_2 fold-change in metabolite expression between *S. aureus* biofilms treated with inosine, and non-treated BHI only (ddH_2O) control data sets (treated to non-treated).
[(d)]Not available, fold change unable to be formulated as peak intensities did not significantly change between sample sets (0 fold change).
[(e)]Not available, fold change unable to be formulated as only detected in the inosine treated biofilm data set and not in the non-treated BHI (ddH_2O) data set.
[(f)]Not available, fold change unable to be formulated as not detected in all sample replicates in the inosine treated biofilm data set.

3.4.3.4 Metabolomic analysis of biofilms treated with adenine

Due to initial metabolomics results identifying changes in purine metabolism between planktonic cells and biofilms, and CV assays and SEM imaging indicating potential changes in biofilm phenotype induced by the addition of exogenous adenine, purine metabolism is hypothesised to be important in biofilm formation. Metabolomic analysis of adenine treated biofilms was performed to investigate the molecular changes induced by the addition of exogenous adenine.

To analyse the metabolic effect of adenine on biofilm metabolism, mature 24 h biofilms of LHSKBClinical were treated with 10 mM adenine spiked into media for 4 h. As a control, mature biofilms were treated with BHI and ddH_2O only under the same conditions. Post-treatment the extraction method described earlier was utilised to extract the metabolome for LC-MS analysis.

Data analysis of biofilm extractions of adenine treated compared to ddH_2O treated biofilms revealed 8 peaks to be highly up-regulated by 2 Log_2 fold change or greater (Table 3-8). In addition to this, the same data set revealed 1 peak to be highly down regulated by 2 Log_2 fold change or greater (Table 3-9). Results had an adjusted P value of <0.05 (null hypothesis: there is no difference between biofilms treated with adenine to BHI, reject null hypothesis).

Since adenine is a purine it was suspected that purine biosynthesis would be significantly changed through the spiking in of this metabolite into the biofilm growth media. Therefore, the metabolites involved in purine biosynthesis could be looked for in the data set comparing adenine treated to non-treated biofilms. This analysis revealed 13 peaks matched to metabolites involved in purine biosynthesis (Table 3-10). Of these, 5 were up-regulated in biofilms treated with inosine with the remaining 8 either not changing in abundance, expression or not identified in one data set (Table 3-10). For full metabolomic data analysis see supplementary data Appendix V.

Table 3-8: Metabolites up-regulated by >2 Log_2 Fold change in biofilms in response to treatment with adenine compared to BHI (ddH_2O) controls.

Peak Number	Mass (Da)	RT (Sec)	Elemental formula	KEGG ID[(a)]	Metabolite Name	Adduct	Metabolite code[(b)]	Log_2 Fold change[(c)]
308	268.104	541.3	$C_{10}H_{13}N_5O_4$	C00212	Adenosine	M+H	$HRMS_a^1$, R_{ta}	6.52
728	252.109	492.1	$C_{10}H_{13}N_5O_3$	C00559	Deoxyadenosine	M+H	$HRMS_a^1$, R_{ta}	6.43
1503	134.047	566.4	$C_5H_5N_5$	C00147	Adenine	M-H	$HRMS_a^1$, R_{ta}	5.79
26	136.062	568.3	$C_5H_5N_5$	C00147	Adenine	M+H	$HRMS_a^1$, R_{ta}	4.40
1125	150.077	496.3	$C_6H_7N_5$	C00913	3-Methyladenine	M+H	$HRMS_{PL}^1$	2.66
			$C_6H_7N_5$	C02241	7-Methyladenine	M+H	$HRMS_{PL}^1$	
			$C_6H_7N_5$	C02216	1-Methyladenine	M+H	$HRMS_{PL}^1$	
			$C_6H_7N_5$	C08434	6-Methylaminopurine	M+H	$HRMS_{PL}^1$	
1593	135.031	593.6	$C_5H_4N_4O$	C00262	Hypoxanthine	M-H	$HRMS_a^1$, R_{ta}	2.34
1892	118.051	752.4	$C_4H_9NO_3$	C00188	L-Threonine	M-H	$HRMS_a^1$, R_{ta}	2.22
2007	104.035	803.3	$C_3H_7NO_3$	C00065	L-Serine	M-H	$HRMS_a^1$, R_{ta}	2.08

[(a)]See reference Kanehisa and Goto, (2000).
[(b)]See reference Sumner *et al*. (2014).
[(c)]Log_2 fold-change in metabolite expression between *S. aureus* biofilms treated with adenine, and non-treated BHI only (ddH_2O) control data sets (treated to non-treated).

Table 3-9: Metabolites down-regulated by >2 Log_2 fold change in biofilms in response to treatment with adenine compared to BHI (ddH_2O) controls.

Peak Number	Mass (Da)	RT (Sec)	Elemental formula	KEGG ID[(a)]	Metabolite Name	Adduct	Metabolite code[(b)]	Log_2 Fold change[(c)]
846	228.098	566.9	$C_9H_{13}N_3O_4$	C00881	Deoxycytidine	M+H	$HRMS_{PL}^1$	-2.04
			$C_7H_{10}N_2O_4$	C13672	AMPA	M+ACN+H	$HRMS_{PL}^1$	

[(a)]See reference Kanehisa and Goto, (2000).
[(b)]See reference Sumner *et al*. (2014).
[(c)]Log_2 fold-change in metabolite expression between *S. aureus* biofilms treated with adenine, and non-treated BHI only (ddH_2O) control data sets (treated to non-treated).

Table 3-10: Purine metabolites identified from biofilms treated with adenine compared to BHI (ddH_2O) controls

Peak Number	Metabolite	Elemental formula	KEGG ID[(a)]	Metabolite code[(b)]	Adduct	Mass (Da)	R_t (sec)	Log_2 fold change[(c)]
308	Adenosine	$C_{10}H_{13}N_5O_4$	C00212	$HRMS^1_a$, R_{ta}	M+H	268.104	541.3	6.52
308	Deoxyguanosine	$C_{10}H_{13}N_5O_4$	C00330	$HRMS^1_{PL}$	M+H	268.104	541.3	6.52
728	Deoxyadenosine	$C_{10}H_{13}N_5O_3$	C00559	$HRMS^1_a$, R_{ta}	M+H	252.109	492.1	6.43
1503	Adenine	$C_5H_5N_6$	C00147	$HRMS^1_a$, R_{ta}	M-H	134.047	566.4	5.79
1593	Hypoxanthine	$C_5H_4N_4O$	C00262	$HRMS^1_a$, R_{ta}	M+H	135.031	593.6	2.34
552	L-Glutamine	$C_5H_{10}N_2O_3$	C00064	$HRMS^1_a$, R_{ta}	M+H	147.076	775.0	n/a[(d)]
2155	Guanine	$C_5H_5N_5O$	C00242	$HRMS^1_a$, R_{ta}	M-H	150.042	692.1	n/a[(d)]
1387	Glycine	$C_2H_5NO_2$	C00037	$HRMS^1_a$, R_{ta}	M+H	76.039	802.6	n/a[(d)]
1591	Xanthine	$C_5H_4N_4O_2$	C00385	$HRMS^1_a$, R_{ta}	M-H	151.026	634.2	n/a[(d)]
918	3',5'-cyclic AMP/2',3'-cyclic AMP	$C_{10}H_{12}N_5O_6P$	C02353/C00575	$HRMS^1_{PL}$	M+H	330.06	511.0	n/a[(d)]
1846	Carbamoyl phosphate	CH_4NO_5P	C00169	$HRMS^1_{PL}$	M-H	139.976	866.9	n/a[(d)]
726	Guanosine	$C_{10}H_{13}N_5O_5$	C00387	$HRMS^1_{PL}$	M+Na	306.081	698.1	n/a[(e)]
493	Inosine	$C_{10}H_{12}N_4O_5$	C00294	$HRMS^1_a$, R_{ta}	M+H	269.088	623.7	n/a[(e)]

[(a)]See reference Kanehisa and Goto, (2000).
[(b)]See reference Sumner *et al.* (2014).
[(c)]Log_2 fold-change in metabolite expression between *S. aureus* biofilms treated with adenine, and non-treated BHI only (ddH_2O) control data sets (treated to non-treated).
[(d)]Not available, fold change unable to be formulated as peak intensities did not significantly change between sample sets (0 fold change).
[(e)]Not available, fold change unable to be formulated as only detected in the adenine treated biofilm data set and not in the non-treated BHI (ddH_2O) data set.

3.4.3.5 Biofilms treated with DNase post inosine treatment

Purine metabolism is involved in the synthesis of nucleobases for the production of DNA. In addition, extracellular DNA (eDNA) is a component of the extracellular matrix of biofilms. The hypothesis that purine metabolism is up regulated in biofilms for the production of eDNA was tested. A DNase was tested against biofilms to look for biofilm dispersal action and if DNase treatment reversed the effect of the observation of biofilm increasing with inosine treatment (Figure 3-15). Results show that DNase decreases the biofilm biomass in inosine treated and BHI control samples (Figure 3-15). A significant difference (P=0.01) was observed in the decrease of biofilm biomass with 4 mg/ml DNase challenge in biofilms treated with inosine compared to BHI controls (Figure 3-15). Other concentrations of DNase did not demonstrate significant changes in biomass between inosine treated and non-treated biofilms (Figure 3-15).

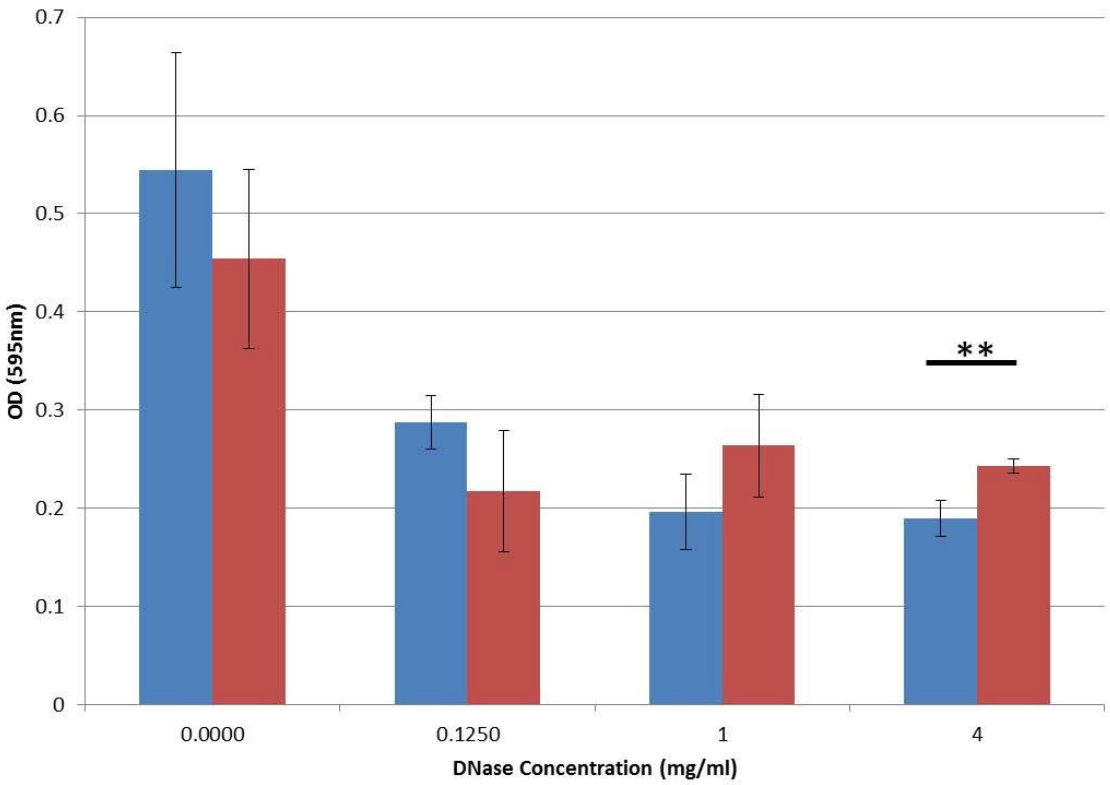

Figure 3-15: DNase treatment of *S. aureus* biofilms.
Biomass in *S. aureus* biofilms after DNase treatment proceeding treatment with or without 10 mM inosine for 4 h. A CV assay of biofilm biomass was used to quantify biofilms. Error bars ± S.D. (n=3), **Unpaired t-test between 4 mg/ml DNase treated biofilms after treatment with or without 10 mM inosine, significant difference, P = 0.01 (two tailed).

3.4.3.6 Formycin B modulates *S. aureus* biofilms by blocking purine metabolism

A structural analogue of inosine, formycin B was investigated for biofilm modulation effects due to observed changes in biofilm phenotype after inosine treatment. Formycin B at 10 mM had a decreasing effect on mature biofilms of LHSKBClinical when treated for 4 h compared to 10 mM inosine for the same time (Figure 3-16). When inosine and formycin B were added simultaneously they had a detrimental effect on the biofilm compared to inosine alone but retained more biofilm biomass than if treated with formycin B alone (Figure 3-16). These results suggest that formycin B can block inosine metabolism in the biofilm (Figure 3-16). Due to large variation in samples no significant difference was observed between inosine-only treated biofilms and other compound treated biofilms. However, a general increase in biofilm biomass was observed as previously shown but with a large standard deviation.

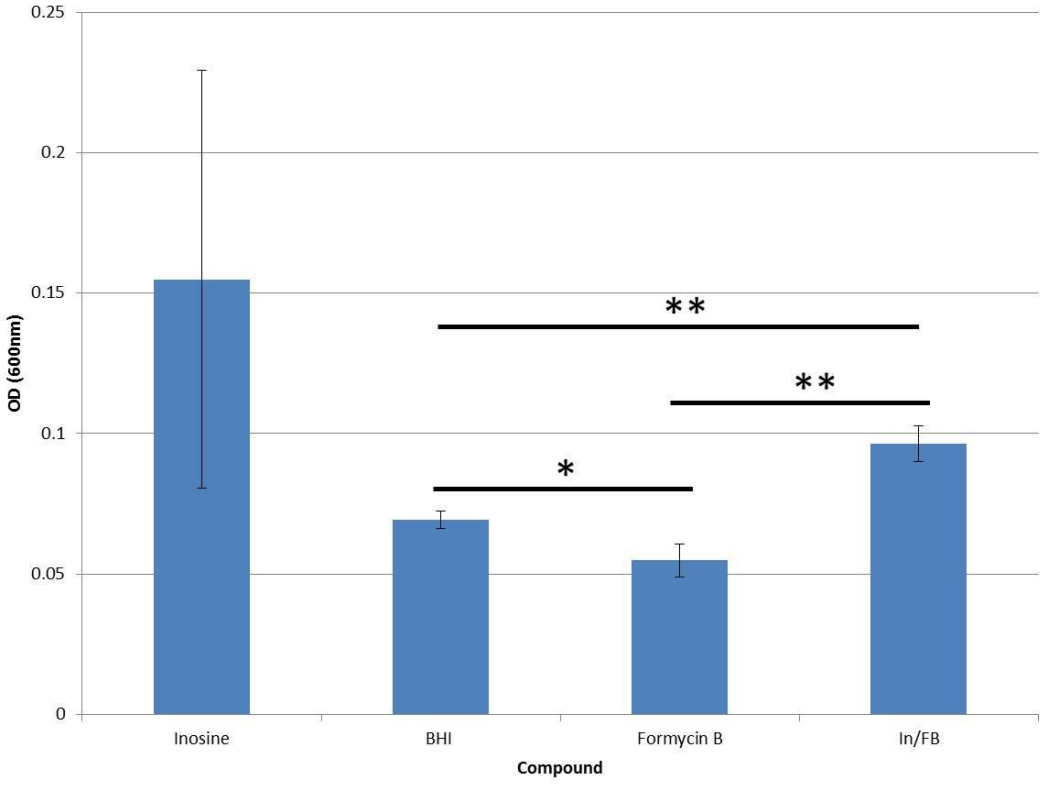

Figure 3-16: Inosine and formycin B treatment of *S. aureus* biofilms.
Biofilm biomass after 10 mM inosine, 10 mM formycin B or 10 mM inosine/10 mM formycin B treatment (In/FB). Biofilms with fresh BHI only added were set up as a negative control. Biofilms were cultured for 24 h in a 96-well microtitre plate at 37°C, followed by a wash and then treatment with the varying compounds and mixes for 4 h at 37°C. A crystal violet assay was used to quantify biofilm biomass. Error bars ± S.D (n=3). **Unpaired t-tests between formycin B and formycin B/inosine treated biofilms, and formycin B/inosine treated biofilms and BHI only biofilms, very significant difference, P = 0.0012 and 0.0028 respectively, (two-tailed). *Unpaired t-test between formycin B treated and BHI only biofilms, significant difference, P = 0.0201, (two-tailed).

Formycin B does not inhibit *S. aureus* planktonic cell growth

An MIC experiment of formycin B was carried out on planktonic culture of LHSKBClinical (Figure 3-17). Results show that formycin B did not have a killing effect on planktonic cells (Figure 3-17). Low overnight growth was most likely due to the slow shaking (50 RPM) and therefore reduced aeration of the culture. In addition, due to experimental variation, the OD_{595} of only 50 µl of culture was measured. Culture OD_{595} appeared to have increased at 10 mM, however this was possibly due to formycin B dropping out of solution during the overnight incubation period because of solution saturation.

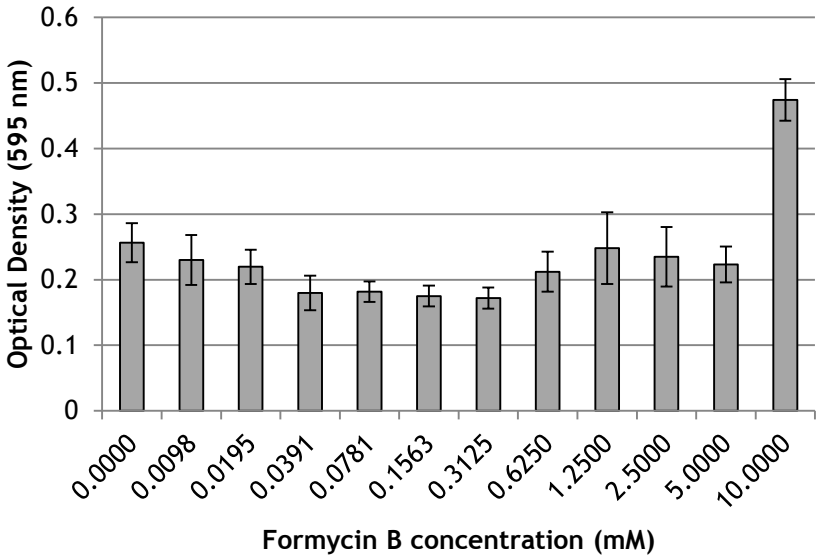

Figure 3-17: MIC testing of formycin B on *S. aureus* LHSKBClinical cells
MIC testing was carried out by testing a concentration gradient of formycin B against *S. aureus* planktonic cell culture overnight in a 96-well microtitre plate, at 37°C, shaking at 50 RPM. An OD_{595} measurement of 50 µl of each concentration was then measured, Error bars ± S.D (n=3).

After establishing that formycin B did not have a detrimental effect on planktonic culture it was tested against biofilms to assess whether it would block inosine metabolism and have a synergistic effect, when coupled with antibiotics, on biofilms.

Synergistic effect of Formycin B and Gentamycin

It was tested to see whether the addition of formycin B would have a synergistic detrimental effect on biofilms when coupled with the antibiotic gentamycin, thus making *S. aureus* biofilms more susceptible to antibiotic therapies.

Initial experiments were carried out to look at the effect of gentamycin on the *S. aureus* biofilm. MIC testing of gentamycin against planktonic cells of LHSKBClinical showed that growth was inhibited at a concentration of >0.004 mg/ml gentamycin (Figure 3-18), whereas it is seen that biofilm biomass decreases with increasing gentamycin concentration but is still present at high gentamycin concentrations (Figure 3-19). The negative control (0 mg/ml gentamycin concentration) for the MIC testing revealed a decrease in OD compared to low gentamycin concentration treated samples. This was most likely because of experimental error or possibly re-growth of the culture after initial antimicrobial challenge.

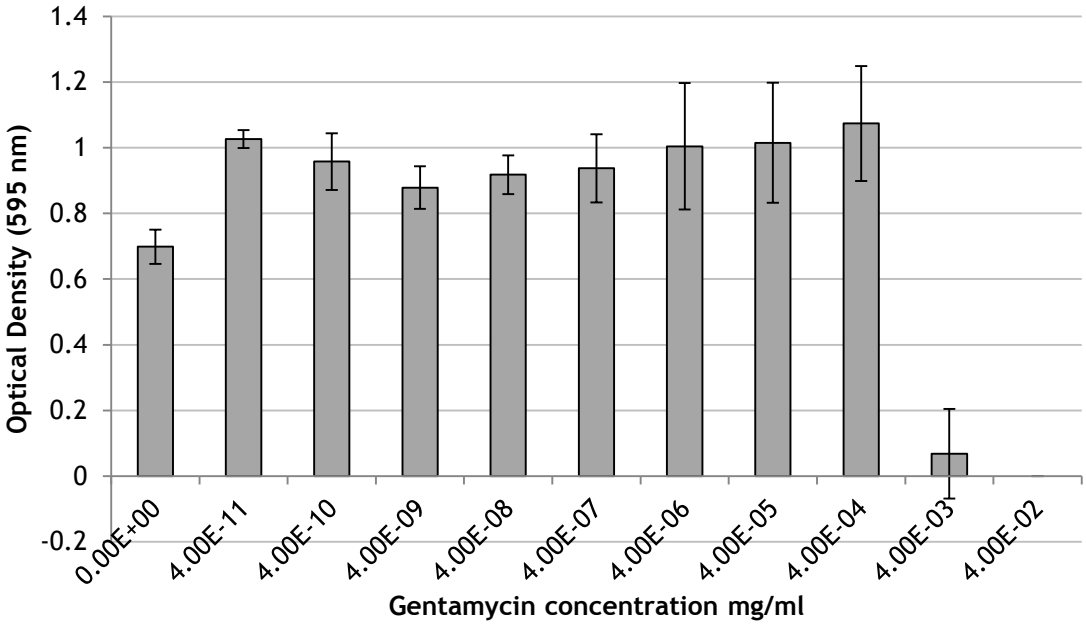

Figure 3-18: MIC testing of gentamycin against *S. aureus*
Varying concentrations of gentamycin were tested against planktonic culture of LHSKBClinical overnight, at 37°C, shaking at 50 RPM. An OD_{595} measurement of each concentration was then taken. Error bars +S.D. (n=8).

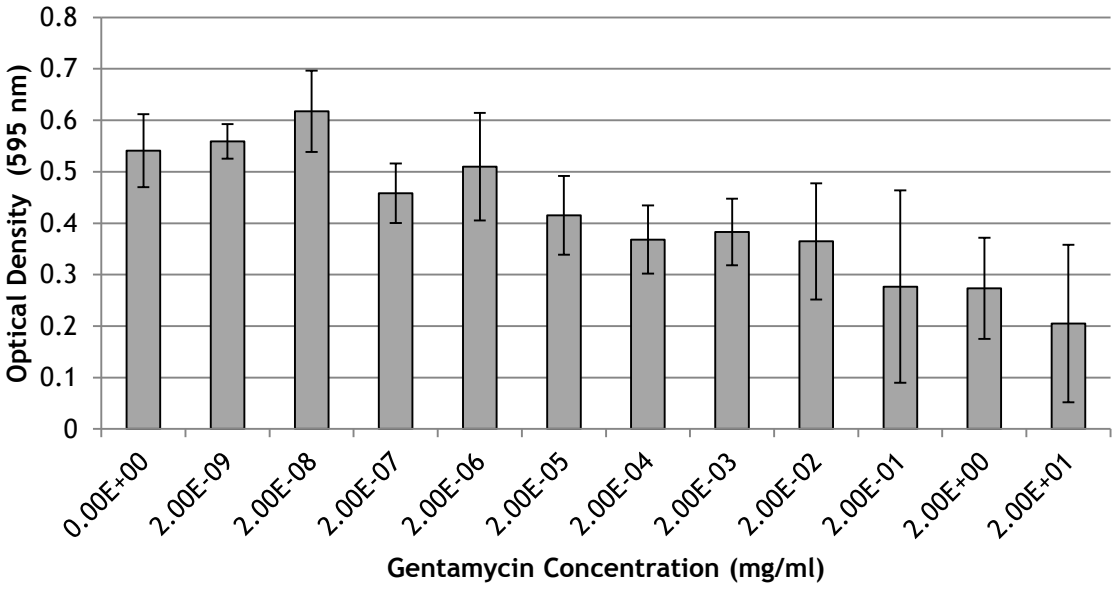

Figure 3-19: CV assay of an inhibitory concentration range of gentamycin tested on *S. aureus* biofilms
Varying gentamycin concentrations were tested against 24 h biofilms of LHSKBClinical in a 96-well microtitre plate. CV staining was used to stain biofilm biomass, solubilised and the OD_{595} of solubilised stain measures. Error bars ±S.D. (n=8).

After a range of antibiotic for biofilm dispersal was established, formycin B was added at 10 mM with the varying concentrations of gentamycin to look for a synergistic effect when used together (Figure 3-20). Figure 3-20 illustrates a synergistic effect when formycin B is added in cooperation with an antibiotic. More dispersal is observed at lower concentrations of gentamycin with the addition of formycin B than without (Figure 3-20). A significant ($P = 0.032$) difference is seen between biofilms treated and non-treated with formycin B when challenged with gentamycin at a concentration of 0.002 mg/ml (Figure 3-20). Other concentrations of gentamycin showed no significant difference between formycin B treated and non-treated biofilms (Figure 3-20). Lowered OD_{595} readings in Figure 3-20 compared to Figure 3-19 are most probably due to small technical and experimental variations in conditions leading to changes in biofilm phenotype.

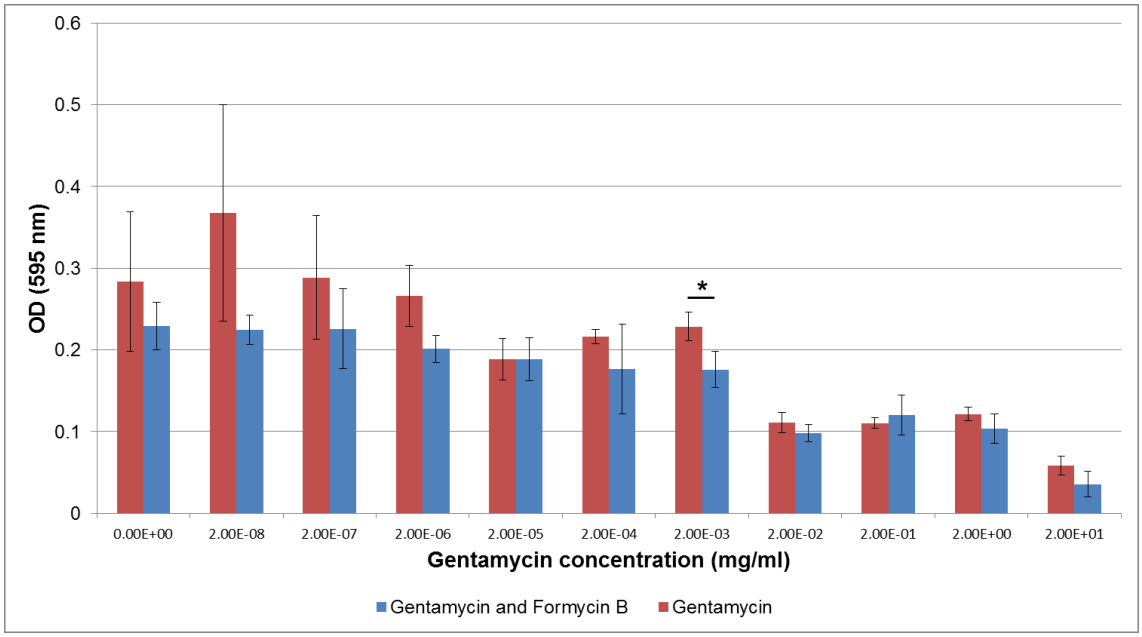

Figure 3-20: CV assay of 24 h *S. aureus* biofilms treated with varying concentrations of gentamycin solution with or without formycin B

LHSKBClinical 24 h biofilms treated with varying gentamycin concentrations with (blue bars) or without (red bars) 10 mM formycin B added, in wells of 96-well microtitre plate. CV stain used to stain biofilm biomass and solubilised. Solubilised stain OD measured. Error bars ± S.D., n=3. *Unpaired t-test between 0.002 mg/ml gentamycin treated 24 h *S. aureus* biofilms with or without 10 mM formycin B, significant difference, P = 0.032, (two-tailed).

3.5 Discussion

3.5.1 Method development and optimisation for biofilm metabolomics

Untargeted metabolomics aims to measure the metabolic profile of a biological system. To sample this, a metabolome extraction method has to be used. Here, we aimed to develop a metabolome extraction method from staphylococcal biofilms for LC-MS metabolomics, with the hypothesis that with the developed metabolome extraction method, significant changes in metabolism will be observed between planktonic cells and biofilms. Significant changes were observed between *S. aureus* planktonic cell and biofilm metabolism with the application of the extraction method; therefore we can accept the hypothesis.

Biofilm formation, involving ECM production and surface adherence, introduces complications and challenges in extracting the metabolome, requiring method development and optimisation. Challenges include poor quenching due to the biofilm structure shielding internal cells and the need for additional steps to get the biofilm material into suspension.

Appropriate preparation of the sample is an important step in optimising the extraction method. Here, all wash stages, to remove spent media, were performed with ammonium bicarbonate due to its LC-MS compatibility, moderate pH buffering and to reduce osmotic stress (Cassou et al., 2014; Faijes et al., 2007; Hedges et al., 2013). Inducing unnecessary osmotic stress can alter the bacterial cell metabolome (Wood, 2015).

Following preparation of the samples, metabolism must be quenched and the metabolites extracted from the cells and separated from cell debris. Metabolic quenching methods that can be utilised, to slow or stop metabolism, include snap-freezing in liquid nitrogen or quenching through the addition of ice cold methanol (Bolten et al., 2007). Inadequate quenching can introduce metabolite degradation and some quenching methods may not be suitable for samples such as biofilms due to their protective properties. Poor quenching may lead to stress responses and altered metabolism. Here, samples were quenched when ice cold extraction solvent mix was added containing 60% methanol as previously

described (Faijes et al., 2007), allowing for simultaneous quenching and metabolome extraction, described below.

Following quenching, a lysis step is required to extract the intracellular metabolites from the cells. Metabolome extraction from staphylococcal biofilms has two major challenges to overcome: firstly, to lyse the thick peptidoglycan cell wall, which provides protection and rigidity to Gram-positive cells, and secondly to overcome the protective ECM (Flemming and Wingender, 2010). Described and optimised herein is a metabolite extraction method employing mechanical bead beating for metabolome extraction from Gram-positive cells and from biofilms adhered to a surface. Bead-beating has previously been shown to be beneficial in the extraction of DNA and metabolites from planktonic cultures of Gram-positive bacteria (Liebeke et al., 2012), pathogenic yeasts (Bolano et al., 2001) and filamentous fungi (Burik et al., 1998).

In the comparison of lysis by sonication versus bead beading, the increase in the number of viable cells remaining after sonication treatment compared to the overnight culture, shown in Figure 3-1, is possibly due to bacterial cell clump homogenisation, an application of sonication previously exploited (Fux et al., 2004). This homogenisation effect of clumped cells can cause an increase in the viable cell count and variability of counts by allowing bacteria to form more CFUs compared to the overnight culture count. However, as this study only incorporated 3 replicates, this effect would have to be confirmed with a larger study. It may be a plausible explanation that the culture may have also grown during the 30 mins sonication treatment, however, this was controlled for by taking the cell count of the overnight culture at the same time, having been treated in the same conditions without sonication as the treated samples. Sonication treatment is unsuitable for Gram-positive cell lysis; bead beating causes greater cell death (Figure 3-1).

Other published methods utilise surface scraping and sonication (Takahashi et al., 2010). However, sonication was found to be unsuitable for Gram-positive cell lysis as it resulted in significant numbers of viable bacteria remaining (Figure 3-1), although has been shown to be useful technique for removing viable cells from orthopaedic appliances (Tunney et al., 1998), as used in the previous chapter.

Other lysis methods such as enzymatic disruption methods, as previously described (Salazar and Asenjo, 2007), require ambient temperature for enzyme activation, potentially resulting in metabolite degradation through thermal decomposition thus resulting in an altered metabolome. Temperature fluctuations can also alter cellular metabolism inducing a stress response if metabolism hasn't been efficiently quenched. This concept follows the Arrhenius equation, which states the empirical relationship between temperature and reaction rates, increased temperature causes an increase in reaction rate and subsequent metabolome change (Laidler, 1984).

Previous metabolomic literature has also reported a number of different solvent mixtures, demonstrating that the solvent used and the temperature of extraction determines the diversity of extracted metabolites (A et al., 2005). Here, chloroform, methanol, water at a ratio of 1:3:1 respectively, is shown as an optimal extraction solvent mix for our chromatography system (t'Kindt et al., 2010).

Comparing published methods for Gram-positive planktonic cell extractions (Soga et al., 2002, 2003; Takahashi et al., 2010), CFU counts after metabolome extraction suggested equivalent levels of cell death between all three extraction methods. However, LC-MS metabolomics results of these extractions revealed that the solvent extraction on its own (filtration method) was less effective than either bead beating or sonication. The sonication method was comparable to bead beating, with similar results but with greater variation between replicates. Both methods can be considered feasible for analysis of planktonic Gram-positive cells.

However, the sonication and filtering methods are not suitable for direct extraction from biofilms attached to a surface, due to complexities of sonicating uniformly across a multiwell plate and the time taken for bath sonication methods; therefore the bead beating method was employed for future cell and biofilm metabolome analyses.

It was decided to utilise the 96-well microtitre plate format to implement biofilm cultivation and metabolome extraction so that biofilms could be extracted *in situ*, therefore standardised planktonic cell extractions could also

be performed under identical conditions. Overall this ensured that results were directly comparable for downstream analysis. In addition, the CapMat provided a tight seal, while plastic-paraffin film failed, causing sample leakage and cross contamination between samples.

This metabolome extraction method, coupling bead beating and solvent mix extraction, proved to be effective for Gram-positive cells when compared with other published planktonic cell lysis methods, was reproducible (Figure 3-4), and additionally allowed for effective metabolomics analysis of biofilms (Figure 3-3). These results demonstrate both its utility for general bacterial metabolomics, and its specialist application to biofilm metabolomics, allowing for comparison between the two.

3.5.1.1 Method limitations

The metabolome extraction method developed here was based on biofilms grown statically on the base of microtitre plates for the ease of multiplexing samples. However, this bead beating method can be applied to biofilms grown in alternative platforms incorporating different substrates in different systems, for example, biofilms cultivated on cover-slips cultured in a dynamic liquid flow system. Universality of an extraction method to different platforms is important as biofilm phenotype can change if cultivated in a static or flow system (Weaver et al., 2012; Yarwood et al., 2004). Arthroplasty implants are typically made of metal alloy. However; plastic *in vitro* models provide a reproducible format to study biofilms. A future step would be to confirm observations using more advanced *in vitro* or *in vivo* models to take into account culture dynamics and host interactions.

A practical concern with using solvents such as chloroform in cell-culture plastics is they can etch and degrade plastic (Bawn and Wajid, 1956). Glass culture materials can be used however previous work has demonstrated that biofilm formation is altered on different substrates (Jansen and Kohnen, 1995; Passerini de Rossi et al., 2007; Ramage et al., 2003). Here the effects of plastic degradation on metabolomic results was minimal, possibly due to the poor retention of hydrophobic compounds on the pHILIC column used, and if present could be compensated for with the use of a negative control. In addition, any

plastic debris would be pelleted along with the beads and cell debris at the end of the extraction process.

Further, this extraction method does not discriminate between the intracellular metabolome of cells in the biofilm and the metabolome of the ECM, as both are lysed and extracted simultaneously. Through applying an appropriate ECM and cell extraction method, suitable for LC-MS metabolomic samples, it may be possible to separate biofilm cells and the ECM, a possible further application of sonication. This is an area for future method development.

Finally, there are two processes to be taken into account when evaluating the results. Firstly, due to the time taken for full lysis and extraction, as a result of the adhered biofilm and the resilience of the cells, rapid metabolic processes may still occur during this time and so this should be considered when evaluating the results as a whole. And secondly, a change in oxygen availability during static biofilm culture should be considered, as metabolism can be different under aerobic and anaerobic conditions.

3.5.2 A metabolomics study looking at planktonic cells compared to biofilm samples of a clinical isolate of *S. aureus*, LHSKBClinical

This study aimed to characterise differences in metabolism between planktonic cells and biofilms of the same clinically relevant *S. aureus* strain. We hypothesised that significant differences in metabolism exist between planktonic cells and biofilm samples, and that biofilm formation will be altered by modulating these metabolic pathways.

Metabolomic analysis of planktonic cells compared to biofilms revealed significant changes in metabolism between the two sample sets. Furthermore through modulating these pathways with exogenous metabolites and small molecule structural analogues, changes in the biofilm phenotype were observed; therefore we can accept our hypothesis.

Replicate clustering identified through PCA of biofilm metabolome data compared to planktonic data demonstrates high reproducibility of the extraction

method while discriminating between biofilm and planktonic samples (Figure 3-3). This highlights the extraction method as a valuable tool for bacterial metabolomics. An outlier in the biofilm data set demonstrates the importance of using sufficient replicates in a study.

A number of fundamental pathways in cellular metabolism were shown to be significantly changing between data sets (Table 3-1). Several mammalian pathways not in bacteria have been described as present here, highlighting database bias towards mammalian metabolism. Mammalian pathways have been included in the results because metabolites detected may still be present in samples but involved in other bacteria specific metabolic processes, providing insight into bacteria metabolism.

Furthermore, when performing statistical analysis on metabolite changes such as T-tests, the assumption is that each metabolite detection is an independent observation. Since all of metabolism is interconnected in pathways and networks, this is obviously incorrect, and therefore a quantitative change should be looked at in context to determine whether something significant is happening in the network. These pathways and networks allow us to use other detected metabolites in them to develop concepts about metabolism. Confident identifications based on R_t matching to standards can be paired with annotations, peaks matched by accurate mass using a database, to provide a clearer picture of a particular pathway, and the magnitude and direction of changes in different metabolites, which can reinforce identifications and annotations of individual metabolites in a pathway. In addition, annotated results can have multiple isomers, meaning one peak can be annotated as multiple molecules; therefore care should be taken when analysing and forming conclusions from annotated results. Further, since metabolites may be present in more than one pathway, only pathways with more than one metabolite detected to be changing between samples sets were listed in Table 3-1.

Changes in amino acid anabolism and catabolism were observed between biofilms and planktonic cells correlating with previous studies (Ammons, 2010; Resch et al., 2005; Zhu et al., 2007).

3.5.2.1 *S. aureus* biofilm arginine metabolism

Significant changes in arginine metabolism, specifically the urea cycle were observed here, with a number of metabolites significantly down regulated in biofilm samples compared to planktonic cells (Figure 3-5). As a fundamental pathway in energy metabolism, changes identified in arginine metabolism highlight significant changes in overall metabolism between the sample sets, correlating with previous studies that show significant changes in energy and cell metabolism between planktonic cells and biofilms (Ammons et al., 2014; Gjersing et al., 2007; Zhang and Powers, 2012).

In addition to the arginine biosynthesis metabolites presented in the results above, the other metabolites in the pathway were seen to be changing between sample sets but identifications for these could not be confirmed. A peak with a mass of 115.004 Da and a R_t of 755.9 sec was identified as fumarate ($C_4H_4O_4$) ($HRMS^1_{PL}$); however, this identification was removed from the analysis as it could not be confirmed. Water loss is a common neutral loss in ESI MS. Malate readily fragments in source to form an ion with identical mass to fumarate, rendering inaccurate identification. Manual analysis of this peak showed a change in relative abundance between planktonic and biofilm samples (Figure 3-21), appearing to be more abundant in planktonic samples. If this is a miss-identification and this peak is in fact an adduct of malate, this too fits the data as malate is in the TCA cycle which is directly linked to the urea cycle. Furthermore, a peak with a mass of 117.019 Da and a R_t of 732.3 sec, annotated as succinate ($C_4H_6O_4$) ($HRMS^1_{PL}$), had a $\log_2$ fold change increase of 1.32 in planktonic cell samples compared to biofilms. This further indicates the presence of fumarate, as fumarate can be converted to succinate in *S. aureus* metabolism.

Figure has been removed due to Copyright restrictions.

Figure 3-21: Peaks matched and annotated as fumarate in *S. aureus* planktonic and biofilm samples.
LHSKBClinical planktonic and biofilm metabolome samples extracted using cell lysis by bead beating and metabolite extraction using chloroform, methanol, water (1:3:1). Peaks matched by mass data base entry ($HRMS^1_{PL}$). Purple replicates represent planktonic cell samples and red replicates represent biofilm samples. Peaks visualised using PeakML viewer.

The amino acid glutamine was identified in both data sets but was seen not to be changing in intensity between planktonic and biofilm samples. *S. aureus* selectively extracts the amino acid glutamine from its medium environment (Zhu et al., 2007).

Two peaks annotated as ornithine ($HRMS^{1}_{PL}$), with the chemical formula $C_5H_{12}N_2O_2$, were resolved from the data both with a mass of 131.082 Da, but with different R_t's of 813.2 sec and 1119.5 sec. Both peaks displayed different levels of expression between sample sets, with one showing a fold change increase in expression in planktonic cells compared to biofilms and the other in reverse. Since this peak was not matched to a standard of ornithine it cannot be concluded which peak is ornithine without further fragmentation analysis. Subsequently, it was removed from the results of metabolites relating to arginine biosynthesis.

Previous studies by Zhu *et al.* (2007) and Ammons *et al.* (2014) suggest that changes in amino acid metabolism are a key feature differing in biofilms compared to planktonic samples (Ammons et al., 2014; Zhu et al., 2007). Furthermore, these studies and Wu *et al.* (2010) suggest that arginine metabolism and catabolism play an important role in biofilm survival (Wu et al., 2010). *S. aureus* extract arginine from the culture medium suggesting it may be important in *S. aureus* survival and pathogenesis (Zhu et al., 2007). Zhu *et al.*, (2007) show that mature biofilms of *S. aureus* maintain a dynamic flux of carbon and amino acid uptake and excretion, unlike previous studies in *S. epidermidis* biofilms where biofilm growth leads to low metabolic activity (Yao et al., 2005; Zhu et al., 2007).

We hypothesise that *S. aureus* may amplify flux through the urea cycle in biofilms to generate ammonia to restore pH balance in response to the production of acids (lactic acid, acetic acid, and formic acid) in the biofilm ECM (Resch et al., 2005), due to anaerobic glycolysis. Suggesting why a low abundance of metabolites was seen in biofilm samples compared to planktonic cell samples. This correlates with other studies that suggest that amino acid catabolism is crucial for biofilm pH balance (Beenken et al., 2004; Resch et al., 2005, 2006; Zhu et al., 2007). Furthermore, a study by Friedman *et al.* (2006)

shows that a decrease in pH is induced by iron starvation (Friedman et al., 2006). This hypothesis has previously been tested through genetic enzyme inactivation decreasing ammonia levels which showed no change in ambient pH (Zhu et al., 2007), however the study only inactivated arginine transport when ammonia can be produced in other metabolic pathways including purine metabolism, therefore our hypothesis may still be the case.

Microarray analyses have previously shown the up-regulation of urea cycle genes in response to the formation of biofilms in *S. aureus* (Resch et al., 2005). An up-regulation in urea cycle genes suggests the pathway is up regulated thus increasing flux through the pathway, a reason for seeing lower abundance of urea cycle metabolites in biofilms in comparison to planktonic cells.

Arginine can be involved in cell signalling through the synthesis of nitric oxide (Barraud et al., 2006; Jardeleza et al., 2011; McDougald et al., 2012) produced through the production of the precursor metabolite N-(omega)-hydroxyarginine. Here, a peak with a mass of 232.141 Da and a R_t of 837.2 sec, detected to have the formulae $C_6H_{14}N_4O_3$ (adduct M+ACN+H), was annotated to be N-(omega)-hydroxyarginine ($HRMS^1_{PL}$). The peak had a significant (adj. P value = 1.14×10^{-43}) $\log_2$ fold change increase of 6.1384 in biofilms compared to planktonic cells, thus suggesting nitric oxide production in biofilms. Nitric oxide has been implicated as a biofilm dispersal agent (Barraud et al., 2006; Jardeleza et al., 2011). An increase in the precursor metabolite to nitric oxide in biofilms leads to two hypotheses: 1) the enzyme responsible for the production of nitric oxide has been blocked; or 2) nitric oxide production is increased to induce biofilm dispersal in the mature biofilm due to limited nutrient availability. Conversely, results may show a decrease in relative abundance in planktonic cells compared to biofilms. This may be a consequence of signalling in the stationary phase cell culture reducing levels of nitric oxide to induce biofilm formation. Furthermore, depletion of arginine through the arginine deiminase pathway is a reported mechanism of nitric oxide reduction, aiding survival and subsequent pathogenesis (Diep et al., 2006).

The urea cycle is also a precursor pathway to the tricarboxylic acid (TCA) cycle through fumarate. In the TCA cycle fumarate is metabolised into malate through

the addition of H_2O. This coupled with other metabolites including succinate, were found to be significantly up-regulated in expression in planktonic cells compared to biofilms, indicating significant alteration in energy metabolism. A decrease in the TCA cycle intermediates has been reported to be a consequence of nutrient deficiency, including a reduction in oxygen and iron availability (Ledala et al., 2014). Iron restriction has been shown to induce biofilm formation and alter *S. aureus* metabolism (Johnson et al., 2005). Iron is an important nutrient for metabolism and enzyme activity in bacteria (Friedman et al., 2006; Ledala et al., 2014), and is an environmental factor influencing biofilm formation along with osmotic stresses (Lim et al., 2004; Rachid et al., 2000), anaerobic growth (Cramton et al., 2001) and glucose availability (Lim et al., 2004). *S. aureus* uptake iron from heme using the iron regulated surface determinant (isD) system (Skaar and Schneewind, 2004).

3.5.2.2 *S. aureus* biofilm purine metabolism

A further pathway to express significant changes between planktonic cells and biofilms was purine metabolism. It has been reported that purine metabolism may be involved in antibiotic resistance (Fox et al., 2007; Mongodin et al., 2003). A microarray analysis study revealed correlations between vancomycin resistance and the regulation of a putative purine metabolism regulator (*PurR)* (Fox et al., 2007; Mongodin et al., 2003). However, Fox *et al*. (2007) further report that biochemical and physiological studies to test this correlation proved unsuccessful and concluded that there was a lack of relationship between purine biosynthesis and vancomycin resistance (Fox et al., 2007), highlighting discrepancies between microarray data and phenotypic tests. Despite this, analysis of purine metabolism in *S. aureus* may provide further understanding of resistance mechanisms.

Adenosine, which was found at a lower intensity in biofilms compared to planktonic cells, can feed into the urea cycle via ammonia, further indicating flux through this pathway thus reinforcing findings in arginine metabolism.

Interestingly, the metabolite to show the greatest up regulation in biofilms compared to planktonic cells was hypoxanthine, indicating an intracellular pool of hypoxanthine in biofilms, which could be a precursor for the production of

nucleobases (Lieberman and Marks, 2009). Purine metabolism is involved in the anabolism and catabolism of purines/pyrimidines, including the synthesis of ATP for energy and of nucleotides for DNA and RNA. Extracellular DNA is a component of the ECM of the biofilm. Significant changes identified in purine metabolism are hypothesised here to be involved in the synthesis of DNA. We hypothesise that flux through purine metabolism is up regulated in the biofilm to produce eDNA for use in the biofilm. With this hypothesis the literature was examined. Traditionally eDNA production is through auto cell lysis of a sub-population of cells encased in the biofilm (Rice et al., 2007), however, some organisms have been shown to secrete eDNA from intact cells, including *Bacillus cereus* and *Staphylococcus lugdunensis*, through type iv secretion mechanisms, a similar mechanism the authors hypothesise to exist in *S. aureus* (Rajendran et al., 2015). Thus, more ECM induces antibiotic resistance.

Untargeted metabolomics is hypothesis generating and our observations in purine metabolism led us to focus investigations on this pathway. Using further metabolomics experiments and biochemical analyses we looked for biofilm modulation effects of exogenous metabolites and structural analogues, with the hypothesis that flooding the metabolic pathway with exogenous metabolites will modulate the biofilm phenotype.

Here, inosine and adenine proved to have an effect on the biofilm. The exogenous addition of adenine caused a slight decrease in biofilm biomass. However, SEM imaging showed variable results and the difference between treated samples and the control was not as significant as other modulation effects caused by inosine. We show that adenine had no effect on planktonic cells or cell growth and although metabolomics revealed significant changes in purine biosynthesis when adenine was added, this was not as vast as when inosine was added. Additionally, adenine results act as a control for the inosine modulation effects, demonstrating that the changes are not just a result of exogenous addition of any purine. This also highlights that purines are infiltrating the biofilm and cells.

Through the addition of inosine, biofilm biomass significantly increased (Figure 3-7). SEM imaging of inosine treated and non-treated biofilms identifies an increase in the biomass of the biofilm in treated samples (Figure 3-8, Figure 3-9,

Figure 3-10). In the SEM imaging controls for this experiment, 24 h biofilms treated with BHI only for 4 h, low biomass was observed on the surface with an adhered covering of cells but no presence of 3-dimensional structures. This was possibly caused by the 24 h biofilm cultivation followed by 4 h treatment inducing/causing dispersal or the wash stage causing detachment before the 4 h treatment (Figure 3-8).

Interestingly, when qPCR analysis was performed, to provide estimation on the cell density, no change in cell density was observed between treated and non-treated samples. However, this observation should be confirmed with another approach, for example a biofilm cell live/dead stain. The thickening in biofilm and increase in biomass is likely due to the production of ECM possibly through the production of eDNA as discussed earlier; therefore no change in cell density would be apparent. SEM sample preparation involves numerous fixing and drying stages which will have detrimental effects on the ECM. Therefore, SEM imaging is not a good way to image the ECM and may be why not a lot is seen on the surface of the biofilm. The inosine treatment could be causing increased surface adhesion by ECM production, therefore resulting in the retention of the biofilm during SEM preparation, compared to the controls. Furthermore, SEM imaging performed here was not quantifiable and therefore represents qualitative data. It is important to note that either detrimental sample preparation in the SEM imaging approach or an error in the qPCR analysis could have been responsible for the discrepancies between the SEM imaging and qPCR approach, therefore requiring further analysis.

The observation that inosine increases biofilm biomass has been identified previously in *E. coli* where an ackA (acetyl phosphate) mutant exhibited increased biofilm amounts in the presence of inosine (Mugabi et al., 2012). Further, Kusada *et al.* (2014) show in *E. coli* that expression of a cloned gene responsible for encoding adenosine deiminase (catalysing the conversion of adenosine to inosine) could be induced using known biofilm-inducing molecules, suggesting a biofilm regulation network involving the production of inosine (Kusada et al., 2014). According to the KEGG database this enzyme may not be present in *S. aureus*. However, through NCBI pBLAST analysis of the gene responsible for the enzyme searched against *S. aureus* genomes, alignment and

regions of heterogeneity were identified suggesting some *S. aureus* stains do have the capability to synthesise this enzyme.

To further demonstrate the role of eDNA in the biofilm ECM, we have shown a reduction in biofilm biomass when treated with DNase (Figure 3-15). However, pre-treating the biofilm with inosine and subsequently treating with DNase resulted in an even greater reduction in biofilm biomass. We hypothesise that this is due to the inosine contributing to purine biosynthesis, producing DNA for the biofilm ECM.

Metabolomics of biofilms treated with exogenous purine metabolites revealed significant changes in purine metabolism. We show a relationship between purine metabolism and biofilm regulation. Results from a study by Zielinska *et al*. (2012) also demonstrated this relationship (Zielinska et al., 2012). Using a proteomics approach, they employed gene knockouts in bacteria and murine models of implant-associated biofilm infection and *S. aureus* bacteraemia to compare virulence of a *sarA* mutant and strain derivatives in USA 300 strains. They report that *sarA* is involved in virulence factor regulation, as *sarA* mutation increases extracellular proteases and causes a decrease in biofilm formation and extracellular toxins. They show a decrease in the accumulation of 253 proteins in the *sarA* mutant compared to the parent strain (Zielinska et al., 2012). From interrogating the study's supplementary proteomic data, it was found that the purine nucleoside phosphorylase enzyme, encoded by the *deoD* gene, was down-regulated, with a decreased total spectral count in the *sarA* mutant compared to the parental strain. This enzyme is involved in purine metabolism, responsible for the reversible reaction of inosine into hypoxanthine. This correlates with the results presented here, where hypoxanthine is higher in biofilm samples compared to planktonic cell samples. Furthermore, when exogenous inosine is added to biofilm samples, biofilm biomass increases and hypoxanthine is found to be up regulated, showing a correlation between the purine metabolic pathway and biofilm biomass, and thus highlighting the importance of purine metabolism in biofilm regulation. We hypothesise that *sarA* is involved in the regulation of purine metabolism, and subsequent biofilm formation, in *S. aureus*.

Additionally, defective purine metabolism in *S. aureus* mutants was found to result in deficient biofilm formation (Ge et al., 2008; Yee et al., 2015).

Small structural analogous of inosine have been used to target purine metabolism of other organisms and have been proven successful. One such analogue is formycin B, a structural analogue of inosine (Figure 3-22). Formycin B has been used as an anti-parasitic against *Leishmania* species (Rainey and Santi, 1983). In *Leishmania*, formycin B is first converted to formycin B 5'-monophosphate by nucleoside phosphotransferase. It is then converted to cytotoxic adenosine nucleotide analogues of formycin A that become incorporated into RNA (Rainey and Santi, 1983). In addition it has been shown to have purine nucleoside phosphorylase (E.C. 2.4.2.1) enzymatic inhibitory action in *E. coli* (Bzowska et al., 1992). However, host toxicity has limited its use. Formycin B potentially has a similar mechanism of action in *S. aureus* as it does in *E. coli* and *Leishmania*, inhibiting purine nucleoside phosphorylase and causing toxic effects to RNA.

Here, formycin B was tested against biofilms (Bzowska et al., 1992). Results show a reduction in biofilm after being treated with formycin B and a potential synergistic effect when added with the antibiotic gentamycin; however results need to be confirmed with a larger study as only one concentration of gentamycin showed statistical significance and the sample size here was small. This suggests that formycin B or similar small structural analogues could be used to block a crucial metabolic pathway in biofilms making them more susceptible to antibiotic therapies, reducing resistance.

Figure has been removed due to Copyright restrictions.

Figure 3-22: Structures of inosine and its structural analogue, formycin B.
R = ribose. Adapted from Bzowska *et al.*, (1992).

3.5.3 Conclusions

Here the aim was to characterise and compare the metabolome of the clinically important bacteria *S. aureus,* living in a planktonic or biofilm state using LC-MS. Through the development of a low-temperature, rapid and mechanical method coupled with an extraction solvent, to lyse Gram-positive bacteria and extract the intracellular metabolome, reproducible results were obtained allowing for comparison in *S. aureus* metabolism between planktonic cells and biofilms. The

method optimised here could be used for future metabolomic analyses of biofilms, providing insight into resistance mechanisms.

An important consideration to be taken into account with this study is the different culturing approaches used for planktonic cell and biofilm preparations. Planktonic cells were cultured under shaking conditions whereas biofilm growth was carried out under static conditions. It is therefore a valid argument that difference between conditions led to a difference in aerobic conditions leading to the production of different metabolites or different metabolite expression intensities. However; changes in aerobic conditions are known to induce biofilm formation (Cramton et al., 2001), therefore results describing the difference between these two states under these conditions are still valid and important. To overcome this in future work; monitoring of oxygen availability in the media could be employed and biofilm formation under dynamic conditions could be incorporated into such a study, therefore increasing oxygen availability.

Studies revealed that through modulating purine metabolism an altered biofilm phenotype was observed. Furthermore, the use of a structural analogue, formycin B, provided synergistic effects when coupled with an antibiotic, gentamycin, providing increased biofilm dispersal.

Initial studies looking at stable isotope labelling of biofilms through utilising ^{13}C labelled glucose spiked into biofilm growth media, of treated biofilms with formycin B were carried out. However, due to time constraints the data could not be analysed. This represents further work. This data would provide flux analysis of metabolism and the effect of formycin B on the *S. aureus* biofilm to be studied. In addition to this, to look at the fate of exogenous inosine when added; labelled inosine with ^{15}N spiked into the biofilm media could be used. This could then be traced using targeted metabolomics.

Further future work could employ the use of a live/dead stain for biofilm cells. Such stains could be used to verify the qPCR result and would provide evidence of the number of viable cells in the biofilm, therefore showing if inosine was inducing cell growth in the biofilm, or retaining live or dead cells through increased ECM production.

Proteomic analysis of planktonic cells and biofilms could also constitute future work. Proteomic studies could be incorporated with metabolomic data showing present enzymes in metabolic pathways and networks, and not just gene annotations of possible encoded proteins. Proteomics allows for the detection of synthesised proteins in a system.

In addition, the analyses carried out here represent observations based on one strain of *S. aureus* and future studies should look for similar modulation effects in metabolism across other strains. Another way to study the effects of purine metabolism in the staphylococcal biofilm could be through utilising gene knock out mutants. Knock out libraries exist for *S. aureus* and could be used to further understand the effects of knocking down enzyme activity.

Chapter 4 A metabolomics approach to study the mode of action of triclosan on *Staphylococcus aureus* biofilm formation and dispersal

4.1 Introduction

Triclosan (Irgasan; 5-chloro-2-(2,4-dichlorophenoxy)phenol)) is an antibacterial compound that has been used for multiple applications for the best part of three decades (Bhargava and Leonard, 1996). The drug has been applied to topical preparations, including personal and surgical soaps (Bhargava and Leonard, 1996); dental hygiene applications, for example a component of dentifrices (Riley and Lamont, 2013); and is regularly used in the cosmetic industry (Bhargava and Leonard, 1996). Triclosan effectiveness changes in response to increasing concentrations: bacteriostatic at low concentrations (inhibiting fatty acid biosynthesis) and bactericidal at high concentrations (causing cytoplasm and membrane damage) (Suller and Russell, 1999, 2000). Triclosan is a broad spectrum drug, effective against a wide range but not all Gram-positive and Gram-negative bacteria (Russell, 2004). High triclosan activity has been reported against staphylococci, some streptococci, some mycobacteria, *Escherichia coli* and *Proteus* species (Russell, 2004; Schweizer, 2001). Such bacteria have shown low minimum inhibitory concentrations (MICs) in the range of 0.01-0.1 mg/L (Russell, 2004; Schweizer, 2001). However, triclosan is often applied at much higher concentrations than the reported MICs ensuring bactericidal activity (Suller and Russell, 1999, 2000). The antimicrobial agent has also been shown to be anti-fungal against some fungi (Bhargava and Leonard, 1996).

Recently the Food and Drug Administration (FDA) have been examining the use of triclosan (FDA, 2013). The effects of the drug are still largely unknown and concerns over a link between the over usage of triclosan and antibiotic resistance persist (McMurry et al., 1998b). FDA concerns have led to some states in the USA banning the use of triclosan. More research is needed into the mechanism of action (MOA) and its effects on different bacterial growth states.

Triclosan has been reported to follow the Z-shape pattern of biocide interaction, whereby effectiveness shows a sharp break followed by enhanced uptake (Denyer and Maillard, 2002). Reasons for this may be because the concentration of adsorbed species is causing breakdown of the cell structure subsequently generating new adsorption sites (Denyer and Maillard, 2002).

The MOA of triclosan in bacteria has previously been characterised. Previous work using sequencing and gene knockout approaches, has shown triclosan to block lipid synthesis in *S. aureus* and *E. coli* (Heath and Rock, 2000; Heath et al., 2000; Levy et al., 1999; McMurry et al., 1998a). Triclosan activity occurs through binding too and inhibiting an NADH-dependent enoyl-acyl carrier protein (ACP) reductase (FABI), encoded by *FABI* gene (Heath and Rock, 2000; Heath et al., 2000; Levy et al., 1999; McMurry et al., 1998a; Slater-Radosti et al., 2001). This binding increases the enzyme's affinity for nicotinamide adenine dinucleotide (NAD^+) and results in the formation of FABI-NAD^+-triclosan, poisoning fatty acid synthesis (Heath et al., 1999).

Further to inhibiting lipid biosynthesis, the antimicrobial agent can employ other toxic and bactericidal effects including potassium ion leakage, and detrimental membrane effects, including damage and destabilizing behaviour, thus highlighting multiple bacteriostatic and bactericidal mechanisms of action (Suller and Russell, 1999, 2000; Villalain et al., 2001), which are not yet fully understood. It has been shown that *S. aureus* adaption to triclosan challenge involves multiple genetic pathways possibly highlighting multiple MOAs (Nielsen et al., 2013). Untargeted metabolomics provides a novel tool to elucidate these mechanisms.

4.2 Aims

The aims of this project were to:

1. Assess the effects of triclosan on *S. aureus* biofilm formation using biochemical and imaging approaches.

2. Determine the metabolic effects of triclosan on *S. aureus* planktonic cells and biofilms by metabolic profiling.

Here we aim to investigate the metabolic effect of triclosan on a clinical isolate of *S. aureus*, LHSKBClinical using an untargeted LC-MS metabolomics approach. In addition, differences between planktonic and biofilm cell metabolism in response to triclosan will be explored. The lack of agreement in the MOA of

triclosan and the increased concern over its use lead us to hypothesise that we can highlight MOAs of triclosan in *S. aureus* using untargeted metabolomics.

4.3 Materials and methods

4.3.1 Cell culture

The *S. aureus* clinical isolate LHSKBClinical characterised in chapter 3 of this thesis was cultured as described in section 2.3.2.1.

4.3.2 Biofilm cultivation

In vitro biofilms of clinical isolate LHSKBClinical were cultivated at described in section 2.3.3.1. Biofilms were cultivated for 10 h and washed in ddH_2O as described in section 2.3.3.1.

4.3.3 Triclosan

Triclosan (Irgasan) (Sigma-Aldrich) was dissolved in 95% ethanol for all experiments.

4.3.4 Triclosan challenge of *S. aureus* planktonic cells

To establish dose-response curves varying drug concentrations of triclosan were tested against planktonic cells of LHSKBClinical. In a sterile 96-well microtitre plate (Corning Costar, Sigma, UK), decreasing triclosan concentrations in equivalent volumes of 95% ethanol were added to a 1:6 dilution of overnight stationary phase culture in BHI to make final triclosan concentrations of 0 nM, 0.01 nM, 0.1 nM, 1 nM, 0.01 µM, 0.1 µM, 1 µM, 0.01 mM, and 0.1 mM. This approach meant each treatment had the same amount of ethanol added. Each treatment was carried out in triplicate (technical replicates). The plate was then incubated for 4 h, at 37°C, in a Bio-Rad orbital shaker at 75 RPM. Cell growth of planktonic bacteria cells in response to triclosan was measured by OD_{595} measurements.

A sub-set of triclosan concentrations were selected for further metabolomic analysis based on the results of the dose response experiments. The contents of the wells containing the dilutions for metabolomic analysis were transferred to a sterile 1.5 ml reaction tubes (Greiner Bio-One) for metabolite extraction. For a positive control, cell samples were treated with 95% ethanol (solvent) only.

Ethanol was added at an equivalent volume as added to triclosan challenged samples. A negative control was treated with sterile BHI only.

4.3.5 Triclosan challenge of *S. aureus* biofilms

Varying drug concentrations of the triclosan were tested against biofilms of LHSKBClinical. Following biofilm cultivation and washing, 200µl of fresh BHI media was added to each well containing biofilm. Next, decreasing triclosan concentrations in equivalent volumes of 95% ethanol were added to each well to make final triclosan concentrations of 0 nM, 0.01 nM, 0.1 nM, 1 nM, 0.01 µM, 0.1 µM, 1 µM, and 0.01 mM. This approach meant each treatment had the same amount of ethanol added. Each treatment was carried out in a replicate of 8 (technical replicates). Appropriate negative controls were utilised including biofilm samples treated with BHI only and biofilm samples treated with 95% ethanol only. The contents of the wells were mixed gently by agitating the plate in a circular motion. The plate was then incubated at 37°C, for 4 h, in a static incubator as previously described. Next, spent media was removed and the samples were washed as described in section 2.3.3.1. Following the wash biofilm biomass was assessed.

For triclosan challenge of biofilms for metabolite extraction, biofilms were cultivated as above in a second 96-well cell culture plate. Metabolomic analysis was performed on biofilms challenged with triclosan concentrations; 0 nM, 0.1 nM, 1 nM, 0.01 µM, 0.1 µM, 1 µM, and 0.01 mM. Biofilm extractions were performed on 11 parallel replicate samples. For negative controls, 0 mM biofilm samples were treated with 95% ethanol only. Ethanol was added at an equivalent volume as added to triclosan challenged samples. Another negative control was treated with sterile BHI only.

4.3.6 Biofilm crystal violet (CV) assay

The CV biofilm assay as described in section 2.3.3.2 was used to quantify biofilms following treatment. CV experiments were carried out in replicates of 8.

4.3.7 Scanning electron Microscopy (SEM)

For SEM imaging, biofilms were grown on Thermanox™ coverslips for 10 h as described in section 2.3.3.1. To the biofilms, sterile BHI was then added together with triclosan to a final concentration of 0.01mM, or equivalent volume of 95 % ethanol or BHI as negative controls. The plate was then mixed gently and incubated for 4 h, at 37°C, static humidified incubator. Following triclosan treatment slips were then washed as described in section 2.3.3.1, and processed for SEM and imaged as described in section 2.3.3.3. Three technical replicates were made and processed for SEM.

4.3.8 Metabolomics

4.3.8.1 Sample extractions and preparations

Planktonic cells and biofilms were initially washed with 10mM ammonium bicarbonate as described in section 2.3.3.1. After washing, the metabolome from cells in reaction-tubes or biofilms in 96-well plates, were extracted using the bead-beating methods described in sections 3.3.3 and 3.3.4, respectively.

4.3.8.2 Metabolomic workflow, data acquirement and analysis

Samples were then analysed by hydrophilic interaction liquid chromatography-mass spectrometry as described in section 3.3.6.

4.3.8.3 Metabolomic data analysis and statistics

Metabolomic data analysis and statistics was performed as described in section 3.3.7.

4.3.8.4 Metabolomic data presentation

Metabolomic data presentation was performed as described in section 3.3.8.

4.4 Results

4.4.1 Crystal violet assays and scanning electron microscopy (SEM) imaging reveals a detrimental effect of triclosan on *S. aureus* planktonic cells and biofilms

Diluted stationary phase planktonic cells and biofilms of the *S. aureus* strain *LHSKBClinical* were incubated with varying triclosan concentrations.

For planktonic cells, a triclosan dose response curve was established though incubating cells with a range of triclosan concentrations. A sub lethal triclosan concentration range was tested for 4 h against planktonic cells, until the lag phase had lapsed and the culture had started the exponential growth phase, (as seen in section 2.4.2.1) when the cells are most metabolically active (Figure 4-1-A). Increased concentration of triclosan had a detrimental effect, correlating with dose, on planktonic cell growth (Figure 4-1-A).

For biofilm dose response curves, bacterial cells were left to adhere to a surface subsequently forming a biofilm. Following biofilm formation, samples were treated with varying concentrations of triclosan for 4 hours. Varying triclosan concentrations demonstrated different levels of biofilm dispersal, correlating with concentration. Dose response experiments showed increased biofilm dispersal with increasing triclosan concentration (Figure 4-1-B).

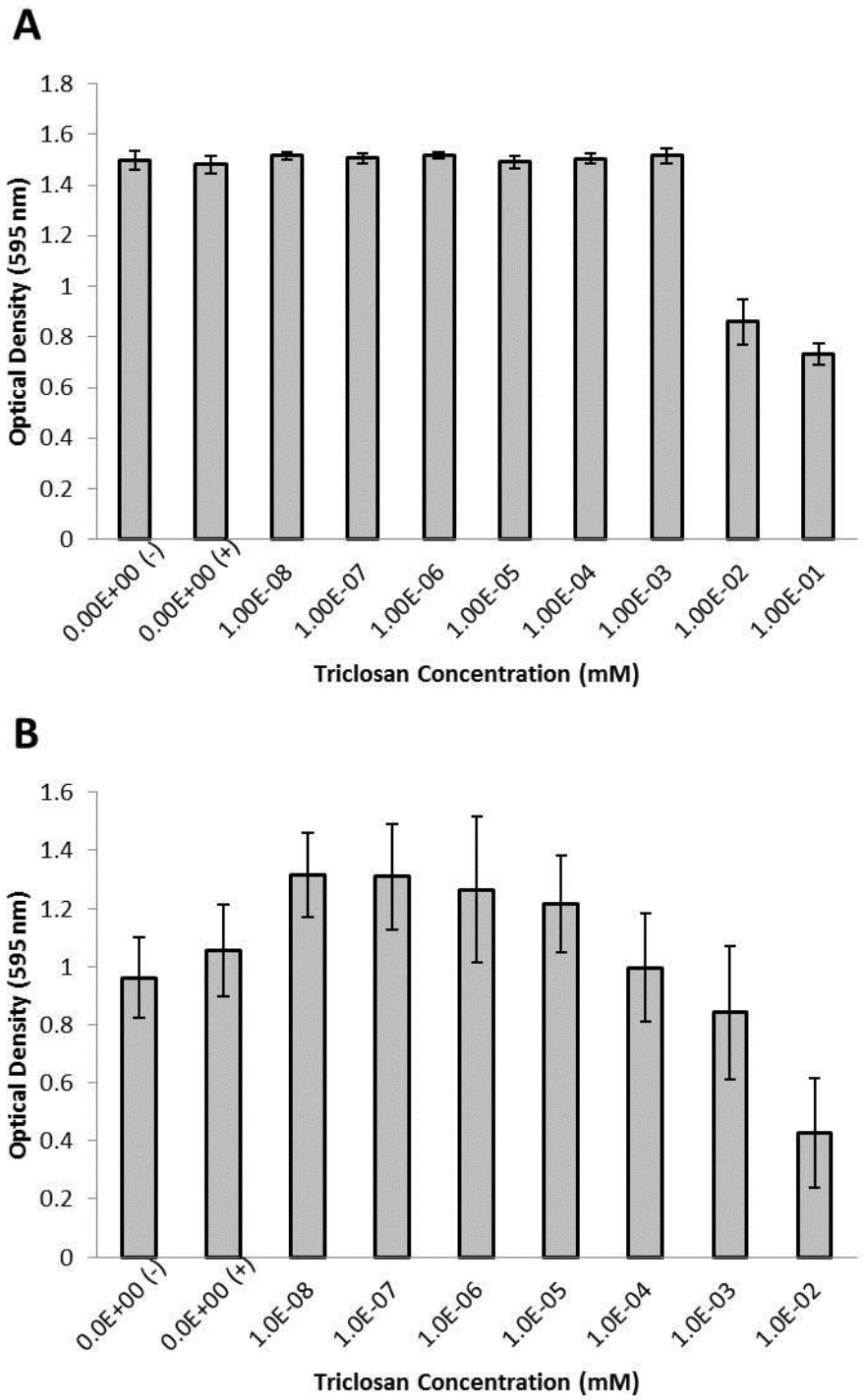

Figure 4-1: Dose response curves of varying triclosan concentrations on planktonic cells (A) and biofilms (B) of *S. aureus* strain LHSKBClinical
(A) OD measurements of planktonic cell culture after 4 h treatment with varying triclosan concentrations, n=3. (B) Biofilms grown for 10 h biofilm and then treated for 4 h with varying triclosan concentrations. Biofilms stained with CV. CV stain was solubilised and the OD_{595} was measured, error bars ± S.D, n=8.

Images of CV stained biofilms in wells of a 96-well plate demonstrated the effect of biofilm dispersal in response to a triclosan concentration of 0.001mM compared to non-treated wells and wells treated with 95 % ethanol (triclosan solvent) (Figure 4-2). A visual decrease in biofilm biomass is apparent in triclosan treated wells.

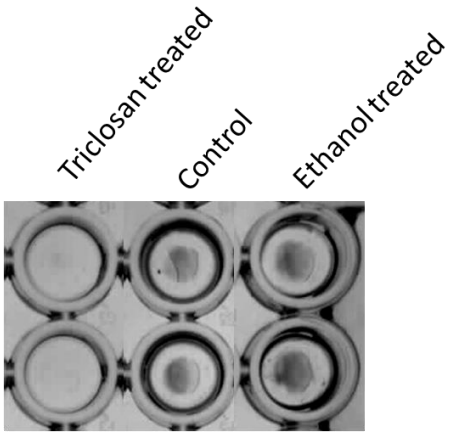

Figure 4-2: CV stained *S. aureus* biofilms treated with triclosan
Biofilms of LHSKBClinical cultivated in the wells of a 96-well microtitre plate for 10 h and treated with triclosan (0.001mM), 95 % ethanol treated (triclosan solvent) or non-treated (control), for 4 h. Following treatment samples were washed, stained with CV and imaged.

Further to using CV staining to look at the effect of triclosan on biofilms, SEM imaging was utilised to provide qualitative data to look at biofilms in detail after triclosan challenge, and to see if triclosan would disperse the *S. aureus* biofilm (Figure 4-3, Figure 4-4, and Figure 4-5). SEM imaging highlighted the detrimental effect of Triclosan on the *S. aureus* biofilm compared to biofilms treated with 95 % ethanol and non-treated samples (Figure 4-3, Figure 4-4 and Figure 4-5). A decrease in biofilm and adhered cells covering the surface is visible in samples treated with triclosan (Figure 4-3, Figure 4-4, and Figure 4-5). It is clear in comparing Figure 4-4 and Figure 4-5 that there is a substantial reduction in three-dimensional structures. In addition, to show that detrimental effects are not caused by the solvent used for triclosan, comparison between 95% ethanol treated and non-treated samples indicates no difference in biofilm coverage or structure. This meaning biofilm dispersal is being induced by the addition of triclosan.

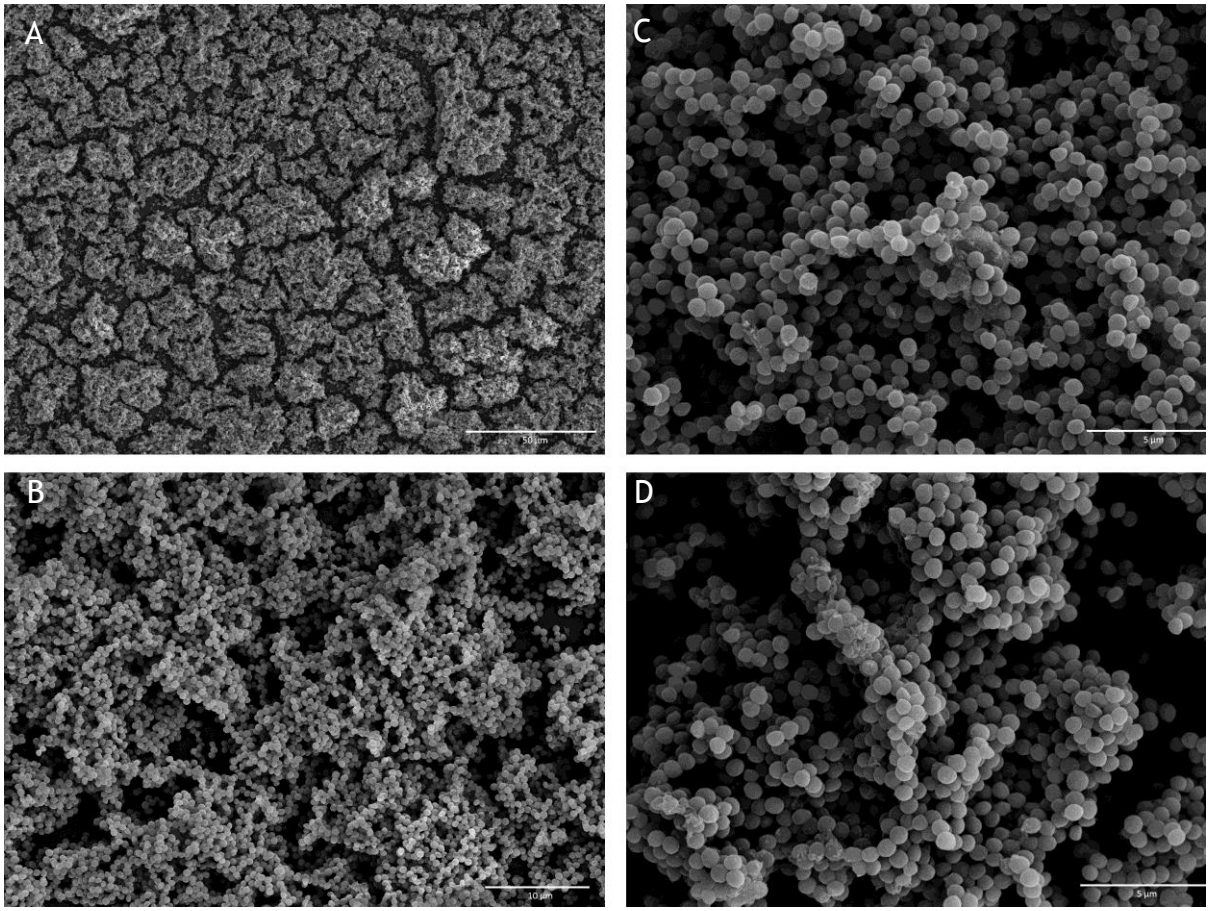

Figure 4-3: SEM of *S. aureus* biofilm, 10 h growth, followed by 4 h incubation with BHI only. Biofilms cultured on a *Thermanox* coverslip, A, 500X magnification, scale bars represent 50 µm. B, 2000X magnification, scale bar represents 10 µm. C and D, 5000X magnification, scale bars represent 5µm. A/C and B/D are 2 technical replicates.

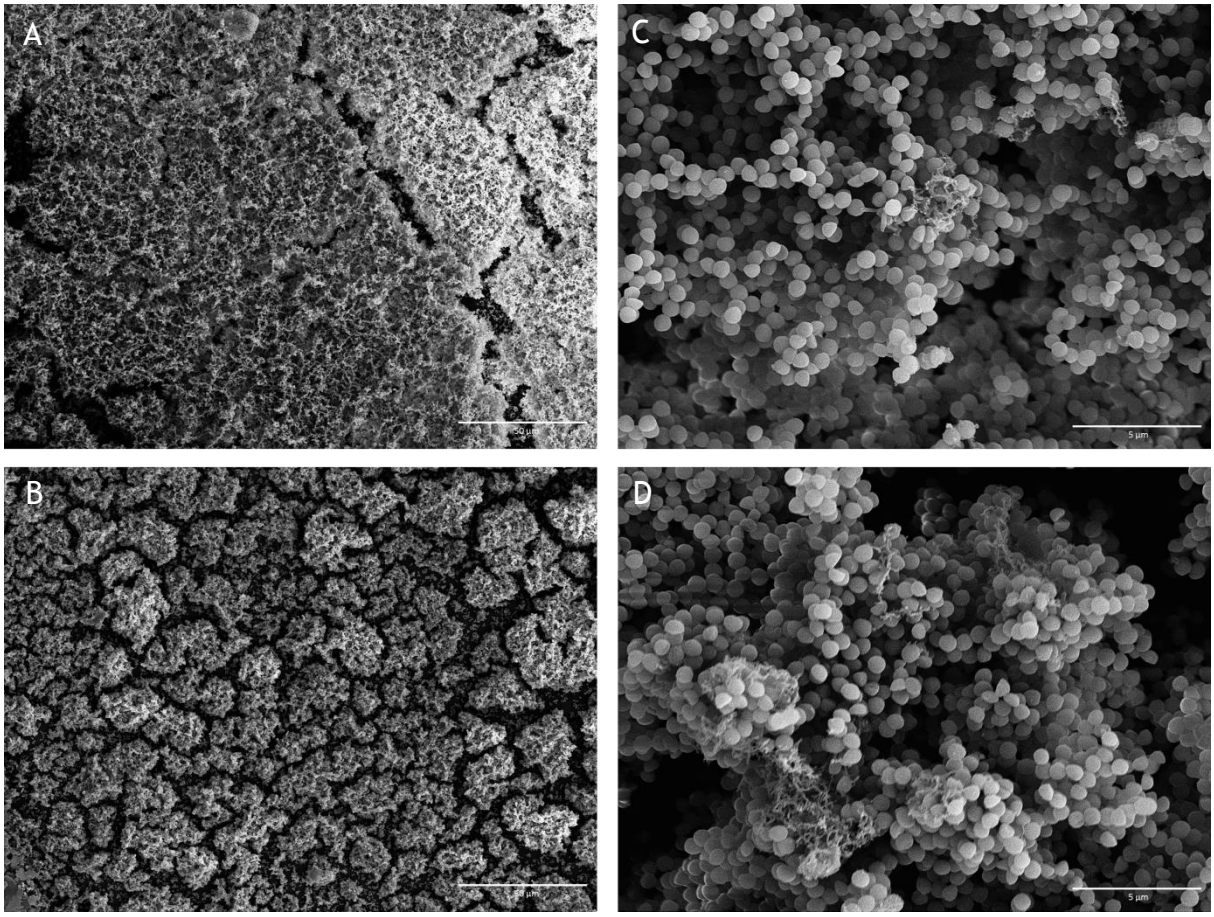

Figure 4-4: SEM of a 10 h *S. aureus* biofilm treated with 95% ethanol.
Biofilms cultured on a *Thermanox* coverslip. A and B, 500X magnification, scale bars represent 50 µm. C and D, 5000X magnification, scale bars represent 5 µm. A/C and B/D are 2 technical replicates

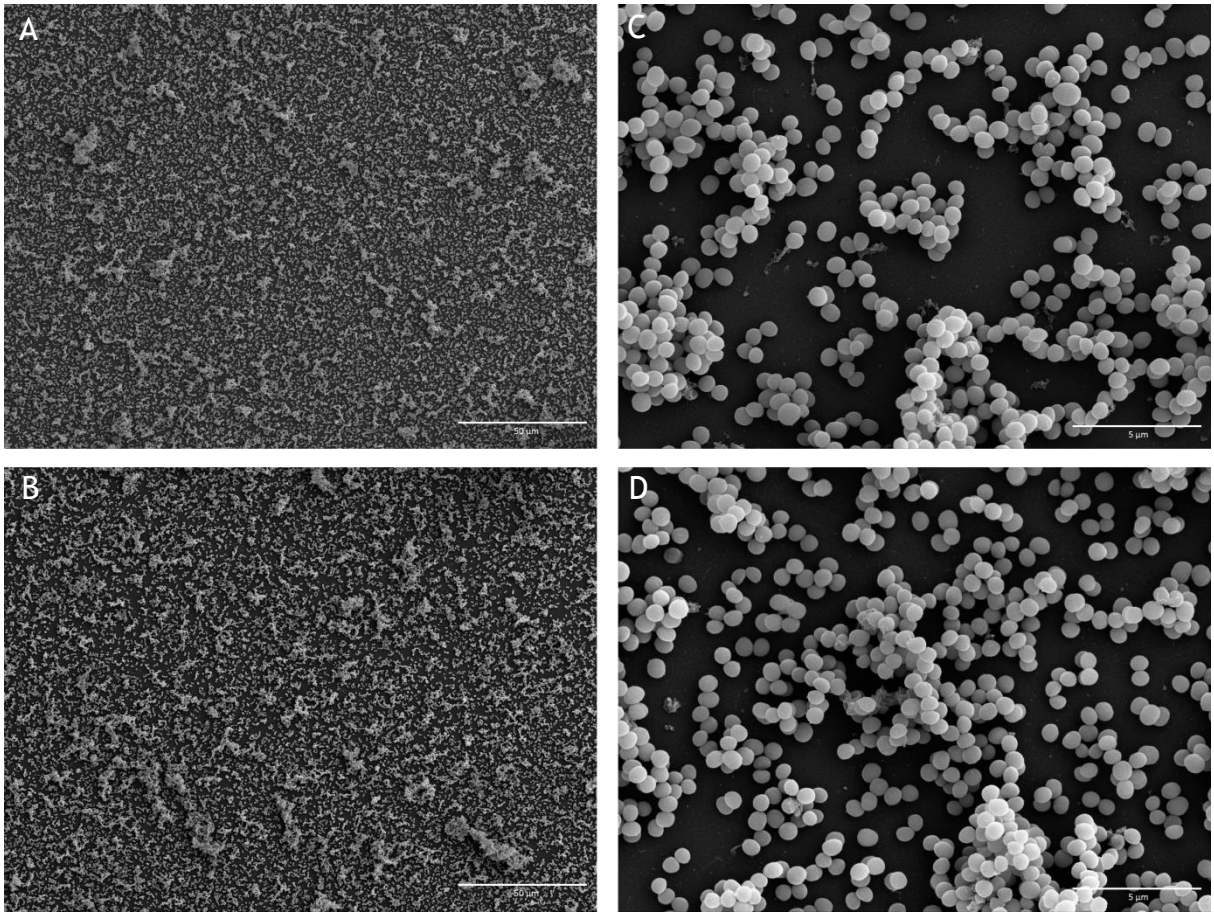

Figure 4-5: SEM of a 10 h *S. aureus* biofilm treated with 0.01 mM Triclosan.
Biofilms cultured on a *Thermanox* coverslips. A and B, 500X magnification, scale bars represent 50 µm. C and D, 5000X magnification, scale bars represent 5 µm. A/C and B/D are 2 technical replicates.

4.4.2 Studying the effect of triclosan on planktonic *S. aureus* cells and biofilms using LC-MS metabolomics

Metabolomic analysis was performed by carrying out metabolite extractions on planktonic cells treated with a triclosan concentration range ascertained by OD dose response experiments (Figure 4-1-A), for 4 h. In addition, metabolomics analysis was performed by carrying out metabolite extractions on biofilms of *S. aureus* treated with the triclosan concentration range tested in dose response experiments (Figure 4-1-B), for 4 h. Once the metabolite extracts were created, the extraction mixtures were separated using LC and analysed using accurate MS.

4.4.2.1 Triclosan detection

Initial analysis was carried out to identify triclosan in the sample sets allowing for evaluation of the serial dilution and triclosan uptake. Intracellular triclosan concentration was detected to be decreasing correlating to a decreasing dose added (Figure 4-6). The spent media from the extracted planktonic cells was also analysed. At a triclosan concentration of 0.01mM, triclosan was only detected intracellularly in the bacterial cells and not exogenously in the culture media.

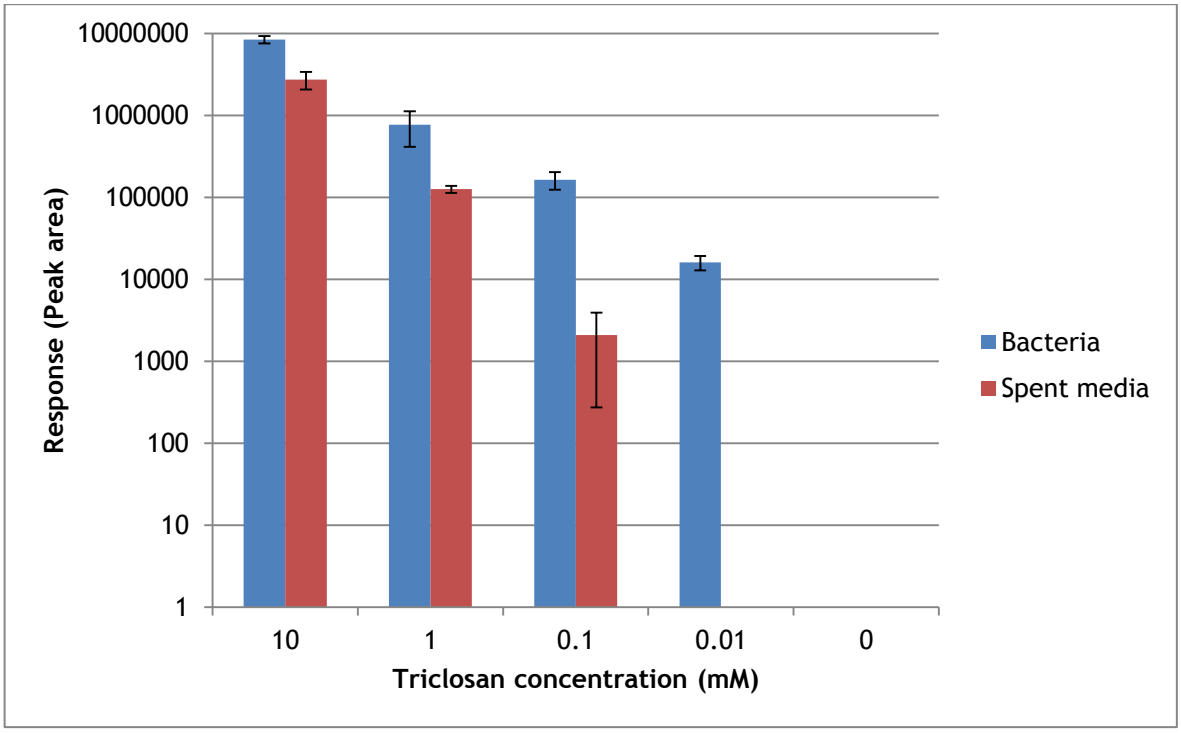

Figure 4-6: Mass-spectrometry detection response (peak area) of triclosan in *S. aureus* and spent media.
Intracellular detection of triclosan in LHSKBClinical planktonic bacteria (blue) and extracellular detection of triclosan in spent media (red) of samples treated with various concentrations of triclosan for 4 h. Samples with 0mM treated with 95% ethanol only as a solvent control (n=3, error bars ± S.D.).

4.4.2.2 Untargeted metabolite detection in samples

Principal component analysis (PCA) plots of the planktonic cell and biofilm metabolomic data sets illustrated clustering of replicate groups and displayed clear differentiation between high drug concentrations compared to low/no drug concentrations (Figure 4-7). A strong correlation was observed between metabolite variance and drug concentration (Figure 4-7-B) in the biofilm dataset. In planktonic samples, changes in the metabolome variation in principle components 1 and 2 are only seen in concentrations above 0.01mM. In biofilm samples, changes in the metabolome variation in principle components 1 and 2 are only seen in concentrations above 0.0001mM. Clustering of sample replicates gave confidence that the extraction method is reproducible and that we can expect strong changes in metabolic profiles between drug concentrations.

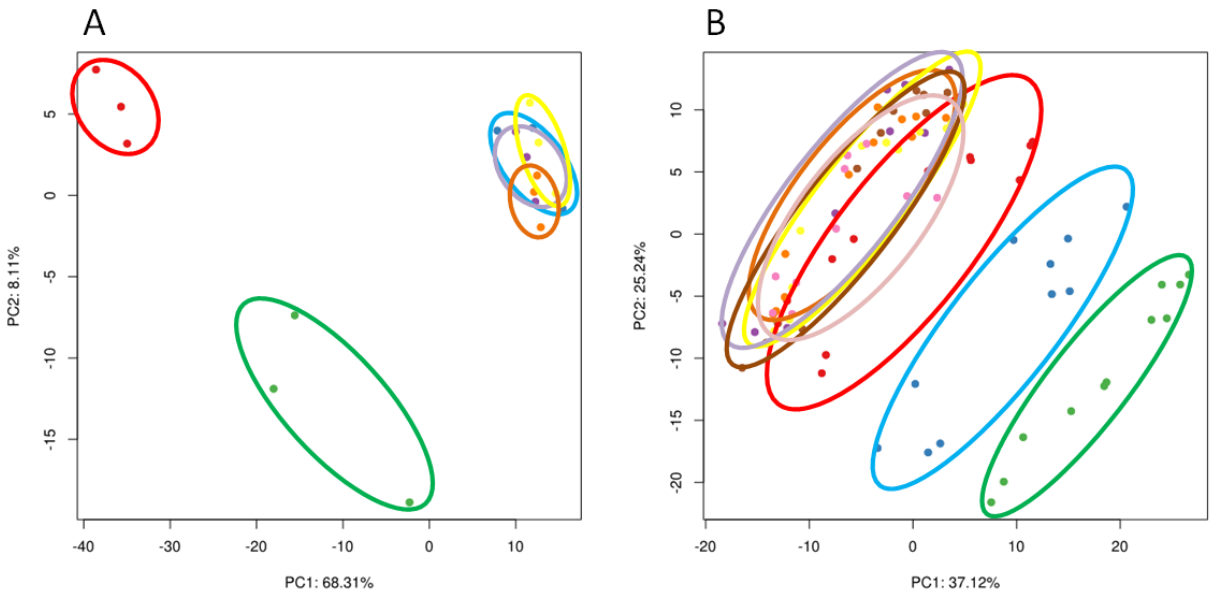

Figure 4-7: Principal component analysis (PCA) plots of *S. aureus* treated with triclosan. (A) Planktonic cells in response to varying concentrations of triclosan: Red = 0.1mM; Green = 0.01mM; Purple = 0.001mM; Blue = 0.0001mM; Orange = 0mM (Ethanol treated); and Yellow = 0mM. Cells were treated with varying triclosan concentrations for 4 h. Bead beating lysis and metabolite extraction using chloroform: methanol: water solvent mix (1:3:1) was used to extract the intracellular metabolome. (B) Biofilm in response to varying concentrations of triclosan: Green = 0.01mM; Blue = 0.001mM; Red = 0.0001mM; Yellow = 0.00001mM; Orange = 0.000001mM; Purple = 0.0000001mM; Brown = 0mM (Ethanol treated); and Pink = 0mM. 10 h biofilms were treated with varying triclosan concentrations for 4 h followed by direct bead beating lysis and chloroform: methanol: water metabolome extraction.

In the metabolome extractions from the planktonic cells, 780 metabolites were detected to have shown a change in abundance in response to triclosan. Of these, and after the data had been corrected for multiple testing, 227 metabolites detected were significantly down-regulated by >2 fold change in correlation with an increasing triclosan concentration. In the same samples, 25 metabolites detected were significantly up-regulated by >2 fold change in correlation with an increasing triclosan concentration. As indicated in the PCA plots above, most and greatest changes in metabolite abundance were seen in concentrations above 0.01mM.

In the metabolome extractions from biofilms, 546 metabolites were detected to have shown a change in abundance in response to triclosan. Of these, a number of metabolites detected were significantly down-regulated by >2 fold change in correlation with an increasing triclosan concentration. In the same samples, a number metabolites detected were significantly up-regulated by >2 fold change in correlation with an increasing triclosan concentration. As indicated in the PCA

plots above, most and greatest changes in metabolite abundance were seen in concentrations above 0.0001mM. This result suggests that lower concentrations of triclosan affect biofilm metabolism when compared to the concentrations required for metabolic changes in planktonic cells.

4.4.2.3 Metabolism pathway analysis

In the planktonic samples, 154 pathways were shown to have significant changes in metabolites in response to 0.1 mM triclosan. Of these, 106 were shown to have 2 or more metabolites detected to have significantly changed in response to 0.1 mM triclosan, with the number of metabolites changing increasing with increasing triclosan concentration (Figure 4-8). For full metabolomic data analysis see supplementary data Appendix VI.

The biofilm sample data displayed 128 pathways shown to have significant changes in metabolites in response to 0.01 mM triclosan. Of these, 74 pathways were shown to have 2 or more metabolites detected to have significantly changed in response to 0.01 mM triclosan, with the number of metabolites changing increasing with increasing triclosan concentration (Figure 4-9). Due to database searches not being species specific, some pathways listed show non-bacteria-related pathways for example Bile secretion. These pathways, although not found in or related to bacteria still help in the understanding of the synthesis, anabolism or catabolism of the detected metabolites so have been included in results. For full metabolomic data analysis see supplementary data Appendix VII.

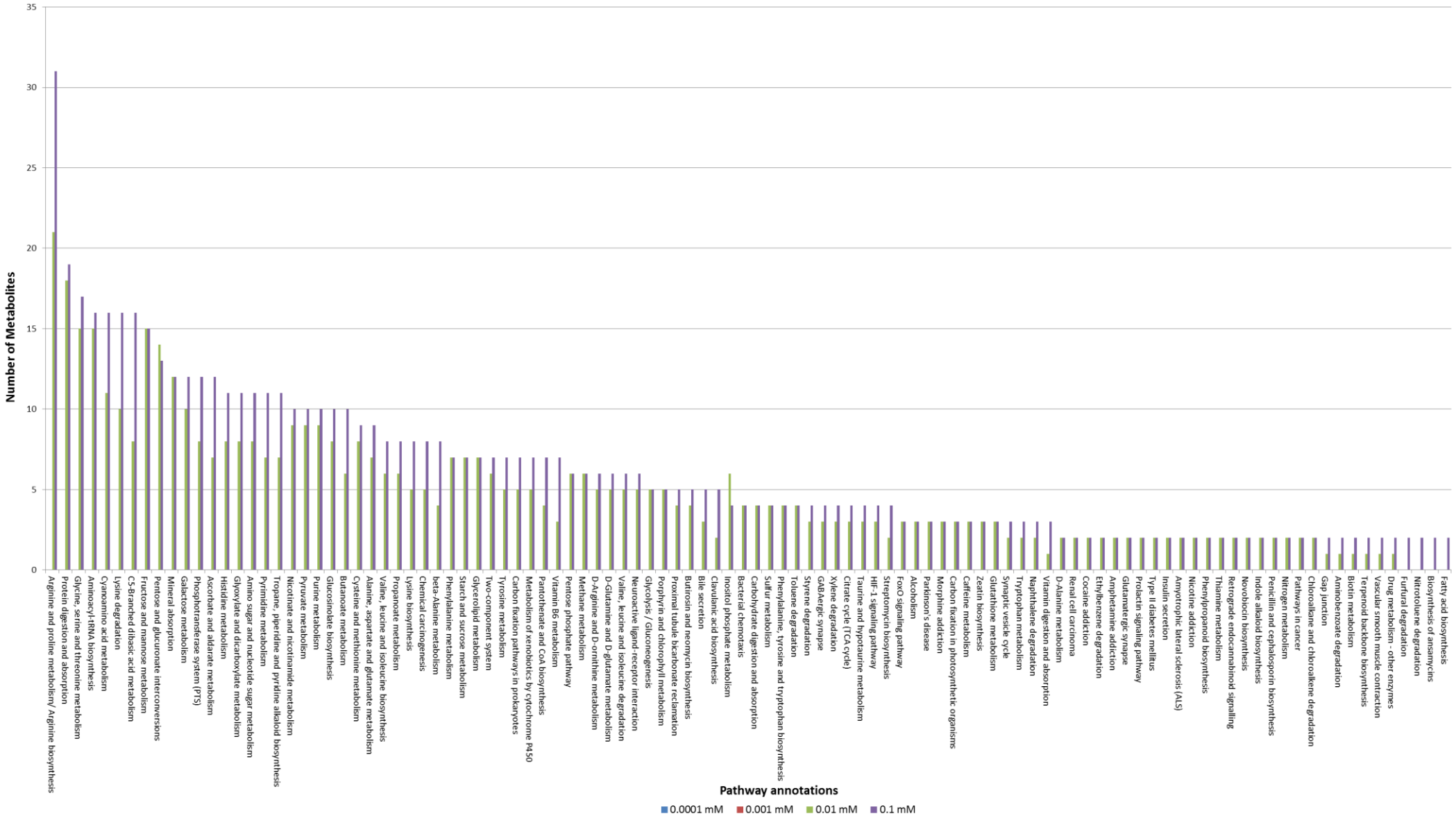
Number of Metabolites
0
5
10
15
20
25
30
35
Arginine and proline metabolism/ Arginine biosynthesis
Protein digestion and absorption
Glycine, serine and threonine metabolism
Aminoacyl-tRNA biosynthesis
Cyanoamino acid metabolism
Lysine degradation
C5-Branched dibasic acid metabolism
Fructose and mannose metabolism
Pentose and glucuronate interconversions
Mineral absorption
Galactose metabolism
Phosphotransferase system (PTS)
Ascorbate and aldarate metabolism
Histidine metabolism
Glyoxylate and dicarboxylate metabolism
Amino sugar and nucleotide sugar metabolism
Pyrimidine metabolism
Tropane, piperidine and pyridine alkaloid biosynthesis
Nicotinate and nicotinamide metabolism
Pyruvate metabolism
Purine metabolism
Glucosinolate biosynthesis
Butanoate metabolism
Cysteine and methionine metabolism
Alanine, aspartate and glutamate metabolism
Valine, leucine and isoleucine biosynthesis
Propanoate metabolism
Lysine biosynthesis
Chemical carcinogenesis
beta-Alanine metabolism
Phenylalanine metabolism
Starch and sucrose metabolism
Glycerolipid metabolism
Two-component system
Tyrosine metabolism
Carbon fixation pathways in prokaryotes
Metabolism of xenobiotics by cytochrome P450
Pantothenate and CoA biosynthesis
Vitamin B6 metabolism
Pentose phosphate pathway
Methane metabolism
D-Arginine and D-ornithine metabolism
D-Glutamine and D-glutamate metabolism
Valine, leucine and isoleucine degradation
Neuroactive ligand-receptor interaction
Glycolysis / Gluconeogenesis
Porphyrin and chlorophyll metabolism
Proximal tubule bicarbonate reclamation
Butirosin and neomycin biosynthesis
Bile secretion
Clavulanic acid biosynthesis
Inositol phosphate metabolism
Bacterial chemotaxis
Carbohydrate digestion and absorption
Sulfur metabolism
Phenylalanine, tyrosine and tryptophan biosynthesis
Toluene degradation
Styrene degradation
GABAergic synapse
Xylene degradation
Citrate cycle (TCA cycle)
Taurine and hypotaurine metabolism
HIF-1 signaling pathway
Streptomycin biosynthesis
FoxO signaling pathway
Alcoholism
Parkinson's disease
Morphine addiction
Carbon fixation in photosynthetic organisms
Caffeine metabolism
Zeatin biosynthesis
Glutathione metabolism
Synaptic vesicle cycle
Tryptophan metabolism
Naphthalene degradation
Vitamin digestion and absorption
D-Alanine metabolism
Renal cell carcinoma
Cocaine addiction
Ethylbenzene degradation
Amphetamine addiction
Glutamatergic synapse
Prolactin signaling pathway
Type II diabetes mellitus
Insulin secretion
Amyotrophic lateral sclerosis (ALS)
Nicotine addiction
Phenylpropanoid biosynthesis
Thiamine metabolism
Retrograde endocannabinoid signaling
Novobiocin biosynthesis
Indole alkaloid biosynthesis
Penicillin and cephalosporin biosynthesis
Nitrogen metabolism
Pathways in cancer
Chloroalkane and chloroalkene degradation
Gap junction
Aminobenzoate degradation
Biotin metabolism
Terpenoid backbone biosynthesis
Vascular smooth muscle contraction
Drug metabolism - other enzymes
Furfural degradation
Nitrotoluene degradation
Biosynthesis of ansamycins
Fatty acid biosynthesis
Pathway annotations
0.0001 mM
0.001 mM
0.01 mM
0.1 mM

Figure 4-8: Pathways identified to be changing in response to varying triclosan concentrations in *S. aureus* planktonic cells
Metabolome extractions from stationary phase planktonic LHSKBClinical cells analysed using LC-MS. Graph depicts the number of metabolites identified or annotated to be changing in each pathway. Pathway annotations come from pathway names in the KEGG database (Kanehisa and Goto, 2000).

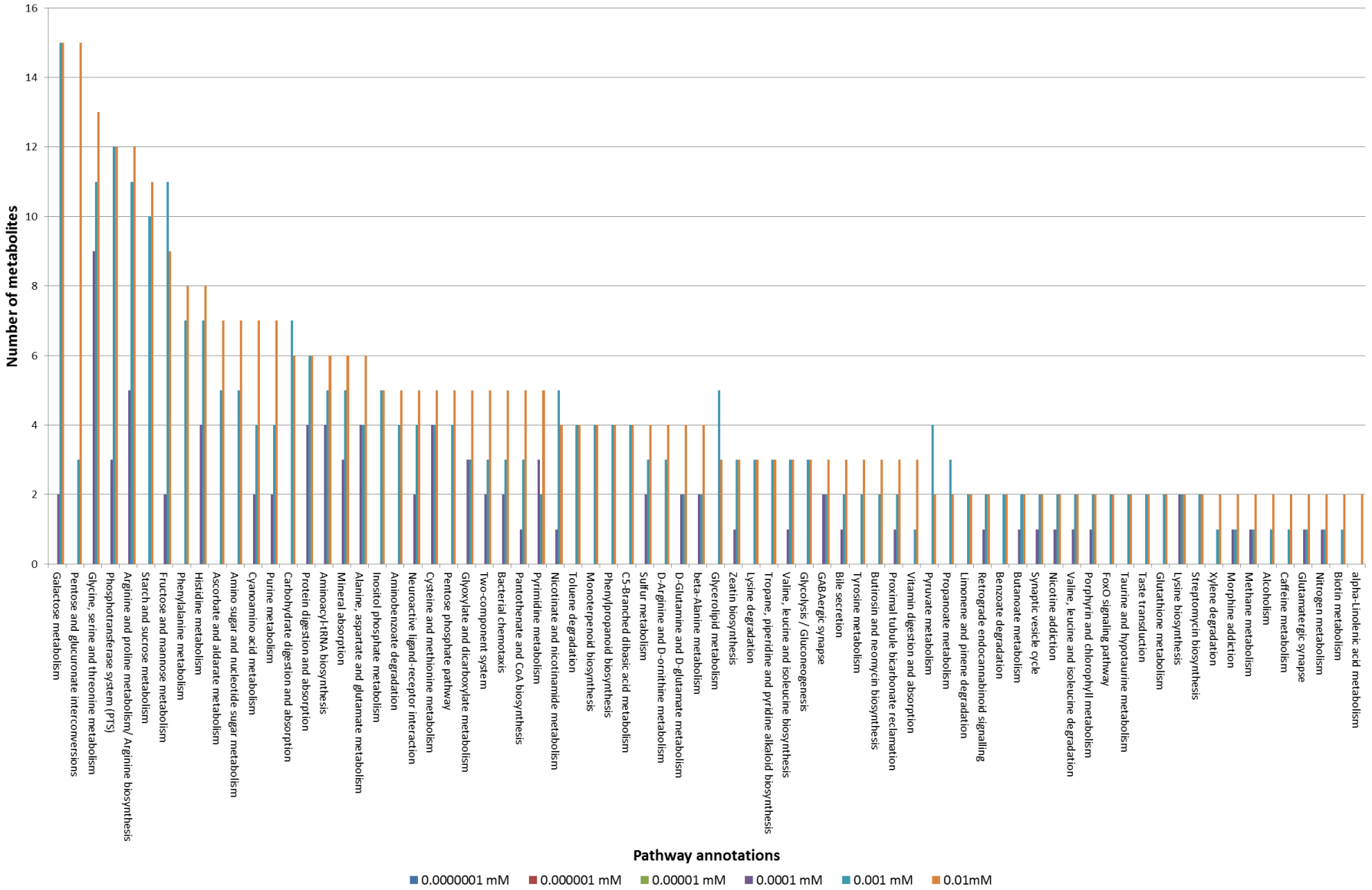
Number of metabolites
0
2
4
6
8
10
12
14
16
Galactose metabolism
Pentose and glucuronate interconversions
Glycine, serine and threonine metabolism
Phosphotransferase system (PTS)
Arginine and proline metabolism/ Arginine biosynthesis
Starch and sucrose metabolism
Fructose and mannose metabolism
Phenylalanine metabolism
Histidine metabolism
Ascorbate and aldarate metabolism
Amino sugar and nucleotide sugar metabolism
Cyanoamino acid metabolism
Purine metabolism
Carbohydrate digestion and absorption
Protein digestion and absorption
Aminoacyl-tRNA biosynthesis
Mineral absorption
Alanine, aspartate and glutamate metabolism
Inositol phosphate metabolism
Aminobenzoate degradation
Neuroactive ligand-receptor interaction
Cysteine and methionine metabolism
Pentose phosphate pathway
Glyoxylate and dicarboxylate metabolism
Two-component system
Bacterial chemotaxis
Pantothenate and CoA biosynthesis
Pyrimidine metabolism
Nicotinate and nicotinamide metabolism
Toluene degradation
Monoterpenoid biosynthesis
Phenylpropanoid biosynthesis
C5-Branched dibasic acid metabolism
Sulfur metabolism
D-Arginine and D-ornithine metabolism
D-Glutamine and D-glutamate metabolism
beta-Alanine metabolism
Glycerolipid metabolism
Zeatin biosynthesis
Lysine degradation
Tropane, piperidine and pyridine alkaloid biosynthesis
Valine, leucine and isoleucine biosynthesis
Glycolysis / Gluconeogenesis
GABAergic synapse
Bile secretion
Tyrosine metabolism
Butirosin and neomycin biosynthesis
Proximal tubule bicarbonate reclamation
Vitamin digestion and absorption
Pyruvate metabolism
Propanoate metabolism
Limonene and pinene degradation
Retrograde endocannabinoid signalling
Benzoate degradation
Butanoate metabolism
Synaptic vesicle cycle
Nicotine addiction
Valine, leucine and isoleucine degradation
Porphyrin and chlorophyll metabolism
FoxO signaling pathway
Taurine and hypotaurine metabolism
Taste transduction
Glutathione metabolism
Lysine biosynthesis
Streptomycin biosynthesis
Xylene degradation
Morphine addiction
Methane metabolism
Alcoholism
Caffeine metabolism
Glutamatergic synapse
Nitrogen metabolism
Biotin metabolism
alpha-Linolenic acid metabolism
Pathway annotations
0.0000001 mM
0.000001 mM
0.00001 mM
0.0001 mM
0.001 mM
0.01mM

Figure 4-9: Pathways identified to be changing in response to varying triclosan concentrations in *S. aureus* biofilms
Metabolome extractions from 24 h biofilms of LHSKBClinical analysed using LC-MS. Graph depicts the number of metabolites identified or annotated to be changing in each pathway. Showing the number of metabolites identified to be changing in each pathway. Pathway annotations come from pathway names in the KEGG database (Kanehisa and Goto, 2000).

4.4.2.4 Observed changes in *S. aureus* planktonic cell and biofilm metabolism in response to varying triclosan concentrations

4.4.2.4.1 Amino acid metabolism

Arginine metabolism

In planktonic cell samples arginine was detected ($HRMS_a^1$, R_{ta}) to have an increasing abundance as triclosan concentration increased (Figure 4-10). Furthermore, in the urea cycle, 4 of the 5 intermediate metabolites, namely: ornithine; citrulline; aspartate; and fumarate, were detected, with all, with the exception of fumarate, matched against internal standards. These 4 metabolites were shown to be significantly down-regulated in response to increasing drug concentrations above 0.001mM (Figure 4-11). These results suggest a possible block in the urea cycle induced by triclosan.

In biofilm samples, arginine was not matched to an internal standard so can only be described as an annotated, putative result ($HRMS_{PL}^1$) which showed no change in abundance. Despite this, intermediate metabolites of arginine metabolism and the urea cycle: ornithine (identified, $HRMS_a^1$, R_{ta}); citrulline (identified, $HRMS_a^1$, R_{ta}); and aspartate (annotated, $HRMS_{PL}^1$) were again observed to be significantly down regulated with triclosan concentrations above 0.00001mM (Figure 4-12).

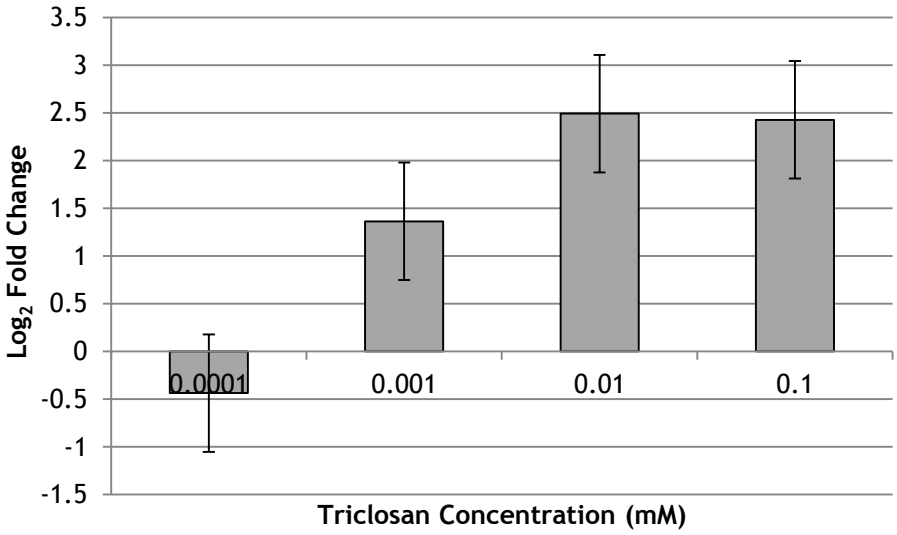

Figure 4-10: Arginine abundance in *S. aureus* planktonic cells in relation to increasing triclosan concentration.
Metabolome samples of LHSKBClinical cells extracted using bead beating cell lysis and metabolite extraction using chloroform, methanol and water (1:3:1). Samples analysed using LC-MS. Log_2 fold change of relative metabolite abundance in samples treated with varying triclosan concentrations against 0 mM treated samples. M+H, $HRMS_a^1$, R_{ta}, error bars C.I. 0.025 and 0.975.

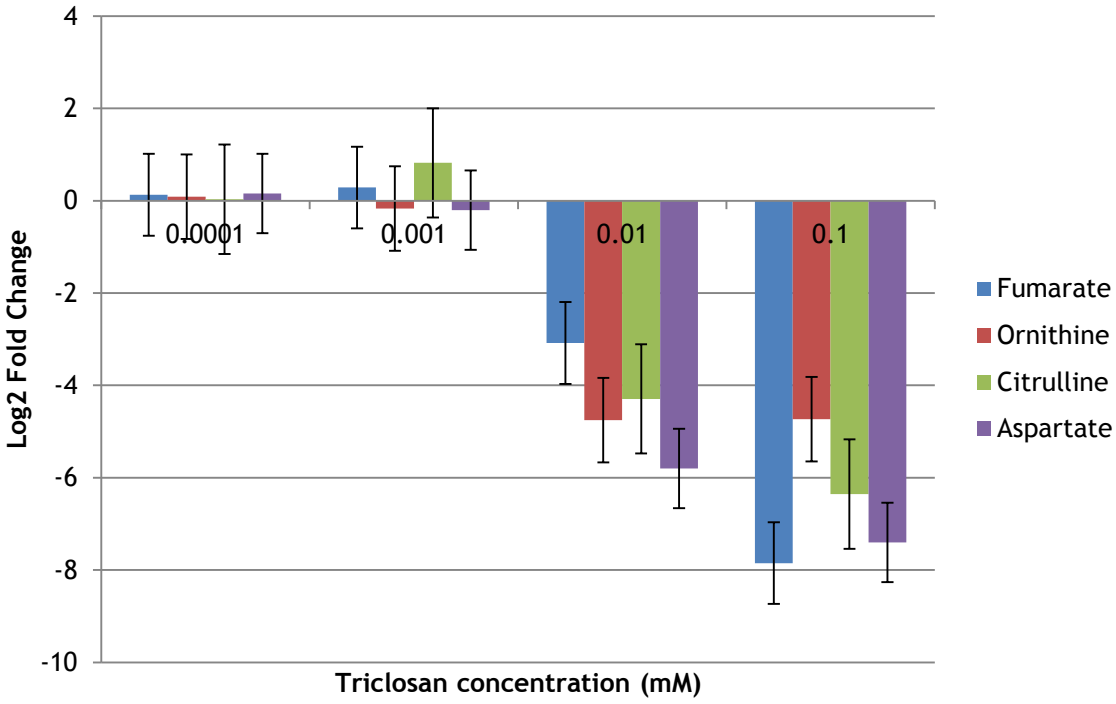

Figure 4-11: Metabolites detected in planktonic S. aureus cells belonging to the Urea cycle that are down-regulated in response to increasing triclosan concentration.
Metabolome samples of LHSKBClinical cells treated with triclosan for 4 h, extracted using bead beating cell lysis and metabolite extraction using chloroform, methanol and water (1:3:1). Samples analysed using LC-MS. Log_2 fold change of relative metabolite abundance in samples treated with varying triclosan concentrations against 0 mM treated samples. Ornithine (M-H, $HRMS_a^1$, R_{ta}); citrulline (M-H, M+H, $HRMS_a^1$, R_{ta}); aspartate (M-H, M+H, $HRMS_a^1$, R_{ta}); fumarate (M+ACN+H, $HRMS_{PL}^1$). Error bars C.I. 0.025 and 0.975.

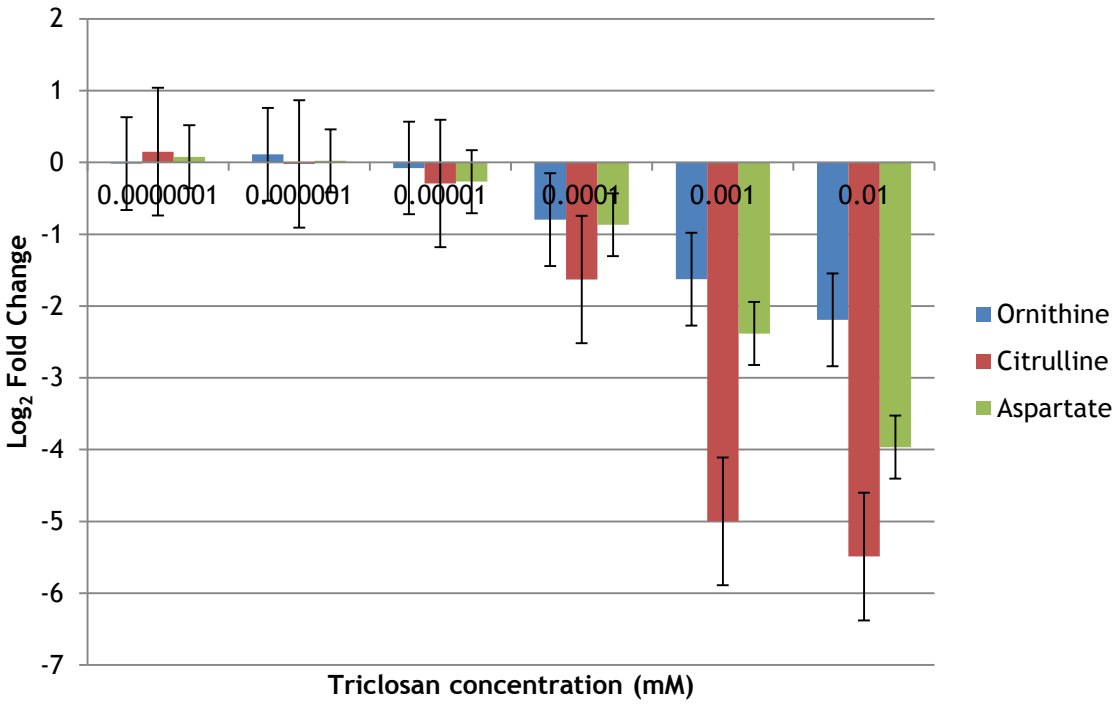

Figure 4-12: Metabolites detected in *S. aureus* biofilm extractions belonging to the Urea cycle that are down-regulated in response to increasing triclosan concentration.
Metabolome samples of 10 h LHSKBClinical biofilms treated with triclosan for 4 h, extracted using bead beating cell lysis and metabolite extraction using chloroform, methanol and water (1:3:1). Samples analysed using LC-MS. Log_2 fold change of relative metabolite abundance in samples treated with varying triclosan concentrations against 0 mM treated samples. Ornithine (M+H, $HRMS_a^1$, R_{ta}); citrulline (M-H, $HRMS_a^1$, R_{ta}); aspartate (M+ACN+Na, $HRMS_{PL}^1$). Error bars C.I. 0.025 and 0.975.

Serine metabolism

A further amino acid to demonstrate altered metabolism in response to increasing triclosan concentration was serine. Serine was found to be significantly up-regulated in planktonic cells with increasing drug concentration above 0.001mM (Figure 4-13), while pyruvate, a metabolite precursor and product of serine metabolism was significantly down-regulated. These changes could subsequently lead to altered pyruvate metabolism. Here, significant changes in serine were not observed in biofilms treated with triclosan.

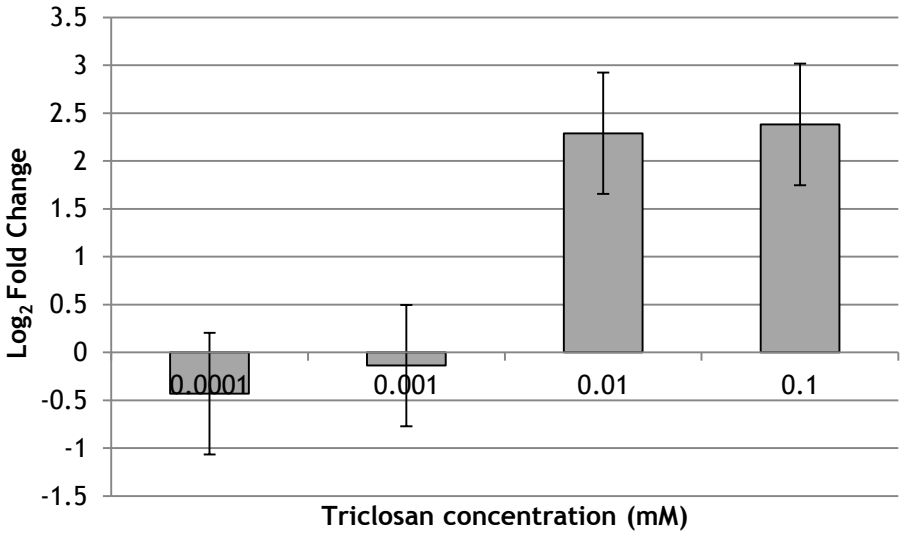

Figure 4-13: Serine abundance in *S. aureus* planktonic cells in relation to increasing triclosan concentration.
Metabolome samples of LHSKBClinical cells treated with triclosan for 4 h, extracted using bead beating cell lysis and metabolite extraction using chloroform, methanol and water (1:3:1). Samples analysed using LC-MS. Log_2 fold change of relative metabolite abundance in samples treated with varying triclosan concentrations against 0 mM treated samples. M+H, $HRMS^1_a$, R_{ta}, error bars C.I. 0.025 and 0.975.

Phenylalanine metabolism

The α-amino acid phenylalanine, displays an altered expression in planktonic cells compared to that of the biofilm in response to an increasing triclosan concentration. In the planktonic cells phenylalanine appeared to be significantly down-regulated in response to increasing triclosan concentration (Figure 4-14). However, in the biofilm it displayed no significant change in expression as triclosan concentration increased.

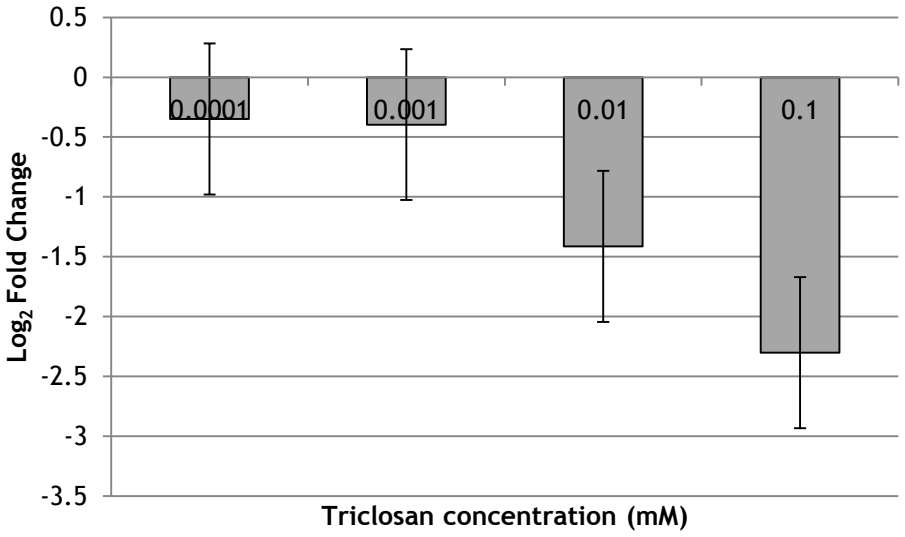

Figure 4-14: Phenylalanine abundance in *S. aureus* planktonic cells in relation to increasing triclosan concentration.
Metabolome samples of LHSKBClinical cells treated with triclosan for 4 h, extracted using bead beating cell lysis and metabolite extraction using chloroform, methanol and water (1:3:1). Samples analysed using LC-MS. Log_2 fold change of relative metabolite abundance in samples treated with varying triclosan concentrations against 0 mM treated samples. M+H, $HRMS_a^1$, R_{ta}, error bars C.I. 0.025 and 0.975.

Lysine biosynthesis and degradation

Metabolites associated with the biosynthesis of the amino acid lysine displayed an altered expression in response to triclosan concentration. Planktonic cells displayed a down-regulation in lysine as well as a number of metabolites involved in the lysine biosynthesis metabolic pathway including aspartate, 2-oxoglutarate, 2-amino-adipate, 2-aminoadipate 6-semialdehyde, 3-Methylornithine, 2-Amino-6-oxopimelate, and L-homoserine in response to an increasing triclosan concentration. Lysine had a >4-fold decrease in expression in planktonic cells at a 0.1mM triclosan concentration compared to no significant change in the biofilm cells. Metabolites are classed as annotated ($HRMS_{PL}^1$) in planktonic cell samples with the exception of aspartate, also involved in other metabolic pathways as described above, which was matched to standards ($HRMS_a^1$, R_{ta}).

In biofilm samples the metabolites belonging to the lysine biosynthesis pathway largely remained unaltered in expression with the exception of L-homoserine ($HRMS_a^1$, R_{ta}) which was increased, and aspartate ($HRMS_{PL}^1$) which was decreased in abundance in response to an increasing triclosan concentration.

L-homoserine, a metabolite involved in lysine biosynthesis and a precursor to serine metabolism, increased significantly in the biofilm samples (Figure 4-15-A) compared to a significant decrease in the planktonic cells (Figure 4-15-B). Both data sets display a significant decrease in L-aspartate expression which can subsequently lead to the synthesis of L-homoserine.

In addition to lysine biosynthesis, significant changes in lysine degradation caused by an increase in triclosan concentration were noted in both planktonic cells and biofilms. Metabolites including N-acetyl lysine, 5-amino-pentanoate, N6-Acetyl-N6-hydroxy-L-lysine, 3,5-Diaminohexanoate, 5-Amino-3-oxohexanoic acid, 6-amino-2-oxohexanoate, delta1-Piperideine-2-carboxylate, 2,5-diaminohexanoate, 2-Amino-5-oxohexanoate, L-pipecolate, delta1-piperideine-6-L-carboxylate, L-2-Aminoadipate 6-semialdehyde, and L-2-Aminoadipate, were all annotated identifications ($HRMS^{1}_{PL}$) and displayed a lowered expression in planktonic cells in response to an increasing triclosan concentration. These changes may be in response to an overall down regulation of lysine biosynthesis which feeds into the lysine degradation pathway.

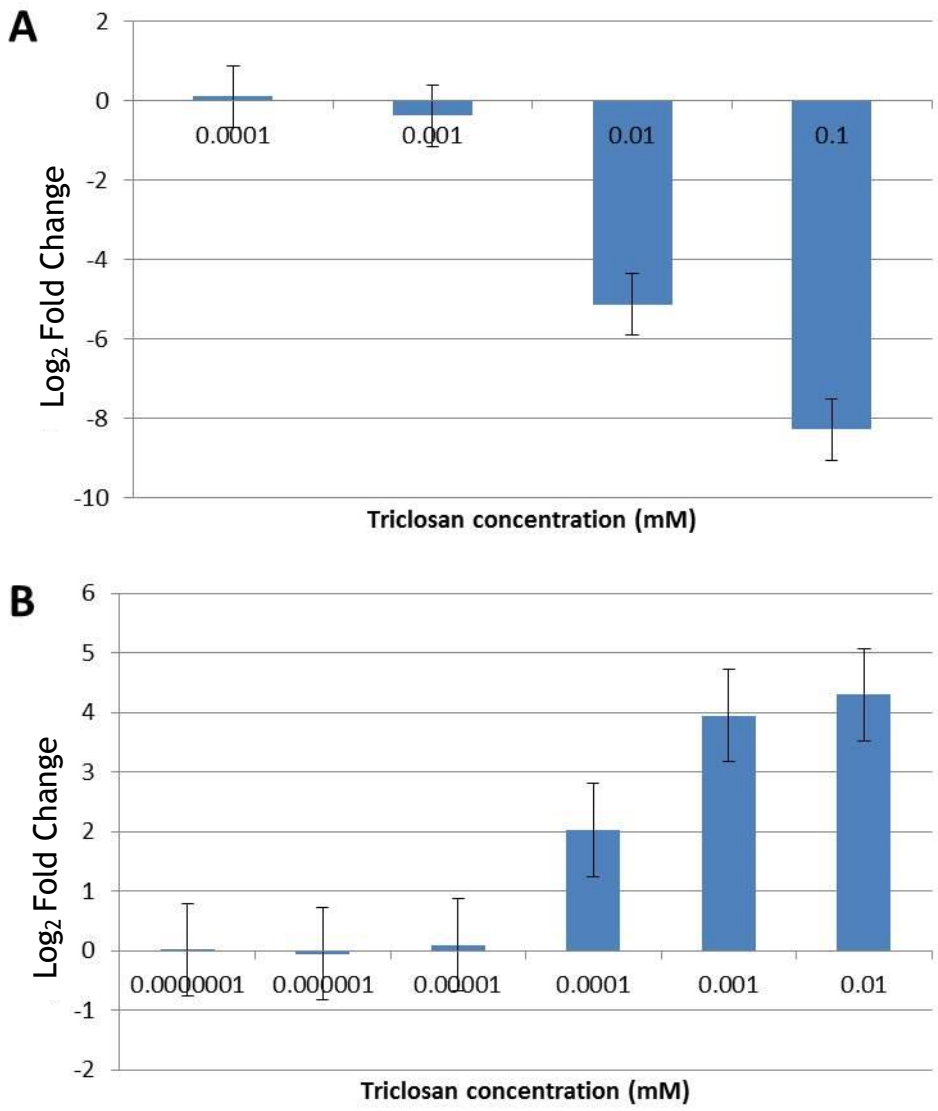

Figure 4-15: L-Homoserine abundance in *S. aureus* in response to increasing triclosan concentration.
Metabolome samples of LHSKBClinical planktonic cells (A) and biofilms (B) treated with triclosan for 4 h, extracted using bead beating cell lysis and metabolite extraction using chloroform, methanol and water (1:3:1). Samples analysed using LC-MS. Log_2 fold change of relative metabolite abundance in samples treated with varying triclosan concentrations against 0 mM treated samples. A; M+ACN+H, $HRMS^1_{PL}$. B; M-H, $HRMS^1_a$, R_{ta}. Error bars C.I. 0.025 and 0.975.

4.4.2.5 Citrate cycle (TCA cycle)

The planktonic data set displayed altered malate metabolism in response to increasing triclosan concentration above a triclosan concentration of 0.001mM. Malate was identified ($HRMS_a^1$, R_{ta}) to have a significant decrease in abundance in response to an increasing triclosan concentration (Figure 4-16). Fumarate and pyruvate were annotated ($HRMS_{PL}^1$) from the data to also be down-regulated. In the biofilm samples, these changes in pyruvate metabolism were not seen.

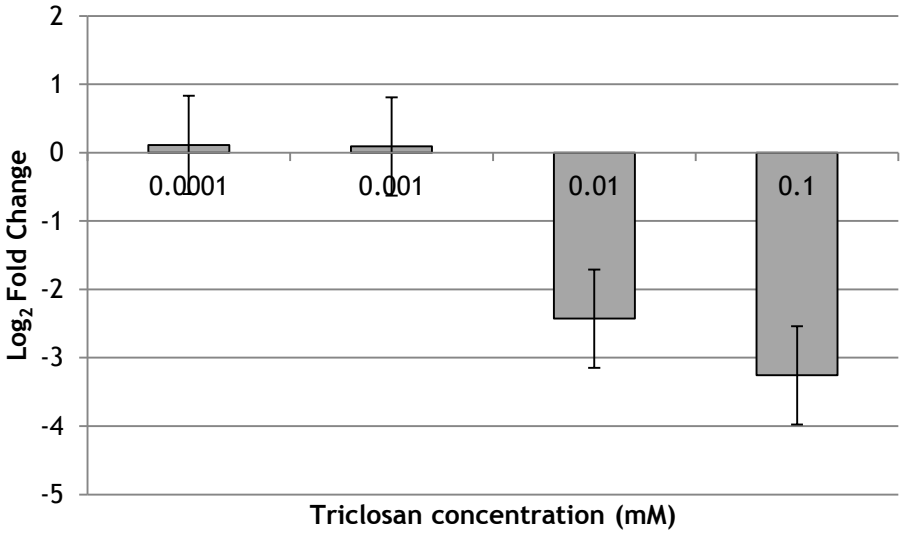

Figure 4-16: Malate abundance in *S. aureus* planktonic cells in relation to increasing triclosan concentration.
Metabolome samples of LHSKBClinical cells treated with triclosan for 4 h, extracted using bead beating cell lysis and metabolite extraction using chloroform, methanol and water (1:3:1). Samples analysed using LC-MS. Log_2 fold change of relative metabolite abundance in samples treated with varying triclosan concentrations against 0 mM treated samples. M-H, $HRMS_a^1$, R_{ta}, error bars C.I. 0.025 and 0.975.

4.4.2.6 Biotin metabolism

A metabolite of biotin metabolism demonstrated a similar response in planktonic cells and biofilms in response to changing triclosan concentration. The metabolomic data demonstrated that 8-Amino-7-oxononanoate ($HRMS^1_{PL}$) was significantly down-regulated in response to increasing triclosan concentration (Figure 4-17). Further to this, significant changes in glycerolipid metabolism in planktonic cells and biofilms were identified, with a number of metabolites significantly down-regulated.

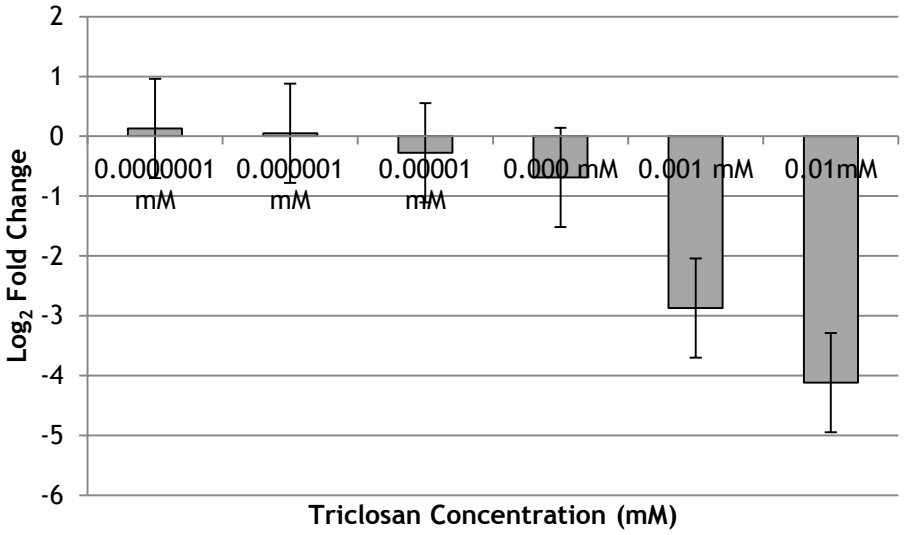

Figure 4-17: 8-Amino-7-oxononanoate abundance in *S. aureus* biofilms in response to increasing triclosan concentration
Metabolome samples of 10 h LHSKBClinical biofilms treated with triclosan for 4 h, extracted using bead beating cell lysis and metabolite extraction using chloroform, methanol and water (1:3:1). Samples analysed using LC-MS. Log_2 fold change of relative metabolite abundance in samples treated with varying triclosan concentrations against 0 mM treated samples. M+ACN+H, $HRMS^1_{PL}$. Error bars C.I. 0.025 and 0.975

4.4.2.7 Galactose metabolism

Galactose metabolism demonstrated a similar response in planktonic cells and biofilms in response to an increasing triclosan concentration. Significant changes in metabolite abundance were observed in a number of metabolites involved in the pathway. In biofilm samples metabolites including: galactose, lactose, glucose, fructose, melibiose, and sucrose were up-regulated in response to high concentrations of triclosan. Figure 4-18 shows the increase in metabolite abundance of sucrose as the concentration of triclosan increases. All

identifications were annotated identifications ($HRMS^1_{PL}$) with the exception of sucrose which was matched to a standard ($HRMS^1_a$, R_{ta}). In planktonic cell samples although most metabolites displayed an up regulation in expression, a metabolite called stachyose was annotated from the analysis to display a down-regulated expression in response to an increasing triclosan concentration.

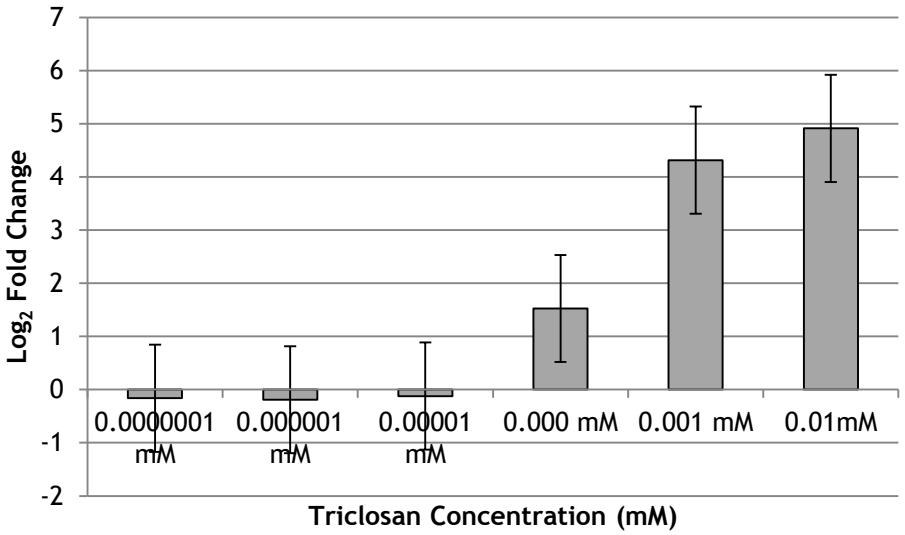

Figure 4-18: Sucrose abundance in *S. aureus* biofilms in response to increasing triclosan concentration.
Metabolome samples of 10 h LHSKBClinical biofilms treated with triclosan for 4 h, extracted using bead beating cell lysis and metabolite extraction using chloroform, methanol and water (1:3:1). Samples analysed using LC-MS. Log_2 fold change of relative metabolite abundance in samples treated with varying triclosan concentrations against 0 mM treated samples. M-H, $HRMS^1_a$, R_{ta}, error bars C.I. 0.025 and 0.975.

4.4.2.8 Metabolic pathways that demonstrate different responses in planktonic cells and biofilms in response to changing triclosan concentration

Further to the changes in metabolic pathways described, a number of pathways where found to have significantly altered expression rates in planktonic cells compared to the biofilm samples in response to triclosan. Pathways to demonstrate significant changes in expression patterns included: purine Metabolism; carbohydrate metabolism; Glyoxylate and dicarboxylate metabolism; Inositol phosphate metabolism; pantothenate and CoA biosynthesis; pyrimidine metabolism; monoterpenoid biosynthesis; limonene and pinene degradation; streptomycine biosynthesis; phenylpropanoid biosynthesis;

glycolysis/gluconeogenesis; vitamin digestion and absorption; and adenine biosynthesis. In addition to this, clavalanic acid metabolism and the citrate cycle displayed significant changes in expression of identified metabolites only in the planktonic cell data and not in the biofilm data, thus highlighting the altered metabolism of the biofilm compared to planktonic cells.

4.5 Discussion

Previously triclosan has been shown to prevent *S. aureus* from forming a biofilm (tested at 10g/L in urinary catheters) (Jones et al., 2006), highlighting the use of triclosan as an anti-biofilm or biofilm dispersal agent. Here, we carried out a study looking at the metabolic effects of varying triclosan concentrations on *S. aureus* planktonic and biofilm metabolism.

We hypothesised that using untargeted metabolomics we could further resolve the MOA of triclosan in *S. aureus* and show that it has multiple effects on bacterial metabolism, as alluded to in these studies: Suller & Russell (1999); Suller & Russell (2000); Villalain et al. (2001); Nielsen et al. (2013). We show a cascade of detrimental effects in *S. aureus* metabolism and further show differences in triclosan MOA depending on whether it was living in a planktonic or biofilm culture, therefore we can accept the hypothesis.

A time point of 4 h was selected as a constant triclosan exposure time because this was when this strain of *S. aureus* left the lag growth phase and had started its exponential growth phase. Drug-time kinetics were not analysed here but could represent a future study. Furthermore, 10 h biofilm cultivation was selected as it is at this time point that biofilm formation has occurred but will still be growing and maturing (Moormeier et al., 2014).

Initial results employing CV assays and SEM imaging revealed detrimental effects of triclosan on *S. aureus* (Figure 4-1 - Figure 4-5) and highlighted a concentration gradient to be tested further in a MOA study. Triclosan treatment appeared to be more effective in planktonic cells compared to biofilms with ~58% reduction in planktonic cell growth compared to ~45% reduction in biofilm biomass with 0.01 mM triclosan treatment (Figure 4-1). This could be a consequence of the protective nature of the biofilm and ECM, previously reported (Drenkard and Ausubel, 2002; Rajendran et al., 2013; Ramage et al., 2003; Soto, 2013; Stewart and Costerton, 2001). However, lower concentrations of triclosan had a detrimental impact on the biofilm while not affecting planktonic cell growth (Figure 4-1).

4.5.1 Untargeted metabolomics

Using untargeted metabolomic approaches, the metabolic response of *S. aureus* to triclosan was explored. Results highlight significant changes in metabolism caused by triclosan. Furthermore, significant metabolic differences in response to the drug were identified between the same *S. aureus* strain living planktonically or as a biofilm.

The PCA plots show a correlation between triclosan concentration and metabolic effect (Figure 4-7). However, metabolic effects as indicated in the PCA plots occur at different triclosan concentrations depending on whether the bacteria were planktonic or living as a biofilm. Differences may be because of bacteria cell concentrations and metabolic rate being different between the different growth states.

4.5.1.1 Triclosan MOA

The NADH or NADPH-dependent ACP reductase is reported to be the target and MOA of triclosan in *S. aureus,* inhibiting bacterial fatty acid biosynthesis (Heath and Rock, 2000; Heath et al., 2000; Levy et al., 1999; McMurry et al., 1998a, 1998b; Slater-Radosti et al., 2001). Possibly due to the methods used here, for example the pHILIC LC column not being optimal for retaining hydrophilic compounds such as lipids, and the data bases exploited for metabolite analysis not being complete, changes in fatty acid synthesis were not detected. However, it has previously been shown that this target will induce a cascade of detrimental metabolic events in metabolism especially in processes that rely on bacterial fatty acid biosynthesis (Escalada et al., 2005a, 2005b), therefore it has also been hypothesised that the effect of triclosan will extend to other cellular functions including aerobic respiration (Boshoff et al., 2004). Furthermore alternative targets of triclosan in other cells including the parasite *Trypanosoma brucei*, have highlighted alternative MOAs for triclosan leading to changes in metabolism (Paul et al., 2004).

The data did show changes in precursor pathways to fatty-acid synthesis but also a number of other metabolic pathways suggesting multiple MOAs. One fatty-acid synthesis precursor pathway was the biotin pathway. This result may correlates

with previous work that show that triclosan has an effect on fatty-acid biosynthesis in *S. aureus* (Heath and Rock, 2000; Heath et al., 2000). However, only a putative identification of one metabolite belonging to the biotin metabolic pathway was observed. In addition, biotin is only involved in fatty acid biosynthesis by acting as a cofactor bound to biotin carboxylase and decarboxylases, which capture CO_2 and catalyse its transfer to organic acids (Chapman-Smith and Cronan Jr, 1999). Therefore this result may not truly reflect changes in fatty acid biosynthesis.

Through testing a range of bacteria species including *S. aureus*, Escalada *et al.*, (2005b), suggest that triclosan challenge may induce a stress response and suggest other MOAs other than the inhibition of the fatty acid biosynthesis are also involved in triclosan MOA (Escalada et al., 2005b). They show that at low concentrations, bacterial growth was severely affected, but at high concentrations triclosan had a rapid bactericidal effect, indicating a more damaging effect such as membrane activity as previously highlighted (Villalain et al., 2001). Concluding that the inhibition of key metabolic pathways is a part of triclosan MOA and that the interactions of triclosan with bacteria is multifactorial, as metabolic pathways are affected at low concentrations of triclosan but only at high concentrations is triclosan bactericidal.

Changes seen here in amino acid metabolism in response to triclosan could be perceived as a bacterial stress response. It has previously been shown that amino acid biosynthesis is increased in *S. aureus* due to temperature and stringent response (Anderson et al., 2006). Here, it was observed that arginine was up-regulated in *S. aureus* planktonic samples, whereas the other urea-cycle metabolites were down-regulated in both planktonic and biofilm samples in response to increasing triclosan concentration. The urea cycle is a crucial metabolic process in bacteria cells and is a known precursor to many other metabolic pathways including the TCA cycle through the production of fumarate and multiple amino acid metabolic pathways. The importance of arginine and its metabolism has been linked to biofilm formation as shown and discussed in Chapter 3 of this thesis. It has been speculated and shown that *S. aureus* catabolise amino acids including arginine to aid its survival and pathogenesis (Beenken et al., 2004; Resch et al., 2005, 2006; Zhu et al., 2007). The up regulation of the arginine deiminase pathway aids its survival and pathogenesis

by maintaining pH homeostasis through ammonia production, as discussed in Chapter 3, and it has been shown in *S. pyogenes* that arginine deiminase aids in the evasion of the host immune response by inhibiting the proliferation of human peripheral blood mononuclear cells (Degnan et al., 1998, 2000; Diep et al., 2006).

Furthermore, changes were observed in lysine metabolism in planktonic cells but not in triclosan treated biofilms. Differences such as these when looked at alone could potentially highlight the previously reported protective nature of biofilms against antimicrobials (Drenkard and Ausubel, 2002; Rajendran et al., 2013; Ramage et al., 2003; Soto, 2013; Stewart and Costerton, 2001). However, when included with other results this conclusion should be taken with caution for two reasons: i) Lower concentrations of triclosan had an impact on the biofilm compared to that in planktonic cells (Figure 4-1); and ii) Planktonic and biofilm samples showed similar responses to triclosan in other metabolic pathways. Other results therefore contradict findings that observed metabolic differences between planktonic cells and biofilms treated with triclosan are due to the protective nature of biofilms.

The difference in the effect of triclosan on planktonic cells and biofilms may be caused by the different metabolic states of planktonic bacteria compared to the indwelling biofilm bacteria. Triclosan effectiveness has been reported to change depending on the metabolic state of the bacteria. Escalada, Russell *et al*. (2005), highlight that metabolically inactive bacteria are more resilient to triclosan through the measurement of the speed at which triclosan lethality occurred (Escalada et al., 2005b). Lethality was induced more rapidly in metabolically active bacteria compared to slower efficacy in stationary phase cells. A further example of this was seen in galactose metabolism where in planktonic cell samples the intermediate metabolite stachyose was significantly down regulated in response to an increase in triclosan concentration while a number of proceeding metabolites appear to be up regulated, an effect not replicated in biofilm samples. Galactose metabolism has been described as playing a crucial role in biofilm formation of some bacteria and the production of ECM (Chai et al., 2012).

A decrease in expression was observed in malate metabolism and the TCA cycle in planktonic cells in response to increasing triclosan concentrations. Boshoff *et al*. (2004), present a transcriptional profile study using microarray analysis to look at the MOA of triclosan in the bacterium *Mycobacterium tuberculosis* (Boshoff et al., 2004). They report that triclosan can induce fatty acid degradation through the up regulation of enzymes in β-oxidation but further report triclosan up regulates citrate synthase, which controls flux through the TCA cycle and enzymes belonging to the pyruvate dehydrogenase complex, subsequently controlling levels of acetyl-CoA. They also found that triclosan caused a dose-dependent inhibition of the membrane-bound quinol reductase, succinate dehydrogenase. They conclude that triclosan has a cell wall component to its MOA but its mechanism of toxicity is complex (Boshoff et al., 2004). These results correlate with ours suggesting that triclosan up regulates flux in the TCA cycle thus depleting metabolite abundance.

TCA cycle expression has been found to be increased in biofilm formation (Resch et al., 2006). Through comparative proteomic analysis, Resch *et al*. (2006) report the up-regulation of nine proteins found to be part of pyruvate metabolism in *S. aureus* biofilms compared to their planktonic living counterparts (Resch et al., 2006). Since pyruvate metabolism has been reported to increase in biofilms a drug such as triclosan that down regulates components of the pathway could be seen to be an anti-biofilm agent. Pyruvate is also a precursor to a number of metabolic pathways including fatty acid biosynthesis.

4.5.2 Triclosan uptake analysis

It was observed from the results that at a concentration of 0.01mM no exogenous triclosan was found in the used bacteria culture media but was found in the bacteria cells. At this concentration triclosan was entirely taken up by a confluent culture of *S. aureus*, subsequently depleting it from the environment. This is important when considering previous research carried out on triclosan found in fresh water systems having adverse effects on the natural environment and ecological niche of fresh water rivers (Lubarsky et al., 2012). Such results aid the understanding of the concentration of triclosan required to prevent bacterial growth but also protect the ambient environment from triclosan

poisoning. It was only at concentrations of 0.01mM and above that a majority of metabolic changes where observed in planktonic cells and biofilms.

4.5.3 Conclusions

Although the use of triclosan has come under increasing speculation, its full MOAs are still largely unknown. The effect of triclosan on planktonic cells and biofilm dispersal of *S. aureus* has been analysed using metabolomics. We have shown that increasing triclosan concentration inhibits the cells living in a planktonic state and significantly alters their metabolism, potentially related to altering their ability to initiate biofilm formation. This could be looked at as further evidence and a positive argument for the use of triclosan as a bacterial biofilm prevention drug. Furthermore, we have been able to provide evidence of changes to the metabolism of bacteria living as a biofilm in response to triclosan challenge, thus highlighting the drugs MOAs in biofilm treatment. Metabolomics has demonstrated that triclosan creates a cascade of events in *S. aureus* cell metabolism. It is possible to conclude from our data that triclosan has multiple effects on bacterial metabolism and is not confined to specifically only one mechanism affecting fatty acid biosynthesis.

Chapter 5 General Discussion

S. aureus is commonly found as a commensal on the skin, however infection can lead to life threatening diseases including septicaemia and meningitis (Aires de Sousa and De Lencastre, 2004; Bien et al., 2011). In addition, *S. aureus* can form biofilms *in vivo*, adhered to a surface and encased in an ECM. Biofilm formation is a virulence factor employed by pathogens increasing pathogenicity and exacerbating antibiotic resistance. Staphylococcal biofilm formation is considered to be a contributor to the onset of orthopaedic infection through forming on the implant surface potentially leading to implant loosening and the requirement for a replacement.

The overall aim of this research project was to provide greater understanding of orthopaedic infection caused by *S. aureus* and biofilm formation on the implant surface. The number of orthopaedic infections and the lack of knowledge regarding biofilm involvement led us to hypothesise that *S. aureus* is a leading cause of orthopaedic infection and metabolomic approaches can be used to study *S. aureus* biofilms, and find significant metabolic differences between different bacterial growth states, and in response to antimicrobial challenge.

Results presented here allow us to accept the hypothesis.

We first provide further evidence of *S. aureus* as the primary cause of orthopaedic infection through a microbiome study and then focussing *in vitro* studies on a clinically relevant *S. aureus* strain. Such research is important due to the number of orthopaedic infection cases occurring and the increasing number of orthopaedic surgeries carried out (National Health Service (NHS), 2014).

5.1 Microbiome study of the infected hip prosthesis

Even though staphylococcal species are the most common bacteria associated with orthopaedic infection (Dempsey et al., 2007; Esteban et al., 2010; Montanaro et al., 2011; Zimmerli et al., 2004), some studies have highlighted that infections can be polymicrobial, where more than one species is present (Bereza et al., 2013; Gomez et al., 2012; Makaritsis et al., 2009; Moran et al., 2007). In addition, culturing methods to detect present bacterial species in infections have been criticised due to selective bias caused by media and culture

conditions employed. Furthermore, PCR based methods introduce primer bias. Metagenome analysis was employed here to look at polymicrobial infection of orthopaedic implants.

Metagenome analysis, coupled with microbial DNA enrichment protocols improves the accuracy and efficiency of sequencing results and eliminates the need for traditional culture methods previously used to study prosthetic hip infections (Atkins et al., 1998; Moran et al., 2007; Tunney et al., 1998). Using metagenomics rather than PCR based methods also permits greater genomic research to be carried out as more than one region of DNA is identified and sequenced, reducing associated problems with PCR and the use of specific primers. Through utilising sensitive genomic approaches multiple species can be identified. However, the number of identified species found here was much lower than previous studies looking at prosthetic joint infections (Bereza et al., 2013; Dempsey et al., 2007). This may have been caused by host contamination.

There is still speculation as to the source of orthopaedic infections. Some common theories include: host skin micro-flora pathogens; commensal pathogens from the theatre staff; or commensals from the operating theatre (Dempsey et al., 2007), causing infection in immunocompromised patients. Through carrying out sample collection in controlled ways and using aseptic techniques to reduce the chances of contamination, epidemiological studies can be carried out through tracing the likely initial source of detected pathogens.

S. aureus is known to be a common skin commensal and is most probably initially from the microflora of the skin of hospital staff or the patient. *E. faecium* is known to be a common commensal of the intestine and *C. difficile* is commonly found in the intestine. Therefore, because the wound from the hip replacement surgery has close proximity to the anus, it is potentially possible for contamination to occur either during surgery or post-surgery inducing a wound infection. Wound infection post arthroplasty surgery has previously been hypothesised as a route of infection (Kamme and Lindberg, 1981; McMillan et al., 2011).

Further to epidemiological studies, using whole genome sequencing methods as those outlined here, permits antimicrobial susceptibility conclusions to be drawn

about the infection (Köser et al., 2014). The presence of detected genes responsible for antibiotic resistance, such as MRSA, VRSA and Vancomycin-resistant Enterococcus (VRE) can be looked for, however due to the high levels of contaminant DNA and time constraints, this type of analysis could not be carried out.

A study such as the one presented here showing the identification of *S. aureus* as a primary cause of infection further highlights that orthopaedic infections are commonly caused by staphylococcal species and thus supports the requirement for further research into *S. aureus* as a cause of orthopaedic implant infections. Due to this finding it was decided to focus this PhD research on *S. aureus* as a primary cause of orthopaedic infection.

5.2 Metabolomic analysis of *S. aureus* planktonic cells compared to biofilms

Differences in energy and cell metabolism between planktonic cells and biofilms have been previously documented (Ammons et al., 2014; Gjersing et al., 2007; Resch et al., 2006; Zhang and Powers, 2012). Results here correlate with previous studies and highlight changes in metabolite components of the arginine metabolism, specifically the urea cycle, and purine metabolic pathways. Metabolites can be intermediates or end products of metabolic pathways interconnected to form metabolic networks.

Findings presented here show that metabolism is significantly altered by the same species of bacteria once a sessile growth phase has been initiated. The changes identified between growth states could be evidence of the bacteria responding to their changing environment and trying to maintain a 'status quo' in chemical and pH balance. Bacteria should be thought of as dynamic entities capable of displaying significantly altered phenotypes without the necessity of genetic change. Because of this, research into bacteria, and especially in the field of antimicrobial testing and identification, should consider different effects drugs may have on different stages of growth.

The study of microbial metabolism is challenging but provides crucial insight into the biochemistry of bacteria. The added complication of bacterial physiology

responding to its environment adds to the complexity of such studies. The ability to study metabolism provides the potential for inferences to be gained, such as the MOA of antimicrobials and the identification of new metabolic drug targets. The insurgence of antimicrobial resistance and the finding that biofilm formation induces resistance (Drenkard and Ausubel, 2002; Rajendran et al., 2013; Ramage et al., 2003; Soto, 2013; Stewart and Costerton, 2001) means that research in this area is vitally important.

5.3 Targeting differences in metabolism between planktonic and biofilms to look for biofilm modulation effects

Changes in metabolism between planktonic and biofilm growth states may highlight novel targets to induce biofilm modulation. Antimicrobial compounds have been shown to induce a cascade of detrimental effects on microbial metabolism through inhibiting biological processes (Allen et al., 2004; Brogden, 2005; Escalada et al., 2005a, 2005b; Lynch and Abbanat, 2010; Vincent et al., 2012; Wisseman et al., 1951; Yee et al., 2015; Yi et al., 2007). However, bacteria have been quick to evolve resistance mechanisms, for example efflux pumps to actively displace intracellular compounds, to combat antimicrobial challenge (Costa et al., 2013; Kaatz et al., 1993; Li and Nikaido, 2009; Soto, 2013; Webber, 2002). Therefore, the identification of new targets is crucial to the development of new antimicrobials.

Purine metabolism was explored as a route for biofilm modulation, by flooding the metabolic pathway with exogenous metabolites. Commercially available structural analogues were sought, with the hypothesis that they could be used to modulate biofilm development by blocking metabolism. Interestingly the purine metabolite inosine was shown to increase biofilm biomass and formycin B a structural analogue of inosine, which has been developed as an anti-parasitic drug in the past (Bzowska et al., 1992; Rainey and Santi, 1983), reduced biofilm biomass. It was hypothesised that structural analogues could be used to block fundamental metabolic processes potentially aiding antimicrobial treatment of biofilms through synergistic effects. Synergistic effects have been highlighted in antimicrobial treatment strategies (Bhargava and Leonard, 1996; Rogers et al., 2010; Srinivasan et al., 2013) and may provide a solution to incomplete bacterial

eradication exposing bacteria to sub-lethal drug concentrations, exacerbating resistance.

5.4 Untargeted metabolomics to study Triclosan mechanism of action (MOA) in *S. aureus*

Untargeted metabolomics can be used to look at the MOA of an antimicrobial across bacterial metabolism, through studying a drug's response on metabolism (Taylor et al., 2010). Two types of MOA study can be employed:

1) Looking at the effects on metabolism caused by a drug concentration gradient at a constant exposure time.

2) Looking at the effects on metabolism caused by a constant concentration of drug over an exposure time range.

Here, we demonstrate a metabolomic approach to study drug MOAs in Gram-positive bacteria. This study further highlights the utility of the developed metabolomic method.

An untargeted metabolomics MOA study in *S. aureus*, looking at the effects of a concentration gradient of triclosan on planktonic cells and biofilms, was carried out. Understanding the effects of triclosan on biofilm formation is crucial to the understanding of the complete actions of the drug. In addition, as with many antimicrobial compounds, there is growing concern with triclosan resistance (Heath et al., 2000; McMurry et al., 1998b, 1999; Schweizer, 2001), its involvement in resistance to other antimicrobials (Russell, 2004; Suller and Russell, 2000), and its effect when released into the surrounding environment (Dann and Hontela, 2011; Lubarsky et al., 2012); prompting the Food and Drug Administration (FDA) to examine this more closely (FDA, 2013).

Although the use of triclosan has come under increasing speculation, its full effects are still largely unknown. Without further research into the MOA of triclosan in bacteria, conclusions on its use cannot be made. Without having all evidence it cannot be decided whether a drug is fit for purpose or not.

Results presented here could be viewed as further evidence and a positive argument for the use of triclosan as a biofilm prevention/treatment strategy. Furthermore, through optimising the metabolomic approaches we have been able to provide evidence of changes to the metabolism of the bacteria cells of the biofilm thus highlighting the drugs MOA through inducing a cascade of events in cell metabolism.

5.5 Summary of Future Work

As with most research, the work presented here does not represent the end and only barely scratches the surface of staphylococcal metabolism. As highlighted in the discussions and conclusions of individual chapters, a number of future experiments and research have been suggested as future works.

To summarise, further method optimisation is a common aspect of the future work emerging from this research. In the microbiome study presented here alternative sample preparation approaches, including implant surface scraping, DNase treatment or direct DNA extraction from the implant surface, should be explored to deplete host contamination and improve sequencing results.

With regards to the biofilm cultivation approaches used, further method optimisation could be incorporated into future work to take into account differences in biofilm formation under static and dynamic cultures. Further experiments could be used to test whether reported changes identified here are apparent in biofilms cultured under dynamic conditions and under different aerobic and anaerobic conditions.

For the metabolomics experiments the extraction methods established here do not discriminate between the intracellular metabolome of cells in the biofilm and the metabolome of the ECM. Future method development should look at applying an approach to initially separate the ECM from the biofilm cell extraction before analysis, for example through enzymatic or sonication disruption. This would allow more accurate analysis of the intracellular metabolome between the different growth states.

The work presented targeting purine metabolism to look for biofilm modulation effects is a preliminary study and future work should be carried out to confirm observations and utilise findings for the understanding of biofilm formation and potentially lead to the development of novel drugs targeting biofilm formation. Metabolomics was used to look at changes in metabolism but results could be confirmed with alternative -omic technologies, for example proteomics look at the changing proteome as well as the metabolome.

The use of *S. aureus* gene knockouts is also a future step in this project. Strains with genes knocked out in identified metabolic pathways shown to play a role in biofilm formation may further highlight metabolic targets for biofilm modulation.

Finally, in the Triclosan MOA study drug-time kinetics were not analysed but could represent a future study. This would look at the differences in metabolism in response to Triclosan over a time course, thus potentially providing more in-depth MOA information on triclosan.

The work and analyses presented here represent observations based on one strain of *S. aureus*. These results and observations should be confirmed in other strains as future work.

5.6 Summary

In summary, the aim of this research project was to provide greater understanding of orthopaedic infection caused by *S. aureus* and biofilm formation on the implant surface. The number of orthopaedic infections and the lack of knowledge regarding biofilm involvement led us to hypothesise that *S. aureus* is a leading cause of orthopaedic infection, and metabolomic approaches can be used to study *S. aureus* biofilms and find significant metabolic differences between different bacterial growth states and in response to antimicrobial challenge.

It was shown that metagenome analysis can be utilised to look at the polymicrobial microbiome of the infected hip prosthesis. As host contamination can lead to inefficient sequencing, commercial kits can be used to deplete

contaminating DNA in microbiome studies, thus enriching microbial DNA. However, we suggest that care should be taken with sample preparations which may damage contaminating DNA, leading to inefficient depletion. Following sequencing, polymicrobial infections were identified in orthopaedic infections. The microbiome study further revealed *S. aureus* as a primary cause of orthopaedic infections.

A clinical orthopaedic isolate of *S. aureus* was characterised and sequenced, named LHSKBClinical. *In vitro* biofilm cultivation methods were used to characterise biofilm formation by LHSKBClinical. A *S. aureus* metabolome extraction method for planktonic cells and biofilms was optimised, using bead beating. Using the method coupled with untargeted LC-MS metabolomics, *S. aureus* planktonic cells were compared to biofilms.

Significant changes in metabolism were identified between *S. aureus* planktonic cells and biofilms, specifically in arginine and purine metabolism. This led to further investigations into purine metabolism, which was explored for biofilm modulation effects using exogenous metabolites and structural analogues, revealing the induction of biofilm modulation effects and possible synergistic effects with antibiotics.

The developed extraction method and untargeted metabolomics were used to study the MOA of triclosan in *S. aureus* planktonic cells, revealing the metabolic effect induced by triclosan. Triclosan MOA was further studied in *S. aureus* biofilms, revealing the metabolic effect induced by triclosan in biofilms and differences in drug metabolism between different growth states of the same species, highlighting the altered metabolic state of biofilms.

Work presented here contributes to the greater understanding of orthopaedic infections, prevention and treatment strategies. Such work helps in the development of novel drugs and informed antimicrobial use, taking steps to reduce and one day stop the occurrence of serious and potentially life threatening orthopaedic infections.

Appendices

Please see attached files.

References

A, J., Trygg, J., Gullberg, J., Johansson, A.I., Jonsson, P.P., Antti, H., Marklund, S.L., and Moritz, T. (2005). Extraction and GC/MS analysis of the human blood plasma metabolome. Anal. Chem. *77*, 8086–8094.

Abraham, N.M., Lamlertthon, S., Fowler, V.G., and Jefferson, K.K. (2012). Chelating agents exert distinct effects on biofilm formation in Staphylococcus aureus depending on strain background: role for clumping factor B. J. Med. Microbiol. *61*, 1062–1070.

Aires de Sousa, M., and De Lencastre, H. (2004). Bridges from hospitals to the laboratory: genetic portraits of methicillin-resistant Staphylococcus aureus clones. FEMS Immunol. Med. Microbiol. *40*, 101–111.

Alenghat, F.J., and Ingber, D.E. (2002). Mechanotransduction: All Signals Point to Cytoskeleton, Matrix, and Integrins. Sci. Signal. *2002*.

Allen, J., Davey, H.M., Broadhurst, D., Rowland, J.J., Oliver, S.G., and Kell, D.B. (2004). Discrimination of Modes of Action of Antifungal Substances by Use of Metabolic Footprinting. Appl. Environ. Microbiol. *70*, 6157–6165.

Almeida Da Silva, P.E., and Palomino, J.C. (2011). Molecular basis and mechanisms of drug resistance in Mycobacterium tuberculosis: classical and new drugs. J. Antimicrob. Chemother. *66* , 1417–1430.

Alonso, A., Marsal, S., and Julià, A. (2015). Analytical Methods in Untargeted Metabolomics: State of the Art in 2015. Front. Bioeng. Biotechnol. *3*, 23.

Altschul, S.F., Gish, W., Miller, W., Myers, E.W., and Lipman, D.J. (1990). Basic local alignment search tool. J. Mol. Biol. *215*, 403–410.

Ammons, M.C.B. (2010). Anti-biofilm strategies and the need for innovations in wound care. Recent Pat. Antiinfect. Drug Discov. *5*, 10–17.

Ammons, M.C.B., Tripet, B.P., Carlson, R.P., Kirker, K.R., Gross, M.A., and Stanisich, J.J. (2014). Quantitative NMR Metabolite Profiling of Methicillin-Resistant and Methicillin-Susceptible Staphylococcus aureus Discriminates between Biofilm and Planktonic Phenotypes. J. Proteome Res. *13*, 2973–2985.

Anderson, K.L., Roberts, C., Disz, T., Vonstein, V., Hwang, K., Overbeek, R., Olson, P.D., Projan, S.J., and Dunman, P.M. (2006). Characterization of the Staphylococcus aureus Heat Shock, Cold Shock, Stringent, and SOS Responses and Their Effects on Log-Phase mRNA Turnover. J. Bacteriol. *188* , 6739–6756.

Andollina, A., De Cesare, A., Bertoni, G., Modelli, L., and Manfreda, G. (2004). Identification and genetic characterisation of orthopaedic Staphylococcus isolates collected in Italy by automated EcoRI ribotyping. FEMS Microbiol. Lett. *234*, 275–280.

Anon (1984). Classics in infectious diseases. “On abscesses”. Alexander Ogston (1844-1929). Rev. Infect. Dis. *6*, 122–128.

Anselme, K., Davidson, P., Popa, A.M., Giazzon, M., Liley, M., and Ploux, L. (2010). The interaction of cells and bacteria with surfaces structured at the nanometre scale. Acta Biomater. *6*, 3824–3846.

Appelbaum, P.C. (2006). The emergence of vancomycin-intermediate and vancomycin-resistant Staphylococcus aureus. Clin. Microbiol. Infect. *12*, 16–23.

Archer, N.K., Mazaitis, M.J., Costerton, J.W., Leid, J.G., Powers, M.E., and Shirtliff, M.E. (2011). Staphylococcus aureus biofilms: Properties, regulation and roles in human disease. Virulence *2*, 445–459.

Arciola, C.R., Campoccia, D., Baldassarri, L., Donati, M.E., Pirini, V., Gamberini, S., and Montanaro, L. (2006). Detection of biofilm formation in Staphylococcus epidermidis from implant infections. Comparison of a PCR-method that recognizes the presence of ica genes with two classic phenotypic methods. J. Biomed. Mater. Res. A *76*, 425–430.

Aros-Calt, S., Muller, B.H., Boudah, S., Ducruix, C., Gervasi, G., Junot, C., and Fenaille, F. (2015). Annotation of the Staphylococcus aureus Metabolome Using Liquid Chromatography Coupled to High-Resolution Mass Spectrometry and Application to the Study of Methicillin Resistance. J. Proteome Res. *14*, 4863–4875.

Atkins, B.L., Athanasou, N., Deeks, J.J., Crook, D.W.M., Simpson, H., Peto, T.E.A., McLardy-Smith, P., Berendt, A.R., and Group, T.O.C.S. (1998). Prospective Evaluation of Criteria for Microbiological Diagnosis of Prosthetic-Joint Infection at Revision Arthroplasty. J. Clin. Microbiol. *36*, 2932–2939.

Aziz, R.K., Bartels, D., Best, A.A., DeJongh, M., Disz, T., Edwards, R.A., Formsma, K., Gerdes, S., Glass, E.M., Kubal, M., et al. (2008). The RAST Server: rapid annotations using subsystems technology. BMC Genomics *9*, 75.

Barken, K.B., Pamp, S.J., Yang, L., Gjermansen, M., Bertrand, J.J., Klausen, M., Givskov, M., Whitchurch, C.B., Engel, J.N., and Tolker-Nielsen, T. (2008). Roles of type IV pili, flagellum-mediated motility and extracellular DNA in the formation of mature multicellular structures in Pseudomonas aeruginosa biofilms. Environ. Microbiol. *10*, 2331–2343.

Barraud, N., Hassett, D.J., Hwang, S.-H., Rice, S.A., Kjelleberg, S., and Webb, J.S. (2006). Involvement of Nitric Oxide in Biofilm Dispersal of Pseudomonas aeruginosa. J. Bacteriol. *188*, 7344–7353.

Bauer, T.W., Parvizi, J., Kobayashi, N., and Krebs, V. (2006). Diagnosis of Periprosthetic Infection. J. Bone Jt. Surg. *88*, 869–882.

Bawn, C.E.H., and Wajid, M.A. (1956). High polymer solutions. Part 7- Vapour pressure of polystyrene solutions in acetone, chloroform and propyl acetate. Trans. Faraday Soc. *52*, 1658–1664.

Beale, D.J., Barratt, R., Marlow, D.R., Dunn, M.S., Palombo, E.A., Morrison, P.D., and Key, C. (2013). Application of metabolomics to understanding biofilms in water distribution systems: a pilot study. Biofouling *29*, 283–294.

Beckonert, O., Keun, H.C., Ebbels, T.M.D., Bundy, J., Holmes, E., Lindon, J.C., and Nicholson, J.K. (2007). Metabolic profiling, metabolomic and metabonomic procedures for NMR spectroscopy of urine, plasma, serum and tissue extracts. Nat. Protoc. *2*, 2692–2703.

Beenken, K.E., Blevins, J.S., and Smeltzer, M.S. (2003). Mutation of sarA in Staphylococcus aureus limits biofilm formation. Infect. Immun. *71*, 4206–4211.

Beenken, K.E., Dunman, P.M., McAleese, F., Macapagal, D., Murphy, E., Projan, S.J., Blevins, J.S., and Smeltzer, M.S. (2004). Global gene expression in Staphylococcus aureus biofilms. J. Bacteriol. *186*, 4665–4684.

Beenken, K.E., Mrak, L.N., Griffin, L.M., Zielinska, A.K., Shaw, L.N., Rice, K.C., Horswill, A.R., Bayles, K.W., and Smeltzer, M.S. (2010). Epistatic Relationships between

sarA and agr in Staphylococcus aureus Biofilm Formation. PLoS One *5*, e10790.

Belas, R. (2014). Biofilms, flagella, and mechanosensing of surfaces by bacteria. Trends Microbiol. *22*, 517–527.

Bereza, P.L., Ekiel, A., Auguåciak-Duma, A., Aptekorz, M., Wilk, I., Kusz, D.J., Wojciechowski, P., and Martirosian, G. (2013). Identification of silent prosthetic joint infection: Preliminary report of a prospective controlled study. Int. Orthop. *37*, 2037–2043.

Bhakdi, S., and Tranum-Jensen, J. (1991). Alpha-toxin of Staphylococcus aureus. Microbiol. Rev. *55*, 733–751.

Bhargava, H.N., and Leonard, P.A. (1996). ARTlCLE Triclosan : Applications and safety. Am. J. Infect. Control *24*, 209–218.

Bien, J., Sokolova, O., and Bozko, P. (2011). Characterization of Virulence Factors of Staphylococcus aureus : Novel Function of Known Virulence Factors That Are Implicated in Activation of Airway Epithelial Proinflammatory Response. J. Pathog. *2011*, 13 pages.

Bishara, J., Goldberg, E., Leibovici, L., Samra, Z., Shaked, H., Mansur, N., and Paul, M. (2012). Healthcare-associated vs. hospital-acquired Staphylococcus aureus bacteremia. Int. J. Infect. Dis. *16*, e457–e463.

Blow, N. (2008). Metabolomics: Biochemistry's new look. Nature *455*, 697–700.

Bolano, A., Stinchi, S., Preziosi, R., Bistoni, F., Allegrucci, M., Baldelli, F., Martini, A., and Cardinali, G. (2001). Rapid methods to extract DNA and RNA from Cryptococcus neoformans. FEMS Yeast Res. *1*, 221–224.

Boles, B.R., and Horswill, A.R. (2008). agr-Mediated Dispersal of Staphylococcus aureus Biofilms. PLoS Pathog. *4*, e1000052.

Bolstad, B.M., Irizarry, R.A., Astrand, M., and Speed, T.P. (2003). A comparison of normalization methods for high density oligonucleotide array data based on variance and bias. Bioinformatics *19*, 185–193.

Bolten, C.J., Kiefer, P., Letisse, F., Portais, J.-C., and Wittmann, C. (2007). Sampling for metabolome analysis of microorganisms. Anal. Chem. *79*, 3843–3849.

Booth, S.C., Workentine, M.L., Wen, J., Shaykhutdinov, R., Vogel, H.J., Ceri, H., Turner, R.J., and Weljie, A.M. (2011). Differences in Metabolism between the Biofilm and Planktonic Response to Metal Stress. J. Proteome Res. *10*, 3190–3199.

Boshoff, H.I.M., Myers, T.G., Copp, B.R., McNeil, M.R., Wilson, M.A., and Barry, C.E. 3rd (2004). The transcriptional responses of Mycobacterium tuberculosis to inhibitors of metabolism: novel insights into drug mechanisms of action. J. Biol. Chem. *279*, 40174–40184.

Bowden, M.G., Visai, L., Longshaw, C.M., Holland, K.T., Speziale, P., and Hook, M. (2002). Is the GehD lipase from Staphylococcus epidermidis a collagen binding adhesin? J. Biol. Chem. *277*, 43017–43023.

Braun, V., Hantke, K., and Koster, W. (1998). Bacterial iron transport: mechanisms, genetics, and regulation. Met. Ions Biol. Syst. *35*, 67–145.

Brogden, K.A. (2005). Antimicrobial peptides: pore formers or metabolic inhibitors in bacteria? Nat Rev Micro *3*, 238–250.

Brown, A.F., Leech, J.M., Rogers, T.R., and McLoughlin, R.M. (2013). Staphylococcus aureus Colonization: Modulation of Host Immune Response and Impact on Human Vaccine Design. Front. Immunol. *4*, 507.

Burik, J.-A.H. van, Schreckhise, R.W., White, T.C., Bowden, R.A., and Myerson, D. (1998). Comparison of six extraction techniques for isolation of DNA from filamentous fungi. Med. Mycol. *36*, 299–303.

Byrnes, R.W., Cotter, D., Maer, A., Li, J., Nadeau, D., and Subramaniam, S. (2009). An editor for pathway drawing and data visualization in the Biopathways Workbench. BMC Syst. Biol. *3*.

Bzowska, A., Kulikowska, E., and Shugar, D. (1992). Formycins A and B and some analogues: selective inhibitors of bacterial (Escherichia coli) purine nucleoside phosphorylase. Biochim. Biophys. Acta *1120*, 239–247.

Careri, M., and Mangia, A. (2011). Trends in analytical atomic and molecular mass spectrometry in biology and the life sciences. Anal. Bioanal. Chem. *399*, 2585–2595.

Cassou, C.A., Sterling, H.J., Susa, A.C., and Williams, E.R. (2014). Electrothermal Supercharging in Mass Spectrometry and Tandem Mass Spectrometry of Native Proteins. Anal. Chem. *85*, 138–146.

Chai, Y., Beauregard, P.B., and Vlamakis, H. (2012). Galactose Metabolism Plays a Crucial Role in Biofilm Formation by Bacillus subtilis. MBio *3*.

Chan, G.H.M., Ho, E.N.M., Leung, D.K.K., Wong, K.S., and Wan, T.S.M. (2016). Targeted Metabolomics Approach To Detect the Misuse of Steroidal Aromatase Inhibitors in Equine Sports by Biomarker Profiling. Anal. Chem. *88*, 764–772.

Chan, W.C., Coyle, B.J., and Williams, P. (2004). Virulence regulation and quorum sensing in staphylococcal infections: competitive AgrC antagonists as quorum sensing inhibitors. J. Med. Chem. *47*, 4633–4641.

Chapman-Smith, A., and Cronan Jr, J.E. (1999). Molecular Biology of Biotin Attachment to Proteins. J. Nutr. *129* , 477S – 484S.

Chatterjee, S., and Fisher, A.B. (2014). Mechanotransduction: Forces, Sensors, and Redox Signaling. Antioxid. Redox Signal. *20*, 868–871.

Chen, M., Yu, Q., and Sun, H. (2013). Novel Strategies for the Prevention and Treatment of Biofilm Related Infections. Int. J. Mol. Sci. *14*, 18488–18501.

Christensen, G., Simpson, W., Younger, J., Baddour, L., Barrett, F., Melton, D., and Beachey, E. (1985). Adherence of coagulase-negative staphylococci to plastic tissue culture plates : a staphylococci to medical devices . Adherence of Coagulase-Negative Staphylococci to Plastic Tissue Culture Plates : a Quantitative Model for the Adherence of Staphylococci. J. Clin. Microbiol. *22*, 996–1006.

Cogen, A.L., Nizet, V., and Gallo, R.L. (2008). Skin microbiota: a source of disease or defence? Br. J. Dermatol. *158*, 442–455.

Conlon, K.M., Humphreys, H., and O'Gara, J.P. (2002). icaR Encodes a Transcriptional Repressor Involved in Environmental Regulation of ica Operon Expression and Biofilm Formation in Staphylococcus epidermidis. J. Bacteriol. *184*, 4400–4408.

Conlon, K.M., Humphreys, H., and O'Gara, J.P. (2004). Inactivations of rsbU and sarA by IS256 Represent Novel Mechanisms of Biofilm Phenotypic Variation in Staphylococcus

epidermidis. J. Bacteriol. *186*, 6208–6219.

Costa, S.S., Viveiros, M., Amaral, L., and Couto, I. (2013). Multidrug Efflux Pumps in Staphylococcus aureus: an Update. Open Microbiol. J. *7*, 59–71.

Costerton, J.W., Lewandowski, Z., Caldwell, D.E., Korber, D.R., and Lappin-Scott, H.M. (1995). Microbial biofilms. Annu. Rev. Microbiol. *49*, 711–745.

Costerton, J.W., Stewart, P.S., and Greenberg, E.P. (1999). Bacterial Biofilms: A Common Cause of Persistent Infections. Science (80-.). *284*, 1318–1322.

Cotter, D., Maer, A., Guda, C., Saunders, B., and Subramaniam, S. (2006). LMPD: LIPID MAPS proteome database. Nucleic Acids Res. *34*, D507–D510.

Cramton, S.E., Gerke, C., Schnell, N.F., Nichols, W.W., and Götz, F. (1999). The Intercellular Adhesion (ica) Locus Is Present in Staphylococcus aureus and Is Required for Biofilm Formation. Infect. Immun. *67*, 5427–5433.

Cramton, S.E., Ulrich, M., Götz, F., and Döring, G. (2001). Anaerobic Conditions Induce Expression of Polysaccharide Intercellular Adhesin in Staphylococcus aureus and Staphylococcus epidermidis. Infect. Immun. *69*, 4079–4085.

Creek, D.J., Jankevics, A., Breitling, R., Watson, D.G., Barrett, M.P., and Burgess, K.E. V (2011). Identification by Retention Time Prediction. Bioinforma. Appl. Note *28*, 8703–8710.

Creek, D.J., Jankevics, A., Burgess, K.E. V, Breitling, R., and Barrett, M.P. (2012). IDEOM: an Excel interface for analysis of LC-MS-based metabolomics data. Bioinformatics *28*, 1048–1049.

Cubbon, S., Antonio, C., Wilson, J., and Thomas-Oates, J. (2010). Metabolomic applications of HILIC-LC-MS. Mass Spectrom. Rev. *29*, 671–684.

Cucarella, C., Solano, C., Valle, J., Amorena, B., Lasa, Í., and Penadés, J.R. (2001). Bap, a Staphylococcus aureus Surface Protein Involved in Biofilm Formation. J. Bacteriol. *183*, 2888–2896.

Cue, D., Lei, M.G., Luong, T.T., Kuechenmeister, L., Dunman, P.M., O'Donnell, S., Rowe, S., O'Gara, J.P., and Lee, C.Y. (2009). Rbf Promotes Biofilm Formation by Staphylococcus aureus via Repression of icaR, a Negative Regulator of icaADBC . J. Bacteriol. *191*, 6363–6373.

Daines, D. a, Bothwell, M., Furrer, J., Unrath, W., Nelson, K., Jarisch, J., Melrose, N., Greiner, L., Apicella, M., and Smith, A.L. (2005). Haemophilus influenzae luxS mutants form a biofilm and have increased virulence. Microb. Pathog. *39*, 87–96.

Dale, S.E., Doherty-Kirby, A., Lajoie, G., and Heinrichs, D.E. (2004). Role of Siderophore Biosynthesis in Virulence of Staphylococcus aureus: Identification and Characterization of Genes Involved in Production of a Siderophore . Infect. Immun. *72*, 29–37.

Dancer, S.J. (2004). How do we assess hospital cleaning? A proposal for microbiological standards for surface hygiene in hospitals. J. Hosp. Infect. *56*, 10–15.

Danielsson, A.P.H., Moritz, T., Mulder, H., and Spegel, P. (2010). Development and optimization of a metabolomic method for analysis of adherent cell cultures. Anal. Biochem. *404*, 30–39.

Dann, A.B., and Hontela, A. (2011). Triclosan: environmental exposure, toxicity and mechanisms of action. J. Appl. Toxicol. *31*, 285–311.

Darghouth, D., Koehl, B., Junot, C., and Romeo, P.-H. (2010). Metabolomic analysis of normal and sickle cell erythrocytes. Transfus. Clin. Biol. *17*, 148–150.

Darling, A.C.E., Mau, B., Blattner, F.R., and Perna, N.T. (2004). Mauve : Multiple Alignment of Conserved Genomic Sequence With Rearrangements. Genome Res. *14*, 1394–1403.

Davey, M.E., and O'toole, G.A. (2000). Microbial Biofilms: from Ecology to Molecular Genetics. Microbiol. Mol. Biol. Rev. *64*, 847–867.

David, M.Z., Boyle-Vavra, S., Zychowski, D.L., and Daum, R.S. (2011). Methicillin-Susceptible Staphylococcus aureus as a Predominantly Healthcare-Associated Pathogen: A Possible Reversal of Roles? PLoS One *6*.

Davies, D. (2003). Understanding biofilm resistance to antibacterial agents. Nat Rev Drug Discov *2*, 114–122.

Davies, D.G., and Marques, C.N.H. (2009). A Fatty Acid Messenger Is Responsible for Inducing Dispersion in Microbial Biofilms . J. Bacteriol. *191*, 1393–1403.

Davies, D.G., Parsek, M.R., Pearson, J.P., Iglewski, B.H., Costerton, J.W., and Greenberg, E.P. (1998). The involvement of cell-to-cell signals in the development of a bacterial biofilm. Science *280*, 295–298.

Degnan, B.A., Palmer, J.M., Robson, T., Jones, C.E.D., Fischer, M., Glanville, M., Mellor, G.D., Diamond, A.G., Kehoe, M.A., and Goodacre, J.A. (1998). Inhibition of Human Peripheral Blood Mononuclear Cell Proliferation by Streptococcus pyogenes Cell Extract Is Associated with Arginine Deiminase Activity. Infect. Immun. *66*, 3050–3058.

Degnan, B.A., Fontaine, M.C., Doebereiner, A.H., Lee, J.J., Mastroeni, P., Dougan, G., Goodacre, J.A., and Kehoe, M.A. (2000). Characterization of an Isogenic Mutant of Streptococcus pyogenes Manfredo Lacking the Ability To Make Streptococcal Acid Glycoprotein. Infect. Immun. *68*, 2441–2448.

Deininger, P.L. (1983). Random subcloning of sonicated DNA: Application to shotgun DNA sequence analysis. Anal. Biochem. *129*, 216–223.

Dejea, C.M., Wick, E.C., Hechenbleikner, E.M., White, J.R., Mark Welch, J.L., Rossetti, B.J., Peterson, S.N., Snesrud, E.C., Borisy, G.G., Lazarev, M., et al. (2014). Microbiota organization is a distinct feature of proximal colorectal cancers. Proc. Natl. Acad. Sci. *111* , 18321–18326.

Dempsey, K.E., Riggio, M.P., Lennon, A., Hannah, V.E., Ramage, G., Allan, D., and Bagg, J. (2007). Identification of bacteria on the surface of clinically infected and non-infected prosthetic hip joints removed during revision arthroplasties by 16S rRNA gene sequencing and by microbiological culture. Arthritis Res. Ther. *9*, R46.

Denyer, S.P., and Maillard, J.-Y. (2002). Cellular impermeability and uptake of biocides and antibiotics in Gram-negative bacteria. J. Appl. Microbiol. *92*, 35S – 45S.

Devriese, L.A., Van Damme, L.R., and Fameree, L. (1972). Methicillin (cloxacillin)-resistant Staphylococcus aureus strains isolated from bovine mastitis cases. Zentralbl. Veterinarmed. B *19*, 598–605.

Diaz, P.I., Dupuy, A.K., Abusleme, L., Reese, B., Obergfell, C., Choquette, L., Dongari-

Bagtzoglou, A., Peterson, D.E., Terzi, E., and Strausbaugh, L.D. (2012). Using high throughput sequencing to explore the biodiversity in oral bacterial communities. Mol. Oral Microbiol. *27*, 182–201.

Díaz, C., Cortizo, M.C., Schilardi, P.L., Saravia, S.G.G. de, and Mele, M.A.F.L. de (2007). Influence of the nano-micro structure of the surface on bacterial adhesion . Mater. Res. *10* , 11–14.

Diep, B.A., Gill, S.R., Chang, R.F., Phan, T.H., Chen, J.H., Davidson, M.G., Lin, F., Lin, J., Carleton, H.A., Mongodin, E.F., et al. (2006). Complete genome sequence of USA300, an epidemic clone of community-acquired meticillin-resistant Staphylococcus aureus. Lancet (London, England) *367*, 731–739.

Dinges, M.M., Orwin, P.M., and Schlievert, P.M. (2000). Exotoxins of Staphylococcus aureus . Clin. Microbiol. Rev. *13* , 16–34.

Drenkard, E., and Ausubel, F.M. (2002). Pseudomonas biofilm formation and antibiotic resistance are linked to phenotypic variation. Nature *416*, 740–743.

Duckworth, G.J., and Jordens, J.Z.O.E. (1990). Adherence and survival properties of an epidemic met h icill i n- resistant strain of Staphy / ococcus aureus compared with those of methicillin-sensitive strains. J. Med. Microbiol. *32*, 195–200.

Dunn, W.B. (2008). Current trends and future requirements for the mass spectrometric investigation of microbial, mammalian and plant metabolomes. Phys. Biol. *5*, 11001.

Enright, M.C., Day, N.P., Davies, C.E., Peacock, S.J., and Spratt, B.G. (2000). Multilocus sequence typing for characterization of methicillin-resistant and methicillin-susceptible clones of Staphylococcus aureus. J. Clin. Microbiol. *38*, 1008–1015.

Erlandsen, S.L., Kristich, C.J., Dunny, G.M., and Wells, C.L. (2004). High-resolution visualization of the microbial glycocalyx with low-voltage scanning electron microscopy: dependence on cationic dyes. J. Histochem. Cytochem. *52*, 1427–1435.

Escalada, M.G., Harwood, J.L., Maillard, J.-Y., and Ochs, D. (2005a). Triclosan inhibition of fatty acid synthesis and its effect on growth of Escherichia coli and Pseudomonas aeruginosa. J. Antimicrob. Chemother. *55*, 879–882.

Escalada, M.G., Russell, A.D., Maillard, J.-Y., and Ochs, D. (2005b). Triclosan-bacteria interactions: single or multiple target sites? Lett. Appl. Microbiol. *41*, 476–481.

Esteban, J., Molina-Manso, D., Spiliopoulou, I., Cordero-Ampuero, J., Fernández-Roblas, R., Foka, A., and Gómez-Barrena, E. (2010). Biofilm development by clinical isolates of Staphylococcus spp. from retrieved orthopedic prostheses. Acta Orthop. *81*, 674–679.

Fahy, E., Sud, M., Cotter, D., and Subramaniam, S. (2007). LIPID MAPS online tools for lipid research. Nucleic Acids Res. *35*, W606–W612.

Fahy, E., Subramaniam, S., Murphy, R.C., Nishijima, M., Raetz, C.R.H., Shimizu, T., Spener, F., van Meer, G., Wakelam, M.J.O., and Dennis, E.A. (2009). Update of the LIPID MAPS comprehensive classification system for lipids. J. Lipid Res. *50 Suppl*, S9–S14.

Faijes, M., Mars, A.E., and Smid, E.J. (2007). Comparison of quenching and extraction methodologies for metabolome analysis of Lactobacillus plantarum. Microb. Cell Fact. *6*, 27.

Fan, T.W.M., Lane, A.N., Higashi, R.M., Farag, M.A., Gao, H., Bousamra, M., and Miller,

D.M. (2009). Altered regulation of metabolic pathways in human lung cancer discerned by (13)C stable isotope-resolved metabolomics (SIRM). Mol. Cancer *8*, 41.

FDA (2013). FDA Taking Closer Look at “Antibacterial” Soap.

Feehery, G.R., Yigit, E., Oyola, S.O., Langhorst, B.W., Schmidt, V.T., Stewart, F.J., Dimalanta, E.T., Amaral-Zettler, L.A., Davis, T., Quail, M.A., et al. (2013). A Method for Selectively Enriching Microbial DNA from Contaminating Vertebrate Host DNA. PLoS One *8*, e76096.

Fiehn, O. (2002). Metabolomics--the link between genotypes and phenotypes. Plant Mol. Biol. *48*, 155–171.

Fitzpatrick, F., Humphreys, H., and O’Gara, J.P. (2005). The genetics of staphylococcal biofilm formation--will a greater understanding of pathogenesis lead to better management of device-related infection? Clin. Microbiol. Infect. *11*, 967–973.

Flemming, H.-C., and Wingender, J. (2010). The biofilm matrix. Nat. Rev. Microbiol. *8*, 623–633.

Foster, T.J. (2005). Immune evasion by staphylococci. Nat. Rev. Microbiol. *3*, 948–958.

Foster, T.J., and Hook, M. (1998). Surface protein adhesins of Staphylococcus aureus. Trends Microbiol. *6*, 484–488.

Foulston, L., Elsholz, A.K.W., DeFrancesco, A.S., and Losick, R. (2014). The Extracellular Matrix of Staphylococcus aureus Biofilms Comprises Cytoplasmic Proteins That Associate with the Cell Surface in Response to Decreasing pH. mBio *5* .

Fournier, B., Klier, A., and Rapoport, G. (2001). The two-component system ArlS-ArlR is a regulator of virulence gene expression in Staphylococcus aureus. Mol. Microbiol. *41*, 247–261.

Fox, P.M., Climo, M.W., and Archer, G.L. (2007). Lack of Relationship between Purine Biosynthesis and Vancomycin Resistance in Staphylococcus aureus: a Cautionary Tale for Microarray Interpretation . Antimicrob. Agents Chemother. *51* , 1274–1280.

Fraimow, H.S. (2009). Systemic Antimicrobial Therapy in Osteomyelitis. Semin. Plast. Surg. *23*, 90–99.

Frank, K.L., Reichert, E.J., Piper, K.E., and Patel, R. (2007). In vitro effects of antimicrobial agents on planktonic and biofilm forms of Staphylococcus lugdunensis clinical isolates. Antimicrob. Agents Chemother. *51*, 888–895.

Friedman, D.B., Stauff, D.L., Pishchany, G., Whitwell, C.W., Torres, V.J., and Skaar, E.P. (2006). Staphylococcus aureus redirects central metabolism to increase iron availability. PLoS Pathog. *2*, e87.

Froberg, M.K., Palavecino, E., Dykoski, R., Gerding, D.N., Peterson, L.R., and Johnson, S. (2004). Staphylococcus aureus and Clostridium difficile Cause Distinct Pseudomembranous Intestinal Diseases. Clin. Infect. Dis. *39* , 747–750.

Fux, C.A., Wilson, S., and Stoodley, P. (2004). Detachment Characteristics and Oxacillin Resistance of Staphyloccocus aureus Biofilm Emboli in an In Vitro Catheter Infection Model. J. Bacteriol. *186*, 4486–4491.

Ge, X., Kitten, T., Chen, Z., Lee, S.P., Munro, C.L., and Xu, P. (2008). Identification of Streptococcus sanguinis genes required for biofilm formation and examination of their

role in endocarditis virulence. Infect. Immun. *76*, 2551–2559.

Gerding, D.N., Muto, C.A., and Owens, R.C. (2008). Treatment of Clostridium difficile Infection. Clin. Infect. Dis. *46* , S32–S42.

Gerke, C., Kraft, A., Sussmuth, R., Schweitzer, O., and Gotz, F. (1998). Characterization of the N-acetylglucosaminyltransferase activity involved in the biosynthesis of the Staphylococcus epidermidis polysaccharide intercellular adhesin. J. Biol. Chem. *273*, 18586–18593.

Giuliano, M., Barza, M., Jacobus, N. V, and Gorbach, S.L. (1987). Effect of broad-spectrum parenteral antibiotics on composition of intestinal microflora of humans. Antimicrob. Agents Chemother. *31* , 202–206.

Gjersing, E.L., Herberg, J.L., Horn, J., Schaldach, C.M., and Maxwell, R.S. (2007). NMR metabolomics of planktonic and biofilm modes of growth in Pseudomonas aeruginosa. Anal. Chem. *79*, 8037–8045.

Gomez, E., Cazanave, C., Cunningham, S.A., Greenwood-Quaintance, K.E., Steckelberg, J.M., Uhl, J.R., Hanssen, A.D., Karau, M.J., Schmidt, S.M., Osmon, D.R., et al. (2012). Prosthetic Joint Infection Diagnosis Using Broad-Range PCR of Biofilms Dislodged from Knee and Hip Arthroplasty Surfaces Using Sonication. J. Clin. Microbiol. *50*, 3501–3508.

Gong, J.Q., Lin, L., Lin, T., Hao, F., Zeng, F.Q., Bi, Z.G., Yi, D., and Zhao, B. (2006). Skin colonization by Staphylococcus aureus in patients with eczema and atopic dermatitis and relevant combined topical therapy: a double-blind multicentre randomized controlled trial. Br. J. Dermatol. *155*, 680–687.

van der Greef, J., and Smilde, A.K. (2005). Symbiosis of chemometrics and metabolomics: past, present, and future. J. Chemom. *19*, 376–386.

Griffin, J.L., and Nicholls, A.W. (2006). Metabolomics as a functional genomic tool for understanding lipid dysfunction in diabetes, obesity and related disorders. Pharmacogenomics *7*, 1095–1107.

Gross, J.H. (2011). Mass Spectrometry A Textbook (Springer, Analytical Chemistry).

Gross, M., Cramton, S.E., Gotz, F., and Peschel, A. (2001). Key role of teichoic acid net charge in Staphylococcus aureus colonization of artificial surfaces. Infect. Immun. *69*, 3423–3426.

Hall-Stoodley, L., Costerton, J.W., and Stoodley, P. (2004). Bacterial biofilms: from the natural environment to infectious diseases. Nat. Rev. Microbiol. *2*, 95–108.

Harshman, S., Boquet, P., Duflot, E., Alouf, J.E., Montecucco, C., and Papini, E. (1989). Staphylococcal alpha-toxin: a study of membrane penetration and pore formation. J. Biol. Chem. *264*, 14978–14984.

Hartley, J.C., and Harris, K.A. (2014). Molecular techniques for diagnosing prosthetic joint infections. J. Antimicrob. Chemother. *69* , i21–i24.

Haug, K., Salek, R.M., Conesa, P., Hastings, J., de Matos, P., Rijnbeek, M., Mahendraker, T., Williams, M., Neumann, S., Rocca-Serra, P., et al. (2012). MetaboLights—an open-access general-purpose repository for metabolomics studies and associated meta-data. Nucleic Acids Res. .

Heath, R.J., and Rock, C.O. (2000). A triclosan-resistant bacterial enzyme. Nature *406*, 145–146.

Heath, R.J., Rubin, J.R., Holland, D.R., Zhang, E., Snow, M.E., and Rock, C.O. (1999). Mechanism of Triclosan Inhibition of Bacterial Fatty Acid Synthesis. J. Biol. Chem. *274* , 11110–11114.

Heath, R.J., Li, J., Roland, G.E., and Rock, C.O. (2000). Inhibition of the Staphylococcus aureus NADPH-dependent enoyl-acyl carrier protein reductase by triclosan and hexachlorophene. J. Biol. Chem. *275*, 4654–4659.

Hedges, J.B., Vahidi, S., Yue, X., and Konermann, L. (2013). Effects of Ammonium Bicarbonate on the Electrospray Mass Spectra of Proteins: Evidence for Bubble-Induced Unfolding. Anal. Chem. *85*, 6469–6476.

Hendrich, B., and Bird, A. (1998). Identification and Characterization of a Family of Mammalian Methyl-CpG Binding Proteins. Mol. Cell. Biol. *18*, 6538–6547.

Hennig, S., Nyunt Wai, S., and Ziebuhr, W. (2007). Spontaneous switch to PIA-independent biofilm formation in an ica-positive Staphylococcus epidermidis isolate. Int. J. Med. Microbiol. *297*, 117–122.

Hochbaum, A.I., Kolodkin-Gal, I., Foulston, L., Kolter, R., Aizenberg, J., and Losick, R. (2011). Inhibitory Effects of d-Amino Acids on Staphylococcus aureus Biofilm Development . J. Bacteriol. *193*, 5616–5622.

Hochberg, Y., and Benjamini, Y. (1990). More powerful procedures for multiple significance testing. Stat. Med. *9*, 811–818.

Hofmann, F.T., Szostak, J.W., and Seebeck, F.P. (2012). In Vitro Selection of Functional Lantipeptides. J. Am. Chem. Soc. *134*, 8038–8041.

Holtfreter, S., and Broker, B.M. (2005). Staphylococcal superantigens: do they play a role in sepsis? Arch. Immunol. Ther. Exp. (Warsz). *53*, 13–27.

Horai, H., Arita, M., Kanaya, S., Nihei, Y., Ikeda, T., Suwa, K., Ojima, Y., Tanaka, K., Tanaka, S., Aoshima, K., et al. (2010). MassBank: a public repository for sharing mass spectral data for life sciences. J. Mass Spectrom. *45*, 703–714.

Horning, E.C., and Horning, M.G. (1971). Metabolic profiles: gas-phase methods for analysis of metabolites. Clin. Chem. *17*, 802–809.

Houston, P., Rowe, S.E., Pozzi, C., Waters, E.M., and O'Gara, J.P. (2011). Essential Role for the Major Autolysin in the Fibronectin-Binding Protein-Mediated Staphylococcus aureus Biofilm Phenotype . Infect. Immun. *79*, 1153–1165.

Hu, Q., Noll, R.J., Li, H., Makarov, A., Hardman, M., and Graham Cooks, R. (2005). The Orbitrap: a new mass spectrometer. J. Mass Spectrom. *40*, 430–443.

Hussain, M., Herrmann, M., von Eiff, C., Perdreau-Remington, F., and Peters, G. (1997). A 140-kilodalton extracellular protein is essential for the accumulation of Staphylococcus epidermidis strains on surfaces. Infect. Immun. *65*, 519–524.

Iorio, F., Bosotti, R., Scacheri, E., Belcastro, V., Mithbaokar, P., Ferriero, R., Murino, L., Tagliaferri, R., Brunetti-Pierri, N., Isacchi, A., et al. (2010). Discovery of drug mode of action and drug repositioning from transcriptional responses. Proc. Natl. Acad. Sci. *107* , 14621–14626.

Jansen, B., and Kohnen, W. (1995). Prevention of biofilm formation by polymer modification. J. Ind. Microbiol. *15*, 391–396.

Jansen, B., Kirstinsson, K.G., Jansen, S., Peters, G., and Pulverer, G. (1992). In-vitro efficacy of a central venous catheter complexed with iodine to prevent bacterial colonization. J. Antimicrob. Chemother. *30* , 135–139.

Jardeleza, C., Foreman, A., Baker, L., Paramasivan, S., Field, J., Tan, L.W., and Wormald, P.-J. (2011). The effects of nitric oxide on Staphylococcus aureus biofilm growth and its implications in chronic rhinosinusitis. Int. Forum Allergy Rhinol. *1*, 438–444.

Jefferson, K.K., Pier, D.B., Goldmann, D.A., and Pier, G.B. (2004). The Teicoplanin-Associated Locus Regulator (TcaR) and the Intercellular Adhesin Locus Regulator (IcaR) Are Transcriptional Inhibitors of the ica Locus in Staphylococcus aureus. J. Bacteriol. *186*, 2449–2456.

Jenkins, P.J., Teoh, K., Simpson, P.M., Dave, J., Simpson, A.H.W.R., and Breusch, S. (2010). Clostridium difficile in patients undergoing primary hip and knee replacement. J. Bone Jt. Surgery, Br. Vol. *92-B* , 994–998.

Ji, G., Beavis, R., and Novick, R.P. (1997). Bacterial interference caused by autoinducing peptide variants. Science *276*, 2027–2030.

Johnson, C.H., Dejea, C.M., Edler, D., Hoang, L.T., Santidrian, A.F., Felding, B.H., Ivanisevic, J., Cho, K., Wick, E.C., Hechenbleikner, E.M., et al. (2015). Metabolism Links Bacterial Biofilms and Colon Carcinogenesis. Cell Metab. *21*, 891–897.

Johnson, M., Cockayne, A., Williams, P.H., and Morrissey, J.A. (2005). Iron-Responsive Regulation of Biofilm Formation in Staphylococcus aureus Involves Fur-Dependent and Fur-Independent Mechanisms. J. Bacteriol. *187*, 8211–8215.

Jones, G.L., Muller, C.T., O'Reilly, M., and Stickler, D.J. (2006). Effect of triclosan on the development of bacterial biofilms by urinary tract pathogens on urinary catheters. J. Antimicrob. Chemother. *57* , 266–272.

Kaatz, G.W., Seo, S.M., and Ruble, C.A. (1993). Efflux-mediated fluoroquinolone resistance in Staphylococcus aureus. Antimicrob. Agents Chemother. *37*, 1086–1094.

Kakwani, R., Chakrabarti, D., Katam, K., Sinha, A., Okoro, T., and Al-Najjar, M. (2010). Impact of C. Difficile infection in elective orthopaedic surgery patients. J. Bone Jt. Surgery, Br. Vol. *92-B*, 315.

Kallala, R.F., Vanhegan, I.S., Ibrahim, M.S., Sarmah, S., and Haddad, F.S. (2015). Financial analysis of revision knee surgery based on NHS tariffs and hospital costs: does it pay to provide a revision service? . Bone Jt. J. *97-B* , 197–201.

Kamme, C., and Lindberg, L. (1981). Aerobic and anaerobic bacteria in deep infections after total hip arthroplasty: differential diagnosis between infectious and non-infectious loosening. Clin. Orthop. Relat. Res. 201–207.

Kanehisa, M., and Goto, S. (2000). KEGG: kyoto encyclopedia of genes and genomes. Nucleic Acids Res. *28*, 27–30.

Kaneko, J., and Kamio, Y. (2004). Bacterial two-component and hetero-heptameric pore-forming cytolytic toxins: structures, pore-forming mechanism, and organization of the genes. Biosci. Biotechnol. Biochem. *68*, 981–1003.

Kaplan, J.B., Ragunath, C., Ramasubbu, N., and Fine, D.H. (2003). Detachment of Actinobacillus actinomycetemcomitans Biofilm Cells by an Endogenous β-Hexosaminidase Activity. J. Bacteriol. *185*, 4693–4698.

Kell, D.B. (2004). Metabolomics and systems biology: making sense of the soup. Curr. Opin. Microbiol. *7*, 296–307.

Kell, D.B., and Oliver, S.G. (2004). Here is the evidence, now what is the hypothesis? The complementary roles of inductive and hypothesis-driven science in the post-genomic era. Bioessays *26*, 99–105.

Khanna, S., and Pardi, D.S. (2012). Clostridium difficile Infection: New Insights Into Management. Mayo Clin. Proc. *87*, 1106–1117.

Kiefer, P., Portais, J.-C., and Vorholt, J.A. (2008). Quantitative metabolome analysis using liquid chromatography-high-resolution mass spectrometry. Anal. Biochem. *382*, 94–100.

Kim, H.K., and Verpoorte, R. (2010). Sample preparation for plant metabolomics. Phytochem. Anal. *21*, 4–13.

Kim, S., Thiessen, P.A., Bolton, E.E., Chen, J., Fu, G., Gindulyte, A., Han, L., He, J., He, S., Shoemaker, B.A., et al. (2016). PubChem Substance and Compound databases. Nucleic Acids Res. *44*, D1202–D1213.

Kinross, J.M., Darzi, A.W., and Nicholson, J.K. (2011). Gut microbiome-host interactions in health and disease. Genome Med. *3*, 14.

Klemm, K. (1979). [Gentamicin-PMMA-beads in treating bone and soft tissue infections (author's transl)]. Zentralbl. Chir. *104*, 934–942.

Kluytmans, J., Belkum, A. van, and Verbrugh, H. (1997). Nasal Carriage of Staphylococcus aureus : Epidemiology , Underlying Mechanisms , and Associated Risks. Clin. Microbiol. Rev. *10*, 505–520.

Knobloch, J.K.-M., Jäger, S., Horstkotte, M.A., Rohde, H., and Mack, D. (2004). RsbU-Dependent Regulation of Staphylococcus epidermidis Biofilm Formation Is Mediated via the Alternative Sigma Factor σ(B) by Repression of the Negative Regulator Gene icaR . Infect. Immun. *72*, 3838–3848.

Kolari, M. (2003). Attachment mechanisms and properties of bacterial biofilms on non-living surfaces Marko Kolari.

Kolodkin-Gal, I., Romero, D., Cao, S., Clardy, J., Kolter, R., and Losick, R. (2010). D-Amino Acids Trigger Biofilm Disassembly. Science *328*, 627–629.

Komaromy, A.Z., Li, S., Zhang, H., Nicolau, D. V, Boysen, R.I., and Hearn, M.T.W. (2012). Arrays of nano-structured surfaces to probe the adhesion and viability of bacteria. Microelectron. Eng. *91*, 39–43.

Kong, K.-F., Vuong, C., and Otto, M. (2006). Staphylococcus quorum sensing in biofilm formation and infection. Int. J. Med. Microbiol. *296*, 133–139.

de Koning, W., and van Dam, K. (1992). A method for the determination of changes of glycolytic metabolites in yeast on a subsecond time scale using extraction at neutral pH. Anal. Biochem. *204*, 118–123.

Koren, O., Spor, A., Felin, J., Fåk, F., Stombaugh, J., Tremaroli, V., Behre, C.J., Knight, R., Fagerberg, B., Ley, R.E., et al. (2011). Human oral, gut, and plaque microbiota in patients with atherosclerosis. Proc. Natl. Acad. Sci. U. S. A. *108*, 4592–4598.

Köser, C.U., Ellington, M.J., and Peacock, S.J. (2014). Whole-genome sequencing to control antimicrobial resistance. Trends Genet. *30*, 401–407.

Kullik, I., and Giachino (1997). The alternative sigma factor sigmaB in Staphylococcus aureus: regulation of the sigB operon in response to growth phase and heat shock. Arch. Microbiol. *167*, 151–159.

Kumar, N., David, M.Z., Boyle-Vavra, S., Sieth, J., and Daum, R.S. (2015). High Staphylococcus aureus colonization prevalence among patients with skin and soft tissue infections and controls in an urban emergency department. J. Clin. Microbiol. *53*, 810–815.

Kusada, H., Hanada, S., Kamagata, Y., and Kimura, N. (2014). The effects of N-acylhomoserine lactones, beta-lactam antibiotics and adenosine on biofilm formation in the multi-beta-lactam antibiotic-resistant bacterium Acidovorax sp. strain MR-S7. J. Biosci. Bioeng. *118*, 14–19.

Laidler, K. (1984). The development of the Arrhenius equation. J. Chem. Educ. *61*, 494.

Lawley, T.D., Croucher, N.J., Yu, L., Clare, S., Sebaihia, M., Goulding, D., Pickard, D.J., Parkhill, J., Choudhary, J., and Dougan, G. (2009). Proteomic and Genomic Characterization of Highly Infectious Clostridium difficile 630 Spores . J. Bacteriol. *191*, 5377–5386.

Ledala, N., Zhang, B., Seravalli, J., Powers, R., and Somerville, G.A. (2014). Influence of Iron and Aeration on Staphylococcus aureus Growth, Metabolism, and Transcription. J. Bacteriol. *196* , 2178–2189.

Lei, T., Wang, L., Chen, C., and Ji, Y. (2014). Metabolomic investigation of methicillin-resistant Staphylococcus aureus. Methods Mol. Biol. *1085*, 251–258.

Levy, C.W., Roujeinikova, a, Sedelnikova, S., Baker, P.J., Stuitje, a R., Slabas, a R., Rice, D.W., and Rafferty, J.B. (1999). Molecular basis of triclosan activity. Nature *398*, 383–384.

Lewis, H.C., Mølbak, K., Reese, C., Aarestrup, F.M., Selchau, M., Sørum, M., and Skov, R.L. (2008). Pigs as Source of Methicillin-Resistant Staphylococcus aureus CC398 Infections in Humans, Denmark. Emerg. Infect. Dis. J. *14*, 1383.

Lewis, J.D., Meehan, R.R., Henzel, W.J., Maurer-Fogy, I., Jeppesen, P., Klein, F., and Bird, A. (1992). Purification, sequence, and cellular localization of a novel chromosomal protein that binds to methylated DNA. Cell *69*, 905–914.

Li, X.-Z., and Nikaido, H. (2009). Efflux-Mediated Drug Resistance in Bacteria: an Update. Drugs *69*, 1555–1623.

Lichtman, J.W., and Conchello, J.-A. (2005). Fluorescence microscopy. Nat Meth *2*, 910–919.

Licitra, G. (2013). Etymologia: Staphylococcus. Emerg. Infect. Dis. *19*, 1553.

Liebeke, M., Dorries, K., Zuhlke, D., Bernhardt, J., Fuchs, S., Pane-Farre, J., Engelmann, S., Volker, U., Bode, R., Dandekar, T., et al. (2011). A metabolomics and proteomics study of the adaptation of Staphylococcus aureus to glucose starvation. Mol. Biosyst. *7*, 1241–1253.

Liebeke, M., Dorries, K., Meyer, H., and Lalk, M. (2012). Metabolome analysis of gram-positive bacteria such as Staphylococcus aureus by GC-MS and LC-MS. Methods Mol. Biol.

815, 377–398.

Lieberman, M., and Marks, A.D. (2009). Purine and Pyrimidine Metabolism. In Marks' Basic Medical Biochemistry, A Clinical Approach, (Baltimore: Lippincott Williams & Wilkins), p. 789.

Lilly, H.A., and Lowbury, E.J.L. (1974). Disinfection of the Skin with Detergent Preparations of Irgasan DP 300 and Other Antiseptics. Br. Med. J. *4*, 372–374.

Lim, Y., Jana, M., Luong, T.T., and Lee, C.Y. (2004). Control of glucose- and NaCl-induced biofilm formation by rbf in Staphylococcus aureus. J. Bacteriol. *186*, 722–729.

Lim, Y., Shin, H.J., Kwon, A.S., Reu, J.H., Park, G., and Kim, J. (2013). Predictive genetic risk markers for strong biofilm-forming Staphylococcus aureus: fnbB gene and SCCmec type III. Diagn. Microbiol. Infect. Dis. *76*, 539–541.

Lim, Y.W., Haynes, M., Furlan, M., Robertson, C.E., Harris, J.K., and Rohwer, F. (2014). Purifying the impure: sequencing metagenomes and metatranscriptomes from complex animal-associated samples. J. Vis. Exp.

Lina, G., Bohach, G.A., Nair, S.P., Hiramatsu, K., Jouvin-Marche, E., and Mariuzza, R. (2004). Standard nomenclature for the superantigens expressed by Staphylococcus. J. Infect. Dis. *189*, 2334–2336.

Lindsay, J.A., and Holden, M.T.G. (2004). Staphylococcus aureus: superbug, super genome? Trends Microbiol. *12*, 378–385.

Lister, R., Pelizzola, M., Dowen, R.H., Hawkins, R.D., Hon, G., Tonti-Filippini, J., Nery, J.R., Lee, L., Ye, Z., Ngo, Q.-M., et al. (2009). Human DNA methylomes at base resolution show widespread epigenomic differences . Nature *462*, 315–322.

Liu, B., Faller, L.L., Klitgord, N., Mazumdar, V., Ghodsi, M., Sommer, D.D., Gibbons, T.R., Treangen, T.J., Chang, Y.-C., Li, S., et al. (2012). Deep Sequencing of the Oral Microbiome Reveals Signatures of Periodontal Disease. PLoS One *7*, e37919.

Loeffler, A., and Lloyd, D.H. (2010). Companion animals: a reservoir for methicillin-resistant Staphylococcus aureus in the community? Epidemiol. Infect. *138*, 595–605.

Lopez-Ribot, J.L. (2014). Large-Scale Biochemical Profiling of the Candida albicans Biofilm Matrix: New Compositional, Structural, and Functional Insights. MBio *5*.

Lowy, Franklin, D. (1998). Staphylococcus aureus Infections. New Englad J. Med. *339*, 520–532.

Lubarsky, H. V, Gerbersdorf, S.U., Hubas, C., Behrens, S., Ricciardi, F., and Paterson, D.M. (2012). Impairment of the bacterial biofilm stability by triclosan. PLoS One *7*, e31183.

Lynch, A.S., and Abbanat, D. (2010). New antibiotic agents and approaches to treat biofilm-associated infections. Expert Opin. Ther. Pat. *20*, 1373–1387.

Lynch, A.S., and Robertson, G.T. (2008). Bacterial and fungal biofilm infections. Annu. Rev. Med. *59*, 415–428.

Ma, L., Conover, M., Lu, H., Parsek, M.R., Bayles, K., and Wozniak, D.J. (2009). Assembly and Development of the Pseudomonas aeruginosa Biofilm Matrix. PLoS Pathog. *5*, e1000354.

Ma, Y., Xu, Y., Yestrepsky, B.D., Sorenson, R.J., Chen, M., Larsen, S.D., and Sun, H. (2012). Novel Inhibitors of Staphylococcus aureus Virulence Gene Expression and Biofilm Formation. PLoS One *7*, e47255.

Mack, D., Siemssen, N., and Laufs, R. (1992). Parallel induction by glucose of adherence and a polysaccharide antigen specific for plastic-adherent Staphylococcus epidermidis: evidence for functional relation to intercellular adhesion. Infect. Immun. *60*, 2048–2057.

Mack, D., Fischer, W., Krokotsch, A., Leopold, K., Hartmann, R., Egge, H., and Laufs, R. (1996). The intercellular adhesin involved in biofilm accumulation of Staphylococcus epidermidis is a linear beta-1,6-linked glucosaminoglycan: purification and structural analysis. J. Bacteriol. *178*, 175–183.

Maharjan, R.P., and Ferenci, T. (2003). Global metabolite analysis: the influence of extraction methodology on metabolome profiles of Escherichia coli. Anal. Biochem. *313*, 145–154.

Maiden, M.C.J., Bygraves, J.A., Feil, E., Morelli, G., Russell, J.E., Urwin, R., Zhang, Q., Zhou, J., Zurth, K., Caugant, D.A., et al. (1998). Multilocus sequence typing: A portable approach to the identification of clones within populations of pathogenic microorganisms. Proc. Natl. Acad. Sci. United States Am. *95*, 3140–3145.

Makaritsis, K.P., Neocleous, C., Gatselis, N., Petinaki, E., and Dalekos, G.N. (2009). An immunocompetent patient presenting with severe septic arthritis due to Ralstonia pickettii identified by molecular-based assays: a case report. Cases J. *2*, 8125.

Makarov, A., Denisov, E., Kholomeev, A., Balschun, W., Lange, O., Strupat, K., and Horning, S. (2006). Performance Evaluation of a Hybrid Linear Ion Trap/Orbitrap Mass Spectrometer. Anal. Chem. *78*, 2113–2120.

Mamas, M., Dunn, W.B., Neyses, L., and Goodacre, R. (2011). The role of metabolites and metabolomics in clinically applicable biomarkers of disease. Arch. Toxicol. *85*, 5–17.

Maresso, A.W., and Schneewind, O. (2008). Sortase as a target of anti-infective therapy. Pharmacol. Rev. *60*, 128–141.

Marraffini, L.A., Dedent, A.C., and Schneewind, O. (2006). Sortases and the art of anchoring proteins to the envelopes of gram-positive bacteria. Microbiol. Mol. Biol. Rev. *70*, 192–221.

Martin, M. (2011). Cutadapt removes adapter sequences from high-throughput sequencing reads. EMBnet.journal; Next Gener. Seq. Data Anal. *17*.

Mashego, M.R., van Gulik, W.M., Vinke, J.L., and Heijnen, J.J. (2003). Critical evaluation of sampling techniques for residual glucose determination in carbon-limited chemostat culture of Saccharomyces cerevisiae. Biotechnol. Bioeng. *83*, 395–399.

Mashego, M.R., Rumbold, K., De Mey, M., Vandamme, E., Soetaert, W., and Heijnen, J.J. (2007). Microbial metabolomics: past, present and future methodologies. Biotechnol. Lett. *29*, 1–16.

Masson, P., Alves, A.C., Ebbels, T.M.D., Nicholson, J.K., and Want, E.J. (2010). Optimization and evaluation of metabolite extraction protocols for untargeted metabolic profiling of liver samples by UPLC-MS. Anal. Chem. *82*, 7779–7786.

Mattila, E., Uusitalo-Seppälä, R., Wuorela, M., Lehtola, L., Nurmi, H., Ristikankare, M., Moilanen, V., Salminen, K., Seppälä, M., Mattila, P.S., et al. (2012). Fecal Transplantation, Through Colonoscopy, Is Effective Therapy for Recurrent Clostridium

difficile Infection. Gastroenterology *142*, 490–496.

Mattila, E., Arkkila, P., Mattila, P.S., Tarkka, E., Tissari, P., and Anttila, V.-J. (2013). Rifaximin in the treatment of recurrent Clostridium difficile infection. Aliment. Pharmacol. Ther. *37*, 122–128.

McCrea, K.W., Hartford, O., Davis, S., Eidhin, D.N., Lina, G., Speziale, P., Foster, T.J., and Hook, M. (2000). The serine-aspartate repeat (Sdr) protein family in Staphylococcus epidermidis. Microbiology *146 (Pt 7*, 1535–1546.

McDougald, D., Rice, S. a, Barraud, N., Steinberg, P.D., and Kjelleberg, S. (2012). Should we stay or should we go: mechanisms and ecological consequences for biofilm dispersal. Nat. Rev. Microbiol. *10*, 39–50.

McLean, J.S., Ona, O.N., and Majors, P.D. (2007). Correlated biofilm imaging, transport and metabolism measurements via combined nuclear magnetic resonance and confocal microscopy. ISME J. *2*, 121–131.

McMillan, D.J., Lutton, C., Rosenzweig, N., Sriprakash, K.S., Goss, B., Stemberger, M., Schuetz, M.A., and Steck, R. (2011). Prevention of Staphylococcus aureus biofilm formation on metallic surgical implants via controlled release of gentamicin. J. Biomed. Sci. Eng. *04*, 535–542.

McMurry, L.M., Oethinger, M., and Levy, S.B. (1998a). Triclosan targets lipid synthesis. Nature *394*, 531–532.

McMurry, L.M., Oethinger, M., and Levy, S.B. (1998b). Overexpression of marA, soxS, or acrAB produces resistance to triclosan in laboratory and clinical strains of Escherichia coli. FEMS Microbiol. Lett. *166*, 305–309.

McMurry, L.M., McDermott, P.F., and Levy, S.B. (1999). Genetic evidence that InhA of Mycobacterium smegmatis is a target for triclosan. Antimicrob. Agents Chemother. *43*, 711–713.

Medema, M.H., Blin, K., Cimermancic, P., de Jager, V., Zakrzewski, P., Fischbach, M.A., Weber, T., Takano, E., and Breitling, R. (2011). antiSMASH: rapid identification, annotation and analysis of secondary metabolite biosynthesis gene clusters in bacterial and fungal genome sequences. Nucleic Acids Res. *39*, W339–W346.

Melzer, M., Eykyn, S.J., Gransden, W.R., and Chinn, S. (2003). Is Methicillin-Resistant Staphylococcus aureus More Virulent than Methicillin-Susceptible S. aureus? A Comparative Cohort Study of British Patients with Nosocomial Infection and Bacteremia. Clin. Infect. Dis. *37* , 1453–1460.

Menestrina, G., Serra, M.D., and Prevost, G. (2001). Mode of action of beta-barrel pore-forming toxins of the staphylococcal alpha-hemolysin family. Toxicon *39*, 1661–1672.

Merino, N., Toledo-Arana, A., Vergara-Irigaray, M., Valle, J., Solano, C., Calvo, E., Lopez, J.A., Foster, T.J., Penadés, J.R., and Lasa, I. (2009). Protein A-Mediated Multicellular Behavior in Staphylococcus aureus . J. Bacteriol. *191*, 832–843.

Merritt, J.H.J., Kadouri, D.D.E., and O'Toole, G.G. a (2005). Growing and analyzing static biofilms. Curr. Protoc. … *Chapter 1*, Unit 1B.1.

Meyer, H., Liebeke, M., and Lalk, M. (2010). A protocol for the investigation of the intracellular Staphylococcus aureus metabolome. Anal. Biochem. *401*, 250–259.

Miles, A.A., and Misra, S.S. (1938). The etimation of the bactericidal power of the

blood. J. Hyg. (Lond). *38*, 732–749.

Mittelman, M.W. (1998). Structure and Functional Characteristics of Bacterial Biofilms in Fluid Processing Operations. J. Dairy Sci. *81*, 2760–2764.

Monds, R.D., and O'Toole, G.A. (2009). The developmental model of microbial biofilms: ten years of a paradigm up for review. Trends Microbiol. *17*, 73–87.

Mongodin, E., Finan, J., Climo, M.W., Rosato, A., Gill, S., and Archer, G.L. (2003). Microarray Transcription Analysis of Clinical Staphylococcus aureus Isolates Resistant to Vancomycin. J. Bacteriol. *185*, 4638–4643.

Montanaro, L., Speziale, P., Campoccia, D., Ravaioli, S., Cangini, I., Pietrocola, G., Giannini, S., and Arciola, C.R. (2011). Scenery of Staphylococcus implant infections in orthopedics. Future Microbiol. *6*, 1329–1349.

Moormeier, D.E., Bose, J.L., Horswill, A.R., and Bayles, K.W. (2014). Temporal and Stochastic Control of Staphylococcus aureus Biofilm Development. mBio *5* .

Moran, E., Masters, S., Berendt, A.R., McLardy-Smith, P., Byren, I., and Atkins, B.L. (2007). Guiding empirical antibiotic therapy in orthopaedics: The microbiology of prosthetic joint infection managed by debridement, irrigation and prosthesis retention. J. Infect. *55*, 1–7.

Mowat, E., Butcher, J., Lang, S., Williams, C., and Ramage, G. (2007). Development of a simple model for studying the effects of antifungal agents on multicellular communities of Aspergillus fumigatus. J. Med. Microbiol. *56*, 1205–1212.

Moxon, E.R., Sweetman, W. a, Deadman, M.E., Ferguson, D.J.P., and Hood, D.W. (2008). Haemophilus influenzae biofilms: hypothesis or fact? Trends Microbiol. *16*, 95–100.

MSI Board Members (2007). The Metabolomics Standards Initiative. Nat Biotech *25*, 846–848.

Mugabi, R., Sandgren, D., Born, M., Leith, I., Horne, S.M., and Prubeta, B.M. (2012). The role of activated acetate intermediates in the control of Escherichia coli biofilm amounts. Webmedcentral *3*.

Murphy, T.F., and Kirkham, C. (2002). Biofilm formation by nontypeable Haemophilus influenzae: strain variability, outer membrane antigen expression and role of pili. BMC Microbiol. *2*, 7.

Nair, S.P., Bischoff, M., Senn, M.M., and Berger-Bächi, B. (2003). The σ(B) Regulon Influences Internalization of Staphylococcus aureus by Osteoblasts . Infect. Immun. *71*, 4167–4170.

Namiki, T., Hachiya, T., Tanaka, H., and Sakakibara, Y. (2012). MetaVelvet: an extension of Velvet assembler to de novo metagenome assembly from short sequence reads. Nucleic Acids Res. 1–12.

National Health Service (NHS) (2014). Scottish Arthroplasty Project Biennial Report 2014, Biennial report. Inf. Serv. Div.

National Health Service (NHS) Scotland (2015). Health Protection Scotland (HPS) Weekly Report. HPS Surveill. Rep. *49*, 25–28.

Nelson, J.L., Rice, K.C., Slater, S.R., Fox, P.M., Archer, G.L., Bayles, K.W., Fey, P.D.,

Kreiswirth, B.N., and Somerville, G.A. (2007). Vancomycin-Intermediate Staphylococcus aureus Strains Have Impaired Acetate Catabolism: Implications for Polysaccharide Intercellular Adhesin Synthesis and Autolysis. Antimicrob. Agents Chemother. *51* , 616–622.

Nguyen, H.M., and Graber, C.J. (2010). Limitations of antibiotic options for invasive infections caused by methicillin-resistant Staphylococcus aureus: is combination therapy the answer? J. Antimicrob. Chemother. *65*, 24–36.

Nicholas, R.O., Li, T., McDevitt, D., Marra, A., Sucoloski, S., Demarsh, P.L., and Gentry, D.R. (1999). Isolation and Characterization of a sigB Deletion Mutant of Staphylococcus aureus. Infect. Immun. *67*, 3667–3669.

Nicholson, J.K., and Lindon, J.C. (2008). Systems Biology: Metabonomics. Nature, News Views Q&A *455*, 1054–1056.

Nielsen, L.N., Larsen, M.H., Skovgaard, S., Kastbjerg, V., Westh, H., Gram, L., and Ingmer, H. (2013). Staphylococcus aureus but not Listeria monocytogenes adapt to triclosan and adaptation correlates with increased fabI expression and agr deficiency. BMC Microbiol. *13*, 177.

Nilsson, I.-M., Hartford, O., Foster, T., and Tarkowski, A. (1999). Alpha-Toxin and Gamma-Toxin Jointly Promote Staphylococcus aureus Virulence in Murine Septic Arthritis. Infect. Immun. *67*, 1045–1049.

Nisman, B. (1954). The Stickland reaction. Bacteriol. Rev. *18*, 16–42.

Novick, R.P. (2003). Mobile genetic elements and bacterial toxinoses: the superantigen-encoding pathogenicity islands of Staphylococcus aureus. Plasmid *49*, 93–105.

O'Toole, G.A. (2011). Microtiter Dish Biofilm Formation Assay. J. Vis. Exp. 2437.

O'Toole, G.A., and Kolter, R. (1998). Initiation of biofilm formation in Pseudomonas fluorescens WCS365 proceeds via multiple, convergent signalling pathways: a genetic analysis. Mol. Microbiol. *28*, 449–461.

O'Toole, G., Kaplan, H.B., and Kolter, R. (2000). Biofilm Formation as Microbial Development. Annu. Rev. Microbiol. *54*, 49–79.

Oldiges, M., Lutz, S., Pflug, S., Schroer, K., Stein, N., and Wiendahl, C. (2007). Metabolomics: current state and evolving methodologies and tools. Appl. Microbiol. Biotechnol. *76*, 495–511.

Oliver, S.G., Winson, M.K., Kell, D.B., and Baganz, F. (1998). Systematic functional analysis of the yeast genome. Trends Biotechnol. *16*, 373–378.

Olszewski, K.L., Mather, M.W., Morrisey, J.M., Garcia, B.A., Vaidya, A.B., Rabinowitz, J.D., and Llinas, M. (2010). Branched tricarboxylic acid metabolism in Plasmodium falciparum. Nature *466*, 774–778.

Opperman, T.J., Kwasny, S.M., Williams, J.D., Khan, A.R., Peet, N.P., Moir, D.T., and Bowlin, T.L. (2009). Aryl Rhodanines Specifically Inhibit Staphylococcal and Enterococcal Biofilm Formation . Antimicrob. Agents Chemother. *53*, 4357–4367.

Osmon, D.R., and Berbari, E.F. (2002). Outpatient intravenous antimicrobial therapy for the practicing orthopaedic surgeon. Clin. Orthop. Relat. Res. 80–86.

Osmon, D.R., Berbari, E.F., Berendt, a. R., Lew, D., Zimmerli, W., Steckelberg, J.M.,

Rao, N., Hanssen, A., and Wilson, W.R. (2012). Diagnosis and Management of Prosthetic Joint Infection: Clinical Practice Guidelines by the Infectious Diseases Society of America (IDSA). Clin. Infect. Dis. *56*, e1–e25.

Otto, M. (2008). Staphylococcal Biofilms. Curr. Top. Microbiol. Immunol. *322*, 207–228.

Overbeek, R., Olson, R., Pusch, G.D., Olsen, G.J., Davis, J.J., Disz, T., Edwards, R.A., Gerdes, S., Parrello, B., Shukla, M., et al. (2014). The SEED and the Rapid Annotation of microbial genomes using Subsystems Technology (RAST). Nucleic Acids Res. *42*, D206–D214.

Pamp, S.J., Frees, D., Engelmann, S., Hecker, M., and Ingmer, H. (2006). Spx Is a Global Effector Impacting Stress Tolerance and Biofilm Formation in Staphylococcus aureus. J. Bacteriol. *188*, 4861–4870.

Pane-Farre, J., Jonas, B., Forstner, K., Engelmann, S., and Hecker, M. (2006). The sigmaB regulon in Staphylococcus aureus and its regulation. Int. J. Med. Microbiol. *296*, 237–258.

Panmanee, W., Taylor, D., Shea, C.J.A., Tang, H., Nelson, S., Seibel, W., Papoian, R., Kramer, R., Hassett, D.J., and Lamkin, T.J. (2013). High-throughput screening for small-molecule inhibitors of Staphylococcus epidermidis RP62a biofilms. J. Biomol. Screen. *18*, 820–829.

Panousis, K., Grigoris, P., Butcher, I., Rana, B., Reilly, J.H., and Hamblen, D.L. (2005). Poor predictive value of broad-range PCR for the detection of arthroplasty infection in 92 cases. Acta Orthop. *76*, 341–346.

Panousis, K., Grigoris, P., Butcher, I., Rana, B., Reilly, J.H., and Hamblen, D.L. (2006). Poor predictive value of broad-range PCR for the detection of arthroplasty infection. J. Bone Jt. Surgery, Br. Vol. *88-B*, 82–83.

Pantosti, A., Sanchini, A., and Monaco, M. (2007). Mechanisms of antibiotic resistance in Staphylococcus aureus. Future Microbiol. *2*, 323–334.

Passerini de Rossi, B., Calenda, M., Vay, C., and Franco, M. (2007). Biofilm formation by Stenotrophomonas maltophilia isolates from device-associated nosocomial infections. Rev. Argent. Microbiol. *39*, 204–212.

Patti, G.J., Yanes, O., and Siuzdak, G. (2012). Metabolomics: the apogee of the omic triology. Nat. Rev. Mol. Cell Biol. *13*, 263–269.

Patti, J.M., Allen, B.L., McGavin, M.J., and Hook, M. (1994). MSCRAMM-mediated adherence of microorganisms to host tissues. Annu. Rev. Microbiol. *48*, 585–617.

Paul, K.S., Bacchi, C.J., and Englund, P.T. (2004). Multiple triclosan targets in Trypanosoma brucei. Eukaryot. Cell *3*, 855–861.

Pelaez-Vargas, A., Carvalho, A., Grenho, L., F.J. Monteiro, 2, Gallego-Perez, D., Higuita-Castro, N., Hansford, D.J., Arismendi, J.A., Fernandes, M.H., and Ferraz, M.P. (2012). Micropatterned Coatings for Guided Tissue Regeneration in Dental Implantology. In Cell Interaction, S. Gowder, ed.

Pence, H.E., and Williams, A. (2010). ChemSpider: An Online Chemical Information Resource. J. Chem. Educ. *87*, 1123–1124.

Periasamy, S., Joo, H.-S., Duong, A.C., Bach, T.-H.L., Tan, V.Y., Chatterjee, S.S., Cheung, G.Y.C., and Otto, M. (2012). How Staphylococcus aureus biofilms develop their

characteristic structure. Proc. Natl. Acad. Sci. U. S. A. *109*, 1281–1286.

Peschel, A., Vuong, C., Otto, M., and Gotz, F. (2000). The D-alanine residues of Staphylococcus aureus teichoic acids alter the susceptibility to vancomycin and the activity of autolytic enzymes. Antimicrob. Agents Chemother. *44*, 2845–2847.

Pierce, C.G., Uppuluri, P., Tristan, A.R., Wormley, F.L., Mowat, E., Ramage, G., and Lopez-Ribot, J.L. (2008). A simple and reproducible 96-well plate-based method for the formation of fungal biofilms and its application to antifungal susceptibility testing. Nat. Protoc. *3*, 1494–1500.

Del Pozo, J.L., and Patel, R. (2009). Infection Associated with Prosthetic Joints. N. Engl. J. Med. *361*, 787–794.

Price, L.B., Stegger, M., Hasman, H., Aziz, M., Larsen, J., Andersen, P.S., Pearson, T., Waters, A.E., Foster, J.T., Schupp, J., et al. (2012). Staphylococcus aureus CC398: Host Adaptation and Emergence of Methicillin Resistance in Livestock. mBio *3* .

Psychogios, N., Hau, D.D., Peng, J., Guo, A.C., Mandal, R., Bouatra, S., Sinelnikov, I., Krishnamurthy, R., Eisner, R., Gautam, B., et al. (2011). The human serum metabolome. PLoS One *6*, e16957.

Public Health England (2015). Annual Epidemiological Commentary : Mandatory MRSA , MSSA and E . coli bacteraemia and C . difficile infection data, 2014/15. Annu. Epidemiol. Comment.

Qazi, S., Middleton, B., Muharram, S.H., Cockayne, A., Hill, P., O'Shea, P., Chhabra, S.R., Cámara, M., and Williams, P. (2006). N-Acylhomoserine Lactones Antagonize Virulence Gene Expression and Quorum Sensing in Staphylococcus aureus. Infect. Immun. *74*, 910–919.

Qiagen (2006). DNeasy Blood & Tissue Handbook, Protocol: Pretreatment of Gram-Positive Bacteria. 45–46.

Rachid, S., Ohlsen, K., Wallner, U., Hacker, J., Hecker, M., and Ziebuhr, W. (2000). Alternative Transcription Factor ç(B) Is Involved in Regulation of Biofilm Expression in a Staphylococcus aureus Mucosal Isolate. J. Bacteriol. *182*, 6824–6826.

Rahman, S.A., and Schomburg, D. (2006). Observing local and global properties of metabolic pathways: "load points" and "choke points" in the metabolic networks. Bioinforma. *22* , 1767–1774.

Rainey, P., and Santi, D. V (1983). Metabolism and mechanism of action of formycin B in Leishmania. Proc. Natl. Acad. Sci. U. S. A. *80*, 288–292.

Rajendran, N.B., Eikmeier, J., Becker, K., Hussain, M., Peters, G., and Heilmann, C. (2015). Important Contribution of the Novel Locus comEB to Extracellular DNA-Dependent Staphylococcus lugdunensis Biofilm Formation. Infect. Immun. .

Rajendran, R., Williams, C., Lappin, D.F., Millington, O., Martins, M., and Ramage, G. (2013). Extracellular DNA Release Acts as an Antifungal Resistance Mechanism in Mature Aspergillus fumigatus Biofilms. Eukaryot. Cell *12*, 420–429.

Ramage, G., Vande Walle, K., Wickes, B.L., and Lopez-Ribot, J.L. (2001). Standardized method for in vitro antifungal susceptibility testing of Candida albicans biofilms. Antimicrob. Agents Chemother. *45*, 2475–2479.

Ramage, G., Tunney, M.M., Patrick, S., Gorman, S.P., and Nixon, J.R. (2003). Formation

of Propionibacterium acnes biofilms on orthopaedic biomaterials and their susceptibility to antimicrobials. Biomaterials *24*, 3221–3227.

Rao, V.K., Krasan, G.P., Hendrixson, D.R., Dawid, S., and St Geme, J.W. (1999). Molecular determinants of the pathogenesis of disease due to non-typable Haemophilus influenzae. FEMS Microbiol. Rev. *23*, 99–129.

Resch, A., Rosenstein, R., Nerz, C., and Go, F. (2005). Differential Gene Expression Profiling of Staphylococcus aureus Cultivated under Biofilm and Planktonic Conditions Differential Gene Expression Profiling of Staphylococcus aureus Cultivated under Biofilm and Planktonic Conditions. Appl. Environ. Microbiol. *71*, 2663–2676.

Resch, A., Leicht, S., Saric, M., Pásztor, L., Jakob, A., Götz, F., and Nordheim, A. (2006). Comparative proteome analysis of Staphylococcus aureus biofilm and planktonic cells and correlation with transcriptome profiling. Proteomics *6*, 1867–1877.

Rice, K.C., Mann, E.E., Endres, J.L., Weiss, E.C., Cassat, J.E., Smeltzer, M.S., and Bayles, K.W. (2007). The cidA murein hydrolase regulator contributes to DNA release and biofilm development in Staphylococcus aureus. Proc. Natl. Acad. Sci. U. S. A. *104*, 8113–8118.

Riley, P., and Lamont, T. (2013). Triclosan / copolymer containing toothpastes for oral health. Cochrane Collab.

Le Roch, K.G., Johnson, J.R., Ahiboh, H., Chung, D.-W.D., Prudhomme, J., Plouffe, D., Henson, K., Zhou, Y., Witola, W., Yates, J.R., et al. (2008). A systematic approach to understand the mechanism of action of the bisthiazolium compound T4 on the human malaria parasite, Plasmodium falciparum. BMC Genomics *9*, 513.

Roessner, U., and Bowne, J. (2009). What is metabolomics all about? Biotechniques *46*, 363–365.

Rogers, S.A., Huigens, R.W., Cavanagh, J., and Melander, C. (2010). Synergistic Effects between Conventional Antibiotics and 2-Aminoimidazole-Derived Antibiofilm Agents . Antimicrob. Agents Chemother. *54*, 2112–2118.

Rohde, H., Burdelski, C., Bartscht, K., Hussain, M., Buck, F., Horstkotte, M.A., Knobloch, J.K.-M., Heilmann, C., Herrmann, M., and Mack, D. (2005). Induction of Staphylococcus epidermidis biofilm formation via proteolytic processing of the accumulation-associated protein by staphylococcal and host proteases. Mol. Microbiol. *55*, 1883–1895.

Rohde, H., Burandt, E.C., Siemssen, N., Frommelt, L., Burdelski, C., Wurster, S., Scherpe, S., Davies, A.P., Harris, L.G., Horstkotte, M.A., et al. (2007). Polysaccharide intercellular adhesin or protein factors in biofilm accumulation of Staphylococcus epidermidis and Staphylococcus aureus isolated from prosthetic hip and knee joint infections. Biomaterials *28*, 1711–1720.

Roilides, E., Simitsopoulou, M., Katragkou, A., and Walsh, T.J. (2015). How Biofilms Evade Host Defenses. Microbiol. Spectr. *3*.

Russell, A. (2004). Whither triclosan? J. Antimicrob. Chemother. *53*, 693–695.

Sadykov, M.R., Olson, M.E., Halouska, S., Zhu, Y., Fey, P.D., Powers, R., and Somerville, G.A. (2008). Tricarboxylic acid cycle-dependent regulation of Staphylococcus epidermidis polysaccharide intercellular adhesin synthesis. J. Bacteriol. *190*, 7621–7632.

Sadykov, M.R., Zhang, B., Halouska, S., Nelson, J.L., Kreimer, L.W., Zhu, Y., Powers, R., and Somerville, G.A. (2010). Using NMR metabolomics to investigate tricarboxylic acid cycle-dependent signal transduction in Staphylococcus epidermidis. J. Biol. Chem. *285*, 36616–36624.

Salazar, O., and Asenjo, J. a (2007). Enzymatic lysis of microbial cells. Biotechnol. Lett. *29*, 985–994.

Salmenlinna, S., Lyytikäinen, O., and Vuopio-Varkila, J. (2002). Community-Acquired Methicillin-Resistant Staphylococcus aureus, Finland. Emerg. Infect. Dis. J. *8*, 602.

Sambanthamoorthy, K., Gokhale, A.A., Lao, W., Parashar, V., Neiditch, M.B., Semmelhack, M.F., Lee, I., and Waters, C.M. (2011). Identification of a Novel Benzimidazole That Inhibits Bacterial Biofilm Formation in a Broad-Spectrum Manner. Antimicrob. Agents Chemother. *55*, 4369–4378.

Sarkar, S., and Pires, M.M. (2015). d-Amino Acids Do Not Inhibit Biofilm Formation in Staphylococcus aureus. PLoS One *10*, e0117613.

Saunders, E.C., DE Souza, D.P., Naderer, T., Sernee, M.F., Ralton, J.E., Doyle, M.A., Macrae, J.I., Chambers, J.L., Heng, J., Nahid, A., et al. (2010). Central carbon metabolism of Leishmania parasites. Parasitology *137*, 1303–1313.

Scheltema, R.A., Kamleh, A., Wildridge, D., Ebikeme, C., Watson, D.G., Barrett, M.P., Jansen, R.C., and Breitling, R. (2008). Increasing the mass accuracy of high-resolution LC-MS data using background ions: a case study on the LTQ-Orbitrap. Proteomics *8*, 4647–4656.

Scheltema, R.A., Jankevics, A., Jansen, R.C., Swertz, M. a, and Breitling, R. (2011). PeakML/mzMatch: a file format, Java library, R library, and tool-chain for mass spectrometry data analysis. Anal. Chem. *83*, 2786–2793.

Schirmer, M., Ijaz, U.Z., D'Amore, R., Hall, N., Sloan, W.T., and Quince, C. (2015). Insight into biases and sequencing errors for amplicon sequencing with the Illumina MiSeq platform. Nucleic Acids Res. .

Schweizer, H.P. (2001). Triclosan: a widely used biocide and its link to antibiotics. FEMS Microbiol. Lett. *202*, 1–7.

Secor, P.R., Jennings, L.K., James, G.A., Kirker, K.R., Pulcini, E.D., McInnerney, K., Gerlach, R., Livinghouse, T., Hilmer, J.K., Bothner, B., et al. (2012). Phevalin (aureusimine B) production by Staphylococcus aureus biofilm and impacts on human keratinocyte gene expression. PLoS One *7*, e40973.

Segata, N., Waldron, L., Ballarini, A., Narasimhan, V., Jousson, O., and Huttenhower, C. (2012). Metagenomic microbial community profiling using unique clade-specific marker genes. Nat. Methods *9*, 811–814.

Shah, N., Tang, H., Doak, T.G., and Ye, Y. (2011). Comparing bacterial communities inferred from 16S rRNA gene sequencing and shotgun metagenomics. Pac. Symp. Biocomput. 165–176.

Shin, M.H., Lee, D.Y., Liu, K.-H., Fiehn, O., and Kim, K.H. (2010). Evaluation of sampling and extraction methodologies for the global metabolic profiling of Saccharophagus degradans. Anal. Chem. *82*, 6660–6666.

Singh, R., Ray, P., Das, A., and Sharma, M. (2009). Role of persisters and small-colony

variants in antibiotic resistance of planktonic and biofilm-associated Staphylococcus aureus: an in vitro study. J. Med. Microbiol. *58*, 1067–1073.

Singh, R., Ray, P., Das, A., and Sharma, M. (2010). Enhanced production of exopolysaccharide matrix and biofilm by a menadione-auxotrophic Staphylococcus aureus small-colony variant. J. Med. Microbiol. *59*, 521–527.

Skaar, E.P., and Schneewind, O. (2004). Iron-regulated surface determinants (Isd) of Staphylococcus aureus: stealing iron from heme. Microbes Infect. *6*, 390–397.

Slater-Radosti, C., Van Aller, G., Greenwood, R., Nicholas, R., Keller, P.M., DeWolf, W.E.J., Fan, F., Payne, D.J., and Jaworski, D.D. (2001). Biochemical and genetic characterization of the action of triclosan on Staphylococcus aureus. J. Antimicrob. Chemother. *48*, 1–6.

Smith, C. a, Want, E.J., O'Maille, G., Abagyan, R., and Siuzdak, G. (2006). XCMS: processing mass spectrometry data for metabolite profiling using nonlinear peak alignment, matching, and identification. Anal. Chem. *78*, 779–787.

Smith, C.A., O'Maille, G., Want, E.J., Qin, C., Trauger, S.A., Brandon, T.R., Custodio, D.E., Abagyan, R., and Siuzdak, G. (2005). METLIN: a metabolite mass spectral database. Ther. Drug Monit. *27*, 747–751.

Smith, K., Perez, A., Ramage, G., Lappin, D., Gemmell, C.G., and Lang, S. (2008). Biofilm formation by Scottish clinical isolates of Staphylococcus aureus. J. Med. Microbiol. *57*, 1018–1023.

Smyth, G.K. (2004). Linear models and empirical bayes methods for assessing differential expression in microarray experiments. Stat. Appl. Genet. Mol. Biol. *3*, Article3.

Soda, K. (2011). The mechanisms by which polyamines accelerate tumor spread. J. Exp. Clin. Cancer Res. *30*, 1–9.

Soga, T., Ueno, Y., Naraoka, H., Ohashi, Y., Tomita, M., and Nishioka, T. (2002). Simultaneous Determination of Anionic Intermediates for Bacillus subtilis Metabolic Pathways by Capillary Electrophoresis Electrospray Ionization Mass Spectrometry. Anal. Chem. *74*, 2233–2239.

Soga, T., Ohashi, Y., Ueno, Y., Naraoka, H., Tomita, M., and Nishioka, T. (2003). Quantitative Metabolome Analysis Using Capillary Electrophoresis Mass Spectrometry. J. Proteome Res. *2*, 488–494.

Solano, C., García, B., Valle, J., Berasain, C., Ghigo, J.-M., Gamazo, C., and Lasa, I. (2002). Genetic analysis of Salmonella enteritidis biofilm formation: critical role of cellulose. Mol. Microbiol. *43*, 793–808.

Somerville, G.A., Beres, S.B., Fitzgerald, J.R., DeLeo, F.R., Cole, R.L., Hoff, J.S., and Musser, J.M. (2002). In Vitro Serial Passage of Staphylococcus aureus: Changes in Physiology, Virulence Factor Production, and agr Nucleotide Sequence. J. Bacteriol. *184*, 1430–1437.

Soto, S.M. (2013). Role of efflux pumps in the antibiotic resistance of bacteria embedded in a biofilm. Virulence *4*, 223–229.

Speziale, P., Pietrocola, G., Rindi, S., Provenzano, M., Provenza, G., Di Poto, A., Visai, L., and Arciola, C.R. (2009). Structural and functional role of Staphylococcus aureus surface components recognizing adhesive matrix molecules of the host. Future

Microbiol. *4*, 1337–1352.

Spratt, B.G. (1999). Multilocus sequence typing: molecular typing of bacterial pathogens in an era of rapid DNA sequencing and the internet. Curr. Opin. Microbiol. *2*, 312–316.

Srinivasan, A., Leung, K.P., Lopez-Ribot, J.L., and Ramasubramanian, A.K. (2013). High-throughput nano-biofilm microarray for antifungal drug discovery. MBio *4*.

Stewart, P.S., and Costerton, J.W. (2001). Antibiotic resistance of bacteria in biofilms. Lancet *358*, 135–138.

Stipetic, L.H., Hamilton, G., Dalby, M.J., Davies, R.L., Meek, R.M.D., Ramage, G., Smith, D.G.E., and Burgess, K.E. V (2015). Draft Genome Sequence of Isolate Staphylococcus aureus LHSKBClinical, Isolated from an Infected Hip. Genome Announc. *3*.

Stowe, S.D., Richards, J.J., Tucker, A.T., Thompson, R., Melander, C., and Cavanagh, J. (2011). Anti-biofilm compounds derived from marine sponges. Mar. Drugs *9*, 2010–2035.

Sud, M., Fahy, E., Cotter, D., Brown, A., Dennis, E.A., Glass, C.K., Merrill, A.H.J., Murphy, R.C., Raetz, C.R.H., Russell, D.W., et al. (2007). LMSD: LIPID MAPS structure database. Nucleic Acids Res. *35*, D527–D532.

Suller, M.T.E., and Russell, A.D. (1999). Antibiotic and biocide resistance in Stuphylococcus aureus and vancomycin-resistant enterococcus. J. Hosp. Infect. *43*, 281–291.

Suller, M.T.E., and Russell, A.D. (2000). Triclosan and antibiotic resistance in Staphylococcus aureus. J. Antimicrob. Chemother. *46*, 11–18.

Sumner, L., Lei, Z., Nikolau, B., Saito, K., Roessner, U., and Trengove, R. (2014). Proposed quantitative and alphanumeric metabolite identification metrics. Metabolomics *10*, 1047–1049.

t'Kindt, R., Jankevics, A., Scheltema, R., Zheng, L., Watson, D., Dujardin, J.-C., Breitling, R., Coombs, G., and Decuypere, S. (2010). Towards an unbiased metabolic profiling of protozoan parasites: optimisation of a Leishmania sampling protocol for HILIC-orbitrap analysis. Anal. Bioanal. Chem. *398*, 2059–2069.

Takahashi, N. (2005). Microbial ecosystem in the oral cavity: Metabolic diversity in an ecological niche and its relationship with oral diseases. Int. Congr. Ser. *1284*, 103–112.

Takahashi, N., and Washio, J. (2011). Metabolomic Effects of Xylitol and Fluoride on Plaque Biofilm in Vivo . J. Dent. Res. *90* , 1463–1468.

Takahashi, N., Washio, J., and Mayanagi, G. (2010). Metabolomics of supragingival plaque and oral bacteria. J. Dent. Res. *89*, 1383–1388.

Takahashi, N., Washio, J., and Mayanagi, G. (2012). Metabolomic approach to oral biofilm characterization—A future direction of biofilm research. J. Oral Biosci. *54*, 138–143.

Tang, J. (2011). Microbial metabolomics. Curr. Genomics *12*, 391–403.

Taylor, N.S., Weber, R.J.M., White, T.A., and Viant, M.R. (2010). Discriminating between different acute chemical toxicities via changes in the daphnid metabolome. Toxicol. Sci. *118*, 307–317.

Terstappen, G.C., Schlupen, C., Raggiaschi, R., and Gaviraghi, G. (2007). Target deconvolution strategies in drug discovery. Nat Rev Drug Discov *6*, 891–903.

The NIH HMP Working Group, Peterson, J., Garges, S., Giovanni, M., McInnes, P., Wang, L., Schloss, J.A., Bonazzi, V., McEwen, J.E., Wetterstrand, K.A., et al. (2009). The NIH Human Microbiome Project. Genome Res. *19*, 2317–2323.

Theobald, U., Mailinger, W., Baltes, M., Rizzi, M., and Reuss, M. (1997). In vivo analysis of metabolic dynamics in Saccharomyces cerevisiae : I. Experimental observations. Biotechnol. Bioeng. *55*, 305–316.

Tomita, T., and Kamio, Y. (1997). Molecular biology of the pore-forming cytolysins from Staphylococcus aureus, alpha- and gamma-hemolysins and leukocidin. Biosci. Biotechnol. Biochem. *61*, 565–572.

Tornero, E., Senneville, E., Euba, G., Petersdorf, S., Rodriguez-Pardo, D., Lakatos, B., Ferrari, M.C., Pilares, M., Bahamonde, A., Trebse, R., et al. (2014). Characteristics of prosthetic joint infections due to Enterococcus sp. and predictors of failure: a multi-national study. Clin. Microbiol. Infect. *20*, 1219–1224.

Trampuz, A., Piper, K.E., Jacobson, M.J., Hanssen, A.D., Unni, K.K., Osmon, D.R., Mandrekar, J.N., Cockerill, F.R., Steckelberg, J.M., Greenleaf, J.F., et al. (2007). Sonication of removed hip and knee prostheses for diagnosis of infection. N. Engl. J. Med. *357*, 654–663.

Truong, D.T., Franzosa, E.A., Tickle, T.L., Scholz, M., Weingart, G., Pasolli, E., Tett, A., Huttenhower, C., and Segata, N. (2015). MetaPhlAn2 for enhanced metagenomic taxonomic profiling. Nat Meth *12*, 902–903.

Tsang, L.H., Cassat, J.E., Shaw, L.N., Beenken, K.E., and Smeltzer, M.S. (2008). Factors Contributing to the Biofilm-Deficient Phenotype of Staphylococcus aureus sarA Mutants. PLoS One *3*, e3361.

Tucker, K.L. (2001). Methylated cytosine and the brain: a new base for neuroscience. Neuron *30*, 649–652.

Tunney, M.M., Patrick, S., Gorman, S.P., Nixon, J.R., Anderson, N., Davis, R.I., Hanna, D., and Ramage, G. (1998). Improved detection of infection in hip replacements. A Currently Underestimated Problem. J. Bone Jt. Surg. *80-B*, 568–572.

Tunney, M.M., Patrick, S., Curran, M.D., Ramage, G., Hanna, D., Nixon, J.R., Gorman, S.P., Davis, R.I., and Anderson, N. (1999). Detection of prosthetic hip infection at revision arthroplasty by immunofluorescence microscopy and PCR amplification of the bacterial 16S rRNA gene. J. Clin. Microbiol. *37*, 3281–3290.

Tzagoloff, H., and Novick, R. (1977). Geometry of cell division in Staphylococcus aureus. J. Bacteriol. *129* , 343–350.

Ulrich, M., Bastian, M., Cramton, S.E., Ziegler, K., Pragman, A.A., Bragonzi, A., Memmi, G., Wolz, C., Schlievert, P.M., Cheung, A., et al. (2007). The staphylococcal respiratory response regulator SrrAB induces ica gene transcription and polysaccharide intercellular adhesin expression, protecting Staphylococcus aureus from neutrophil killing under anaerobic growth conditions. Mol. Microbiol. *65*, 1276–1287.

Valle, J., Toledo-Arana, A., Berasain, C., Ghigo, J.-M., Amorena, B., Penades, J.R., and Lasa, I. (2003). SarA and not sigmaB is essential for biofilm development by Staphylococcus aureus. Mol. Microbiol. *48*, 1075–1087.

Vanhegan, I.S., Malik, A.K., Jayakumar, P., Ul Islam, S., and Haddad, F.S. (2012). A financial analysis of revision hip arthroplasty: the economic burden in relation to the national tariff. J. Bone Joint Surg. Br. *94*, 619–623.

Varella Coelho, M.L., Santos Nascimento, J. dos, Fagundes, P.C., Madureira, D.J., Oliveira, S.S. de, Vasconcelos de Paiva Brito, M.A., and Freire Bastos, M. do C. de (2007). Activity of staphylococcal bacteriocins against Staphylococcus aureus and Streptococcus agalactiae involved in bovine mastitis. Res. Microbiol. *158*, 625–630.

Ventura, M., O'Flaherty, S., Claesson, M.J., Turroni, F., Klaenhammer, T.R., van Sinderen, D., and O'Toole, P.W. (2009). Genome-scale analyses of health-promoting bacteria: probiogenomics. Nat. Rev. Microbiol. *7*, 61–71.

Villalain, J., Mateo, C.R., Aranda, F.J., Shapiro, S., and Micol, V. (2001). Membranotropic effects of the antibacterial agent Triclosan. Arch. Biochem. Biophys. *390*, 128–136.

Villar, M., Ayllón, N., Alberdi, P., Moreno, A., Moreno, M., Tobes, R., Mateos-Hernández, L., Weisheit, S., Bell-Sakyi, L., and de la Fuente, J. (2015). Integrated Metabolomics, Transcriptomics and Proteomics Identifies Metabolic Pathways Affected by Anaplasma phagocytophilum Infection in Tick Cells. Mol. Cell. Proteomics *14* , 3154–3172.

Vincent, I.M., Creek, D., Watson, D.G., Kamleh, M. a, Woods, D.J., Wong, P.E., Burchmore, R.J.S., and Barrett, M.P. (2010). A molecular mechanism for eflornithine resistance in African trypanosomes. PLoS Pathog. *6*, e1001204.

Vincent, I.M., Creek, D.J., Burgess, K., Woods, D.J., Burchmore, R.J.S., and Barrett, M.P. (2012). Untargeted metabolomics reveals a lack of synergy between nifurtimox and eflornithine against Trypanosoma brucei. PLoS Negl. Trop. Dis. *6*, e1618.

Vincent, I.M., Weidt, S., Rivas, L., Burgess, K., Smith, T.K., and Ouellette, M. (2014). Untargeted metabolomic analysis of miltefosine action in Leishmania infantum reveals changes to the internal lipid metabolism. Int. J. Parasitol. Drugs Drug Resist. *4*, 20–27.

Vogt, M., Flemming, H.C., and Veeman, W.S. (2000). Diffusion in Pseudomonas aeruginosa biofilms: a pulsed field gradient NMR study. J. Biotechnol. *77*, 137–146.

Vuong, C., Saenz, H.L., Gotz, F., and Otto, M. (2000). Impact of the agr quorum-sensing system on adherence to polystyrene in Staphylococcus aureus. J. Infect. Dis. *182*, 1688–1693.

Vuong, C., Gerke, C., Somerville, G.A., Fischer, E.R., and Otto, M. (2003). Quorum-sensing control of biofilm factors in Staphylococcus epidermidis. J. Infect. Dis. *188*, 706–718.

Vuong, C., Kocianova, S., Yao, Y., Carmody, A.B., and Otto, M. (2004). Increased colonization of indwelling medical devices by quorum-sensing mutants of Staphylococcus epidermidis in vivo. J. Infect. Dis. *190*, 1498–1505.

Vuong, C., Kidder, J.B., Jacobson, E.R., Otto, M., Proctor, R.A., and Somerville, G.A. (2005). Staphylococcus epidermidis polysaccharide intercellular adhesin production significantly increases during tricarboxylic acid cycle stress. J. Bacteriol. *187*, 2967–2973.

Walencka, E., Rozalska, S., Wysokinska, H., Rozalski, M., Kuzma, L., and Rozalska, B. (2007). Salvipisone and aethiopinone from Salvia sclarea hairy roots modulate staphylococcal antibiotic resistance and express anti-biofilm activity. Planta Med. *73*,

545–551.

Watson, D.G. (2010). The potential of mass spectrometry for the global profiling of parasite metabolomes. Parasitology *137*, 1409–1423.

Weaver, W.M., Milisavljevic, V., Miller, J.F., and Di Carlo, D. (2012). Fluid Flow Induces Biofilm Formation in Staphylococcus epidermidis Polysaccharide Intracellular Adhesin-Positive Clinical Isolates. Appl. Environ. Microbiol. *78* , 5890–5896.

Webber, M. a. (2002). The importance of efflux pumps in bacterial antibiotic resistance. J. Antimicrob. Chemother. *51*, 9–11.

van der Werf, M.J., Overkamp, K.M., Muilwijk, B., Coulier, L., and Hankemeier, T. (2007). Microbial metabolomics: toward a platform with full metabolome coverage. Anal. Biochem. *370*, 17–25.

Whipps, J.M., Lewis, K., and Cooke, R.C. (1988). Mycoparasitism and plant disease control. In Fungi in Biological Control Systems, M.N. Burge, ed. (Manchester: Manchester University Press), pp. 141–161.

Willey, J.M., and van der Donk, W.A. (2007). Lantibiotics: peptides of diverse structure and function. Annu. Rev. Microbiol. *61*, 477–501.

Williams, R.J. (1951). Biochemical Institute Studies IV. Individual Metabolic Patterns and Human Disease: An Exploratory Study Utilizing Predominantly Paper Chromatographic Methods (Austin: U. Texas).

Williams, R.E.O., and Harper, G.J. (1947). Staphylococcal hæmolysins on sheep-blood agar with evidence for a fourth hæmolysin. J. Pathol. Bacteriol. *59*, 69–78.

Wilson, I.D., Plumb, R., Granger, J., Major, H., Williams, R., and Lenz, E.M. (2005). HPLC-MS-based methods for the study of metabonomics. J. Chromatogr. B, Anal. Technol. Biomed. Life Sci. *817*, 67–76.

Wishart, D.S., Tzur, D., Knox, C., Eisner, R., Guo, A.C., Young, N., Cheng, D., Jewell, K., Arndt, D., Sawhney, S., et al. (2007). HMDB: the Human Metabolome Database. Nucleic Acids Res. *35*, D521–D526.

Wishart, D.S., Knox, C., Guo, A.C., Eisner, R., Young, N., Gautam, B., Hau, D.D., Psychogios, N., Dong, E., Bouatra, S., et al. (2009). HMDB: a knowledgebase for the human metabolome. Nucleic Acids Res. *37*, D603–D610.

Wishart, D.S., Jewison, T., Guo, A.C., Wilson, M., Knox, C., Liu, Y., Djoumbou, Y., Mandal, R., Aziat, F., Dong, E., et al. (2013). HMDB 3.0--The Human Metabolome Database in 2013. Nucleic Acids Res. *41*, D801–D807.

Wisseman, C.L., Jackson, E.B., Hahn, F.E., Ley, A.C., and Smadel, J.E. (1951). Metabolic Studies of Rickettsiae: I. The Effects of Antimicrobial Substances and Enzyme Inhibitors on the Oxidation of Glutamate by Purified Rickettsiae . J. Immunol. *67* , 123–136.

Wistrom, J., Norrby, S.R., Myhre, E.B., Eriksson, S., Granstrom, G., Lagergren, L., Englund, G., Nord, C.E., and Svenungsson, B. (2001). Frequency of antibiotic-associated diarrhoea in 2462 antibiotic-treated hospitalized patients: a prospective study. J. Antimicrob. Chemother. *47*, 43–50.

Wood, J.M. (2015). Bacterial responses to osmotic challenges. J. Gen. Physiol. *145*, 381–388.

Workentine, M.L., Harrison, J.J., Weljie, A.M., Tran, V.A., Stenroos, P.U., Tremaroli, V., Vogel, H.J., Ceri, H., and Turner, R.J. (2010). Phenotypic and metabolic profiling of colony morphology variants evolved from Pseudomonas fluorescens biofilms. Environ. Microbiol. *12*, 1565–1577.

Wright, G.D. (2005). Bacterial resistance to antibiotics: Enzymatic degradation and modification. Adv. Drug Deliv. Rev. *57*, 1451–1470.

Wu, L., Mashego, M.R., van Dam, J.C., Proell, A.M., Vinke, J.L., Ras, C., van Winden, W.A., van Gulik, W.M., and Heijnen, J.J. (2005). Quantitative analysis of the microbial metabolome by isotope dilution mass spectrometry using uniformly 13C-labeled cell extracts as internal standards. Anal. Biochem. *336*, 164–171.

Wu, X.-H., Yu, H.-L., Ba, Z.-Y., Chen, J.-Y., Sun, H.-G., and Han, B.-Z. (2010). Sampling methods for NMR-based metabolomics of Staphylococcus aureus. Biotechnol. J. *5*, 75–84.

Wyatt, M.A., Wang, W., Roux, C.M., Beasley, F.C., Heinrichs, D.E., Dunman, P.M., and Magarvey, N.A. (2010). Staphylococcus aureus Nonribosomal Peptide Secondary Metabolites Regulate Virulence. Sci. *329* , 294–296.

Wynne, A.G., McCartney, A.L., Brostoff, J., Hudspith, B.N., and Gibson, G.R. (2004). An in vitro assessment of the effects of broad-spectrum antibiotics on the human gut microflora and concomitant isolation of a Lactobacillus plantarum with anti-Candida activities. Anaerobe *10*, 165–169.

Yamada, Y., Kuzuyama, T., Komatsu, M., Shin-ya, K., Omura, S., Cane, D.E., and Ikeda, H. (2015). Terpene synthases are widely distributed in bacteria. Proc. Natl. Acad. Sci. *112* , 857–862.

Yao, Y., Sturdevant, D.E., and Otto, M. (2005). Genomewide analysis of gene expression in Staphylococcus epidermidis biofilms: insights into the pathophysiology of S. epidermidis biofilms and the role of phenol-soluble modulins in formation of biofilms. J. Infect. Dis. *191*, 289–298.

Yarwood, J.M., Bartels, D.J., Volper, E.M., and Greenberg, E.P. (2004). Quorum Sensing in Staphylococcus aureus Biofilms. J. Bacteriol. *186* , 1838–1850.

Yee, R., Cui, P., Shi, W., Feng, J., and Zhang, Y. (2015). Genetic Screen Reveals the Role of Purine Metabolism in Staphylococcus aureus Persistence to Rifampicin. Antibiotics *4*, 627–642.

Yi, Z.-B., Yu, Y., Liang, Y.-Z., and Zeng, B. (2007). Evaluation of the antimicrobial mode of berberine by LC/ESI-MS combined with principal component analysis. J. Pharm. Biomed. Anal. *44*, 301–304.

Yigit, E., Hernandez, D.I., Trujillo, J.T., Dimalanta, E., and Bailey, C.D. (2014). Genome and metagenome sequencing: Using the human methyl-binding domain to partition genomic DNA derived from plant tissues. Appl. Plant Sci. *2*.

Zhang, B., and Powers, R. (2012). Analysis of bacterial biofilms using NMR-based metabolomics. Future Med. Chem. *4*, 1273–1306.

Zhang, B., Halouska, S., Schiaffo, C.E., Sadykov, M.R., Somerville, G.A., and Powers, R. (2011). NMR Analysis of a Stress Response Metabolic Signaling Network. J. Proteome Res. *10*, 3743–3754.

Zheng, Z., Clark, N., Keremane, M., Lee, R., Wallis, C., Deng, X., and Chen, J. (2014).

Whole-Genome Sequence of “Candidatus Liberibacter solanacearum” Strain R1 from California. Genome Announc. *2*, e01353–14.

Zhu, Y., Weiss, E.C., Otto, M., Fey, P.D., Smeltzer, M.S., and Somerville, G.A. (2007). Staphylococcus aureus biofilm metabolism and the influence of arginine on polysaccharide intercellular adhesin synthesis, biofilm formation, and pathogenesis. Infect. Immun. *75*, 4219–4226.

Ziebuhr, W., Krimmer, V., Rachid, S., Lossner, I., Gotz, F., and Hacker, J. (1999). A novel mechanism of phase variation of virulence in Staphylococcus epidermidis: evidence for control of the polysaccharide intercellular adhesin synthesis by alternating insertion and excision of the insertion sequence element IS256. Mol. Microbiol. *32*, 345–356.

Zielinska, A.K., Beenken, K.E., Mrak, L.N., Spencer, H.J., Post, G.R., Skinner, R.A., Tackett, A.J., Horswill, A.R., and Smeltzer, M.S. (2012). sarA-mediated repression of protease production plays a key role in the pathogenesis of Staphylococcus aureus USA300 isolates. Mol. Microbiol. *86*, 1183–1196.

Zimmerli, W., Trampuz, A., and Ochsner, P.E. (2004). Prosthetic-joint infections. N. Engl. J. Med. *351*, 1645–1654.